Quantifying Aircraft Lead Emissions at Airports

DETAILS

217 pages | 8.5 x 11 | PAPERBACK
ISBN 978-0-309-43255-9 | DOI 10.17226/22142

AUTHORS

Jeremy Heiken; Airport Cooperative Research Program; Transportation Research Board; National Academies of Sciences, Engineering, and Medicine

THE NATIONAL ACADEMIES

Advisers to the Nation on Science, Engineering, and Medicine

The **National Academy of Sciences** is a private, nonprofit, self-perpetuating society of distinguished scholars engaged in scientific and engineering research, dedicated to the furtherance of science and technology and to their use for the general welfare. Upon the authority of the charter granted to it by the Congress in 1863, the Academy has a mandate that requires it to advise the federal government on scientific and technical matters. Dr. Ralph J. Cicerone is president of the National Academy of Sciences.

The **National Academy of Engineering** was established in 1964, under the charter of the National Academy of Sciences, as a parallel organization of outstanding engineers. It is autonomous in its administration and in the selection of its members, sharing with the National Academy of Sciences the responsibility for advising the federal government. The National Academy of Engineering also sponsors engineering programs aimed at meeting national needs, encourages education and research, and recognizes the superior achievements of engineers. Dr. C. D. Mote, Jr., is president of the National Academy of Engineering.

The **Institute of Medicine** was established in 1970 by the National Academy of Sciences to secure the services of eminent members of appropriate professions in the examination of policy matters pertaining to the health of the public. The Institute acts under the responsibility given to the National Academy of Sciences by its congressional charter to be an adviser to the federal government and, upon its own initiative, to identify issues of medical care, research, and education. Dr. Victor J. Dzau is president of the Institute of Medicine.

The **National Research Council** was organized by the National Academy of Sciences in 1916 to associate the broad community of science and technology with the Academy's purposes of furthering knowledge and advising the federal government. Functioning in accordance with general policies determined by the Academy, the Council has become the principal operating agency of both the National Academy of Sciences and the National Academy of Engineering in providing services to the government, the public, and the scientific and engineering communities. The Council is administered jointly by both Academies and the Institute of Medicine. Dr. Ralph J. Cicerone and Dr. C. D. Mote, Jr., are chair and vice chair, respectively, of the National Research Council.

The **Transportation Research Board** is one of six major divisions of the National Research Council. The mission of the Transportation Research Board is to provide leadership in transportation innovation and progress through research and information exchange, conducted within a setting that is objective, interdisciplinary, and multimodal. The Board's varied activities annually engage about 7,000 engineers, scientists, and other transportation researchers and practitioners from the public and private sectors and academia, all of whom contribute their expertise in the public interest. The program is supported by state transportation departments, federal agencies including the component administrations of the U.S. Department of Transportation, and other organizations and individuals interested in the development of transportation. **www.TRB.org**

www.national-academies.org

Table of Contents

List of Figures

List of Tables

1. EXECUTIVE SUMMARY

Lead (Pb) is a well-known air pollutant that can lead to a variety of adverse health impacts, including neurological effects in children that lead to behavioral problems, learning deficits, and lowered IQ. Concerns regarding the adverse health effects of exposure to airborne Pb resulted in its classification as an air pollutant pursuant to the Clean Air Act in 1976, followed by the requisite enactment of a health-based National Ambient Air Quality Standard (NAAQS) for Pb in 1978 (set at 1.5 micrograms per cubic meter based on quarterly average concentration).

During the 1970s, the primary source of airborne Pb in the United States was the combustion of leaded gasoline in motor vehicles. Phase-out of leaded gasoline use in motor vehicles began in the mid-1970s with the introduction of catalytic converters, and the use was banned after December 31, 1995. The elimination of leaded gasoline use in motor vehicles left ore and metals processing, waste incinerators, utilities, lead-acid battery manufacturing, as well as the combustion of leaded aviation gasoline in piston-engine powered aircraft, as the major sources of airborne lead emissions.

In October 2008, the U.S. Environmental Protection Agency (EPA) promulgated a new Pb NAAQS that lowered the acceptable level by an order of magnitude, to 0.15 micrograms per cubic meter based on a rolling three-month average concentration. In addition to promulgating the new Pb NAAQS, in December 2010 EPA revised requirements for ambient Pb monitoring around facilities known to have substantial Pb emissions. These facilities include airports with sufficient piston-powered aircraft activity that they are estimated to have annual Pb emissions of 1.0 ton or more. In addition, EPA is currently engaged in a monitoring study of 15 additional airports with estimated annual Pb emissions between 0.5 and 1.0 ton to investigate whether airports with this range of Pb emissions that meet additional criteria described by EPA that may have the potential to cause violations of the Pb NAAQS (U.S. EPA 2013).

In light of the above, the Airport Cooperative Research Program (ACRP) initiated ACRP Project 02-34 entitled “Quantifying Aircraft Lead Emissions at Airports.” The first primary objective of this study is to review and improve upon existing methodologies to quantify and characterize aircraft-related Pb emissions at airports with significant populations of aircraft that use leaded aviation gasoline. The second primary objective is to create a guidance document that explains the refined methodology for quantifying airport Pb emissions such that it can be readily implemented by airports around the country seeking to assess the importance of aircraft-related Pb emissions at their facilities. This report focuses only on the first objective.

Given the objective of reviewing and improving methods for quantifying aircraft-related lead emissions, the study involved the following five major phases:

1. A review of existing methodologies for quantifying aircraft-related Pb emissions;

2. Development of a refined methodology for estimating aircraft-related Pb emissions inventories that addresses shortcomings with existing methodologies identified during the critical review;

3. Conducting month-long field studies at each of three selected airports to gather site-specific data regarding aircraft activity, the lead content of aviation gasoline used at the airport, and data regarding ambient Pb concentrations, Pb particle size distributions, and Pb isotope ratios;

4. Application of the refined methodology to develop Pb emission inventories for three selected airports using both readily available activity data as well as the site-specific data; and

5. Validation of the refined methodology through comparison of dispersion modeling results based on the inventory computed using site-specific data with ambient Pb measurements made during the field study.

During the course of the review of existing aircraft Pb quantification methodologies, issues and data gaps were identified in the following key areas:

- Information regarding airframes and engines;
- Engine fuel consumption rates and modal load assumptions;
- Aviation gasoline lead concentrations;
- Engine lead retention;
- Aircraft time in mode;
- Total aircraft operations, aircraft fleet operations, and temporal variations;
- Contribution of non-combustion sources of lead;
- Validation of emission estimates; and
- Proper documentation of data and results.

Based on the results of the critical review, a refined methodology for quantifying aircraft-related Pb emissions was developed and applied to estimate calendar year 2008 and 2011 aircraft-related Pb emissions. Emissions inventories resulting from engine exhaust were prepared using publicly available data for three selected airports with substantial piston-engine aircraft operations: Richard Lloyd Jones Jr. Airport (RVS) in Tulsa, OK; Centennial Airport (APA) in Denver, CO; and Santa Monica Municipal Airport (SMO) in Santa Monica, CA. The key differences between the refined methodology and the existing methodologies include the following:

- Expansion of the number of aircraft and engine types considered;
- Use of brake specific fuel consumption and engine load data by mode to estimate fuel consumption instead of volumetric fuel flow rates;
- Use of the Federal Aviation Administration's (FAA's) Traffic Flow Management System Counts (TFMSC) database at *https://aspm.faa.gov/TFMS/sys/* for the distribution of piston-powered aircraft operations;
- Use of FAA's Type Certificate Data Sheets (TCDS) to obtain engine characteristics data for piston-powered aircraft;
- Use of FAA's U.S. registration counts for the distribution of engines within a given piston-powered aircraft; and
- Use of FAA's General Aviation and Air Taxi Activity (GAATA) Survey defined at the regional level for the fraction of civilian operations of total piston-powered aircraft operations.

In addition, the refined methodology was applied for calendar year 2011 at each airport using site-specific data gathered during the field studies regarding aircraft fleet characteristics, activity, and gasoline Pb content to estimate engine exhaust emissions.

Annual Pb exhaust emissions as estimated using the refined methodology with publicly available data for 2008 are compared to the estimates obtained using existing methods in Table 1. The two results for Santa Monica Airport reflect differing assumptions regarding operational modes that were also used with the refined methodology. As shown, the differences in emission estimates for APA and RVS were relatively large and of opposite sign, while those for SMO were smaller. Also of note is that the refined methodology predicated higher emissions for two of the three airports.

Annual Pb exhaust emissions as estimated using the refined methodology with publicly available data for 2011 are compared to the estimates obtained using the refined methodology with site-specific data in Table 2. Again, two results are shown for Santa Monica Airport based on the use of publicly available data reflecting the differing assumptions in operational modes discussed above, but both are compared to a single value obtained using the site-specific data gathered during the field study. As shown, use of the site-specific data resulted in lower estimated Pb emissions in all cases, with the differences being substantial in most cases.

The site-specific data gathered during the field studies were also used to develop temporally and spatially resolved inventories for selected days on which ambient Pb concentrations were measured. These inventories were used as input to the AERMOD dispersion model to compute 12-hour average "modeled" concentrations that could be

Table 1
Estimated Calendar Year 2008 Pb Emissions (tons per year)

	APA	RVS	SMO 1	SMO 2
Existing Methodologies	0.73	1.17	0.33	0.13
Refined Methodology	1.95	0.69	0.43	0.16

Note: The two results for Santa Monica Airport reflect differing assumptions regarding operational modes.

Table 2
Estimated Calendar Year 2011 Pb Emissions (tons per year)

	APA	RVS	SMO 1	SMO 2
Refined Methodology – Publicly Available Data	1.76	0.48	0.38	0.14
Refined Methodology – Site-Specific Data	0.26	0.18	0.12	0.12

Note: The two results for Santa Monica Airport reflect differing assumptions regarding operational modes.

compared to the monitored values in order to evaluate the performance of the refined methodology. These data are shown in Figure 1 for RVS, where the best agreement between modeled and monitored concentrations was observed. Data for APA, where the poorest agreement was observed are shown in Figure 2 and indicate an overprediction of ambient Pb levels. Finally, as shown in Figure 3, data for SMO indicated relatively good agreement except for two weekend days (shown as triangles) when the monitored concentrations were far higher than those modeled. Similar comparisons of modeled versus monitored concentrations made using the refined methodology but with publicly available data all showed poor agreement.

Finally, the field study data also allowed assessment of the relative importance of resuspended lead (as opposed to Pb from only exhaust emissions) to total lead concentrations. Based on the comparisons of Pb concentrations in total suspended particulate (TSP) and fine particulate matter ($PM_{2.5}$) measured at the three field study sites, what is believed to be resuspended lead in the coarse particle size range was observed to account for about 20–30% of the lead found in TSP. Furthermore, based on analysis of lead isotopes present in the samples collected at the field sites, the original source of the lead found in the coarse particle range appears to be the combustion of leaded aviation gasoline.

Figure 1
Modeled versus Measured $PM_{2.5}$-PbAt the RVS North Site

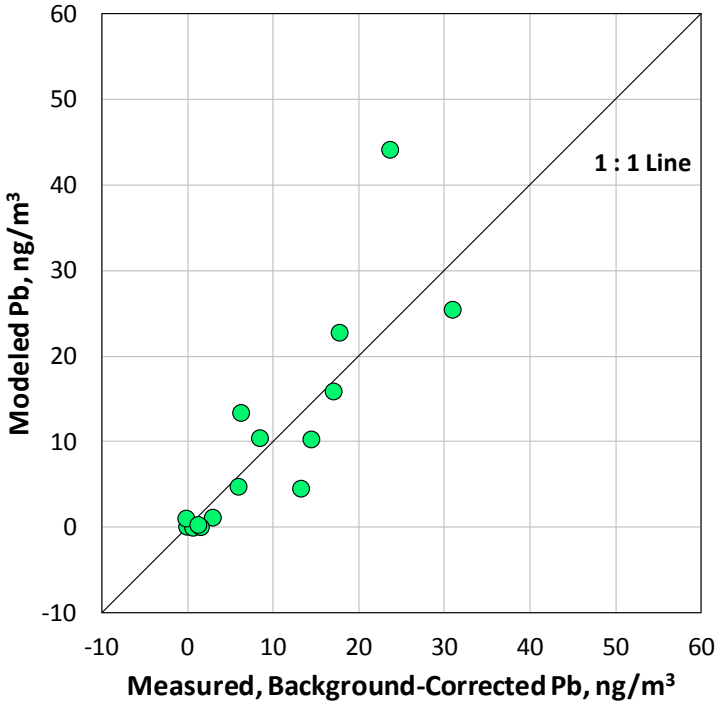

Figure 2
Modeled versus Measured $PM_{2.5}$-Pb at the APA Central Site

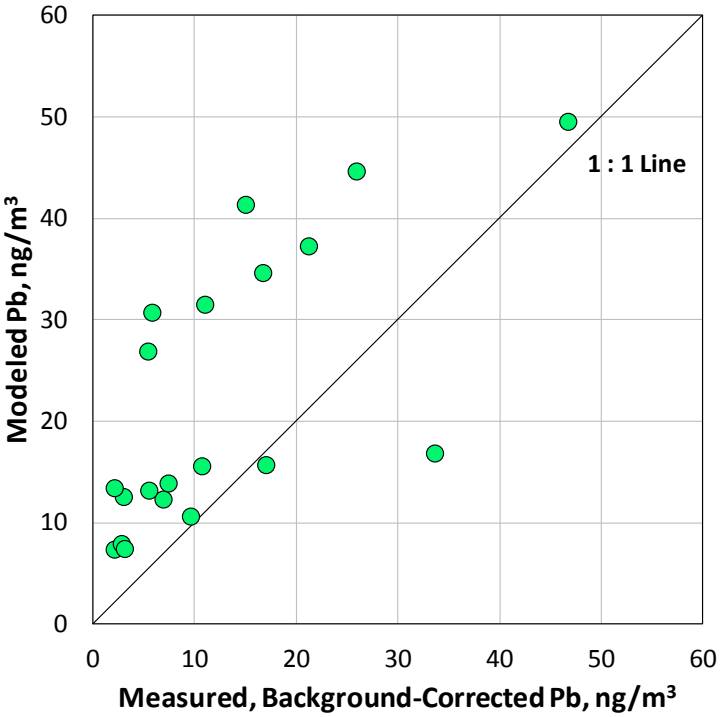

Figure 3
Modeled versus Measured $PM_{2.5}$-Pb Concentrations at the SMO Northeast Site

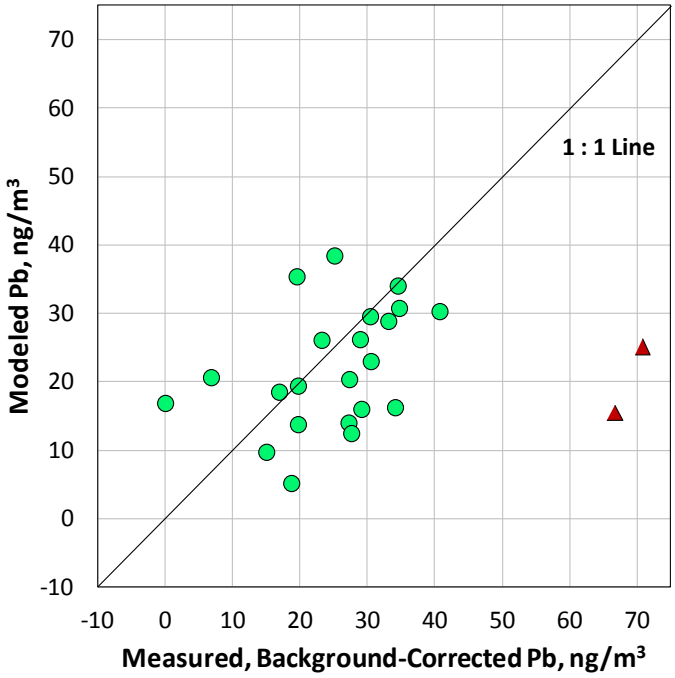

###

2. INTRODUCTION

Lead (Pb) is a well-known air pollutant that can lead to a variety of adverse health impacts, including neurological effects in children that lead to behavioral problems, learning deficits, and lowered IQ. Concerns regarding the adverse health effects of exposure to airborne Pb resulted in its classification as an air pollutant pursuant to the Clean Air Act in 1976, followed by the requisite enactment of a health-based National Ambient Air Quality Standard (NAAQS) for Pb in 1978 (set at 1.5 micrograms per cubic meter based on quarterly average concentration).

During the 1970s, the primary source of airborne Pb in the United States was the combustion of leaded gasoline in motor vehicles. Phase-out of leaded gasoline use in motor vehicles began in the mid-1970s with the introduction of catalytic converters, and the use was banned after December 31, 1995. The elimination of leaded gasoline use in motor vehicles left ore and metals processing, waste incinerators, utilities, lead-acid battery manufacturing, as well as the combustion of leaded aviation gasoline in piston-engine powered aircraft, as the major sources of airborne lead emissions.

In October 2008, the U.S. Environmental Protection Agency (EPA) promulgated a new Pb NAAQS that lowered the acceptable level by an order of magnitude, to 0.15 micrograms per cubic meter based on a rolling three-month average concentration. In addition to promulgating the new Pb NAAQS, in December 2010 EPA revised requirements for ambient Pb monitoring around facilities known to have substantial Pb emissions. These facilities include airports with sufficient piston-powered aircraft activity that they are estimated to have annual Pb emissions of 1.0 ton or more. In addition, EPA is currently engaged in a one-year monitoring study of 15 additional airports with estimated annual Pb emissions between 0.5 and 1.0 ton to investigate whether airports with this range of Pb emissions that meet additional criteria described by EPA may have the potential to cause violations of the Pb NAAQS (U.S. EPA 2013).

In light of the above, the Airport Cooperative Research Program initiated ACRP Project 02-34 entitled “Quantifying Aircraft Lead Emissions at Airports.” The first primary objective of this study is to review and improve upon existing methodologies to quantify and characterize aircraft-related Pb emissions at airports with significant populations of aircraft that use leaded aviation gasoline. The second primary objective is to create a guidance document that explains the refined methodology for quantifying airport Pb emissions such that it can be readily implemented by airports around the country seeking to assess the importance of aircraft-related Pb emissions at their facilities. This report focuses only on the first objective.

Given the objective of reviewing and improving methods for quantify aircraft-related lead emissions, the study involved five major phases:

1. A review of existing methodologies for quantifying aircraft-related Pb emissions;

2. Development of a refined methodology for estimating aircraft-related Pb emissions inventories that addresses shortcomings with existing methodologies identified during the review for application at three selected airports;

3. Conducting month-long field studies at each of three selected airports to gather site-specific data regarding aircraft activity, the lead content of aviation gasoline used at the airport, and data regarding ambient Pb concentrations, Pb particle size distributions and Pb isotope ratios;

4. Application of the refined methodology to develop Pb emission inventories for three selected airports using site-specific data; and

5. Validation of the refined methodology through comparison of dispersion modeling results based on the inventory computed using site-specific data with ambient Pb measurements made during the field study.

The results for each phase of the study are documented in the five chapters that follow.

###

3. REVIEW OF EXISTING METHODS FOR QUANTIFYING AIRCRAFT-RELATED LEAD EMISSIONS

In its simplest form, the methodology for quantifying lead emissions from an individual aircraft during a given airport operation (e.g., taxiing) requires only the following information:

- The engine fuel flow rate during the operation in units of volume or mass of fuel consumed per unit time;
- The lead content of the fuel in units of mass of lead per unit volume or mass of fuel consumed;
- The amount of lead that is retained in the engine or exhaust system as a percentage of total lead consumed; and
- The amount of time required to conduct the operation.

However, the amount of information needed expands dramatically when quantifying the aircraft-related lead emissions at a given airport over any significant length of time. The expanded data needs typically include the following:

- Relationships between engine fuel flow and engine load for all of the different types of engines used in aircraft operating at the airport;
- Engine loads during each aircraft operating mode (idle/taxi, run-up, takeoff, climb-out, and approach) for all of the different types of aircraft in operation at the airport;
- The gasoline lead content and lead retention rate for all of the different types of aircraft in operation at the airport;
- The duration of each of the different operating modes for all of the different types of aircraft in operation at the airport; and
- The number of each type of aircraft in operation at the airport and the operations in which they are engaged.

Furthermore, to the extent that one seeks to use aircraft-related Pb emissions data in combination with air quality models to estimate ambient Pb concentrations at points in and around the airport, information is also needed regarding spatial and temporal patterns of aircraft activity as well as relevant meteorological data.

Because of the scope and complexity of the information needed to quantify aircraft-related lead emissions for a given airport and the resources required to obtain that information, many simplifying assumptions are typically required. Obviously the types of information that are actually used and the nature of the assumptions that are made have the potential to substantially affect the quality of the estimates of Pb emissions occurring at an airport. Given this, the goal of this phase of the study was to critically review existing methods used to quantify aircraft-related Pb emissions in order to assess the information and assumptions upon which they are based and to develop approaches that can be used to improve quantification of airport Pb emissions.

3.1 Literature Search

The review began with a search of the technical literature related to the quantification of aircraft-related lead emissions. Over 70 related documents were identified and are summarized in the annotated bibliography provided in Appendix A. As a review of the bibliography shows, many of the identified documents, while related to aircraft lead emissions, were not directly relevant to existing methodologies used for quantification of Pb emissions at airports. The methodologies described in the directly relevant studies are summarized below, along with key sources of existing information.

3.2 Summary of Existing Methodologies and Information Sources for Quantifying Aircraft-Related Lead Emissions

3.2.1 EPA Methodologies

AP-42 – The general method by which air emissions are quantified from aircraft had its origination in the *Compilation of Air Pollutant Emissions Factors, Third Edition (AP-42)* published by the U.S. Environmental Protection Agency (EPA) (U.S. EPA 1977). Therein, times in mode of operation (TIM) for piston-powered general aviation (GA) and military aircraft within the Landing-Takeoff Cycle (LTO)—representing taxi-out, takeoff, climb-out, approach and taxi-in operations—are presented. Additionally, modal fuel flow rates and emissions factors for select criteria pollutants emitted from the Continental O-200 and Lycoming O-320 model piston engines are provided. The fuel flow rates reported for these engines are summarized in Table 3 below. Notably, a methodology for quantifying aircraft Pb emissions is not addressed in this document.

Table 3
Original Fuel Flow Rates from AP-42

Engine Model	Fuel Flow Rate per Mode of Operation (lb/hr)			
	Taxi/Idle	Takeoff	Climb-out	Approach
Continental O-200	7.68	48.4	48.4	21.3
Lycoming O-320	13.0	65.7	63.5	23.1

Source: U.S. EPA, "Compilation of Air Pollutant Emissions Factors, Third Edition" (1977)

As part of the Emissions Inventory Improvement Program (EIIP) in the early 1990s, EPA updated its guidance for preparing emissions inventories in a ten-volume series. The updated guidance for aircraft emissions inventories was presented in *Procedures for Emission Inventory Preparation Volume IV: Mobile Sources* (known as *Procedures Volume IV)* (U.S. EPA 1992).

With respect to GA aircraft emissions, the methodology was updated to provide an approach for quantifying emissions if the specific aircraft fleet mix and engines were known, as well as an alternate approach involving fleet average emissions factors if the only data available were the level of LTOs at a facility as reported in the FAA's *Air Traffic Activity* publication.

Procedures Volume IV also improved the methodology by providing guidance on the adjustment of approach and climb-out TIM calculations to account for local mixing height, generally defined as the atmospheric ceiling above which vertical mixing of air (and air pollutants) does not occur. Again, however, no methodology specific to estimating Pb emissions from piston-engine aircraft was provided, although the fuel consumption data provided for piston engines were expanded slightly to include the Continental TSIO-360C engine model.

Table 4 summarizes the fuel consumption and TIM information for piston-engine aircraft provided in *Procedures Volume IV*. Values published for the O-200 and O-320 engine differ slightly than those previously provided in *AP-42*.

National Emissions Inventory – Pursuant to the Consolidated Emissions Reporting Rule (CERR) promulgated in June 2002, EPA began preparing the National Emissions Inventory (NEI) on a three-year cycle (U.S. EPA 2002). The NEI catalogs emissions from point, non-point, area, mobile, and stationary sources by state and county.

In estimating aircraft lead emissions for the 2002 and 2005 NEI, EPA relied on a methodology developed for use with on-road vehicles designed to operate on leaded gasoline (U.S. EPA 1998). The methodology accounted for piston-engine Pb emissions by taking the total gallons of aviation gasoline (avgas) produced in 2002 and 2005 and

Table 4
Updated Fuel Flow Rates from AP-42

Engine Model	Fuel Flow Rate per Mode of Operation (lb/hr)			
	Taxi/Idle	Takeoff	Climb-out	Approach
Continental O-200	8.4	45.0	45.0	25.8
Continental TSIO-360C	11.4	133.2	99.6	61.2
Lycoming O-320	9.6	88.8	66.6	46.8

Source: U.S. EPA, Procedures for Emissions Inventory Preparation Volume IV: Mobile Sources (1992)

factoring it by the American Society of Testing and Materials (ASTM) maximum allowable Pb concentration in 100 low-lead (100LL) aviation gasoline (2.12 grams Pb/gallon avgas) and assuming that 25% of the Pb consumed was retained in aircraft engines. The 25% Pb retention assumption was developed using data from measurements made in the exhaust from vehicles operating on leaded fuel. The resulting national Pb aircraft emissions estimates were then apportioned to 3,410 airports based on the level of piston-engine aircraft activity reported in the FAA's Terminal Area Forecast (FAA TAF) for the year in question.

In a technical support document and guidance document issued in 2008, EPA first described the calculation of Pb emissions from piston-powered aircraft based on the use of aircraft-specific emission factors and activity data (U.S. EPA 2008). This methodology focused on refining Pb estimates specific to the LTO cycle. These refinements are summarized below.

1. Computing single- and twin-piston-engine LTOs based on the FAA's General Aviation and Air Taxi Activity Survey (GAATA) compiled in 2005.

2. Applying times in mode for piston-engine aircraft operations contained in *Procedures Volume IV* to fuel flow rates for piston-engine aircraft available in the FAA's Emissions and Dispersion Modeling System (EDMS) to compute single- and twin-engine fuel consumption values per LTO in combination with an aviation gasoline density of 6 lbs/gallon. Table 5 presents the EDMS engine fuel flow data.

3. Computing a weighted-average fuel consumption value per LTO, according to the proportions that 90% of landings reported in the GAATA Survey were completed by single-engine aircraft and 10% were completed by twin engine aircraft. The resulting factor was 7.34 g Pb/LTO.

4. Reducing the assumed Pb retention factor from 25% to 5%.

Table 5
EDMS Fuel Flow Rates

Engine Model	Fuel Flow Rates by Mode of Operation (lb/hr)			
	Taxi/Idle	Takeoff	Climb-out	Approach
Continental 6-285-B	72.1	153.0	166.0	83.3
Continental IO-360-B	8.1	103.0	71.7	36.6
Continental O-200	8.3	45.2	45.2	25.5
Continental TSIO-360C	11.5	133.3	99.2	61.0
Lycoming IO-320-D1AD	7.8	91.7	61.4	37.6
Lycoming O-320	9.4	88.9	66.7	46.5
Lycoming TIO-540-J2B2	25.0	259.7	204.5	99.2
Wright R-1820	88.9	1165.9	861.9	323.0

Source: Federal Aviation Administration Emissions and Dispersion Modeling System (version 5.0.2)

This general methodology was also used with some revisions to generate the 2008 NEI estimates. (ERG 2011). For example, EPA expanded the list of data sources used to compute LTOs at GA facilities for which data are available (ERG 2011). These sources include the FAA Form 5010, FAA's Operations Network (OPSNET) and ATADS and TAF databases, and the Bureau of Transportation Statistics (BTS) T-100 database. Furthermore, an approach was outlined to estimate LTO activity based on the number of GA aircraft based at a facility if LTO data are unavailable:

$$\text{LTOs} = 1293 + 203 * (\#\text{ based aircraft}) + 0.0019 * (\text{county population}) - 473 * [\text{Alaska} - 144 * (\text{AlaskaXaircraft})]$$

Where:

- LTOs = Landing Takeoff Operations (i.e., 1 landing + 1 takeoff)
- [Alaska – 144 * (AlaskaXaircraft)] = correction factor to account for the effect that aircraft based in Alaska have on the suitability of the equation

For facilities with neither LTO data nor aircraft-based data, EPA proposed that the bottom 10% of LTO values calculated according to the equation above was representative of the missing activity. Additionally, EPA considered the median number of LTOs reported at heliports as representative of helicopter activity at facilities where data are unavailable. Finally, EPA provided an estimate of Pb emissions occurring outside of the

LTO cycle during the cruise mode of operation, apportioned to individual states based on their share of the national general aviation and air taxi LTOs used in the NEI.

The NEI documentation acknowledges that its methodology would benefit from the following improvements (ERG 2011):

1. Use of airport-specific LTO and TIM data, and an improved process by which LTOs are computed from the number of aircraft based at the airport if LTO information is not available;

2. Use of gasoline Pb concentrations based on data specific to the fuel being supplied at an airport; and

3. Fuel consumption rates specific to the fleet mix operating at an airport.

3.2.2 Other Methodologies

Harris and Davidson calculated Pb emissions from piston aircraft operating within the South Coast Air Basin (SCAB) of southern California by inputting 2001 LTO data from facilities within the basin into EDMS (Harris and Davidson 2005). For this assessment, aircraft activity was modeled in EDMS using the Cessna 172, Piper PA28 and Cessna 150 aircraft types, assuming a 64.9-minute total flight duration, and that 42.1% of this average flight activity occurs below the local atmospheric mixing height (27.3 minutes). Sulfur dioxide (SO_2) emissions calculated by EDMS were converted to Pb emissions by applying a speciation factor of 0.739 and an uncertainty estimate of 17.5%, resulting in an overall emissions inventory of 267 kg of Pb per year in the SCAB.

Detailed studies of Pb emissions have also been conducted at SMO, each of which included emissions inventories prepared using distinct methodologies. At the behest of the Santa Monica Airport Working Group, Piazza (1999) computed emissions of Pb at SMO using SMO-supplied aircraft fleet and activity data, engine emission factors from AP-42 and the FAA's Aircraft Engine Emission Database (FAEED), and the calculations outlined in *Procedures Volume IV*. Notably, default LTO times in mode were applied in the study.

On behalf of EPA, ICF International prepared a Pb emissions inventory based on 2008 piston-engine aircraft activity at SMO (ICF International and T&B Systems 2010, Carr et al. 2011). Activity data were obtained directly from the airport and used as inputs to the 2008 NEI methodology to estimate Pb emissions. Fuel consumption was calculated based on an 11.8-minute LTO cycle (compared to the 27.3 minutes used in previous studies). The ICF methodology applied at SMO included two modes of operation that were previously unaccounted for in the then-existent methodologies: aircraft run-up and landing. The inclusion of engine run-up was a significant improvement, as this mode commonly occurs in order to perform safety checks. Moreover, sensitivity analysis conducted by ICF showed engine run-up to be one of the most important factors related to total aircraft-related Pb emissions at SMO. The study also accounted for fuel

consumption during landing based on the assumption that engines would operate at full load.

Run-up fuel consumption rates were obtained from operational manuals for the IO-360, IO-320, GSO-480, IO-550, TIO-540-J2B2, and TSIO-550 engines. When averaged, these yielded a rate of 13 gallons per hour for twin-engine aircraft and 7 gallons per hour for single-engine aircraft. Based on the two most common piston engines in the aircraft fleet at SMO (i.e., the IO-360 and the IO-320), a fuel consumption rate of 5 gallons per hour was ultimately selected.

Piston-powered helicopter activity was accounted in the ICF study based on a 20-minute LTO cycle and an average Pb emission rate of 6.6 grams per LTO. Notably, 25% of the LTO activity reported for helicopters was assumed to be conducted by piston-engine powered machines, based on estimates from the airport operator.

3.2.3 Swiss Federal Office of Civil Aviation Methodologies and Data

The Switzerland Federal Office of Civil Aviation (FOCA) has collected emissions and fuel consumption data on many types of piston-powered aircraft and helicopter engines, and has published guidance on the calculation of emissions and fuel consumption resulting from their operation. Table 6 summarizes piston-engine fuel consumption rates per mode of operation collected by FOCA (Switzerland Federal Office of Civil Aviation 2007).

FOCA has also developed a relationship between fuel flow and shaft horsepower (HP) for piston helicopter engines (Switzerland Federal Office of Civil Aviation 2009). Times in mode associated with the FOCA helicopter emissions estimation methodology comprise 5 minutes total ground idle time, 3 minutes takeoff time, and 5.5 minutes approach time. Notably, fuel flow rates derived for 172 distinct helicopter airframe/ piston-engine combinations, as computed using the equation below, are also provided.

$$\text{Fuel Flow (kg/s)} = 1.9*10^{-12}* SHP^4 - 10^{-9}*SHP^3 + 2.6*10^{-7}*SHP^2 + 4*10^{-5}*SHP + 0.006$$

Where:

- SHP = Shaft Horsepower; assuming operation at 20% maximum SHP during idle;
- 95% maximum SHP during takeoff, 60% maximum SHP during approach; and
- 90% maximum SHP during cruise.

Table 6
Swiss FOCA Fuel Flow Rates

Engine Model	Horsepower (HP)	Fuel Flow Rate per Mode of Operation (lb/hr)			
		Taxi/Idle	Takeoff	Climb-out	Approach
IO-320-DIAD	160	7.9	92.1	61.1	37.3
IO-360-A1B6	200	11.1	107.9	84.1	49.2
IO-540-T4A5D	260	19.8	132.5	117.5	58.7
IO-550-B	300	30.2	144.4	142.9	77.8
O-200	100	7.9	45.2	45.2	25.4
O-320-E2A	150	10.3	79.4	63.5	38.1
O-360-A3A	180	12.7	95.2	81.0	42.9
O-540-J3C5D	235	12.7	131.7	111.1	52.4
Rotax 582 DCDI	64	4.8	31.7	28.6	12.7
Rotax 912	80	9.5	30.2	24.6	14.3
Rotax 912S	100	4.0	42.4	32.7	18.3
Rotax 914	114	14.3	57.1	44.4	23.0
TAE-125-01	135	2.4	50.8	40.5	19.8
TIO-540-J2B2	350	25.4	259.5	204.8	99.2
TSIO-360C	225	11.1	133.3	99.2	61.1
TSIO-520-WB	325	48.4	214.3	182.5	111.1
Unspecified < 200 HP	150	9.5	88.9	66.7	46.8
Unspecified > 500 HP	1200	7.9	1780.2	356.4	174.6
Unspecified 201 to 300 HP	225	11.1	133.3	99.2	61.1
Unspecified 301 to 500 HP	350	25.4	259.5	204.8	99.2

Source: Switzerland Federal Office of Civil Aviation, 2007.

3.2.4 Additional Piston-Engine Fuel Consumption Data

Fuel consumption rates from select piston aircraft engines have also been collected through a series of technical reports prepared by both the FAA and the Coordinating Research Council (CRC) as part of a series of tests conducted on the viability of unleaded fuel alternatives to avgas (Atwood 2007, Atwood 2009, Atwood and Camirales 2004, Atwood and Knopp 1999, Coordinating Research Council 2010). These rates were

collected at varying engine power settings, many of which do not directly correspond to those assumed in the existing emissions inventory methodologies.

Figure 4 shows the covariation of mass fuel flow (in lbs/hr) with brake specific fuel consumption (BSFC, in lbs/hp-hr) for a sample of engine test data taken from these studies, representing a variety of engines (e.g., IO-540-K), power settings (e.g., 100%, 85%, 75%), and fuel blends (e.g., 100LL, UL). Relationships shown by the data in Figure 4 include the following:

- BSFC and mass fuel flow values typically decrease as engine power setting decreases;
- TSIO and TIO series engines typically have the highest fuel consumption rates in the data set in terms of both BSFC as well as mass fuel flow, indicating that these engines operate at higher horsepower ratings;
- The IO-320 series engine consumes the least amount of fuel compared to other engines for which data are available; and
- With a few exceptions, each engine data series shows good linear correlation between BSFC and mass fuel flow ($r^2 > 0.9$).

Most significantly, Figure 4 demonstrates the utility of using BSFC to estimate fuel consumption for estimating Pb emissions from piston-engine aircraft because it allows fuel consumption to be varied as a function of engine load instead of having to obtain measured or estimated mass fuel flow rates for each power rating.

3.3 Issues Identified During the Review

The major issues identified with the information and assumptions used in current methodologies for estimating aircraft-related lead emissions are discussed below.

3.3.1 Information Regarding Airframes and Engines

Fuel consumption rates can vary between fixed-wing, experimental, light-sport, and rotorcraft types of airframes defined by FAA. However, existing emissions inventory methodologies do not segregate aircraft operations by airframe type for the purposes of calculating lead emissions from those aircraft equipped with piston engines. This is due in part to the lack of readily available data sources that adequately characterize operations by airframe type and also indicate how engine technology and usage (i.e., type and number of engines equipped to the airframe) can vary by airframe type.

Figure 4
Covariation of BSFC with Mass Fuel Flow
(Legend: Engine, Fuel, % Throttle)

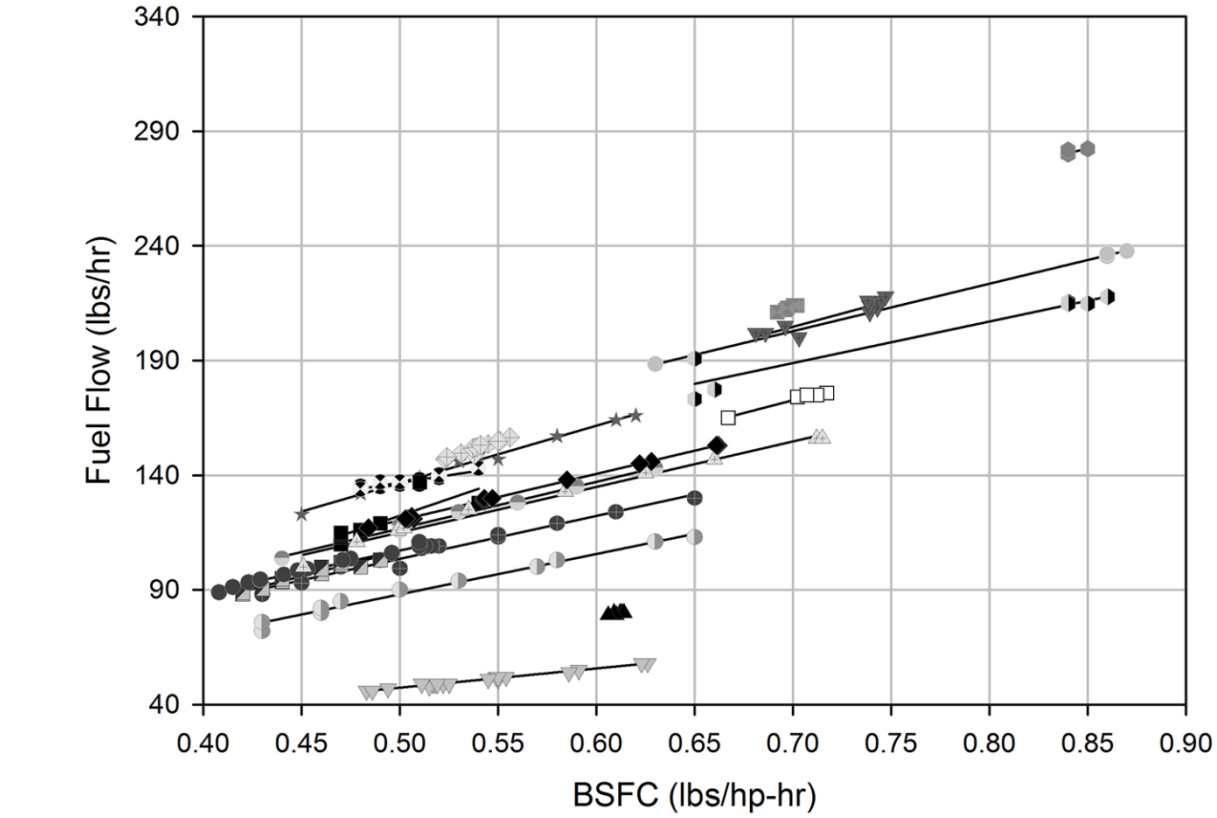

IO-320-B, UL, 100%	IO-540-K, UL, 85%	TSIO-550-E (325), UL, 75%
IO-540-K, 100 LL, 100%	TIO-540-J (325), UL, 85%	IO-320-B, UL, 70%
IO-540-K, UL, 100%	TSIO-550-E (310), UL, 85%	IO-540-K, 100 LL, 65%
IO-550-D, UL, 100%	IO-540-K, 100 LL, 75%	
TIO-540-J (325), UL, 100%	IO-540-K, UL, 75%	
TSIO-550-E (310), UL, 100%	IO-550-D, UL, 75%	
TSIO-550-E (325), UL, 100%	TIO-540-J (325), UL, 75%	
IO-540-K, 100 LL, 85%	TSIO-550-E (310), UL, 75%	

To address this issue, data regarding observed aircraft operations or data from provided airport records could be used in combination with the FAA's Tail Number Registry and Type Certification database to determine specific airframe types and engines in operation at an airport, to the extent tail number information is available for the facility.

Alternatively, the FAA's TFMSC (previously the Enhanced Traffic Management System Counts, ETMSC) database could be used to obtain type data for aircraft using the facility. However, this approach is not likely to be as robust as the approach described above because, although TFMSC captures the vast majority of operations, it may not provide full coverage of certain localized types of flights. TFMSC data report predominantly instrument flight rules (IFR) flights, which are a minority of the types of flights conducted at many general aviation airports where visual flight rules (VFR) flights (e.g., training flights, recreational flying) are a significant fraction of total piston-engine powered aircraft operations. With that understood, cross-referencing of the TFMSC data with state/local level records from the Tail Number Registry could aid in engine selection by highlighting which engines are the "most flown" in the area for a given TFMSC aircraft type.

3.3.2 Engine Fuel Consumption Rates and Modal Load Assumptions

Engine fuel consumption rates in existing methodologies are cast in terms of the mass of fuel used per unit time in a given mode and are generally based on data from EDMS that represent only a limited number of piston engines. Furthermore, these limited data are then averaged to yield one single-engine and one twin-engine fuel consumption rate, which are then combined into a single fuel consumption rate based on the assumed proportions of single- and twin-engine aircraft. It is further assumed that the fuel consumption rates are transferable across aircraft of varying sizes and with different engine technologies. Similarly, as noted previously, during recent assessments of Pb emissions at SMO, the methodology used was improved by accounting for Pb emissions during engine run-up mode. However, the fuel consumption rates for run-up were averaged based on single- and twin-engine aircraft most frequently in use based on the available operational data. Additionally, landing mode fuel consumption rates used in the most recent SMO study incorrectly assumed that engines would be operating at full load when, in fact, they operate at idle.

The issues identified above could be addressed by developing BSFC rates for piston engines rather than using a generalized mass fuel flow rate for a limited set of single- and twin-engine aircraft. Using this approach, modal variations in horsepower and load factor can be incorporated into the fuel consumption and emissions calculations for the taxi/idle, takeoff, climb-out, approach, landing and run-up modes of operation, accounting for variations in engine performance within these modes. BSFC values can be extracted from either manufacturer specifications or from existing data published by the Switzerland FOCA, the FAA, and the CRC. The lack of available BSFC information for every type of engine may, however, preclude a complete characterization of total fuel consumption across the entire piston-powered aircraft fleet at a facility. Where data are unavailable for a specific engine(s), it is possible to estimate BSFC based on data available for other similar engines.

Additionally, although modal load factors are available for the more traditional modes of operation within the LTO cycle, factors for new modes (i.e., run-up/maintenance), as well as refinements to existing modes (i.e., continuous lowering of load during approach and landing), can be developed using assumptions regarding average engine load either assigned directly from available engine test data or interpolated using fuel consumption relationships obtained from the Swiss FOCA data or other similar sources.

3.3.3 Aviation Gasoline Lead Concentrations

The general practice at present is to use a fuel-based Pb emissions factor developed using the ASTM maximum allowable concentration of Pb in 100LL aviation gasoline, which is 2.12 g/gallon. However, a recent survey of 89 aviation gasoline samples from FAA fixed base operators (representing nine refineries) indicated Pb concentrations ranging between about 1.3 and 2.1 g/gallon. Additionally, 23 aviation gasoline samples obtained from engine manufacturers for use in certification testing exhibited Pb concentrations ranging between 0.3 and 2.2 g/gallon (Coordinating Research Council 2011). Material Safety Data Sheets (MSDS) available from aviation gasoline producers (British Petroleum 2011, Chevron Global Aviation 2003, ConocoPhllips 2010, Shell Energy North America 2003, Petro-Canada 2009, Phillips Petroleum 1998) corroborate this variance in the concentration of Pb actually contained in 100LL aviation gasoline blends compared to the ASTM maximum, demonstrating that the local sources of aviation gasoline supply may be influential in refining airport emissions inventories.

Given that aircraft-related Pb emissions are directly proportional to the amount of Pb in the fuel, under ideal circumstances the actual concentration of lead in the fuel being used by each aircraft would be available for use in preparing an airport Pb emission inventory. Given that these data do not exist, the next best alternative is to use data regarding the Pb concentrations present in the fuel being dispensed at the airport.

In general, Pb concentration data should be available for each load of aviation gasoline delivered to an airport or each batch of fuel to the extent that aviation gasoline is delivered to an airport by pipeline. However, these data may be unavailable from airport operators or fuel suppliers, and manufacturers may consider the information proprietary. Alternatives include historic data and forecast Pb usage levels from airport fuel suppliers or the best available existing data regarding Pb concentrations as a function of fuel grade, geographic region, and season from published sources.

3.3.4 Engine Lead Retention

The fraction of total lead in the fuel consumed by an aircraft engine that remains in the engine and exhaust system is another key parameter that has to be accounted for during inventory preparation. Ideally, lead retention data, which would be expected to vary somewhat with engine technology and exhaust system design, would be available on an aircraft-specific basis; however, data at this level of detail are not available.

As noted above, EPA's original methodology for calculating Pb emissions from piston aircraft within the NEI assumed that 25% of the Pb consumed by the engine was retained in the engine oil based on data from automobiles designed to operate on leaded fuel. More recently, Petersen (2008) performed a study that estimated lead retained in aircraft engines to be 5%. This study included quantification of the concentrations of lead in used and new fuel lubricants for a sampling of in-use piston engines, the results of which are summarized in Table 7 to estimate the amount of lead retained in engine oil. A representative value for lead retained in engine oil and an estimate of lead retained in the engine itself from the Swiss FOCA were then used along with an estimate of the lead consumed in fuel to arrive at the 5% retention value.

In the absence of additional data, this 5% retention rate currently represents the best available information for inventory preparation. However, additional research in the area would be useful to confirm the value.

Table 7
Piston-Engine Oil Data

Sample	Lead (ppm)	Test Hours	Sump Capacity (quarts)
IO-360	2,453	50	8
O-300	3,605	25	8
O-320	1,726	20	8
O-320	2,911	20	8
C-85	3,747	21	4.5
IO-360	2,017	40	8
O-235 L2C	5,797	100	6
O-300	4,456	40	8
IO-550	5,536	50	12
O-320 D2J	10,286	100	8
New Unused Oil	226	0	0

Source: Petersen 2008

3.3.5 Time in Mode

The piston-engine aircraft TIM data currently utilized in quantifying aircraft-related lead emissions are summarized in Table 8**.** EPA's NEI methodology has historically utilized the EPA/ICAO (International Civil Aviation Organization) standard TIM reported in Table 8, while the Switzerland FOCA methodology has its own set of standard times.

For comparison purposes, times in mode for select GA airports are also provided in Table 8, demonstrating that facility-specific data, including fleet mix and taxi patterns, are important factors to consider in estimating TIM values. Specifically, taxi times

Table 8
Time-in-Mode Comparison

Facility	Piston Aircraft Times in Mode (minutes)					
	Run-up	Taxi (Idle)	Takeoff	Climb-out	Approach	Total
EPA/ICAO Default	--[a]	16.0	0.3	5.0	6.0	27.3
FOCA Default	--	12.0	0.3	2.5	3.0	17.8
DMW (Carroll County Regional Airport, Maryland)	–	5	1.2	1.7	7.4	15.4
DPA (DuPage Airport, Illinois)	–	13.9	1.6	2.2	8	25.8
GED (Sussex County Airport, Delaware)	–	9.9	1.6	3.1	7.7	22.3
LSZB – circuit (Bern Airport, Switzerland)	–	11.1	0.3	1.3	3.6	16.3
LSZB - LTO	–	11	1.0	3.5	7.5	23.0
MWC (Timmerman Airport, Wisconsin)	–	8.6	1.8	1.9	7.2	19.4
SGJ (Northeast Florida Regional Airport)	–	7.3	2.1	2.4	7.9	19.7
SMO	1.5	7.4	0.3	1.3	1.3[b]	11.8
TPF (Peter O Knight Airport, Florida)	–	3.6	1.6	2.3	7.2	14.5
VDF (Tampa Executive Airport, Florida)	–	5.2	1.5	2.3	7.2	16.1

a. Dashes indicate that data are not available.
b. Includes landing

Sources: Switzerland Federal Office of Civil Aviation, U.S. Environmental Protection Agency, and KB Environmental Sciences, Inc., Carr et al. 2011.

utilized in emissions inventories at the reported facilities are significantly lower than both EPA/ICAO and FOCA defaults. Conversely, takeoff times utilized in the emissions inventories are somewhat higher than both the EPA/ICAO and FOCA default values. For climb-out, the FOCA default TIM approximates the airport-specific times, while the EPA/ICAO default may be more representative for the approach mode of operation based on the presented data. Another important component to TIM calculation for takeoffs and landings is the local atmospheric mixing height above which Pb emissions are not allocated to the airport emission inventory.

Overall, the data show considerable variation in TIM values, and TIM data collected at specific airports show that fleet mix, the local mixing height (which affects TIM for takeoffs and landings), and taxi patterns can have a significant bearing on actual TIM values. Given the above and the importance of accurate TIM data to the accurate quantification of Pb emissions, the best approach is to develop airport-specific TIM values. This could be done through surveys of airport personnel designed to obtain as much airport-specific information regarding TIM as possible or through a dedicated on-site data collection effort. The latter approach should include observations on aircraft speeds, taxi-paths, and taxi-path distances, and applying them to available runway usage data for various types and/or categories of aircraft.

3.3.6 Total Aircraft Operations, Aircraft Fleet Operations, and Temporal Variations

Total Operations – Ideally, the data used to estimate total aircraft operations at a facility should be segregated by engine category (e.g., turboprop) and operational category (e.g., military); however, review of existing methodologies and data sources indicates that robust data are readily available only by operational category. In light of this, the primary approach recommended for this parameter is to acquire data from airport flight strips, counter systems, fixed base operator (FBO) logs, and/or other sources such as direct observations that may be available at a given airport.

Absent the types of data described above, the FAA's ATADS provides another source of total aircraft operations data, with those operations categorized as (1) air carrier, (2) air taxi, (3) general aviation, or (4) military. Furthermore, ATADS data are available for approximately 540 airports within the FAA's National Plan for Integrated Airport Systems (NPIAS). The remainder of the operational data for the over 3,400 hub, non-hub, and general aviation facilities in the NPIAS are based on the FAA's Terminal Area Forecast (TAF) database.

Aircraft Fleet Operations – Ideally, once total operations in each category are computed, they should, as discussed below, be allocated to each airframe in the fleet, with emphasis on being able to adequately represent the proportions of operations within each category at the facility. As above, airport-provided data sources such as flight strips, counters, and data logs would be primarily consulted.

An alternative approach, to be used in instances where the above approach is not feasible, could be to use the FAA's TFMSC database to obtain operational data for each type of aircraft using the facility. TFMSC provides information on operations by category (e.g., air taxi), airframe (e.g., Learjet 35) and engine type (e.g., jet) for the subset of operations conducted under filed flight plans, or recorded under instrument flight rules (IFR). This approach is considered less desirable because, although TFMSC captures the vast majority of operations, it may not provide full coverage of certain localized flight types common to general aviation airports.

Temporal Variations in Aircraft Fleet Operations – In addition to characterizing aircraft fleet operations in general, it may be important—particularly if modeling of ambient Pb

concentrations at an airport is going to be performed—to characterize temporal variations in those operations. For example, given that aircraft usage can vary by season, month, or day of the week, resolution of that variation will improve airport Pb emission inventories that are prepared for similar time frames. Again, the primary recommendation for addressing temporal variations in the aircraft fleet is to use data based on direct observations at airports. Alternatively, the TFMSC database could be used, again with the caveat that it may not provide full coverage of certain localized flight types.

3.3.7 Non-Combustion Sources of Lead

While current methodologies for quantifying aircraft-related lead emissions focus only on emissions from the combustion of leaded aviation gasoline, monitoring studies have identified elevated concentrations of Pb in soils at and surrounding airports, ranging between 21.7 and 232.5 µg of Pb per kg of soil. However, most of the research in this area has failed to demonstrate a clear spatial relationship linking soil concentrations with airport activity (Conor Pacific Environmental Technologies 2000, ICF International and T&B Systems 2010, Lejano and Ericson 2005, Young et al. 2002). Regardless of whether lead in soils at airports is due to aircraft operation, assessments of total Pb emissions at airports and, in particular, studies focused on the contribution of airports to Pb concentrations in TSP or PM_{10} should consider contributions from dust resuspension.

Ideally, in order to estimate total airport lead emissions and airport contributions to ambient lead concentrations, data would be available regarding lead concentrations in soils and dust at the airport, as would data regarding soil entrainment and dust re-suspension rates. Unfortunately, these data are not generally available and are difficult to estimate. In the absence of data addressing non-combustion sources of lead from special airport-specific studies, the alternative is to use some combination of default local airport soil lead concentrations in conjunction with current EPA methodologies for estimating dust re-entrainment.

3.3.8 Validation of Emission Estimates

As discussed in detail above, quantification of aircraft-related Pb emissions is complex and requires many assumptions that are likely to have varying degrees of accuracy. Given this, some studies use air quality modeling and gather ambient Pb monitoring data in order to validate the accuracy of emissions inventories. This type of study requires that the emission inventory include highly detailed information regarding the temporal and spatial distributions of aircraft operation and Pb emissions. Results are usually presented in terms of a comparison of modeled to monitored emissions for specific time periods.

Figure 5 provides an example of data from such a study performed by Carr et al. (2011) at SMO. The model tends to be biased high (especially in the winter) but, overall, there is good agreement between measured and modeled PM-Pb concentration values, with an absolute fractional bias of 0.29 for the winter data and 0.07 for the summer data.

Figure 5
Model-to-Monitor Comparison at SMO

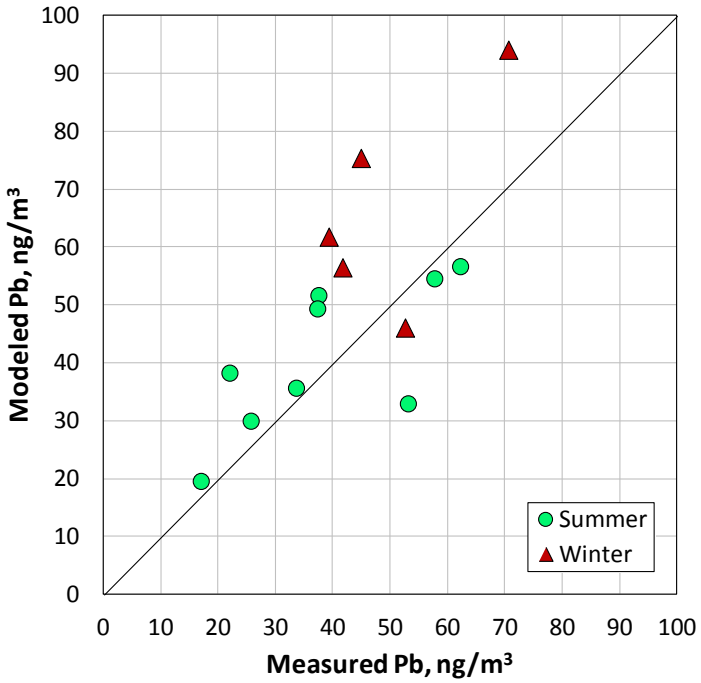

3.3.9 Proper Documentation

A general finding throughout the literature search of existing emissions inventory methodologies, as well as airport-specific emissions inventories, was a lack of sufficient detail to allow emissions inventory results to be recreated. Inadequate documentation included, but was not limited to, the following:

- Specification of operational data sources with inadequate detail on how they were accessed, used, and manipulated for the purposes of preparing an emissions inventory;

- Specification of TIM with inadequate detail on how it was either empirically observed or calculated from obtained data;

- Lack of detail on averaging methods and operational assumptions (i.e., load points, horsepower) in developing fuel consumption rates used for piston-engine aircraft in existing emissions inventories; and

- Incomplete documentation of supporting data or communications that guided underlying assumptions.

Clearly, proper documentation of aircraft Pb inventories is important because it ensures reproducibility, which aids in validation, and helps identify potential sources of erroneous results that could be avoided by refining assumptions or adjusting the fidelity at which each inventory parameter is treated. In order to ensure that proper documentation is being provided, the technical issues outlined below need to be addressed in detail.

Fleet Identification

- For each aircraft category (i.e., GA, air taxi, helicopter), specify which airframe/engine combination was assumed.

- Specify how many engines are equipped to the aircraft and, to the extent possible, how the engine is configured (i.e., HP rating).

- Detail sources of fleet data, when they were accessed, and which time period(s) they cover, and summarize how they were processed or manipulated. Provide end results (i.e., fleet mix).

Operational Specifications

- Specify the level of operations for each aircraft/engine combination in the fleet, which sources of data were consulted to develop the operational levels (and when), and how the operational levels were derived.

- Identify data sources and assumptions used to compute aircraft TIM and how TIM was computed, and summarize results for each fleet member and each operational mode.

- Per mode of operation, indicate assumptions or empirical data used to assign engine load points to aircraft fleet.

Emissions Factor/Fuel Consumption Derivation

- For each member of the fleet, identify sources of modal fuel consumption data and present calculation steps based on observed/assumed operational parameters. Provide all rates utilized in the emissions inventory, per fleet member and operational mode.

- Indicate the fuel Pb concentration(s) used in emissions factor development and present data and the rationale for these values used.

###

4. DEVELOPMENT AND APPLICATION OF A REFINED METHODOLOGY FOR QUANTIFYING AIRCRAFT-RELATED LEAD EMISSIONS

Based on the review of existing methods described in the previous chapter, a refined methodology for quantifying aircraft-related lead emissions was developed and applied at three selected airports for calendar years 2008 and 2011 based on publicly available data sources. The following three airports were selected:

- Richard Lloyd Jones Jr. Airport (RVS) in Tulsa, OK;
- Centennial Airport (APA) in Denver, CO; and
- Santa Monica Municipal Airport (SMO) in Santa Monica, CA.

The selection of these airports was made in light of considerations related to the field studies described in Chapter 5 and the basis for their selection is addressed there.

There were two objectives associated with developing the emission inventories for the three airports. The first of these was to provide a basis for comparison of the results obtained using the refined methodology with those obtained using two existing methodologies: (1) the EPA 2008 NEI methodology (U.S. EPA 2012, ERG 2011), and (2) that applied by ICF at SMO (ICF International and T&B Systems 2010). The second objective was to use the refined inventory results as inputs for air quality modeling that was performed in order to guide the design of the field studies discussed in the next chapter.

Publicly available data were used for development of the refined inventories because aircraft-related Pb emissions historically have generally been quantified using only publicly available data (due at least in part to the resources required to obtain site-specific data) and this approach would also provide a basis for comparing these results with the results obtained using the site-specific data collected in the field studies (as discussed in Chapter 6).

The remainder of this chapter discusses development of the refined methodology, provides a detailed description of the input data and assumptions required, presents the results, and lastly compares the results to results obtained from application of other existing methodologies.

4.1 Methodology Overview

Calendar year 2008 and 2011 inventories were prepared for each airport (APA, RVS, and SMO) using the methods and data sources represented by the flow chart depicted in Figure 6, which presents a schematic overview of the methodology and data sources. The key steps and public data sources used are outlined below.

1. The engine fuel consumption rate data collected for this project were converted to BSFC rates and then extrapolated to include all unique engines found in the underlying activity databases.

2. The ATADS data provided the total airport operations by calendar year.

3. The Traffic Flow Management System Counts (TFMSC) database provided the distribution of piston-powered aircraft operations at each airport.

4. FAA's Type Certificate Data Sheets (TCDS) provided the engine characteristics data of piston-powered aircraft.

5. FAA's U.S. registration counts provided the distribution of engines within a given piston-powered aircraft.

6. The FAA's General Aviation and Air Taxi Activity Survey provided the fraction of civilian operations coming from piston-powered aircraft; note that these data are reported at the national and regional level, but are not airport specific. Use of the regional values is applied in this methodology.

Additional details of the development of the inventory methods are contained in Section 4.2.

Finally, Table 9 provides a comparative summary of the inventory modeling parameters for this analysis versus those used in the 2008 NEI and the ICF SMO study which are also described in Section 4.2.

Figure 6
Flow Chart of Airport Inventory Development Methods

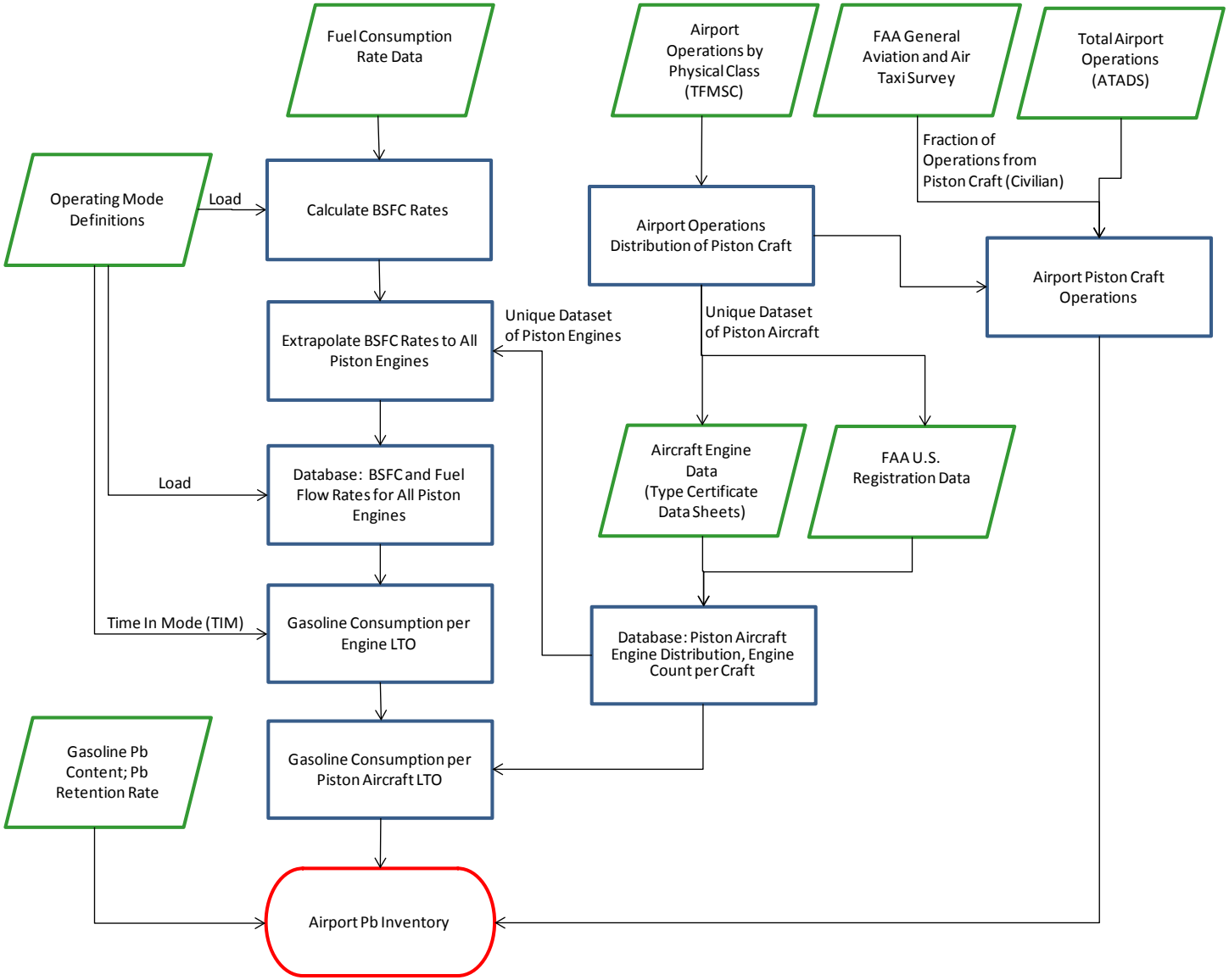

Table 9
Comparative Summary of Methodologies

Parameter	Current Study	2008 NEI	ICF SMO
Aircraft Total Operations	FAA's Air Traffic Activity Data System (ATADS)	FAA's ATADS and Terminal Area Forecast (TAF)	Airport-supplied data
Aircraft Fleet Operations	FAA's Traffic Flow Management System Counts (TFMSC); FAA's General Aviation and Air Taxi Activity Survey	FAA's General Aviation and Air Taxi Activity Survey	Airport-supplied separate fixed-wing and rotorcraft operations
Airframe and Engine Technology	FAA's Type Certificate Data Sheets (TCDS) and U.S. registration counts	None	None
Engine Fuel Consumption Rates	Expanded underlying database to 29 engines; converted fuel consumption rates to BSFC; extrapolated rates to all engines evaluated	Simple average over 7 EDMS engines; separate averages for single- and twin-engine fixed-wing craft	Simple average over 7 EDMS engines; separate averages for single- and twin-engine fixed-wing craft; separate average for rotorcraft
Modal Load Assumptions	EDMS load assumptions; specific approach for run-up	EDMS load assumptions	EDMS load assumptions; specific approach for run-up; specific approach for landing
Time in Mode (TIM)	Used FAA/EPA default and ICF SMO study values	FAA/EPA defaults	SMO-specific assumptions
Lead Concentration in Fuels	2.12 g/gal	2.12 g/gal	2.12 g/gal
Lead Retention Rate	5%	5%	5%

4.2 Required Inputs and Assumptions

Described below are the inputs and modeling assumptions used in the inventory analysis for the three airports of APA, RVS, and SMO in 2008 and 2011. This discussion is divided into the following topics:

- Fuel consumption rates;
- Piston aircraft and engine distributions;
- TIM assumptions;
- Total operations;
- Piston operations; and
- Remaining assumptions.

Fuel Consumption Rates – The fuel consumption rates historically utilized by EPA are based on FAA EDMS data, representing a limited piston-engine database of eight piston engines, of which seven were used by EPA for inventory calculations. These data were augmented with the additional available data identified in this course of this project (Switzerland Federal Office of Civil Aviation 2007, Atwood 2007, Atwood 2009, Atwood and Camirales 2004, Atwood and Knopp 1999, Coordinating Research Council 2010). In aggregate, for the inventory methods described herein, a total of 29 unique engines were identified with suitable fuel consumption data for inventory development, of which 28 were ultimately used in the inventory calculations.

In the inventory analysis, separate fuel consumption rates were estimated for the following five individual engine operation modes:

- Idle/taxi;
- Takeoff;
- Climb-out;
- Approach; and
- Run-up.

Of these modes, the first four are the standard modes preexisting within the EDMS model, and those on which historical airport inventory estimates have been typically based. A greater amount of fuel consumption data exists for the four standard modes. The fifth mode, run-up, is a more recent addition to the inventory methods (it was included in the ICF study but not the 2008 NEI) and is also included in this analysis. As described below, the fuel rate methodology of run-up mode was handled distinctly based on a lesser amount of data available.

The fuel consumption rate method for the four standard modes was further refined for this analysis by converting the fuel rates (i.e., rates reported in the units of mass per unit time) to BSFC rates (i.e., rates reported in terms of mass of fuel consumed per unit work done by the engine). BSFC is a measure of engine efficiency, and is a suitable metric for extrapolating fuel consumption rates from one engine to another, with the implicit assumption that the efficiency of the engine (by operation mode) is equivalent across engines of similar technology.

$$BSFC_{Mode}\left(\frac{lb}{hp-hr}\right)=\frac{Fuel\ Rate_{Mode}\left(\frac{lb}{hr}\right)}{Load_{Mode}\times Rated\ Power(hp)}$$

Load, as defined in this equation, represents the fraction of engine rated power applied at each mode, and load times rated power equals the power output of each mode. Loads for fixed-wing aircraft were assigned as 7, 45, 85, and 100% for idle/taxi, approach, climb-out and takeoff, respectively. Two key points as related to the load assignment of each mode should be noted.

- The assumed 7% load for idle/taxi operation is not exact (whereas the loads assumed for the other three modes are explicitly stated in the test procedures on which the data are based). Fuel consumption testing of idle/taxi was generally completed at "manufacturer recommended settings" and the individual load point or power output may not be reported. Because the load point is variable for the idle/taxi mode, this mode exhibits the greatest variation within the fuel consumption data assembled.

- Load assumptions for rotorcraft differ from fixed-wing aircraft. The Swiss FOCA recommends loads of 20, 60, and 95% for idle/taxi, approach and climb-out/ takeoff, respectively (Switzerland Federal Office of Civil Association 2009). Note that rotorcraft were not present in the activity data used in this inventory analysis.

The BSFC data for 29 engines were organized by the following technology groups:

- 4-stroke horizontal spark ignition (SI) engine, carbureted (8 engines);
- 4-stroke horizontal SI engine, fuel injected (8 engines);
- 4-stroke horizontal SI engine, turbocharged (9 engines);
- 4-stroke radial SI engine (2 engines);
- 2-stroke horizontal SI engine (1 engine); and
- 4-stroke compression ignition (CI) engine (1 engine).

The separation of 4-stroke horizontal engines into three groups was based on a statistical assessment finding that the data from at least one mode of operation were significantly distinct at the 90% confidence level. Generally speaking, the order of efficiency observed is fuel injected > carbureted > turbocharged, which matches engineering expectations. These three engine technologies represent the vast majority of activity at each airport. Of the remaining three technology groups, 2-stroke horizontal SI engines were not found in the activity data, so this engine type did not factor into the inventory analysis; otherwise, both radial SI and CI engines were present in the activity data.

The BSFC data were grouped by technology, manufacturer, and model number. With respect to the model number, suffix letters were not included. For example, the horizontal carbureted Lycoming 320 engine (i.e., Lycoming O-320) has been manufactured with approximately 60 distinct engine models when suffix letters are included (e.g., Lycoming O-320-B1A). Within this analysis, only the base model number was considered and suffix letters were not distinguished in the matching of aircraft to BSFC rates.

For 8 of the 29 engines (3 horizontal SI fuel injected and five horizontal SI turbocharged), fuel consumption rates were collected for only two of the four modes (takeoff and climb-out); the two modes of approach and idle/taxi were not recorded. For these eight engines, the BSFC values for approach and idle/taxi were scaled from the takeoff BSFC rate using the average BSFC ratios calculated from the set of engines within the same technology group that were tested at all four modes. The ratios of 1.015 (idle/taxi-to-takeoff) and 0.971 (approach-to-takeoff) were used for the horizontal fuel injected SI engines, and the ratios of 1.326 (idle/taxi-to-takeoff) and 0.978 (approach-to-takeoff0 were used for the horizontal turbocharged SI engines.

Table 10 shows the final compilation of "gasoline" BSFC data by technology and unique aircraft engine (defined by technology, manufacturer and model number). Key notes on these data are summarized below.

- A "default" value is estimated for each technology group with more than one engine represented. The default value is the average for all engines in that technology group.

- Instances where modal BSFC rates for approach and idle/taxi data include values extrapolated from ratios (as noted above) are shown in bold type in Table 10.

- The BSFC for the horizontal CI engines is intentionally listed as zero, which is how these are treated in the inventory calculations. Because the CI engines are fueled with either diesel or jet fuel, these piston engines do not consume gasoline and produce no lead emissions.

- In reviewing these data, it is pertinent to note that aircraft are engineered for maximum efficiency (i.e., lowest BSFC) at cruise (approximately 65% load). Therefore, engineering expectation is that BSFC would reach a minimum somewhere between the approach and climb-out modes.

Within the activity data collected (described further below), 147 unique piston engines were found to be operating at the three airports in either calendar year. A distinct engine in this case is defined by the unique combination of the following identifiers:

- Technology group (as defined in Table 10);
- Manufacturer;
- Model number (excluding suffix letters); and
- Engine rating (HP).

Table 10
BSFC Data for Fixed-Wing Aircraft Operation Modes

Technology Group	Manufacturer & Model Number	Test Engines	Gasoline BSFC (lb/hp-hr)			
			Takeoff	Climb-out	Approach	Taxi/Idle
4-Stroke Horizontal CI[1]	All	n/a	0.000	0.000	0.000	0.000
4-Stroke Horizontal SI, Carbureted	Default	8	0.514	0.528	0.557	1.370
	Lycoming 320	2	0.561	0.511	0.627	0.938
	Lycoming 360	1	0.529	0.529	0.530	1.008
	Lycoming 540	1	0.560	0.556	0.496	0.772
	Rotax 912	2	0.401	0.373	0.402	1.134
	Continental 200	1	0.452	0.532	0.567	1.186
	Continental 6-285	1	0.537	0.685	0.650	3.614
4-Stroke Horizontal SI, Fuel Injection	Default	8	0.518	0.490	**0.503**	**0.902**
	Lycoming 320	2	0.535	0.459	**0.503**	**0.781**
	Lycoming 360	1	0.540	0.495	0.547	0.793
	Lycoming 540	2	0.490	0.501	**0.479**	**0.953**
	Continental 360	1	0.572	0.469	0.452	0.643
	Continental 550	2	0.493	0.519	**0.533**	**1.158**
4-Stroke Horizontal SI, Turbocharged	Default	9	0.674	0.635	**0.659**	**1.531**
	Lycoming 540	3	0.777	0.725	**0.728**	**1.543**
	Rotax 914	1	0.501	0.458	0.448	1.792
	Continental 360	1	0.592	0.519	0.602	0.730
	Continental 520	1	0.659	0.661	0.760	2.127
	Continental 550	3	0.660	0.634	**0.646**	**1.500**
4-Stroke Radial SI	Default[2]	2	1.325	0.682	0.521	1.270
	Wright 1820	1	1.166	1.014	0.718	1.270
2-Stroke Horizontal SI	Rotax 582	1	0.495	0.526	0.441	1.071

Note: Instances where modal BSFC rates for approach and idle/taxi data include values extrapolated from ratios (as noted above) are shown in **bold** type.
[1] Compression ignition (CI) piston engines do not operate on gasoline.
[2] Within the database, there was one radial engine with an undisclosed manufacturer and model number. This engine was included in the radial SI engine default value reported but is not listed as a separate engine.
Sources: FAA EDMS data, supplemented by data from Switzerland Federal Office of Civil Aviation 2007, Atwood 2007, Atwood 2009, Atwood and Camirales 2004, Atwood and Knopp 1999, Coordinating Research Council 2010.

The assignment of BSFC rates to each of the 147 engines was completed as follows. If the technology group, manufacturer, and model number matched the value listed in Table 10, the BSFC for that specific engine was assigned; if no match was found in Table 10, the "default" for that technology group was assigned. Finally, the engine rating and assumed load by mode were used to convert the BSFC rate back into a fuel consumption rate (rates reported in the units of lb per hour) using the equation below.

$$Fuel\ Rate_{Mode}\left(\frac{lb}{hr}\right) = BSFC_{Mode}\left(\frac{lb}{hp-hr}\right) \times Load_{Mode} \times Rated\ Power(hp)$$

The mass fuel rate above was then used in the inventory calculations. Overall, the procedure followed assigns rates to engines based on BSFC and then factors in the engine rating to determine the final fuel consumption rate (reported in the units of mass per unit time).

Using the Lycoming horizontal fuel-injected 540 engine as an example (i.e., Lycoming IO-540), there were eight distinct engine ratings for this engine model found in the activity database (ranging from 230 to 380 HP). From Table 10, the BSFC assigned to this engine (for all eight engine ratings) was 0.490, 0.501, 0.479, and 0.556 lb/hp-hr for takeoff, climb-out, approach, and idle/taxi modes, respectively. The application of the equation above yields the fuel consumption rates shown in Table 11.

Table 11
Estimated Fuel Consumption Rates for the Lycoming IO-540 Engine

Engine Rating (HP)	Fuel Consumption Rate (lb/hr)			
	Takeoff	Climb-out	Approach	Taxi/Idle
230	112.6	98.0	49.6	15.3
235	115.0	100.1	50.6	15.7
250	122.4	106.5	53.9	16.7
260	127.3	110.8	56.0	17.3
290	142.0	123.6	62.5	19.3
300	146.9	127.8	64.6	20.0
350	171.3	149.1	75.4	23.3
380	186.0	161.9	81.9	25.3

Lastly, the fuel consumption rate for the fifth mode of operation—i.e., the run-up mode was defined. The run-up mode was included in the ICF SMO study; however, the 2008 NEI, and previous EPA efforts omitted it. The run-up is performed as part of the standard operating procedures prior to take off in which instrument checks are performed at a moderate fuel flow rate.

The fuel consumption rate for the run-up mode in this study was defined as a percentage of the maximum fuel consumption rate (i.e., at maximum load and power reported in the units of mass per unit time). Four operations manuals (Lycoming Engines 1997, 2008 and undated; Continental Motors 2011) were examined to determine the manufacturer-suggested run-up procedures, and reported fuel rate curves from those manuals were reviewed to estimate the fuel consumption rates at run-up conditions and at maximum load/power. From these manuals, run-up rates were identified for seven distinct engine models, with individual values ranging from 43 to 68% of the maximum fuel consumption rate. In this study, the average run-up rate from the seven engine models of 52% of the maximum fuel consumption rate was used to represent the run-up mode for all engines in this study.

Piston Aircraft and Engine Distributions – EPA's inventory approach simply averages EDMS engine-specific fuel consumption rates to calculate single-engine and twin-engine fuel consumption rates; in total, seven engines were used to derive these averages in both the 2008 NEI and the ICF study. This approach is potentially problematic, in part because it fails to account for the underlying proportions of these engines in the fleet. The variation in fuel flow rates across engine models is significant, and even significant within the same engine model, depending on engine power rating, as shown in Table 11 for the Lycoming IO-540.

The FAA's TFMSC (Traffic Flow Management System Counts) database (*https://aspm.faa.gov/TFMS/sys/default.asp*) was used in this inventory evaluation for airport-specific operations information, specifically to determine the distribution of piston-powered LTOs by individual aircraft. TFMSC operations are reported based on pilot-filed flight plans and RADAR detections restricted to the subset of flights that fly under IFR. Because reporting is not triggered for each operation at the airport, the distribution of piston-powered aircraft is normalized to sum to 1 with the assumption that the TFMSC captured data are representative of the fleet as whole. Operations data are differentiated by physical class (i.e., piston, turbine and jet) and user class (i.e., air taxi, general aviation, and military). Aircraft are classified according to FAA/ICAO designators (e.g., "PA28 - Piper Cherokee") as found on the FAA database (*https://www.faa.gov/air_traffic/publications/atpubs/CNT/5-2.htm*).

The quantity of piston operations used to estimate the aircraft distribution at each airport is summarized in Table 12. Within these data, 169 distinct aircraft were present. Separate aircraft operation profiles were identified for civilian and military user classes.

Table 12
TFMSC Piston-Powered Operations Used to Determine Aircraft Distributions

Year	APA	RVS	SMO
2008	8,769	12,740	13,541
2011	7,159	6,008	8,170

Source: FAA's Traffic Flow Management System Counts database (https://aspm.faa.gov/TFMS/sys/default.asp)

The engine distribution for each FAA/ICAO designated aircraft type was then determined from the FAA's registration data (*http://registry.faa.gov/aircraftinquiry/AcftRef_Inquiry.aspx)* and the agency's TCDS database (*http://www.airweb.faa.gov/Regulatory_and_Guidance_Library/rgMakeModel.nsf/MainFrame?OpenFrameSet*). From these two resources, the number of aircraft models represented (for each FAA/ICAO designation) and the U.S. total registration counts by model were collected. The TCDS provided the engine manufacturer, technology, model number, and engine rating data for each aircraft model. Technology distinctions of the engines were simplified to the six cases shown in Table 10 (i.e., those with distinct BSFC rates). Model numbers were simplified by excluding suffix letters. Using this engine categorization scheme, a total of 147 unique engines were found to exist for the set of aircraft extracted from the TFMSC database. Each engine is defined by the unique combination of the following identifiers:

- Technology group (as defined in Table 10);
- Manufacturer;
- Model number (excluding suffix letters); and
- Engine rating (HP).

Finally, the normalized engine distribution was then calculated for each FAA/ICAO designated aircraft type. The engine distribution represents the fraction of the 147 unique engines present in each of the 169 unique aircraft. It should again be noted that in the collection and processing of these activity data, there were no rotorcraft models present at the three airports in the two years of TFMSC data examined, although helicopter activity occurs at all three airports. This may be a limitation of the protocol by which the TFMSC data are recorded, as noted above. As such, the inventory results of this analysis are based entirely on the set of fixed-winged aircraft represented by these data.

TIM Assumptions – TIM data for individual airports are not generally in the public domain, and EPA's two distinct TIM assumptions were largely used with minor modifications as described below.

- The FAA/EPA default TIM assumption for piston-powered aircraft covers the four primary modes of operation (idle/taxi, takeoff, climb-out, and approach). For use in this inventory analysis, the run-up mode (i.e., a fifth mode) was added to the default based on the run-up time estimated in the ICF SMO study. The FAA/EPA defaults with the added fifth mode were used at all three airports.

- The ICF study's TIM data for SMO were also used as an alternate assumption (for SMO only). It should be noted, however, that ICF included a distinct "landing" mode that erroneously assumed engine operation at 100% load during landing; this was not used here, and the time allocated to "landing" by ICF was incorporated into the idle/taxi time associated with aircraft arrival for use in this effort.

Table 13 summarizes Times reflect a complete operational cycle. Note that the maximum altitudes of the aloft modes (i.e., climb-out and approach) defined by the FAA/EPA default and ICF SMO study TIM assumptions differ. This accounts for a significant portion of the TIM differences of those two modes, complicating their direct comparison.

Table 13
Time-In-Mode Assumptions (Minutes)

Mode	FAA/EPA Default	ICF SMO Study
Idle/Taxi (Departure)	12.00	5.07
Run-Up	1.48[a]	1.48
Takeoff	0.30	0.27
Climb-out	5.00	1.30
Approach	6.00	1.07
Idle/Taxi (Arrival)	4.00	2.53[b]

[a] The EPA/FAA default does not include the run-up mode; however, for this analysis the run-up mode was added for completeness using the ICF SMO Study value. The time spent in the run-up procedures mode is not airport specific.
[b] The "landing" mode of the ICF SMO study was incorporated into the arrival idle/taxi mode reported here.

Total Operations – The Air Traffic Activity Data System contains the official National Airspace System (NAS) air traffic operations data available for public release; ATADS was the source of total aircraft operations data at each airport for inventory development. The ATADS is a database of air traffic operations from towered facilities managed by the FAA and includes both IFR (instrument flight rules) and VFR (visual flight rules) itinerant operations as well as local operations. Table 14 summarizes ATADS data for years 2008 and 2011. Note that tabulated operations include both landings and takeoffs.

For comparative purposes, Table 15 summarizes the total operations used by the 2008 NEI for the three airports of interest. These data originate from the FAA's Terminal Area Forecast (TAF), which includes historical data as well as forecasts. The data in Table 15 are the historic values reported for 2008 in which ATADS is the source of operations activity for towered facilities reported in the TAF. The TAF includes both towered and non-towered facilities and is used as the source of total operations for the NEI because the NEI estimates airport emission inventories from both towered and non-towered facilities. Given that the TAF data purportedly originate from ATADS for these three airports, the data generally agree (within a few percent), but the agreement is not exact. The source of the discrepancy between total operations reported by ATADS and TAF for matched facilities and historical periods is not known.

Table 14
Total Aircraft Operations by Airport and Year

Year	Facility	Air Carrier (Itinerant)	Air Taxi (Itinerant)	General Aviation (Itinerant)	Military (Local & Itinerant)	Civil (Local)[1]	Total Operations
2008	APA	3	44,376	129,412	3,524	143,634	320,949
	RVS	2,735	1,123	136,382	2,281	191,750	334,271
	SMO	0	9,966	68,399	237	45,912	124,514
2011	APA	68	36,191	126,112	7,195	125,025	294,591
	RVS	5	1,943	90,591	200	106,673	199,412
	SMO	0	6,739	62,938	217	40,875	110,769

[1] In 2008, the FAA changed the labeling of this category from General Aviation (Local) to Civil (Local). This was simply a labeling change—the types of operations covered did not change.
Source: FAA Air Traffic Activity Data System (ATADS)

Table 15
2008 NEI Total Operations by Airport and Year

Year	Facility	Air Carrier (Itinerant)	Air Taxi (Itinerant)	General Aviation (Itinerant)	Military[1] (Local & Itinerant)	Total Operations
2008	APA	10	46,722	279,778	3,542	330,052
	RVS	1,942	1,142	335,255	2,220	340,559
	SMO	6	10,354	113,780	274	124,414

[1] The NEI assumes that all military operations are turboprop or jet.
Source: U.S. EPA 2008 National Emissions Inventory (NEI)

Piston Operations – For this analysis, the two data sources outlined below were used to quantify the piston-powered aircraft share of total airport operations.

- The FAA's annual General Aviation and Part 135 Activity Surveys (http://www.faa.gov/data_research/aviation_data_statistics/general_aviation/) were used to define the fraction of civilian aircraft operations coming from piston-powered craft. The 2008 survey of "landings" activity was used for 2008, and the 2010 survey of landings was used for 2011 since the 2011 survey results had not been published at the time of this effort. Notably, these data are not airport-specific.

- The FAA's TFMSC database described above as the resource used for piston aircraft distribution data was used to define the piston LTO fraction of military operations at each airport. These data are airport specific. It should be noted that

the TFMSC database was also evaluated for potential use in defining the piston operation fraction of civilian aircraft. Using SMO as test case, TFMSC operations showed a 33% share for piston-powered craft at SMO; however, the airport-specific data used in the ICF study showed an 85% LTO share for piston-powered aircraft. As such, it is believed that the protocol by which the TFMSC data are captured undercounts piston aircraft relative to similar counts for jets and turboprops. Excluding TFMSC resulted in no other airport-specific data source, and the General Aviation and Part 135 Activity Survey was used as an alternate method for estimating the piston fraction of civilian operations.

Table 16 summarizes the survey data used for civilian aircraft. The survey data for "landings" were taken from Table 2.4 of the FAA's annual General Aviation and Part 135 Activity Surveys and the fraction of piston-powered landings was calculated and reported in Table 16 for each region and the U.S. total. The regional results were used in this analysis, with APA, RVS, and SMO represented by Northwest Mountain, South Western, and Western-Pacific regions, respectively.

Table 17 summarizes the fraction of military operations coming from piston-powered aircraft at each airport using the TFMSC database.

Table 16
Fraction of General Aviation and Air Taxi Landings from Piston-Powered Aircraft

FAA Region	2008 Survey	2010 Survey
Alaskan	75.9%	82.9%
Central	62.6%	76.0%
Eastern	70.3%	64.6%
Great Lakes	79.9%	82.0%
New England	72.4%	73.6%
Northwest Mountain	66.5%	72.5%
Southern	66.7%	73.2%
South Western	44.8%	41.4%
Western-Pacific	70.6%	63.4%
Total U.S.	65.7%	66.1%

Source: Table 2.4 of FAA's annual General Aviation and Part 135 Activity Surveys, available at *http://www.faa.gov/data_research/aviation_data_statistics/general_aviation/*.

Table 17
Fraction of Military Operations from Piston-Powered Aircraft

Year	APA	RVS	SMO
2008	6.8%	24.4%	40.9%
2011	3.7%	26.1%	71.0%

Source: FAA Traffic Flow Management System Counts database (https://aspm.faa.gov/TFMS/sys/)

For comparative purposes, the 2008 NEI also used the 2008 General Aviation and Part 135 Activity Survey for estimating the fraction of civilian operations coming from piston-powered craft. The NEI assumes that all military operations are turboprop or jet. However, the NEI used hours of operation from the survey data as the surrogate for estimating the piston-engine aircraft proportions of 72.5% for general aviation and 23.1% for air taxi. The use of hours allowed for separate estimated fractions for general aviation and air taxi; however, only national average results are reported. The use of hours versus landings appears to have similar proportions.

For comparison to the ICF SMO study, the airport-provided operations data by physical class in which 85% of operations at SMO in 2008 were estimated from piston-powered aircraft. This piston share (85%) is somewhat greater than that observed in the survey values reported for the Western-Pacific region of 70.6% and 63.4% in 2008 and 2010, respectively. In the absence of airport-specific data, the specification of the fraction of operations from piston-powered aircraft remains a significant source of uncertainty and error in this analysis.

Remaining Modeling Assumptions – Lastly, the emission inventory method requires specifying the lead retention rate, gasoline density, and lead content of aviation gasoline. For each of these three assumptions, the values used by EPA in the NEI and ICF efforts were retained in this analysis, as follows:

- Lead retention rate = 5%;
- Aviation gasoline density (g/gal) = 2,726 (or 6.01 lb/gal); and
- Lead content in aviation gasoline (g/gal) = 2.12.

In addition, given the lack of available data, no effort was made to quantify non-exhaust-related Pb emissions.

4.3 Results

Calendar year 2008 and 2011 inventories were prepared for each airport using the input data and assumptions described above. A complete summary of modeling results obtained using the refined methodology is presented in Tables 18 and 19 for 2008 and 2011, respectively. The modeling parameters of operations (total and piston), percent of

Table 18
Calendar Year 2008 Inventory Results

Modeling Result	APA (Default TIM)	RVS (Default TIM)	SMO (Default TIM)	SMO (ICF TIM)
Operations, Total	320,950	334,272	124,514	124,514
Operations, Piston Craft	211,200	149,278	87,802	87,802
Multi-Engine Piston Operations (% of Piston Total)	47%	14%	13%	13%
Mean Piston-Engine Rating (HP)	283	204	226	226
Gasoline Consumption (Gal./Piston Operation)	4.15	2.08	2.23	0.81
Pb Emissions (g/Piston Operation)	8.35	4.19	4.49	1.63
Pb Inventory (Tons/Year)	1.95	0.69	0.43	0.16

Table 19
Calendar Year 2011 Inventory Results

Modeling Result	APA (Default TIM)	RVS (Default TIM)	SMO (Default TIM)	SMO (ICF TIM)
Operations, Total	294,592	199,412	110,770	110,770
Operations, Piston Craft	208,582	82,616	70,208	70,208
Multi-Engine Piston Operations (% of Piston Total)	41%	23%	15%	15%
Mean Piston-Engine Rating (HP)	283	240	239	239
Gasoline Consumption (Gal./Piston Operations)	3.80	2.63	2.42	0.88
Pb Emissions (g/Piston Operations)	7.64	5.29	4.87	1.76
Pb Inventory (Tons/Year)	1.76	0.48	0.38	0.14

multi-engine aircraft, mean engine rating, and mean gasoline consumption rate are shown to assist in understanding the differences in inventory estimates. As shown, the 2011 inventory results are lower at each airport than the 2008 inventory results owing in large part to the reduction in piston-engine aircraft activity. Other observations are outlined below.

- The refined methodology separates out civilian operation from military, both of which are included in the totals shown; however, the military contribution was negligible relative to the total Pb inventory at these three airports.

- The multi-engine piston operations fractions are due to the TFMSC-based aircraft distribution data. The General Aviation and Part 135 Activity Surveys show a national average fraction of 12% and 10% in 2008 and 2010, respectively. As shown, the multi-engine fractions observed in the TFMSC database are generally above the national average at each of the airports.

- The differences in the two sets of TIM assumptions, shown in Table 13, at SMO lead to inventories that differ by approximately a factor of three. A significant portion of this difference is from differences in maximum altitude assumed for the aloft modes (i.e., climb-out and approach) and this confounds the direct comparison of these results. However, the total taxi/idle time on the ground can be directly compared and is about 50 percent less in the SMO-specific data indicating that airport-specific TIM can be a key modeling variable.

Calendar year 2008 results for these three airports are shown in Table 20. The 2008 NEI inventory results come from the EPA's FTP site (*ftp://ftp.epa.gov*) and the remaining data come from ERG (2011). The 2008 NEI results do not include the run-up mode, which would increase the inventory results by approximately 10%. Values for the ICF Study were derived from ICF International and T&B Systems (2010). Also shown in Table 20 is the ratio of these results to those obtained using the refined methodology. As the ratios shown in Table 20 indicate, the refined methodology results in substantially greater estimates of Pb emissions at APA and somewhat greater Pb emissions at SMO. Conversely, the refined methodology yields substantially lower Pb emissions at RVS.

Table 20
Calendar Year 2008 Inventory Results

Modeling Result	APA (2008 NEI)[1]	RVS (2008 NEI)[1]	SMO (2008 NEI)[1]	SMO (ICF Study)[2]
Operations, Total	332,348	340,558	125,986	124,544
Operations, Piston Craft	214,938	243,322	85,970	105,696
Multi-Engine Piston Operations (% of Piston Total)	10%			N/D[a]
Gasoline Consumption (Gal./Piston Operation)	1.73			0.56
Pb Emissions (g/Piston Operation)	3.67			1.12
Pb Inventory (Tons/Year)	0.73	1.17	0.33	0.13
Ratio to Refined Methodology Result	0.37	1.70	0.77	0.81

[a] No data; based on results reported, multi-engine LTOs were less than 10 percent of the piston LTO total.
[1] Source: 2008 National Emission Inventory, *ftp://ftp.epa.gov*, and ERG (2011)
[2] Source: ICF International and T&B Systems (2010)

Outlined below are key observations from comparing the EPA and ICF results with results from the refined methodology.

- The refined methodology generally estimates greater fuel consumption per operation. This is due in large part to the multi-engine fraction and other fleet characteristics inherent in the TFMSC data used.

- The higher Pb emission estimates for APA and SMO with the refined methodology are due to high fuel consumption estimates and the assumed characteristics of the piston-engine aircraft fleet.

- The lower Pb emission estimates for RVS using the refined methodology are due to a much smaller fraction of total operations estimated from piston-engine aircraft.

###

5. AIRBORNE LEAD AND AIRCRAFT ACTIVITY DATA COLLECTION AT AIRPORTS

During this phase of the project, field studies were conducted at three airports to generate data sets of airborne PM-Pb concentrations to evaluate the emission inventory methodology through dispersion modeling. Detailed aircraft activity data were collected to allow for the development of spatially and temporally resolved emission inventories for each of the three airports. While such fine-grained activity data are not routinely available, this approach was needed for a robust evaluation of emission inventory methodology and sensitivity studies to determine the data collection elements that are most important for an accurate inventory.

In order to select the three airports at which field studies were to be performed, general aviation airports nationwide were systematically evaluated for consideration as a field study site. Desired attributes were identified and criteria were developed to screen and ultimately rank candidate airports. Desired attributes included, but were not limited to, a large Pb emissions load (based on the 2008 NEI), a large share of non-carrier operations and specifically a large share of piston-engine aircraft activity, and favorable meteorology (high wind direction persistence with few calms). A prioritized list of airports was generated and airport operators were contacted to determine their willingness to participate. Listed below are the three airports selected for field studies and the dates the studies were performed.

- Richard Lloyd Jones Jr. (RVS), Tulsa, OK; March 27 to April 28, 2013
- Centennial Airport (APA), Englewood, CO; May 15, 2013 to June 10, 2013
- Santa Monica Airport (SMO), Santa Monica, CA; July 3, 2013 to July 30, 2013

These airports have distinctive characteristics. RVS and APA are among the busiest general aviation airports nationwide and have relatively large footprints with multiple runways. However, the spatial distribution of run-up and LTO activity patterns are quite different because of the runway layouts, and wind directions were more variable at APA than RVS. SMO is a much smaller airport but with concentrated run-up and LTO activity patterns and a history of being the subject of special PM-Pb studies.

5.1 Data Collection Overview

As indicated above, the field studies—each nominally one month in duration—were conducted at each of the three airports by staff from Washington University in St. Louis (WUSTL). A consistent data collection strategy was used across the three field studies, and the data collection plan was reviewed by the Project Panel prior to the first deployment. In this section, generic features of the data collection are summarized; this is followed by a summary for each airport that includes the airport-specific features and select results.

5.1.1 Aircraft Activity Data Collection

Detailed aircraft activity data were collected to inform the development of a spatially and temporally resolved emissions inventory for the model-to-monitor comparisons. These data have been processed and compiled into databases (e.g., MS Excel spreadsheets). The key data collection elements are summarized below.

- Landing and Takeoff Operations (LTOs) – Daily PM-Pb sampling was conducted during the 12-hour daytime period with highest aircraft activity. Video cameras were used to continuously record LTOs during each PM-Pb sampling event. The videos were played back to document takeoff, landing, and touch-and-go operations by runway at 10-minute intervals and these data were rolled up to one-hour periods. LTO data were collected for all fixed-wing aircraft at each airport and at SMO the piston-engine aircraft fraction was also directly measured. At RVS and APA, the piston-engine aircraft fraction was not directly measured from the video data because aircraft in the video images were often too small to be conclusively identified as either piston engine or jet.

- Aircraft Fleet Inventory – LTOs were photographed for 30 hours at each airport. The data collection schedule was generated using a quasi-random process to populate a 2D matrix with dimensions of time of day and day of week (Weekdays / Saturdays / Sundays). The matrix was weighted towards data collection during hours with higher activity and to ensure adequate data collection on weekends. Photographs were reviewed to develop a time-stamped inventory of LTO activities by tail ID. The FAA Registry (*http://registry.faa.gov/aircraftinquiry/*) was used to identify the aircraft and engine characteristics for each recorded tail ID. Data were collected for all aircraft, not just piston-engine aircraft, to provide information about the distribution of activities between piston-engine airplanes and jets. Some aircraft were observed multiple times over the 30 hours of data collection. Given the objective to inventory the fleet from an operations perspective, each observation was an independent entry into the database. Each database record includes the observation time stamp; aircraft type, manufacturer, model, year, and number of engines; engine type, manufacturer, model, and horsepower; and number of times the aircraft was identified in the one-hour observation period and in the overall data set. Tail ID numbers are decoupled from the final database.

- Time in Mode for Run-up – Run-up operations were manually observed for 15 hours at each airport. Data collection was scheduled to capture a range of conditions (time of day, day of week) and included the time aircraft spent in a run-up area (visual observation), the duration of the magneto test (audible changes in engine noise during run-up), and the aircraft tail ID. Some planes bypassed the run-up area prior to takeoff and such instances were recorded. In some cases, the magneto test duration could not be determined because of confounding sources of noise. Each record in the database includes the data collection hour, total run-up time, magneto test time, and the aircraft attributes listed above for the aircraft fleet inventory. Tail ID numbers are decoupled from the final database.

- Time in Mode for Other Activities – Additional piston-engine aircraft activities such as taxiing, takeoffs, and landings were manually observed for 15 hours at each airport. Data collection was scheduled to capture a range of conditions (time of day, day of week). Observation points were chosen to maximize viewing of the entire airport footprint. Activities were tracked by aircraft and recorded by runway or taxiway. For example, a taxi-back would consist of the following data: landing time (time on runway between wheels down and turning onto taxiway); time taxiing and idling on each taxiway; and takeoff time (time on runway between starting rollout and wheels-up). Approach and climb-out times could not be adequately captured because of the difficulty in establishing aloft locations for the start of approach and end of climb-out. Instead, wheels-up and wheels-down locations on the runways were recorded to inform the development of TIM estimates for climb-out and approach and to spatially allocate runway emissions. TIM for touch-and-go operations was recorded as the time between wheels down for the landing portion and wheels-up for the takeoff portion. Each record in the database includes a plane identifier (arbitrary), activity (e.g., landing, takeoff, taxiing, idling), and location (e.g., runway ID, taxiway ID).

Activity data processing was conducted in coordination with the Sierra Research and KB Environmental Services staff. TIM data were processed by the WUSTL field operator (Neil Feinberg) with QA/QC performed by the WUSTL lead investigator (Jay Turner). Most of the LTO video and fleet inventory photographs were processed by other WUSTL staff and in these cases initial QA/QC was performed by the WUSTL field operator with additional QA/QC by the WUSTL lead investigator.

5.1.2 Airborne PM-Pb Data Collection

Airborne PM samples were collected daily and analyzed for Pb. At each airport, four PM sampling sites were selected based on the location of piston-engine aircraft activities, historical winds data, and Pb concentration fields generated from preliminary dispersion modeling. PM-Pb hot spots were predicted downwind of run-up areas and such locations were given high priority. Relatively flat terrain was desired, and it was necessary to stay clear of FAA-restricted areas; for SMO, the siting of samplers in previous studies was also considered. At each airport, the four sampling sites included two “primary” sites and two “secondary” sites. The primary sites were a location downwind of a run-up/takeoff area for prevailing winds, and a location chosen to capture background PM-Pb levels for

prevailing winds. Characteristics for the two secondary sites are described in the airport-specific summaries. Up to four PM samplers were operated during each sampling event. A $PM_{2.5}$ sampler was always operated at each of the two primary sites (except for collocated TSP data collection events to establish TSP-Pb measurement precision) and the remaining two PM samplers were used in one of the three configurations: (i) collocated $PM_{2.5}$ sampling at the primary sites (to establish $PM_{2.5}$-Pb measurement precision); (ii) TSP sampling at the primary sites; or (iii) $PM_{2.5}$ sampling at the secondary sites.

PM samples were collected using Model PQ100 portable samplers (BGI, Waltham, MA). The PQ100 is an EPA Federal Reference Method (FRM) for PM_{10} sampling; for this study, the samplers were used with BGI Very Sharp Cut Cyclones (VSCC) to achieve $PM_{2.5}$ cutpoints. A louvered inlet with PM_{10} impactor—the standard configuration for ambient PM_{10} sampling—was used upstream of the $PM_{2.5}$ cyclone. TSP samples were collected using PQ100 samplers with BGI TSP inlets. The TSP inlets have been previously characterized (Kenny et al. 2005). The design flow rate is 16.7 liters per minute (LPM) for these various inlets. Figure 7 shows the BGI samplers deployed at the APA Central monitoring site with runway 17L/35R in the background.

Figure 7
BGI PQ100 PM samplers for $PM_{2.5}$ (PM_{10} inlet followed by a $PM_{2.5}$ cyclone) (left) and TSP inlet (right)

Twelve-hour integrated PM samples were collected each day. These sampling events were conducted during the 12-hour period of highest piston-engine aircraft activity based on discussions with the airport authorities. This approach was preferred over 24-hour integrated sampling for several reasons. Piston-engine aircraft activity is very low at night and thus the additional 12 hours of sampling would increase the relative contribution from background Pb to the time average concentration. The 24-hour time window for sampling also increases the likelihood of wind direction variability. This is not a hard constraint for the modeling, but persistent winds do simplify the data interpretation. Finally, calm winds are more frequently observed at night and these periods are more difficult to model.

PM sampling and chemical analysis protocols are described in detail in Appendix B and are summarized as follows. PM samplers were mounted on wood platforms. Filter holders containing the Teflon® filter media were installed in the samplers each morning immediately prior to the start of sampling and retrieved each evening immediately following the end of sampling. While Pb is nonvolatile, bromine (Br) is also of interest and it is relatively volatile so cold transport and storage was adopted. Samples were transported to and from the field sites in coolers with ice packs and were stored in a freezer after sampling. For each airport study, a subset of samples was analyzed by X-Ray Fluorescence (XRF) at Cooper Environmental Services (CES, Beaverton, OR) to obtain data for a range of elements. XRF data were reported as areal densities (e.g., ng/cm^2 filter) and converted to ambient concentrations using the filter effective cross-sectional area and the ambient air volume sampled. All samples—including those analyzed by XRF, which is a non-destructive method—were digested and analyzed for Pb at WUSTL using Inductively Coupled Plasma – Mass Spectrometry (ICP-MS). Two sequential digestions were performed using a hot-block at 90 °C with nitric acid and hydrofluoric acid for the first digestion and boric acid for the second digestion. Digestion solutions were diluted to a known volume and filtered to remove any remaining particulate matter. ICP-MS data were reported as concentrations in the diluted digestion solutions and converted to ambient concentrations using the diluted digestion solution volume and the ambient air volume sampled.

All samples were analyzed for Pb isotopes as well as total Pb. ICP-MS analysis for Pb isotopes was not included in the original study design but was added to strengthen the connection between airborne Pb and piston-engine aircraft emissions. The isotopic composition of Pb used to make the avgas additive tetraethlylead (TEL) is distinct from the isotopic composition of native soils at these airports. Thus, isotopic composition can be used to discriminate the origins of Pb in the airborne PM samples. Pb isotopes are stable and therefore cannot be used to distinguish PM-Pb in freshly emitted exhaust from exhaust PM-Pb that has locally deposited over the years and is resuspended by wind or aircraft-induced turbulence during the PM sampling events. The isotopes data were also used to screen PM-Pb samples for contamination. Appendix B presents the analytical protocol and use of the isotopic composition for data validation.

Data collection objectives included 20 sampling events at each airport with 85% data completeness (17 events) for valid $PM_{2.5}$-Pb data at both of the primary sites. Additional data collection objectives were nine events with $PM_{2.5}$ and TSP sampling at the primary sites and nine events with $PM_{2.5}$ sampling at the primary and secondary sites. Table 21

Table 21
PM Data Collection Summary

Parameter	Objective	RVS	APA	SMO
PM Sampling Events[1]	20	31	25	25
$PM_{2.5}$-Pb (two primary sites)	17	31	25	24
$PM_{2.5}$-Pb and TSP-Pb (two primary sites)	9	9	9	9
$PM_{2.5}$-Pb (two primary and two secondary sites)	9	8	9	4

Note: PM-Pb measures include both valid data collection and valid chemical analysis for Pb content.
[1] Excludes collocated TSP sampling events which, by design, do not include $PM_{2.5}$ sample collection.

summarizes the data completeness from the perspective of not only valid sample collection but also valid chemical analysis for Pb. Additional details are provided in the airport-specific summaries. For each airport, the number of attempted PM sampling events and valid $PM_{2.5}$-Pb data collection at the primary sites far exceeded the objectives. $PM_{2.5}$-Pb and TSP-Pb data collection at the primary sites met the objective of nine events per airport. The four-site $PM_{2.5}$-Pb data collection objective of nine events was met at APA; however, RVS included only eight events and SMO only four. Low capture at SMO was from a failed sampler that needed to be returned for repair, which resulted in nine valid samples at one secondary site and five valid samples at the other secondary site. As discussed in the SMO case study summary, this data collection shortcoming did not compromise the data analysis and interpretation.

PM-Pb quality assurance data collection included field blanks and collocated sampling for $PM_{2.5}$ and TSP. Eight $PM_{2.5}$ and four TSP field blanks were collected at each airport by placing filters in the samplers overnight (nominally 12 hours) between scheduled sampling events. A one-way nonparametric analysis of variance test demonstrated the field blanks distributions for each airport were statistically indistinguishable (95% confidence level) and thus the field blanks data were pooled across the airports. Effective ambient concentrations were calculated using the target air volume of 12 m^3 drawn through a 16.7 LPM sampler during a 12-hour sampling event. $PM_{2.5}$-Pb median and 90^{th} percentile field blank concentrations were 0.1 $ng/m^3$and 0.5 ng/m^3, respectively (N = 48). For TSP-Pb the median field blank concentration was 0.4 ng/m^3 (N = 12). The 90^{th} percentile TSP-Pb field blank was 1.8 ng/m^3 but extremes of a distribution, such as the 90^{th} percentile, might be non-representative for small sample sizes such as the 12 samples in this case. The higher field blanks value for TSP compared to $PM_{2.5}$ is consistent with windblown dust intrusion into the sampler in the absence of air sampling. Median field blank Pb levels are similar to the analytical MDL of 0.2 ng/m^3 and thus airborne PM-Pb concentration values were not corrected using the field blanks data.

PM-Pb measurement precision was evaluated by collocating samplers with matched inlets (i.e., operating two matched samplers side-by-side). These measurements were conducted at both of the primary sites at each airport. PM-Pb collocated data are presented in the data tables for each airport summary (see Sections 5.2, 5.3, and 5.4).

Thirty-two $PM_{2.5}$ sample pairs were collected: 16 at RVS, 4 at APA, and 12 at SMO. Ten TSP sample pairs were collected: four at APA and six at SMO. These data were pooled across the airports and the collocated precision was calculated as the root mean square difference over all sample pairs divided by $\sqrt{2}$. Precision estimates are presented in Table 22. Measurement precision for ambient PM sampling typically has two components—an additive (absolute) contribution that dominates at low concentrations approaching the detection limit, and a proportional (relative) contribution that dominates at high concentrations. The concentration dependence of precision was evaluated by splitting the $PM_{2.5}$ data into three groups using tertile concentrations and splitting the TSP data into two groups using the median concentration. Table 22 shows that at low PM-Pb concentrations the absolute precision is 0.35 ng/m^3 for $PM_{2.5}$ and 0.59 ng/m^3 for TSP; at high concentrations, the relative precision is 12% for $PM_{2.5}$ and 5% for TSP (bolded values in Table 22). Precision estimates for TSP might be influenced by the small sample sizes after stratifying the data into two groups (N = 5 for each group).

Table 22
PM-Pb Measurement Precision from Collocated Sampling

Parameter	Sample Pairs	Mean Pb (ng/m^3)	Collocated Precision	
			Absolute (ng/m^3)	Relative[1] (%)
$PM_{2.5}$-Pb				
- All Data	29[a]	10.7	1.8	17
- Bottom 1/3 Concentrations	9	0.83	**0.35**	43
- Middle 1/3 Concentrations	10	4.8	0.85	18
- Top 1/3 Concentrations	10	25.7	3.0	**12**
TSP-Pb				
- All Data	10	15.6	1.2	8
- Bottom 1/2 Concentrations	5	1.8	**0.59**	37
- Top 1/2 Concentrations	5	29.5	1.6	**5**

[1] Relative precision is the absolute collocated precision divided by the pooled mean concentration.
[a] The 7/27/13 SMO Northeast site sample pair was excluded because the concentration difference is an extreme value that exerts high influence on the precision estimates.

Additional analysis, presented in Appendix B, demonstrates the $PM_{2.5}$-Pb relative precision of 12% at high concentrations is a stable estimate. Assuming the additive and proportional contributions to measurement error are independent, sample-specific uncertainties can be estimated by adding the precision contributions in quadrature, i.e.

$$\sigma_{PM_{2.5}-Pb} = \sqrt{0.12 + 0.015 \times C^2_{PM_{2.5}-Pb}}$$

where C is the measured $PM_{2.5}$-Pb concentration and σ is its uncertainty, both in units of ng/m^3. $PM_{2.5}$-Pb measurement precision of ~0.35 ng/m^3 at low concentrations and 12% at high concentrations demonstrate high data quality for use in the model evaluation.

5.1.3 Avgas Data Collection

Avgas dispensed by all FBOs at three airports is 100LL grade, which has a maximum Pb content of 2.12 g/gal (0.56 g/L). The actual Pb content in 100LL can be considerably lower, however, and thus avgas samples were collected at each airport and analyzed for Pb content. Avgas samples were collected from FBOs at RVS and APA. At SMO, however, the FBOs were unwilling to provide avgas samples for this study; therefore, samples were collected from two privately owned, SMO-based piston-engine aircraft. In general, avgas samples were collected from FBOs within days after new fuel deliveries; however, some samples were obtained from FBOs with low avgas sales volumes, resulting in samples drawn as long as 10 months after the most recent delivery. A total of 15 avgas samples were collected and shipped to Intertek Caleb Brett for Pb content analysis using test method ASTM D5059. Airport-specific results are presented in Sections 5.2, 5.3, and 5.4. Pooling over the three airports, mean and median Pb concentrations in avgas were 1.56 g/gal and 1.33 g/gal, respectively, with a maximum Pb content of 2.12 g/gal. The avgas samples were analyzed by ICP-MS for Pb isotopes for comparison to the airborne PM-Pb data.

5.1.4 Soil Data Collection

Bulk soil samples were collected near each of the four PM sampling sites at each airport. A portion of each sample was resuspended in a chamber with $PM_{2.5}$ collected onto filters. These filter samples were digested and analyzed by ICP-MS for Pb mass fraction in the resuspended soil and also Pb isotopes. The remaining portion of each bulk soil sample will be archived at WUSTL until at least January 1, 2016.

5.1.5 Meteorological Data Collection

Automated Surface Observing System (ASOS) data and Integrated Surface Hourly **(**ISH**)** data for each airport have been obtained from the National Climatic Data Center**.** In addition, a 3D sonic anemometer (Model 81000, RM Young Co., Traverse City, MI) was deployed starting midway through the first field study (RVS) and throughout the remaining two studies. 3D wind speeds and temperature at 3 m height were logged at 10 Hz. These data can be used to calculate horizontal wind direction and speed in addition to the vertical wind speed. To further enhance the ASOS routine meteorology data collection, a portable weather station (PortLog, Rainwise Inc., Bar Harbor, ME) was deployed for each study period. The following parameters were recorded as one-minute averages: wind speed and direction at nominally 2 m height; temperature; relative humidity; barometric pressure; rainfall; and solar radiation. While the ASOS 10 m surface winds data are used for all modeling, the additional meteorology data are used to further characterize environmental conditions during sampling.

5.2 RVS Field Study

Figure 8 shows the RVS airport layout. There are three runways: the two north/south runways are used predominantly, while the east/west runway is rarely used. Prevailing winds are from the south.

Figure 8
Airport Diagram and PM Sampling and Activity Data Collection Locations Deployed at RVS

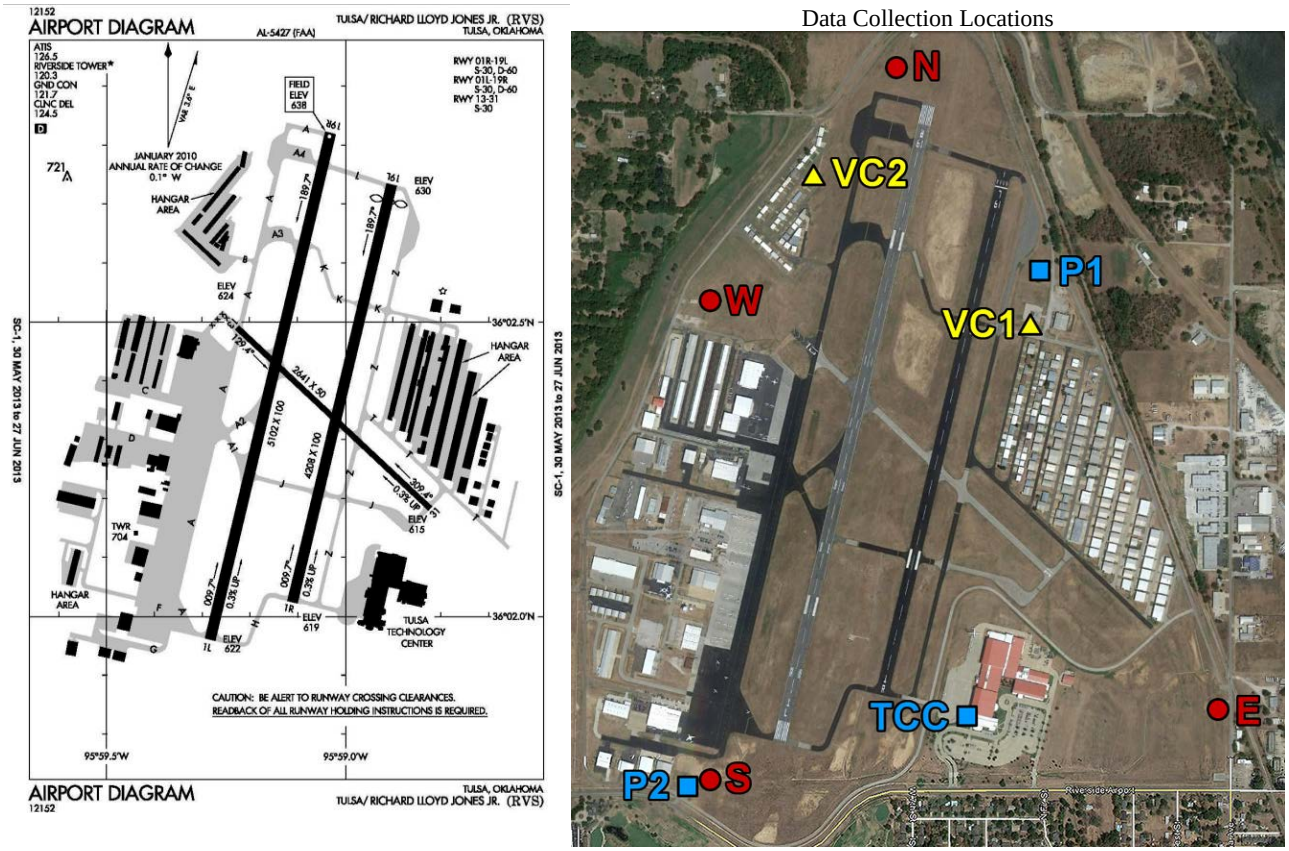

Note: PM sampling was conducted at the North (N), East (E), South (S), and West (W) sites; video cameras were deployed at the VC1 and VC2 sites; and other activity data were manually collected at the P1, P2, and TCC sites.

The field study was conducted from March 27 to April 28, 2013. March 27 was a shakedown day for PM measurements and these data are valid for precision estimates but, for reasons described in Section 5.2.2, should not be used for the model-to-monitor comparison. A video camera to continuously record LTOs was deployed starting on March 27. However, for reasons described in Section 5.2.1, this camera did not adequately capture LTO operations. A second camera was deployed starting on April 4 and the data collected thereafter are most suitable for the model-to-monitor comparison, although the data collected prior to April 4 can be used with additional assumptions about

LTO activity. PM sampling and aircraft activity data were collected from 8 AM to 8 PM CDT.

5.2.1 Aircraft Activity Data Collection

Aircraft activity data collection at RVS is summarized in Table 23; data collection locations are shown in Figure 8. Video cameras were continuously operated during each 12-hour PM sampling event to record LTOs. Initially one camera was deployed at the VC1 location (Figure 8) to capture LTOs for aircraft takeoffs and landings at the north end of both north-south runways, which are the operating conditions for prevailing southerly winds. However, VC1 could not capture the takeoff portion of touch-and-go operations and only partially captured landings that originated at the south end of the north-south runways, which are the operating conditions for northerly winds. Periods with northerly winds were more frequent than anticipated. Starting on April 4, a video camera was also deployed at the VC2 location (Figure 8) to resolve these data collection issues and LTO operations are reported in the database only for the period from April 4 through April 28.

Figure 9 shows the hourly distribution of total operations for all aircraft (not just piston-engine aircraft) as determined from the video camera data. Touch-and-go activities are counted as two operations each and are distinguished from normal takeoffs and landings. Over the study period there were, on average, 19 operations per hour. Total operations peaked between 10 AM and 12 PM, with the lowest levels of activity in the early morning. Operations were nearly evenly distributed between the two north/south oriented runways with 46% on 1R/19L and 49% on 1L/19R. East/west runway (13/31) and helicopter activity were 3.6% and 1.5% of documented operations, respectively. However, the video cameras are not ideal for capturing helicopter activity since they have a different spatial extent of operation. Operations on the north/south runways were evenly split between those originated at the north end (19L/19R) and south end (1L/1R) at 50% each.

Thirty hours of LTOs were photographed from the locations marked as P1 and P2 in Figure 8. The photographs were reviewed to identify tail numbers, which were matched to aircraft and engine specifications in the FAA Registry. The resulting fleet inventory database includes a record for each operation but with the tail numbers removed. Over the 30 hours of observation, 171 unique aircraft were identified. Nine aircraft (5%) accounted for one-third of the operations and 20 aircraft (12%) accounted for half of the operations (19 fixed-wing single-engine aircraft, and one fixed-wing multi-engine aircraft). Table 24 summarizes the distribution of LTOs by aircraft type; more than three-fourths of the operations were single-engine piston aircraft.

TIM data were manually collected. Piston-engine aircraft run-up activities were observed for 15 hours and included 109 run-up operations, with magneto test duration recorded for 76 of these operations. Missing magneto test data primarily resulted from confounding sources of noise. Tail numbers were recorded for 95% of the run-up operations. Twenty-eight planes bypassed the run-up area and did not perform any observed run-ups.

Table 23
RVS Aircraft Activity Data Collection at RVS

Date	Activity Data Collection					
	VC1	VC2	Tail ID	TIM	Run-up	Comments
03/27/2013	P	-	2	0	0	VC1 ran 1200-2000 CDT
03/28/2013	Y	-	2	0	0	
03/29/2013	Y	-	1	1	0	
03/30/2013	Y	-	2	0	1	
03/31/2013	Y	-	1	2	0	
04/01/2013	Y	-	2	0	1	
04/02/2013	N	-	0	0	0	
04/03/2013	Y	-	0	2	0	
04/04/2013	Y	Y	1	0	2	VC2 deployed starting 4/4/2013
04/05/2013	Y	P	0	0	0	VC2 ran 0800-1338 CDT
04/06/2013	Y	N	0	0	0	VC2 hardware failure
04/07/2013	Y	Y	0	0	0	
04/08/2013	Y	Y	2	0	1	
04/09/2013	Y	Y	1	0.5	0	
04/10/2013	N	N	0	0	0	VCs not deployed - severe weather
04/11/2013	Y	Y	0	0	1	
04/12/2013	Y	Y	1	0	0	
04/13/2013	Y	Y	2	2	0	
04/14/2013	Y	Y	2	1	1	
04/15/2013	Y	Y	2	1	0	
04/16/2013	Y	Y	1	2.5	0	
04/17/2013	Y	Y	0	1	0	
04/18/2013	Y	Y	1	0	0	
04/19/2013	Y	Y	1	0	0	
04/20/2013	Y	Y	1	0	2	
04/21/2013	Y	Y	3	1	0	
04/22/2013	Y	Y	1	1	1	
04/23/2013	Y	Y	0	0	0	
04/24/2013	Y	Y	0	0	2	
04/25/2013	Y	Y	0	0	2	
04/26/2013	Y	Y	0	0	0	
04/27/2013	Y	Y	0	0	0	
04/28/2013	Y	P	1	0	1	VC2 ran 0800-1631 CDT
Total Hours			30	15	15	

Notes: VC = video camera for time-resolved takeoffs and landings (Y = yes, N = no, P = portion of the 12 hour period); Tail ID = still photographs of planes for tail number identification; TIM = time-in-mode data collection (e.g., taxiing, takeoff, climb-out); and Run-up = run-up area activity including TIM for magneto testing.

Figure 9
Hourly Average Operations at RVS – All Aircraft
PM sampling was conducted 8 AM to 8 PM CDT

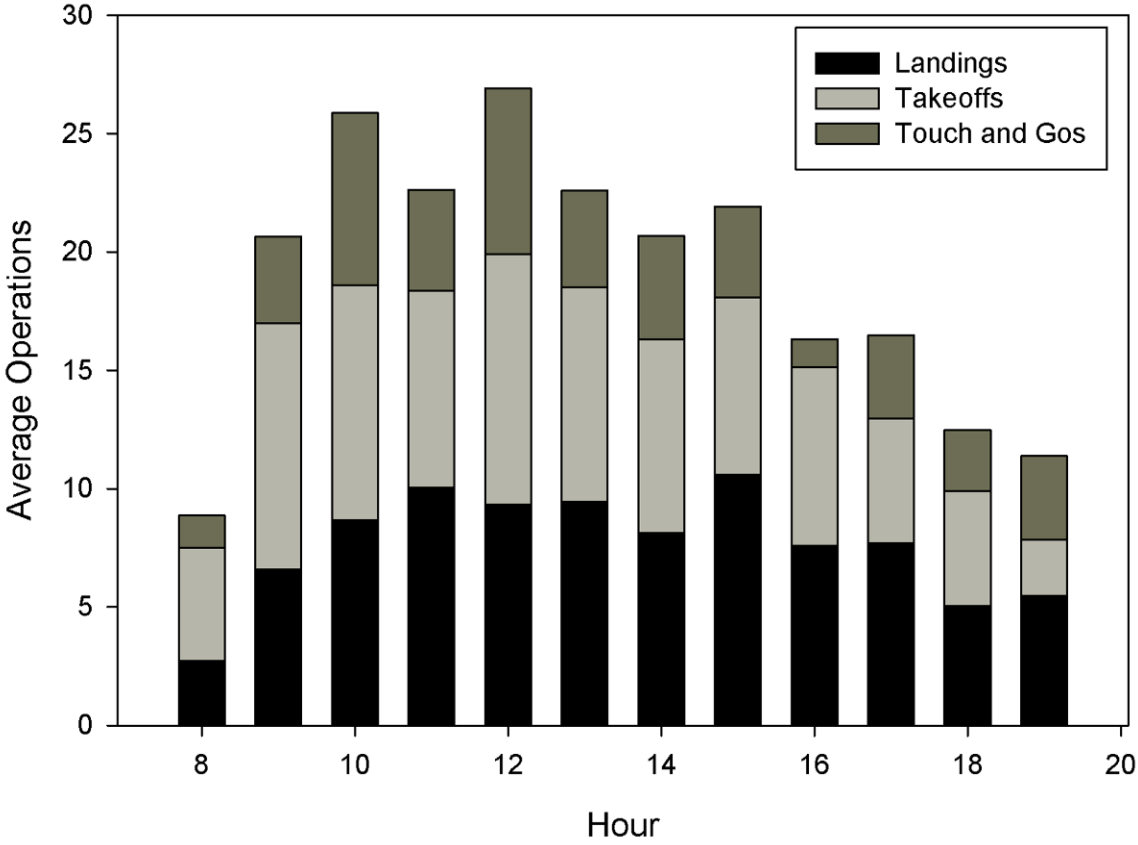

Table 24
Distribution of Aircraft Types Identified by Tail ID at RVS

Plane Type	Count	% of Total
Piston		
Single Engine	437	79%
Multi Engine	59	11%
Turboprop	24	4%
Jet	30	5%

Note: Based on 30 hours of still photography.

Table 25 and Figure 10 summarize the run-up results. Mean TIM values were 69 seconds for the magneto test and 296 seconds for the total time in the run-up area. There was large variation in these times, with standard deviations of about 50% and 80% of the means for total run-up and magneto testing, respectively. Total run-up and magneto test

Table 25
Time in Mode Data Collected for Run-Up Operations at RVS

	Total Run-Up	Magneto Testing
Number of Aircraft	109	76
Mean ± Std Dev (sec)	296 ± 150	69 ± 56
Median (sec)	284	50

Notes: Based on 15 hours of data collection. Means are reported with 1σ standard deviation values.

Figure 10
Time-in-Mode Data for Total Time in the Run-Up Area and Duration of Magneto Testing at RVS

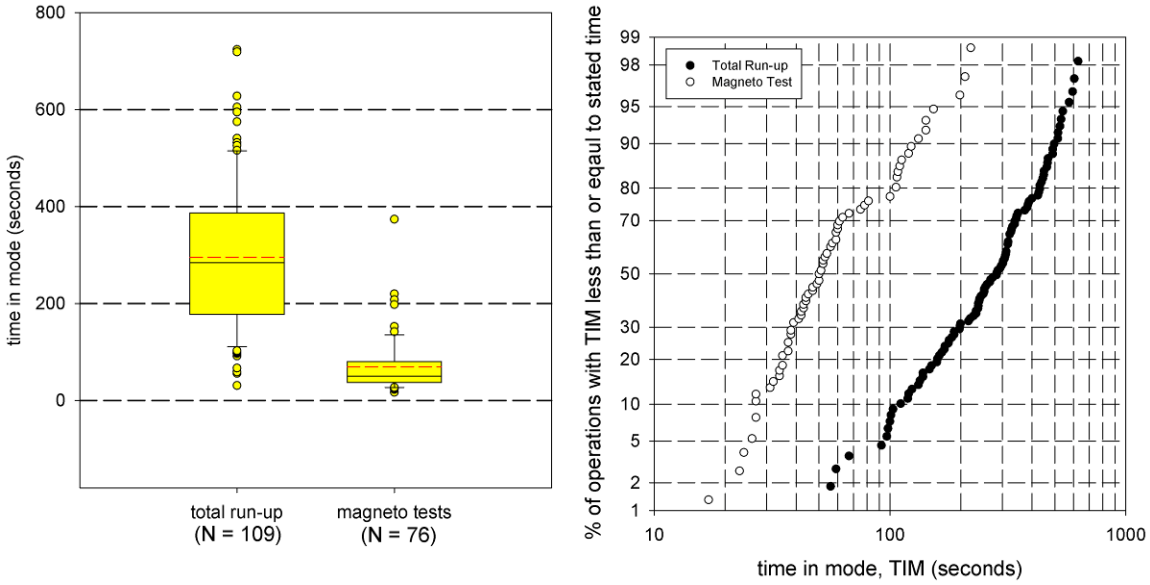

(a) (b)

Notes: (a) box plots (interior solid line is the median, interior dashed line is the arithmetic mean; box boundaries are 25th and 75th percentiles, whiskers are 10th and 90th percentiles, and circles are all records below the 10th percentile and above the 90th percentile); and (b) cumulative distributions as a log-probability plot.

TIM data are shown as box plots in Figure 10(a) and cumulative distributions in Figure 10(b). Both total run-up time and magneto test duration data are approximated relatively well by a lognormal distribution as evidenced by the nearly linear trend for the log-probability plot. This means that a few aircraft have much longer TIM than would be expected from the standard deviations about the mean times.

TIM data were also manually collected for piston-engine aircraft taxiing, idling, landings, and takeoffs. Fifteen hours of operations were viewed from an observation tower. Table 26 shows summary statistics for landing, takeoff, and touch-and-go times, as well as average locations for wheels-up and wheels-down. TIM for touch-and-go operations represents the time between wheels-down on landing and the subsequent wheels-up on takeoff. Wheels-up and wheels-down locations are measured as the distance from the start of the runway. There is less variation in TIM for landing and takeoff activities than for run-up activities. Activities were logged by aircraft so trip-based times can be constructed. Similar TIM data collection and processing has been performed for other aircraft activities, such as taxiing and idling, and the data are included in the database.

Table 26
Summary of Time-in-Mode and Location of Aircraft Landing and Takeoff Operations at RVS

Activity/Location	Mean Time (s)	Std. Dev (s)	Mean Wheels-Up (ft)	Mean Wheels-Down (ft)
Landing				
Runway 1L	25	8	-[a]	562
Runway 1R	22	4	-	1036
Runway 19L	39	29	-	1117
Runway 19R	39	13	-	1016
Takeoff				
Runway 1L	18	9	1064	-
Runway 1R	13	7	727	-
Runway 19L	14	5	1324	-
Runway 19R	20	8	1595	-
Touch-and-Go				
Runway 1L	23	8	3370	976
Runway 1R	17	6	1324	-
Runway 19L	16	8	1371	729
Runway 19R	-	-	-	-

Notes: Based on 15 hours of data collection. TIM means are reported with 1σ standard deviation values.
[a] Dashes indicate no data are available.

5.2.2 Airborne PM-Pb Data Collection

PM sampling locations are shown in Figure 8 with key characteristics summarized in Table 27. The North site is the downwind primary site with presumably high impacts from run-up, taxiing and idling, and takeoff activities on runway 19R for prevailing southerly winds. The East site is the upwind primary site and should capture background Pb concentrations regardless of wind direction with the exception of westerly winds, which were rare during the study. The South site is impacted by climb-out from runway 19R for southerly winds and run-up, taxiing and idling, and takeoffs from runway 1L for

Table 27
Airborne PM Sampling Locations for the RVS Study

Site	Location with Respect to Nearest Runway	Comments
North Downwind Primary	~125m NW of 19R	For prevailing southerly winds, this site was impacted from runway 19R run-ups and takeoffs, as well as idling and taxiing. (Lat: 36.047435° Long: -95.984719°)
East Upwind Primary	~500m SE of 31	For winds from the south, east, and north, this site is upwind of all ground-based activities. It is ~700m east of runway 1R and may be modestly impacted by aircraft operations for winds from the west. (Lat: 36.033631° Long: -95.976139°)
West Downwind Secondary	~250m NW of 13	For prevailing southerly winds, this site was impacted by the southern half of runways 19L and 19R and ground-based activities on the west side of the airport. (Lat: 36.042370° Long: -95.989708°)
South Upwind Secondary	~200m SW of 1L	For winds from the south, east, and west, this site is upwind of all ground-based activities. For northerly winds, it was impacted by ground-based activities on the west site of the airport including run-ups and takeoffs for runway 1L, as well as idling. (Lat: 36.032130° Long: -95.989700°)

northerly winds. Emissions from ground-based operations west of the runways might impact this site for northerly winds. The West site is potentially impacted by ground-based operations on the west side of the airport for southerly winds and runway operations for easterly winds, which were rare during the study. Twelve-hour integrated PM samples were collected each day using up to four PQ100 samplers. Sampling was conducted from 8 AM to 8 PM CDT.

Table 28 shows the PM samples collected each day. Although the goal was to operate four samplers during each event, one of the PQ100 samplers failed early in the study and eight runs were conducted with three samplers until a rental unit could be obtained while the original sampler was being repaired. Due to this and also the relatively high frequency of northerly winds, the campaign was extended an additional week. Samplers were operated on 32 of the 33 days—no sample collection was attempted on 4/2 because of heavy rain. The first day of sampling, conducted on 3/27, was not considered to be an attempted sampling event because it was a hardware shakedown day; the North site

Table 28
Airborne PM Sampling Configurations and Wind Direction Characteristics at RVS

	PM Sampling Configuration				Wind Direction Frequency and Classification					
Date	N	E	S	W	Calm	N	E	S	W	Winds
03/27/2013	{F,F}	F,F			0	2	0	98	0	S
03/28/2013	F,F	F,F			0	2	0	**98**	0	S
03/29/2013	F,F	F,F			0	13	13	**56**	19	var
03/30/2013	F,F	F,[F]			0	6	10	**83**	0	S
03/31/2013	F,F	F,F			0	**94**	6	0	0	N
04/01/2013	F,F	F			0	**100**	0	0	0	N
04/02/2013	*no sample collection*				0	46	54	0	0	var
04/03/2013	F,F	F			0	**69**	25	4	2	N
04/04/2013	F,F	F			0	**88**	0	0	13	N
04/05/2013	F,F	F			4	0	0	**85**	10	S
04/06/2013	F,[F]	F			0	2	0	**94**	4	S
04/07/2013	F,F	F			2	0	4	**94**	0	S
04/08/2013	F	F	[F]		0	2	0	**98**	0	S
04/09/2013	F	F	F		0	2	0	**98**	0	S
04/10/2013	F	F	F		0	52	0	0	48	var
04/11/2013	F	F	F	F	0	21	0	0	**79**	W
04/12/2013	F	F	F	F	4	**71**	6	0	19	N
04/13/2013	F	F	F	[F]	0	2	8	**90**	0	S
04/14/2013	F	F	F	F	0	2	0	**98**	0	S
04/15/2013	F,T	F,T			0	**94**	6	0	0	N
04/16/2013	F,T	F,T			0	**100**	0	0	0	N
04/17/2013	F,T	F,T			2	0	6	**92**	0	S
04/18/2013	F,T	F,T			0	29	0	0	**71**	W
04/19/2013	F	F	F	F	0	4	0	0	**96**	W
04/20/2013	F	F	F	F	0	2	6	**92**	0	S
04/21/2013	F	F	F	F	0	2	0	**98**	0	S
04/22/2013	F	F	F	F	0	2	0	**98**	0	S
04/23/2013	F	F	F	F	0	**100**	0	0	0	N
04/24/2013	F,T	F,T			2	**88**	0	0	10	N
04/25/2013	F,T	F,T			4	0	23	**73**	0	S
04/26/2013	F,T	F,T			0	6	**81**	13	0	E
04/27/2013	F,T	F,T			0	**96**	0	0	4	N
04/28/2013	F,T	F,T			0	2	2	**96**	0	S

Notes: The row following each interior horizontal line is a Monday. PM Sampling: F = $PM_{2.5}$, T = TSP, [ ] = invalid sample; { } = samplers moved during the sampling period; and empty cells indicate no sample collection. Wind Direction: percentage frequency of 15-minute average ASOS 10m wind direction; and wind direction classification for events with at least two-thirds of the 15-minute winds from a given quadrant (var = variable winds).

samplers were moved ~75 m during the sampling period from a temporary location to their permanent location and the South site samplers did not start until 11 AM. Thus, there are 31 events with valid $PM_{2.5}$ sample collection at the North and East sites, which is nearly twice the objective of 17 events. The additional measurement objective of nine events with $PM_{2.5}$ and TSP sampling at the North and East sites was met, while the eight events with $PM_{2.5}$ sampling at four sites was one short of the objective because of a sampler failure. All samples were analyzed for Pb with no identified issues; thus, the sample collection completeness carried through to the overall PM-Pb data completeness.

Figure 11 shows the wind rose for NWS ASOS (10 meter) 15-minute average data over all sampling periods (8 AM to 8 PM CDT). Daytime wind speeds were relatively high throughout the study with only 1.2% calms (operationally defined as wind speeds ≤ 1 m/s) and only 13% of 15-minute periods with wind speeds less than 4 m/s. While prevailing winds were from the south quadrant (46%), winds from the north quadrant were also common (32%).

The model-to-monitor comparison does not require a consistent wind direction throughout the day, but instead relies upon the background site not being significantly impacted by emissions from aircraft operations; however, for many reasons, interpretation of the PM data is simplified when the wind direction is consistent throughout the sampling period. Wind direction persistence was examined by assigning each 15-minute average wind direction to a quadrant centered on the cardinal wind directions. A wind direction was assigned to a sampling event if at least two-thirds of the 15-minute average winds were from a given quadrant; otherwise the winds were deemed to be variable. Table 28 summarizes the daily wind direction patterns. Excluding the first sampling day (shakedown) and the day with no sample collection attempted, the 31 sampling events had the following distribution of winds: southerly, 15 events (48%), including 13 events after April 4 when the second video camera was deployed to improve the LTO data collection; northerly, 10 events (32%); westerly, 3 events (10%); easterly, 1 event (3%); and variable, 3 events (6%). While the criterion of winds being from a given quadrant for two-thirds of the time might seem relatively lax, for 19 of the 29 sampling events with a classified wind direction the winds were from the designated quadrant for at least 90% of the sampling period.

Table 29 shows the PM-Pb data for all ambient PM samples as measured by ICP-MS. Four samples were invalidated, as explained in Appendix B. Of the 99 $PM_{2.5}$ samples, 93 (94%) have a Pb concentration at least three times the $PM_{2.5}$ median field blank level. Of the 18 TSP samples, 16 (89%) have Pb concentrations at least three times higher than the median TSP field blank. These results demonstrate that acceptable detectability was achieved for the airborne Pb data.

Figure 11
Daytime (0800-1959 CDT) 15-minute Average 10m ASOS Winds at RVS, March 25 – April 29, 2013

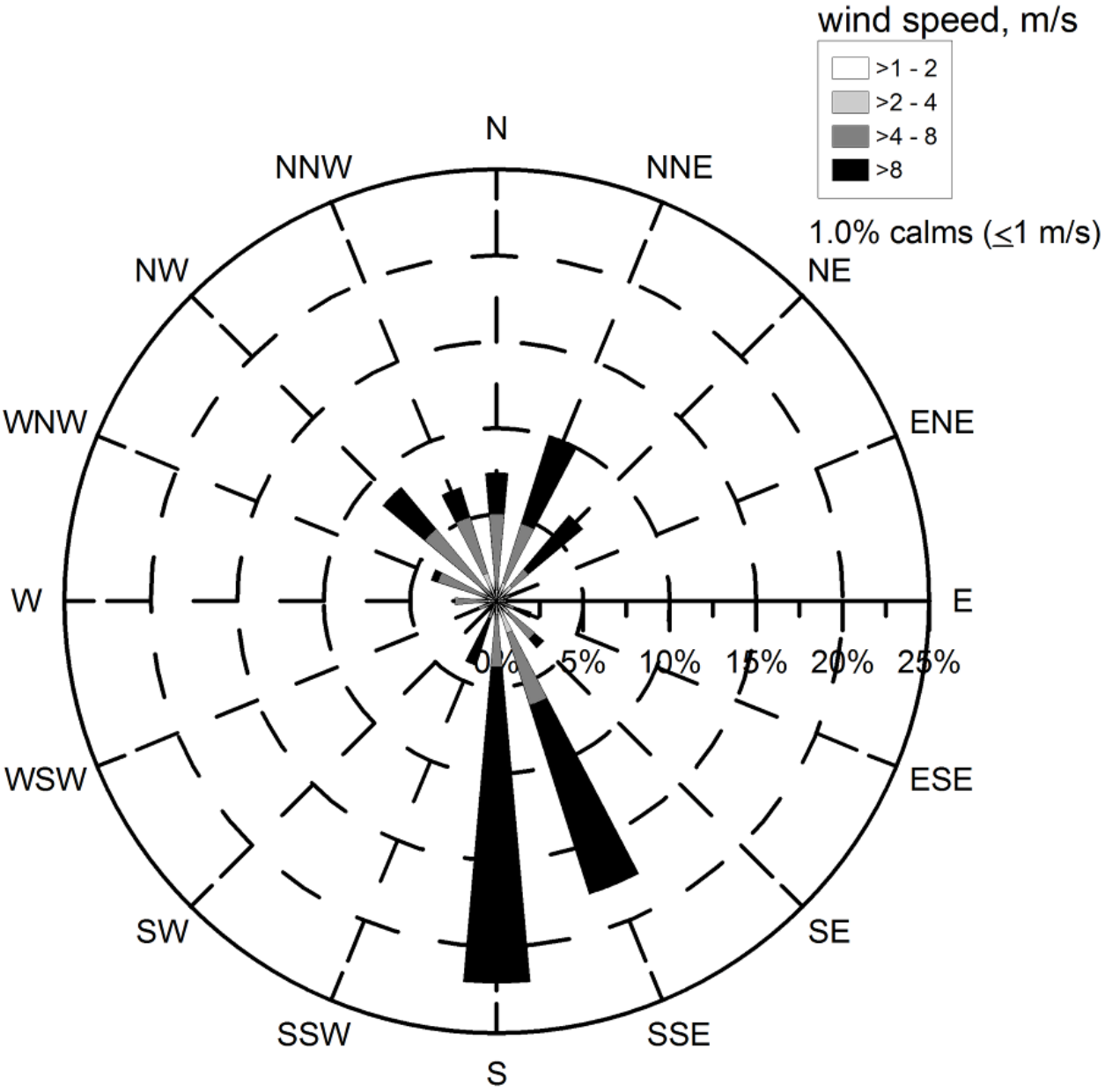

Table 29
Airborne Pb Concentrations Observed at RVS

	Pb Concentration, ng/m^3					
	North		East			
Date	Primary	Collocate	Primary	Collocate	South	West
03/27/2013	{49.6}	{50.1}	4.3	2.6		
03/28/2013	37.7	32.9	2.5	2.4		
03/29/2013	19.1	18.3	7.2	8.0		
03/30/2013	8.6	8.0	1.2	--		
03/31/2013	1.2	1.1	1.2	0.9		
04/01/2013	3.3	2.2	3.6			
04/02/2013						
04/03/2013	2.2	2.3	2.9			
04/04/2013	6.2	2.8	3.3			
04/05/2013	46.9	50.7	3.0			
04/06/2013	17.2	--	3.5			
04/07/2013	7.3	7.0	1.4			
04/08/2013	14.0		0.8		--	
04/09/2013	18.4		1.4		2.4	
04/10/2013	0.5		0.4		0.3	
04/11/2013	0.7		1.9		7.6	0.8
04/12/2013	1.9		2.6		29.2	1.8
04/13/2013	33.2		2.3		2.2	--
04/14/2013	11.0		2.6		1.2	2.1
04/15/2013	1.6	[3.4]	1.6	[3.4]		
04/16/2013	0.9	[3.3]	1.0	[2.2]		
04/17/2013	15.5	[18.0]	1.1	[2.0]		
04/18/2013	0.3	[0.4]	2.4	[2.2]		
04/19/2013	1.2		6.7		9.9	1.2
04/20/2013	31.2		1.6		1.4	7.1
04/21/2013	7.7		1.5		1.4	2.9
04/22/2013	19.4		1.7		2.1	4.9
04/23/2013	1.0		0.4		12.3	0.6
04/24/2013	2.2	[4.2]	2.4	[3.3]		
04/25/2013	26.8	[37.1]	3.2	[3.1]		
04/26/2013	3.9	[4.6]	2.4	[3.2]		
04/27/2013	1.5	[1.9]	0.3	[0.6]		
04/28/2013	14.7	[22.5]	2.7	[2.0]		

Notes: The row following each interior horizontal line is a Monday. Data are $PM_{2.5}$-Pb unless otherwise noted. [ ] = TSP;{ } = samplers moved during the sampling period; "--" = invalid sample; and empty cells indicate no sample collection.

Trends for PM-Pb are presented within the context of wind patterns during sample collection. Figure 12 compares $PM_{2.5}$-Pb at the North and East sites with the data stratified by prevailing wind direction. For southerly winds, $PM_{2.5}$-Pb at the North site is at least five times higher than $PM_{2.5}$-Pb at the East (background) site. This pattern clearly indicates the downwind site is impacted by aircraft operations. In contrast, $PM_{2.5}$-Pb concentrations at the North and East sites are quite similar for northerly winds. There are three events with $PM_{2.5}$-Pb at the East site significantly higher than at the North site (i.e., the inverted triangles along the x-axis in Figure 12). These three events had winds from the west, which led to aircraft emissions impacts at the East site. In summary, the East site appears to represent background Pb levels for all conditions except when the winds are from the west. $PM_{2.5}$-Pb for the North and South sites are compared in Figure 13. Southerly winds yield elevated Pb at the North site while northerly and westerly winds lead to elevated Pb at the South site, which is near a run-up and takeoff area for operations when winds are from the north.

Figure 14 shows TSP-Pb versus $PM_{2.5}$-Pb for the North and East sites. The mean concentration for Pb in the TSP-minus-$PM_{2.5}$ size range (i.e., coarse particles) was 1.8 ng/m^3. For the three samples with elevated Pb levels, $PM_{2.5}$-Pb was 65-86% of TSP-Pb. The low concentrations for Pb in $PM_{TSP-2.5}$ compared to Pb in $PM_{2.5}$ at sites impacted by the piston-engine aircraft strongly suggest that the observed $PM_{2.5}$-Pb in these samples is from direct aircraft exhaust emissions and not the tail of coarse mode PM-Pb extending below 2.5 µm.

Figure 12
$PM_{2.5}$-Pb at the North and East Sites Stratified by the Prevailing Wind Direction During Sample Collection at RVS

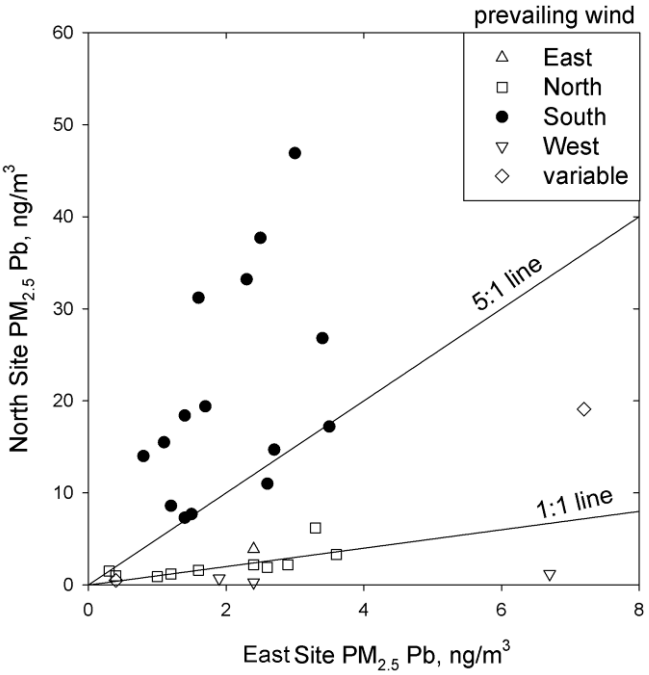

Figure 13
$PM_{2.5}$-Pb at the North and South Sites Stratified by the Prevailing Wind Direction During Sample Collection at RVS

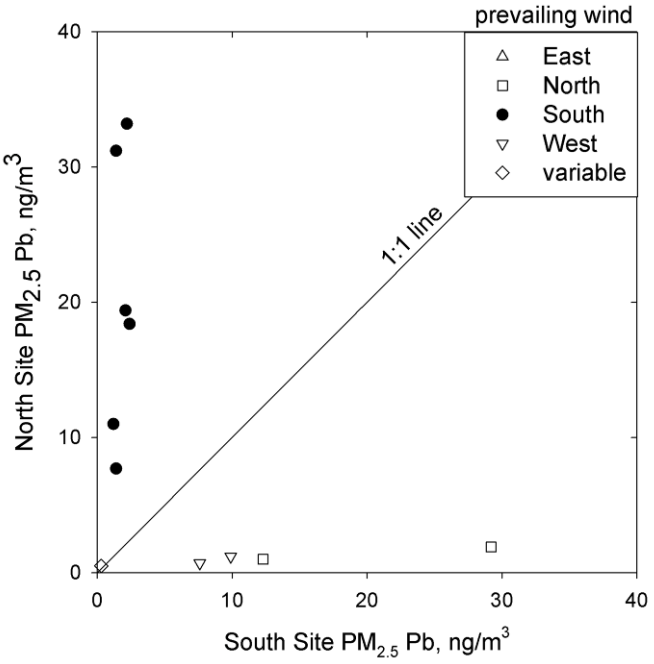

Figure 14
TSP-Pb versus $PM_{2.5}$-Pb at the North and East Sites

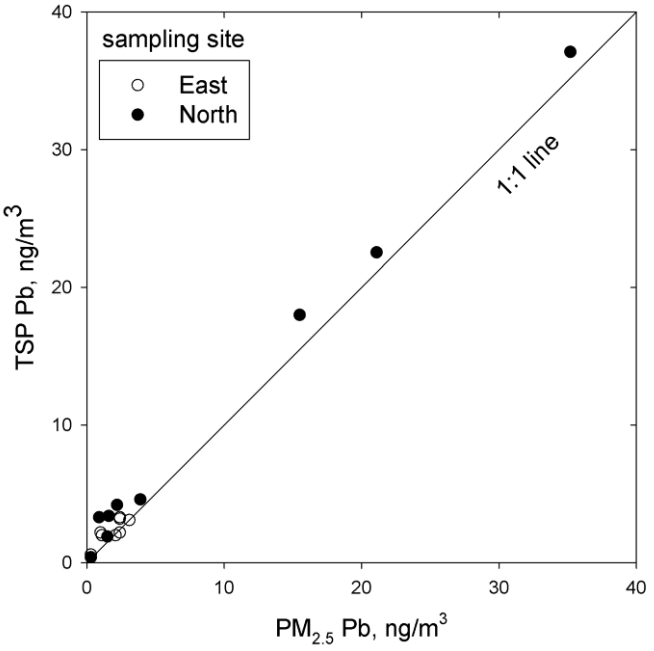

5.2.3 Avgas Data Collection

Four avgas samples were collected from the FBOs. Christiansen Aviation Inc. is the largest FBO at the airport with activities including, but not limited to, a flight school. Avgas samples were obtained from Christiansen after three fuel deliveries. One sample was obtained from Spartan College of Aeronautics and Technology, which operates a flight school. A third flight school—Riverside—obtains avgas from Christiansen. The mean lead content of the seven avgas samples provided by Christiansen and Spartan college was 0.34 ± 0.008 g/L.

5.3 APA Field Study

Figure 15 shows the airport layout. There are three runways. Prevailing winds are from the south but tend to shift throughout the day; however, the east/west runway is still used except at high wind speeds.

Figure 15
Airport Diagram and PM Sampling and Activity Data Collection Locations Deployed at APA

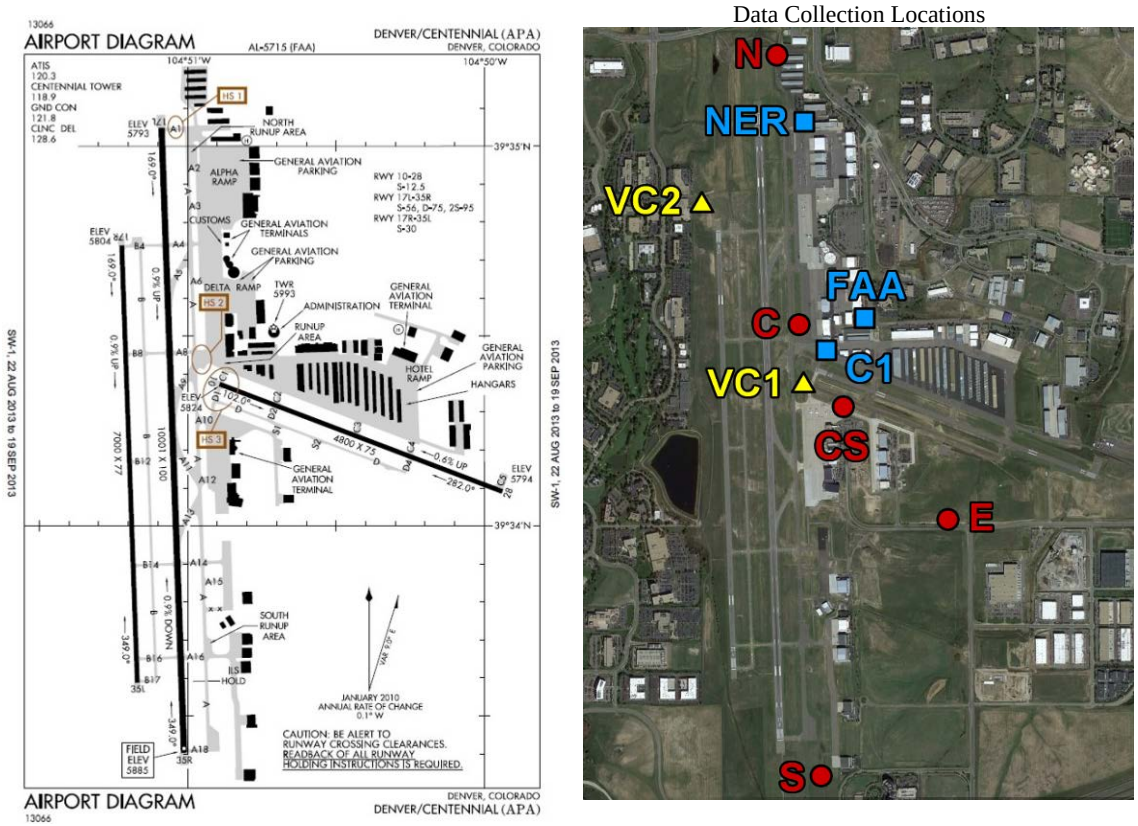

Note: PM sampling was conducted at the North (N), East (E), South (S), Center (C), and Center Secondary (CS) sites; video cameras were deployed at the VC1 and VC2 sites; and other activity data was manually collected at the C1, NER and FAA sites.

The field study was conducted from May 15 to June 10, 2013. Video cameras were deployed to record LTOs starting on April 16. PM sampling and aircraft activity data were collected from 7 AM to 7 PM MDT.

5.3.1 Aircraft Activity Data Collection

Aircraft activity data collection activities at APA are summarized in Table 30 and data collection locations are shown in Figure 15. Video cameras were continuously operated at the VC1 and VC2 locations during each 12-hour sampling event to record LTOs. Given the runway layouts at APA, it was necessary to review the video for both cameras: VC1 was used to capture LTOs on runway 10/28, and VC2 was used to capture LTOs and touch-and-go operations (TGOs) on runways 17L/35R and 17R/35L.

Figure 16 shows average hourly distribution of total operations for all aircraft (not just piston-engine aircraft) as determined from the video camera data. Touch-and-go activities accounted for 25-50% of the total operations depending on the hour with higher proportions of such operations in the mornings. Total operations peaked around 11 AM and the lowest levels were towards the end of the 7 AM to 7 PM MDT sampling periods.

About half (51%) of the operations were on runway 17R/35L, which is normally used only by piston-engine aircraft and has high touch-and-go activity. Forty percent (40%) of operations were on runway 17L/35R, which has all of the jet activity and some of the piston-engine activity. Only 9% of operations were on runway 10/28, which is used exclusively by piston-engine aircraft. For the north/south-oriented runways, 60% of operations originated at the north end (17L/17R) and 40% originated at the south end (25L/35R). For the east/west-oriented runway, 97% of operations originated at the west end (runway 10) and 3% originated at the east end (runway 28).

Thirty hours of LTOs were photographed to develop the active fleet inventory. The photographs were reviewed to identify tail numbers, which were matched to aircraft and engine specifications in the FAA registry. The resulting fleet inventory database includes a record for each operation but with the tail numbers removed. Over the 30 hours of observation, there were 365 unique aircraft identified. Eighteen aircraft (5%) accounted for one-third of the operations and 39 aircraft (11%) accounted for half of the operations (35 fixed-wing single-engine aircraft and four fixed-wing, multi-engine aircraft). Table 31 summarizes the distribution of LTOs by aircraft type; about two-thirds of the operations were single-engine piston aircraft.

Table 30
Aircraft Activity Data Collection at APA

Date	Activity Data Collection					
	VC1	VC2	Tail ID	TIM	Run-up	Comments
05/15/2013	N	N	0	0	0	VCs not deployed during PM sampler shakedown
05/16/2013	Y	Y	0	0	0	
05/17/2013	Y	Y	1	0	1	
05/18/2013	Y	Y	1	2	1	
05/19/2013	Y	Y	1	1	1	
05/20/2013	Y	Y	1	0	0	
05/21/2013	Y	Y	1	1	1	
05/22/2013	Y	Y	2	1	0	
05/23/2013	Y	Y	2	0	1	
05/24/2013	Y	Y	1	1	0	
05/25/2013	Y	Y	2	0	2	
05/26/2013	Y	Y	3	1	0	
05/27/2013	Y	Y	1	1	1	
05/28/2013	Y	Y	2	0	1	
05/29/2013	Y	Y	0	1	1	
05/30/2013	Y	Y	0	0	0	
05/31/2013	Y	Y	0	0	0	
06/01/2013	Y	Y	0	0	0	
06/02/2013	Y	Y	0	0	0	
06/03/2013	Y	Y	2	0	0	
06/04/2013	Y	Y	2	1	0	
06/05/2013	Y	Y	1	1	1	
06/06/2013	Y	N	1	1	1	VC2 hardware failure
06/07/2013	Y	N	0	1	0	VC2 hardware failure
06/08/2013	Y	Y	2	0	2	
06/09/2013	Y	Y	3	0	1	
06/10/2013	Y	Y	1	2	0	
Total Hours			30	15	15	

Note: VC = video camera for time-resolved takeoffs and landings (Y = yes, N = no); Tail ID = still photographs of planes for tail number identification; TIM = time-in-mode data collection (e.g., taxiing, takeoff, climb-out); and Run-up = run-up area activity including time in mode for magneto testing.

Figure 16
Fixed-wing Aircraft Average Hourly Operations at APA
PM sampling was conducted 7 AM to 7 PM MDT

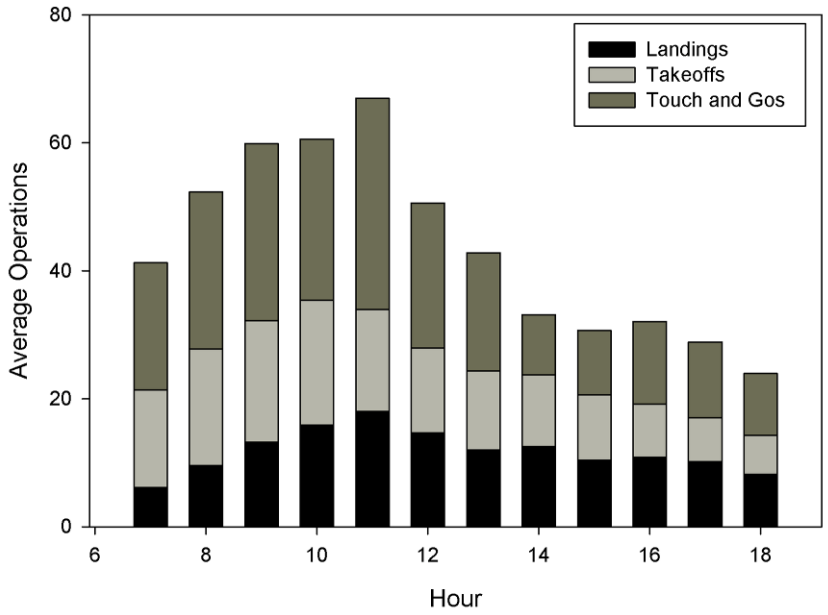

Table 31
Distribution of Aircraft Types Identified by Tail ID APA

Plane Type	Count	% of Total
Piston		
Single Engine	598	64%
Multi Engine	64	7%
Turboprop	93	10%
Jet	182	19%

Note: Based on 30 hours of still photography.

Time-in-mode data were manually collected. Piston-engine aircraft run-up activities were observed for 15 hours and included 53 run-up operations, with magneto test duration recorded for 42 of these operations. Missing magneto test data primarily resulted from confounding sources of noise. Tail numbers were recorded for 89% of the run-up operations. Table 32 and Figure 17 summarize the run-up results. Mean times in mode were 97 seconds for the magneto test and 327 seconds for the total time in the run-up area. There was large variation in these times, with standard deviations of about 60% and 100% of the means for total run-up and magneto testing, respectively. Figure 17(a) shows box plots of the total run-up and magneto test TIM data; Figure 17(b) shows cumulative distributions for the TIM data. The magneto test data are relatively

Table 32
Time in Mode Data Collected for Run-Up Operations at APA

	Total Run-Up	Magneto Testing
Number of Aircraft	53	42
Mean ± Std Dev (sec)[1]	327 ± 189	97 ± 102
Median (sec)	287	71

[1] Means are reported with 1σ standard deviation values.

Figure 17
Time-in-Mode Data for Total Time in the Run-Up Area and Duration of Magneto Testing at APA

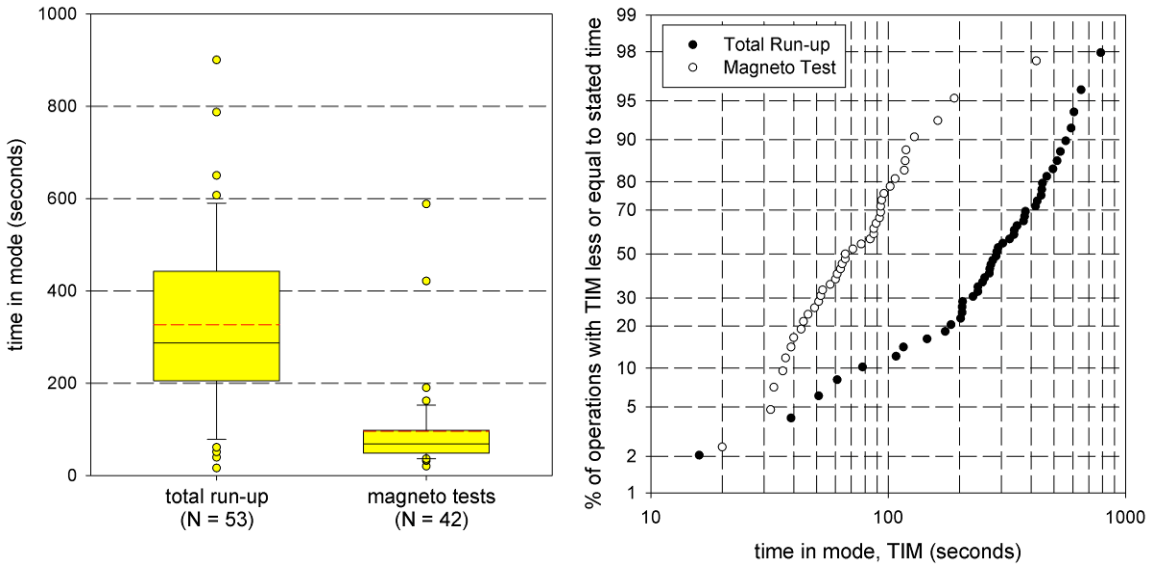

(a) (b)

Notes: (a) box plots (interior solid line is the median, interior dashed line is the arithmetic mean; box boundaries are 25th and 75th percentiles, whiskers are 10th and 90th percentiles, and circles are all records below the 10th percentile and above the 90th percentile); and (b) cumulative distributions as a log-probability plot.

well approximated by a lognormal distribution as evidenced by the nearly linear trend for the log-probability plot. The total run-up time data are not well represented by normal or lognormal distributions. Compared to RVS, the mean total run-up time and mean magneto test time were longer at APA. Both run-up time and magneto test time also showed higher variability at APA compared to RVS.

TIM data were also manually collected for piston-engine aircraft taxiing, landings, and takeoffs. Fifteen hours of operations were viewed from an observation tower. Table 33 shows summary statistics for landing, takeoff, and touch-and go times as well as average locations for wheels-up and wheels down. TIM for touch-and-go operations represents the time between wheels down on landing and the subsequent wheels-up on takeoff. Wheels-up and wheels-down locations are measured as distance from the start of the runway. There is less variation in TIM for landing and takeoff activities than for run-up activities. Wheels-up for touch-and-go operations on Runway 17R were a shorter distance down the runway than wheels-up for takeoffs on the runway; this unexpected pattern likely results from only three regular takeoffs recorded on that runway during the TIM data collection periods. Taxiing activities were logged by aircraft so trip-based taxiing times can be constructed. Similar TIM data collection and processing have been performed for other aircraft activities such as taxiing and idling, and the data are included in the database.

Table 33
Summary of Time-in-Mode and Location of Aircraft Landing and Takeoff Operations at APA

Activity/Location	Mean Time (s)	Std Dev (s)	Avg Wheels-Up (ft)	Avg Wheels-Down (ft)
Landing				
Runway 10	27	2	-[a]	700
Runway 28	37	10	-	600
Runway 17L	45	23	-	1600
Runway 17R	39	11	-	1200
Runway 35L	40	16	-	1500
Runway 35R	57	14	-	2100
Takeoff				
Runway 10	20	7	1700	-
Runway 28	20	4	2700	-
Runway 17L	27	6	2800	-
Runway 17R	-	-	3300	-
Runway 35L	19	-	1800	-
Runway 35R	37	13	3400	-
Touch-and-Go				
Runway 17L	23	-	3200	1700
Runway 17R	23	5	3000	1100
Runway 35L	23	6	2500	1400
Runway 35R	32	-	-	2100

[a] Dashes indicate no data are available.

5.3.2 Airborne PM-Pb Data Collection

PM sampling locations are shown in Figure 15, with key characteristics summarized in Table 34. The Central site is the downwind primary site, with presumably high impacts from run-up and takeoff activities on runway 10 for prevailing southerly winds as well as taxiing on taxiway A. Although information provided prior to the field campaign suggested there was little piston-engine aircraft activity on runway 17L/35R, we were subsequently informed that there is considerable piston-engine activity on this runway that may lead to significant impacts at the Central site. The East site is the upwind primary site and should capture background Pb concentrations because of its distance from airport activity. The South site is impacted by climb-out from runway 17L for southerly winds and run-up, taxiing and idling, and takeoffs from runway 35R for northerly winds. Emissions from ground-based operations east of the runways might impact this site for northerly winds. The North site should be impacted primarily by climb-out from runway 35R for northerly winds and run-up, taxiing and idling, and takeoffs from runway 17L for southerly winds. Sampling was conducted from 7 AM to 7 PM MDT.

Table 35 shows the PM samples collected each day. The goal was to operate four samplers during each event. Valid $PM_{2.5}$ samples were collected at the Central and East sites (i.e., the primary sites) for each event. Thus, there are 25 events with valid $PM_{2.5}$ data collection at the Central and East sites, which is 40% greater the objective of 17 events. The additional measurement objective of nine events with $PM_{2.5}$ and TSP sampling at the Central and East sites was met; the objective of nine events with $PM_{2.5}$ sampling at four sites was exceeded, with three additional valid samples collected at the Central Secondary site instead of the South site. All samples were analyzed for Pb with no identified issues; thus, the sample collection completeness carried through to the overall PM-Pb data completeness.

Figure 18 shows the wind rose for NWS ASOS (10 meter) 15-minute average data over all sampling periods (7 AM to 7 PM MDT). Daytime wind speeds were relatively high throughout the study, with only 1.1% calms (operationally defined as wind speeds $\leq$ 1 m/s) and 76% of 15-minute periods with wind speeds greater than 4 m/s. While prevailing winds were from the south quadrant (36%), winds from the west quadrant (22.7%) and north quadrant (21.3%) were also common. The wind direction was more variable than expected from the climatology for this period. Wind direction persistence was examined by assigning each 15-minute average wind direction to a quadrant centered on the cardinal wind directions. A wind direction was assigned to a sampling event if at least two-thirds of the 15-minute average winds were from a given quadrant; otherwise the winds were deemed to be variable. Table 35 summarizes the daily wind direction patterns. Excluding the two days with mostly missing wind data, the remaining 25 sampling events had the following distribution of winds: southerly, 2 events (8%); northerly, 4 events (16%); westerly, 1 event (4%); easterly, 1 event (4%); and variable, 17 events (68%). In contrast to RVS, there were a high proportion of events with variable winds at APA. However, the variations within sampling periods tended to be distinct shifts followed by persistent winds rather than light and variable winds. Thus, these sampling events are still conducive to dispersion modeling.

Table 34
Airborne PM Sampling Locations for the APA Study

Site	Location with Respect to Nearest Runway	Comments
Central Downwind Primary	~250m NW of 10	For prevailing southerly winds, this site was impacted by runway 10 run-ups and takeoffs. It was also impacted by taxi and idle activities around the center of the airport. (Lat: 39.574860° Long: -104.849210°)
East Upwind Primary	~1km SE of 10	For winds from the south, east, and north, this site is upwind of all ground-based activities. It is ~850m east of runway 35R and was modestly impacted by aircraft operations for winds from the west. (Lat: 39.566290° Long: -104.840830 °)
North Downwind Secondary	~300m NW of 17L	For prevailing southerly winds, this site was impacted by the northern portions of runways 35L and 35R and ground-based activities on the east side of the airport. (Lat: 39.586810° Long: -104.850550°)
South Upwind Secondary	~250m SE of 35R	For winds from the south, east, and west, this site is upwind of all ground-based activities. For northerly winds, it was impacted by ground-based activities on the east side of the airport, including run-ups and takeoffs for runway 35R. (Lat: 39.555010° Long: -104.847950°)
Central Secondary Upwind Tertiary	~200m SE of 10	For winds from the south and east, this site is upwind of all landing and takeoff operations but was impacted by taxiing on the ramp to the south of the site. For northerly winds, it was impacted by activities on runway 10. (Lat: 39.571300° Long: -104.846660°)

Table 35
Airborne PM Sampling Configurations and Wind Direction Characteristics at APA

	PM Sampling Configuration					Wind Direction Frequency and Classification					
Date	C	E	N	S	CS	Calm	N	E	S	W	Winds
05/15/2013	F	F	F		[F]	2	17	8	19	54	var
05/16/2013	F	F	F		F	0	17	17	33	33	var
05/17/2013	F	F	F		F	6	0	8	46	40	var
05/18/2013	F	F	F		F	2	15	31	6	46	var
05/19/2013	F	F	F	F		0	46	4	8	42	var
05/20/2013	F	F	F	F		4	42	23	23	8	var
05/21/2013	F	F	F	F		0	**67**	23	10	0	N
05/22/2013	F	F	F	F		4	10	65	6	15	var
05/23/2013	F	F	F	F		0	2	2	**96**	0	S
05/24/2013	F,T	F,T				*77% of records missing*					
05/25/2013	F,T	F,T				0	8	4	40	48	var
05/26/2013	F,T	F,T				0	29	29	10	31	var
05/27/2013	F,T	F,T				0	17	8	33	42	var
05/28/2013	F,T	F,T				2	15	4	**79**	0	S
05/29/2013	F	F	F	F		0	63	31	0	6	var
05/30/2013	F	F	F	F		0	10	0	2	**88**	W
05/31/2013	F	F	F	F		*77% of records missing*					
06/01/2013	F	F	F	F		0	**77**	19	4	0	N
06/02/2013	F,T	F,T				8	29	42	19	2	var
06/03/2013	F,T	F,T				0	15	0	25	60	var
06/04/2013	F,T	F,T				0	58	40	0	2	var
06/05/2013	F,T	F,T				0	15	85	0	0	E
06/06/2013	F,F	F,F				0	**67**	8	4	21	N
06/07/2013	F,F	F,[F]				0	8	0	31	60	var
06/08/2013	F,F	F,F				0	90	2	0	8	N
06/09/2013	T,T	T,T				0	19	27	23	31	var
06/10/2013	T,T	T,T				0	27	17	38	19	var

Note: The row following each interior horizontal line is a Monday. PM Sampling: F = $PM_{2.5}$, T = TSP; [ ] = invalid sample; and empty cells indicate no sample collection. Wind Direction: percentage frequency of 15-minute average ASOS 10m wind direction; and wind direction classification for events with at least two-thirds of the 15-minute winds from a given quadrant (var = variable winds).

Figure 18
Daytime (0700-1859 MDT) 15-minute Average 10m ASOS winds at APA, May 15 – June 10, 2013

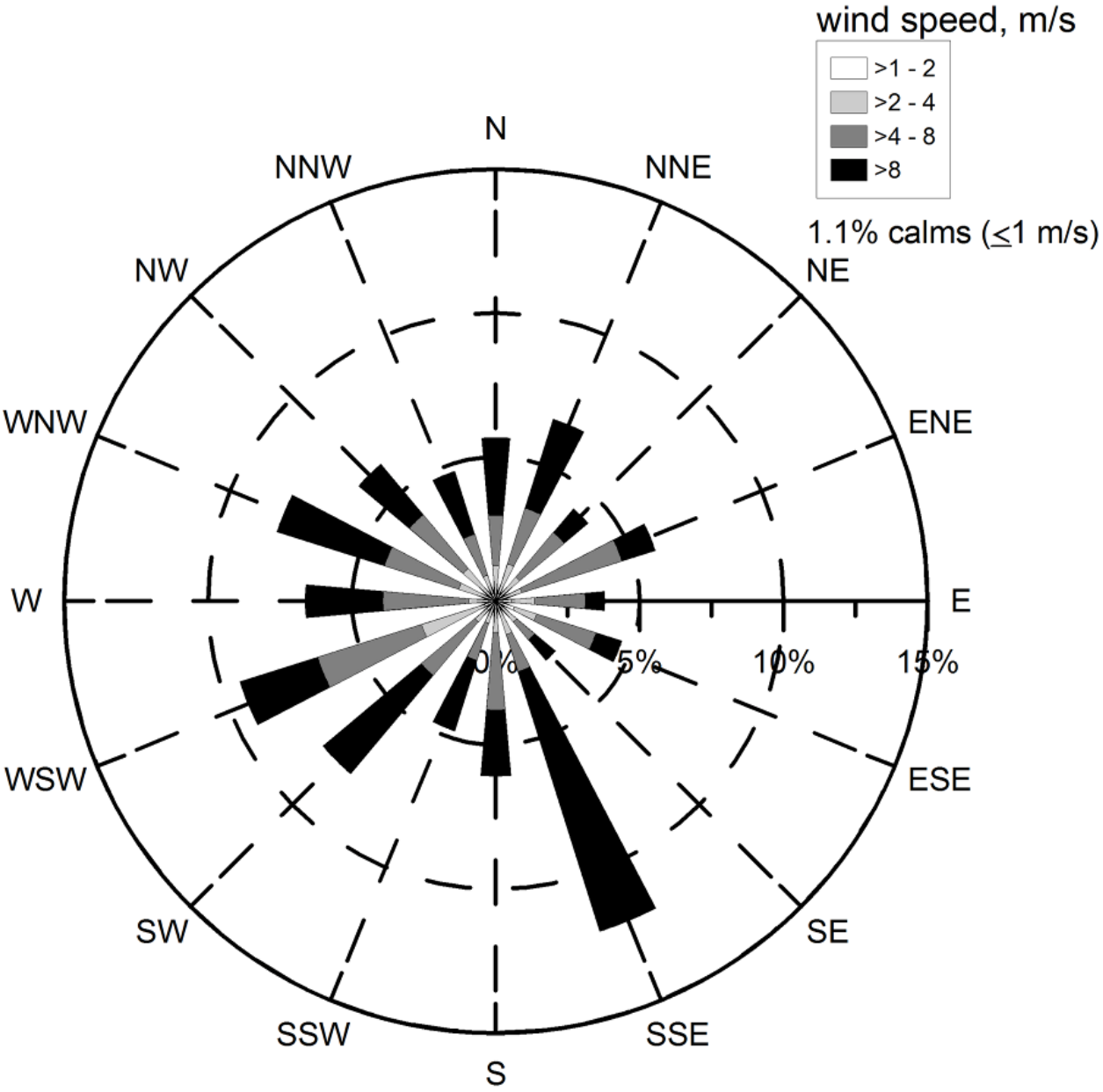

Table 36 shows the PM-Pb data for all PM samples as measured by ICP-MS. Two samples were invalidated and explanations are provided in Appendix B. Of the 80 analyzed $PM_{2.5}$ samples, 79 (99%) have a Pb concentration at least three times the $PM_{2.5}$ median field blank; of the 26 TSP samples, 24 (92%) have Pb concentrations at least three times higher than the median TSP field blank. These results demonstrate that acceptable detectability was achieved for the airborne Pb data.

Table 36
Airborne Pb Concentrations Observed at APA

	Pb Concentration (ng/m^3)						
	Central		East				Central
Date	Primary	Collocate	Primary	Collocate	North	South	Secondary
05/15/2013	16.2		1.4		2.0		--
05/16/2013	22.7		1.5		5.4		4.3
05/17/2013	27.2		1.3		12.0		4.0
05/18/2013	20.5		3.5		2.3		9.3
05/19/2013	8.1		1.2		1.3	3.5	
05/20/2013	7.7		2.2		1.5	1.9	
05/21/2013	35.4		1.8		1.2	3.4	
05/22/2013	8.4		3.0		2.3	2.0	
05/23/2013	47.1		0.4		6.6	0.2	
05/24/2013	18.3	[25.5]	1.6	[2.2]			
05/25/2013	16.9	[21.7]	1.9	[2.6]			
05/26/2013	12.4	[22.0]	2.8	[2.1]			
05/27/2013	12.8	[12.5]	1.8	[1.8]			
05/28/2013	26.1	[27.7]	1.8	[2.1]			
05/29/2013	3.1		1.0		1.0	0.9	
05/30/2013	4.7		1.9		1.6	1.1	
05/31/2013	4.3		1.2		0.3	2.0	
06/01/2013	4.1		1.1		4.9	1.3	
06/02/2013	7.8	[10.1]	2.0	[1.7]			
06/03/2013	8.8	[1.2]	1.4	[2.6]			
06/04/2013	3.3	[4.0]	1.2	[1.8]			
06/05/2013	11.1	[9.8]	0.4	[0.0]			
06/06/2013	17.3	15.4	5.6	4.9			
06/07/2013	19.6	--	1.2				
06/08/2013	5.7	5.5	2.6	2.4			
06/09/2013	[13.2]	[11.7]	[2.3]	[3.8]			
06/10/2013	[13.9]	[15.5]	[1.9]	[0.9]			

Note: The row following each interior horizontal line is a Monday. Data are $PM_{2.5}$-Pb unless otherwise noted. [ ] = TSP; "--" = invalid sample; and empty cells indicate no sample collection.

Figure 19 compares $PM_{2.5}$-Pb at the Central and East sites. The minimum ratio of Central site concentration to East site concentration was 2.2. While it is difficult to stratify the data based on wind direction because of the within-sample wind variations, the highest ratios usually occurred for higher wind frequencies from the south or west.

Figure 19
$PM_{2.5}$-Pb at the Central and East Sites at APA

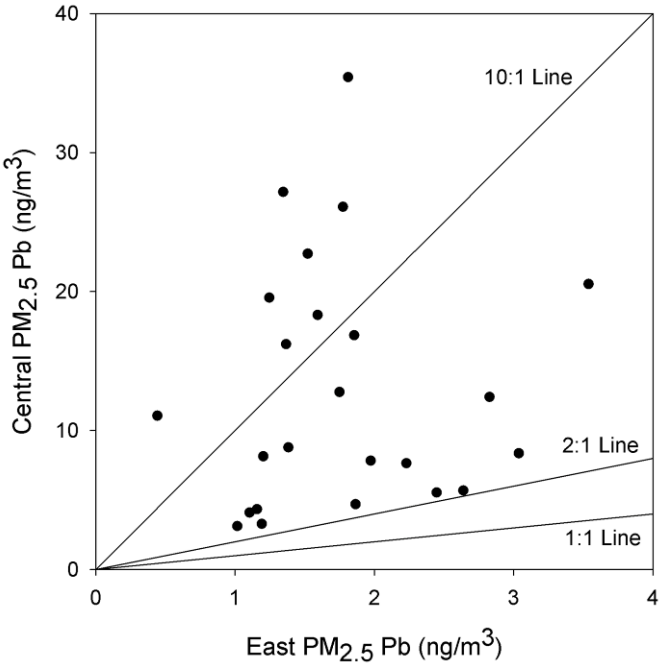

This pattern clearly indicates the downwind Central site is impacted by aircraft operations. In contrast, for sampling events with a higher frequency of northerly or easterly winds the ratios of $PM_{2.5}$-Pb at the Central and East sites are usually lower. In summary, the East site appears to represent background Pb levels for all conditions, with the Central site more strongly impacted for winds from the south or west. The $PM_{2.5}$-Pb levels at the North and South sites were above or within the measurement error, as defined by the collocated precision, of the $PM_{2.5}$-Pb at the East site. This supports the selection of the East site as a proper background site for the airport and also demonstrates the localized nature of concentration hot spots near zones such as the Central site. Additionally, the Central Secondary site was used for three days of sample collection. The $PM_{2.5}$-Pb measured at the Central Secondary site was about three times higher than the East site for each day and the difference between the two sites exceeded the measurement error.

Figure 20 shows TSP-Pb versus $PM_{2.5}$-Pb for the Central and East sites. The high-concentration samples show enrichment of Pb in TSP but most of the Pb is in the $PM_{2.5}$ size range. One sample has a higher Pb concentration in $PM_{2.5}$ than in TSP, which is physically unrealistic; however, this sample may have been contaminated as there were large specks and dirt on the $PM_{2.5}$ filter after sampling (such cases were rare and these observations were flagged in the data set). The mean concentration for Pb in the TSP-minus-$PM_{2.5}$ size range (i.e., coarse particles) was 2.6 ng/m^3, excluding the sample with higher $PM_{2.5}$-Pb than TSP-Pb. For the four samples with elevated Pb levels, $PM_{2.5}$-Pb was 56-94% of TSP-Pb. The relatively low concentrations for Pb in $PM_{TSP-2.5}$ compared to Pb in $PM_{2.5}$ at the piston-engine aircraft-impacted sites strongly suggest that the observed $PM_{2.5}$-Pb in these samples is from direct aircraft exhaust emissions and not the tail of coarse mode PM-Pb extending below 2.5 µm.

Figure 20
TSP-Pb versus $PM_{2.5}$-Pb at the Central and East Sites at APA

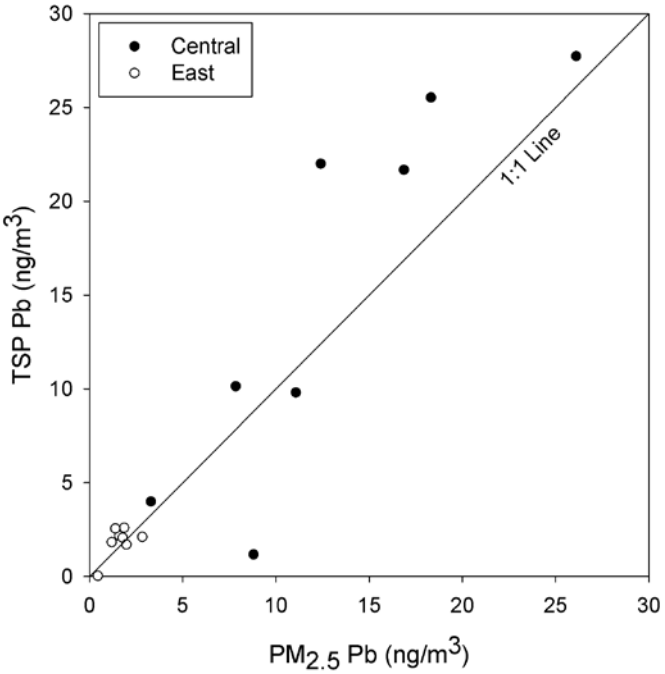

5.3.3 Avgas Data Collection

Nine aviation gasoline (avgas) samples were collected from the FBOs. TAC Air and Denver Jet Center are the largest FBOs at the airport in terms of gasoline distribution. Three avgas samples were obtained from Denver Jet Center and four were obtained from TAC Air. One sample was obtained from Signature Flight Support and another sample was obtained from XOJet. The mean lead content of the seven avgas samples provided by Denver Jet Center and TAC Air was 1.57 ± 0.3 g/gal. The samples from XOJet (1.32 g/gal) and Signature Flight Support (2.08 g/gal) were excluded from this calculation because they are jet-focused FBOs and distribute limited amounts of avgas.

5.4 SMO Field Study

Figure 21 shows the airport layout. There is only one runway at SMO. Prevailing winds were from the southwest throughout the entire field study, which was conducted from July 3 to July 30, 2013.

Figure 21
Airport Diagram and PM Sampling and Activity Data Collection Locations Deployed at SMO

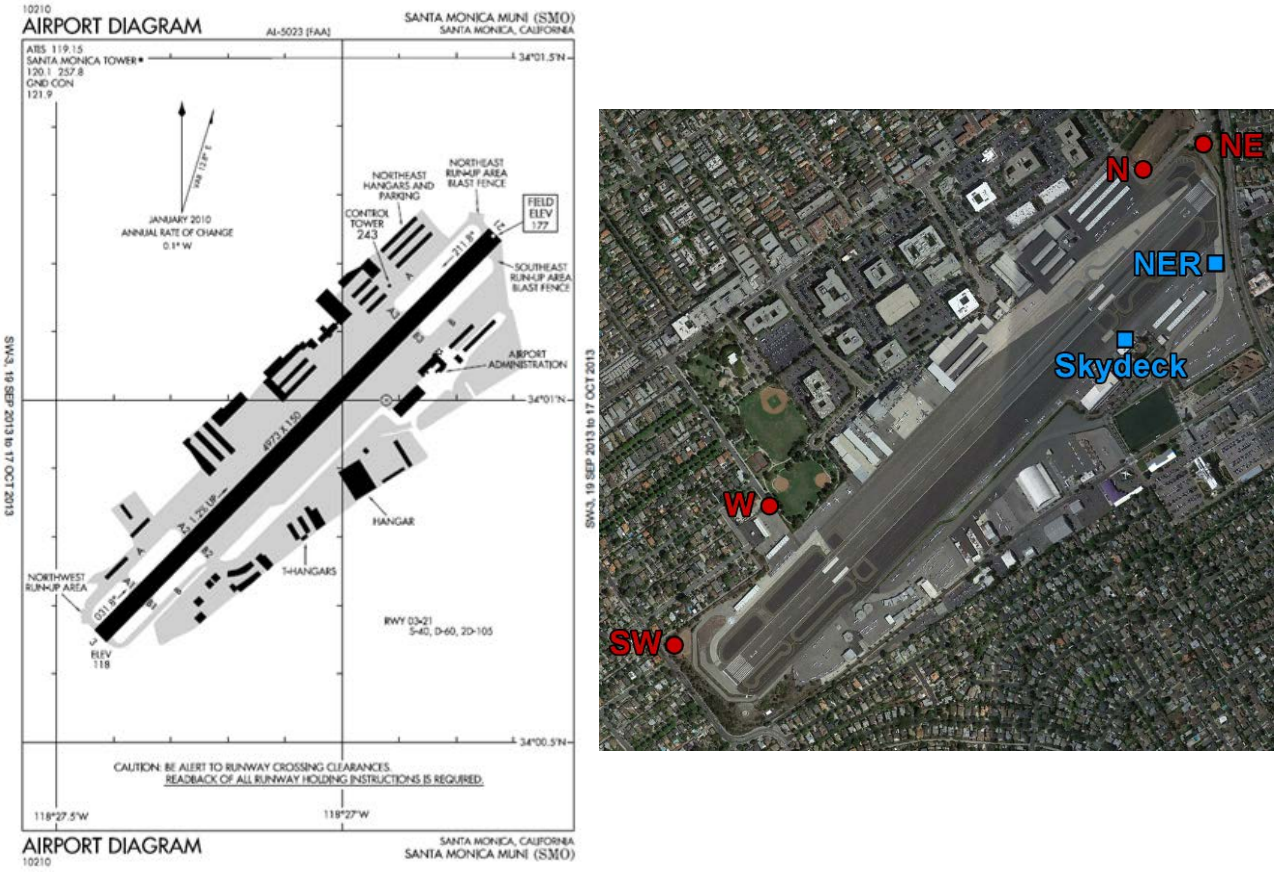

Note: PM sampling was conducted at the North (N), Northeast (NE), West (W), and Southwest (SW) sites; video cameras were deployed at the North site; and other activity data was manually collected at the Skydeck and NER sites.

5.4.1 Aircraft Activity Data Collection

Aircraft activity data collection activities at SMO are summarized in Table 37 and data collection locations shown in Figure 21. Video cameras were continuously operated at

Table 37
Aircraft Activity Data Collection at SMO

Date	Activity Data Collection					
	VC1	VC2	Tail ID	TIM	Run-up	Comments
07/03/2013	Y	Y	0	0	0	
07/04/2013	Y	Y	1	1	0	
07/05/2013	Y	Y	0	0	0	
07/06/2013	Y	Y	2	2	0	
07/07/2013	Y	Y	2	1	0	
07/08/2013	Y	Y	2	0	1	
07/09/2013	Y	Y	0	1	2	
07/10/2013	Y	Y	2	2	0	
07/11/2013	Y	Y	0	1	2	
07/12/2013	Y	Y	1	1	0	
07/13/2013	Y	Y	0	0	0	
07/14/2013	Y	Y	0	0	0	
07/15/2013	Y	Y	0	0	0	
07/16/2013	Y	Y	0	0	0	
07/17/2013	Y	Y	1	0	0	
07/18/2013	Y	Y	2	0	0	
07/19/2013	Y	Y	2	0	1	
07/20/2013	Y	Y	2	0	2	
07/21/2013	Y	Y	2	1	1	
07/22/2013	Y	Y	1	2	0	
07/23/2013	Y	Y	2	1	0	
07/24/2013	Y	Y	0	0	1	No run-up activity during collection period
07/25/2013	Y	Y	2	0	0	
07/26/2013	Y	Y	2	0	0	
07/27/2013	Y	Y	2	0	2	
07/28/2013	Y	Y	2	1	3	
07/29/2013	Y	Y	1	1	0	
07/30/2013	Y	Y	0	0	1	
Total Hours			30	15	15	

Note: VC = video camera for time-resolved takeoffs and landings (Y = yes, N = no); Tail ID = still photographs of planes for tail number identification; TIM = time-in-mode data collection (e.g., taxiing, takeoff, climb-out); and Run-up = run-up area activity including time in mode for magneto testing.

the North site during each 12-hour sampling event to record LTOs. One camera was set up to determine the number of LTOs, while a second camera was set up to enhance run-up time characterization. In contrast to RVS and APA, where the runways covered large footprints, the activities at SMO are more concentrated and the fractions of jets, turboprops, and piston-engine aircraft could be determined from the video camera data. Given the positioning of the video camera, however, it was sometimes difficult to distinguish touch-and-go operations from normal landings; therefore, touch-and-go operations are underrepresented and normal landings are overrepresented in this data set. The TIM data collected at SMO may be able to close this data gap. Figure 22 shows average hourly piston-engine operations for the entire study period (in contrast, Figure 9 for RVS and Figure 16 for APA include all fixed-wing aircraft). Touch-and-go activities are counted as two operations each. From 11 AM to 4 PM, the total hourly operations were relatively high and consistent from hour to hour.

Thirty hours of LTOs were photographed from the Skydeck to develop the active fleet inventory. The photographs were reviewed to identify tail numbers, which were matched to aircraft and engine specifications in the FAA registry. The resulting fleet inventory database includes a record for each operation but with the tail numbers removed. Over the 30 hours of observation, 247 unique aircraft were identified. Twelve aircraft (5%) accounted for one-third of the operations and 25 aircraft (10%) accounted for half of the operations (24 fixed-wing, single-engine aircraft and one fixed-wing, multi-engine aircraft). Table 38 summarizes the distribution of LTOs by aircraft type; more than three-fourths of the operations were single-engine piston aircraft.

TIM data were manually collected. Piston-engine aircraft run-up activities were observed for 15 hours and included 41 run-up operations, with magneto test duration recorded for 36 of these operations. Missing magneto test data primarily resulted from confounding sources of noise. Tail numbers were recorded for 95% of the run-up operations. Twenty-three planes bypassed the run-up area and did not perform run-ups that were observed. Table 39 and Figure 23 summarize the run-up results. Mean TIM was 61 seconds for the magneto test and 328 seconds for the total time in the run-up area. There was a large variation in these times, with standard deviations of about 70% and 80% of the means for total run-up and magneto testing, respectively. Figure 23(a) shows box plots of the total run-up and magneto test TIM data, and Figure 23(b) shows cumulative distributions for the TIM data. Both total run-up time and magneto test data are relatively well approximated by a lognormal distribution as evidenced by the nearly linear trend for the log-probability plot. Mean total run-up times at SMO and APA were similar, with shorter total run-up times at RVS. The highest variability in total run-up time was observed at SMO. Mean magneto test times at SMO were shorter than at RVS and APA. The magneto test times at SMA and RVS had similar variability, with higher variability observed at APA.

Figure 22
Piston-Engine Aircraft Average Hourly Operations at SMO

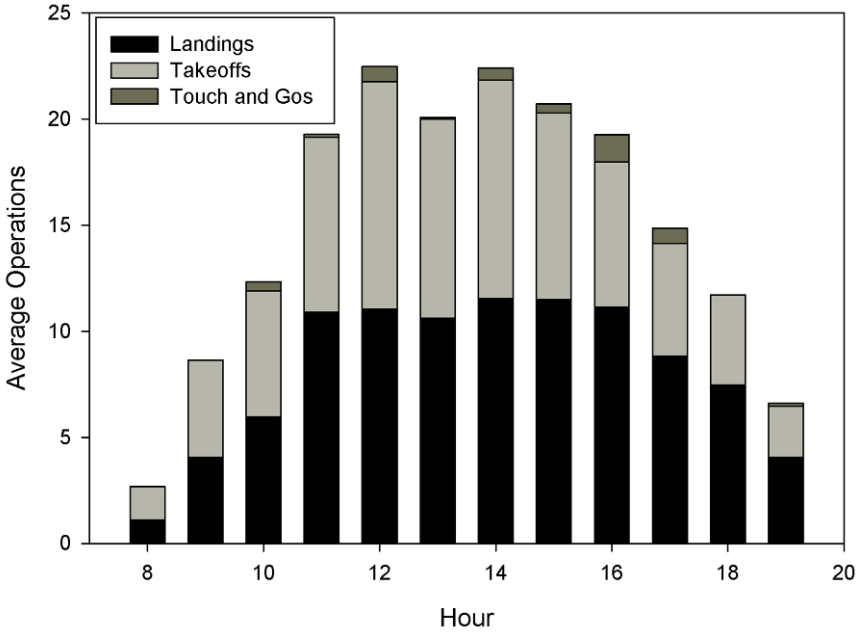

Note: PM sampling was conducted from 8 AM to 8 PM PDT.

Table 38
Distribution of Aircraft Types Identified by Tail ID at SMO

Plane Type	Count	% of Total
Piston		
Single Engine	447	78%
Multi Engine	11	2%
Turboprop	32	6%
Jet	81	14%

Note: Based on 30 hours of still photography.

Table 39
Time-in-Mode Data Collected for Run-Up Operations Including Magneto Testing at SMO

	Total Run-Up	Magneto Testing
Number of Aircraft	41	36
Mean ± Std Dev (sec)[a]	328 ± 215	61 ± 52
Median (sec)	244	42

Notes: Means are reported with 1σ standard deviation values.

Figure 23
Time-in-Mode Data for Total Time in the Run-Up Area and Duration of Magneto Testing at SMO

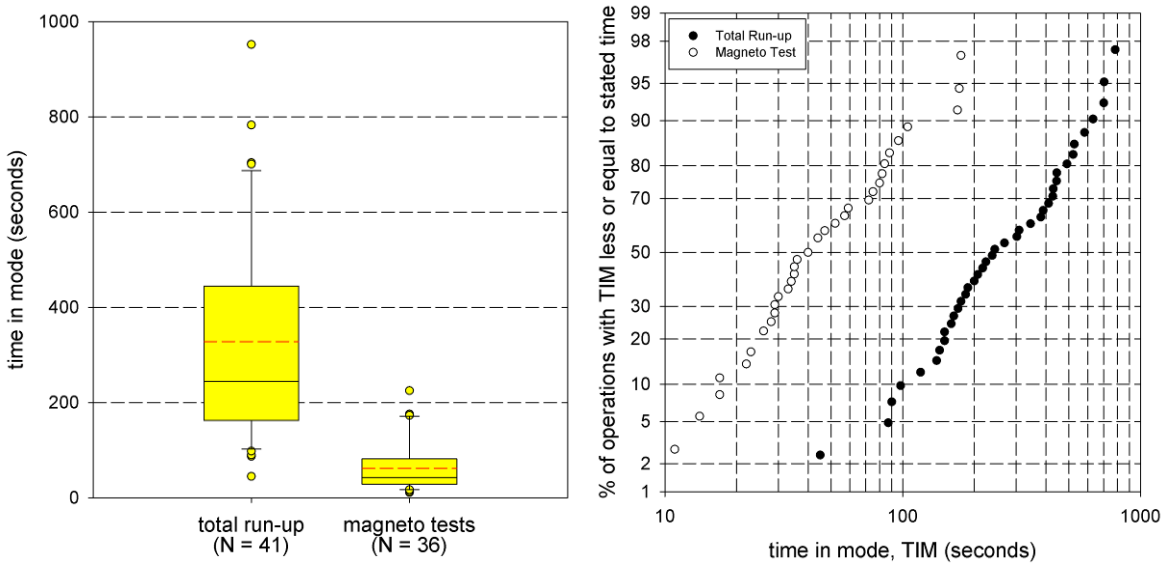

(a) (b)

Notes: (a) box plots (interior solid line is the median, interior dashed line is the arithmetic mean; box boundaries are 25th and 75th percentiles, whiskers are 10th and 90th percentiles, and circles are all records below the 10th percentile and above the 90th percentile); and (b) cumulative distributions as a log-probability plot.

TIM data were also manually collected for piston-engine aircraft taxiing, landings, and takeoffs. Fifteen hours of operations were viewed from an observation deck. Table 40 shows summary statistics for landing, takeoff, and touch-and-go times, as well as average locations for wheels-up and wheels-down. TIM for touch-and-go operations represents the time between wheels down on landing and the subsequent wheels up on takeoff. Wheels-up and wheels-down locations are measured as the distance from the start of the runway. There is less variation in the time-in-mode for landing and takeoff activities than for run-up activities. Taxiing activities were logged by aircraft so trip-based taxiing times can be constructed. Similar time-in-mode data collection and processing has been performed for other aircraft activities such as taxiing and idling and the data are included in the database.

Table 40
Summary of Time-in-Mode and Location of Aircraft Landing and Takeoff Operations at SMO

Activity/Location	Mean Time (s)	Std Dev (s)	Avg Wheels-Up (ft)	Avg Wheels-Down (ft)
Landing				
Runway 21	37	14	-[a]	1200
Takeoff				
Runway 3	21	2	2100	-
Runway 21	15	3	1200	-
Touch-and-Go				
Runway 21	10	4	1600	930

[a] Dashes indicate no data.

5.4.2 Airborne PM-Pb Data Collection

Figure 21 depicts PM sampling locations, and Table 41 summarizes the key characteristics. The Northeast site is the downwind primary site, with presumably high impacts from run-up, taxiing and idling, and takeoff activities on runway 21 for prevailing southwesterly winds. In contrast to RVS and APA, it was not possible to locate the upwind primary site on the airport footprint far removed from aircraft activities. The Southwest site is the upwind primary site and should, to a large extent, capture background Pb concentrations; however, it might be influenced by climb-out, for prevailing southwesterly winds. The North site is impacted by taxiing and climb-out from runways 3 and 21 for southwesterly winds. Emissions from ground-based operations north of the runway might impact this site for prevailing winds. The West site should be impacted primarily by climb-out from runway 3 for southwesterly winds and ground-based activities for southerly and southeasterly winds. Sampling was conducted from 8 AM to 8 PM PDT.

Table 42 shows the PM samples collected each day. Although the goal was to operate four samplers during each event, one of the PQ100 samplers failed on the first day of the study and only three samplers were available until a rental unit could be obtained while the original was being repaired. Valid $PM_{2.5}$ samples were collected at the Northeast and Southwest sites (i.e., the primary sites) for each event. Thus, there are 25 events with valid $PM_{2.5}$ sample collection at the Northeast and Southwest sites, which is nearly 50% greater than the objective of 17 events. The additional measurement objectives of nine events with $PM_{2.5}$ and TSP sampling at the Northeast and Southwest sites was met; however, the objective of nine events with $PM_{2.5}$ sampling at four sites was not met, with only six valid samples collected at the West site because of the sampler failure that required a replacement unit. All samples were analyzed for Pb and three samples were invalidated because of contamination issues (Northeast and Southwest on July 13, and West on July 17). The justification for invalidating samples is provided in Appendix B. This reduced the PM-Pb data completeness to 24 events with $PM_{2.5}$ data at the Northeast and Southwest sites and four events with $PM_{2.5}$ sampling at the two primary sites and two secondary sites. There were eight events with $PM_{2.5}$ sampling at the two primary sites and the North secondary site.

Table 41
Airborne PM Sampling Locations for the SMO Study

Site	Location with Respect to Nearest Runway	Comments
Northeast Downwind Primary	~100m N of 21	For prevailing southwesterly winds, this site was impacted from runway 21 run-ups and takeoffs. It was also significantly impacted by taxiing and idling on Taxiways A and B. (Lat: 34.021490° Long: -118.445531°)
Southwest Upwind Primary	~150m NW of 3	For winds from the southwest, this site is upwind of all ground-based activities but may be impacted by climb-out. It may be impacted by aircraft operations for winds from the east. (Lat: 34.011560° Long: -118.458439°)
North Downwind Secondary	~150m W of 21	For prevailing southwesterly winds, this site was impacted by takeoffs and run-ups on runway 3, as well as most ground-based activities on Taxiways A and B. (Lat: 34.021030° Long: -118.447011°)
West Upwind Secondary	~400m NE of 3	For winds from the southwest, this site is upwind of all activities on runway 21 and the northeast side of the airport. It may be impacted by activities at the southwest end of the airport. For southeasterly winds, it is potentially impacted by ground-based activities at the southern end of the airport. In contrast to the other three sites that were sited in open fetch, the West site was near obstructions (buildings, trees). (Lat: 34.014300° Long: -118.456050°)

Figure 24 shows the wind rose for NWS ASOS (10 meter) 15-minute average data over all sampling periods (8 AM to 8 PM PDT). Daytime wind speeds were relatively high throughout the study with only 7.1% calms (operationally defined as wind speeds ≤ 1 m/s) and 54% of 15-minute periods with wind speeds less than 4 m/s. Prevailing winds were from the southwest quadrant for the vast majority of the study period (94%).

Table 42
Airborne PM Sampling Configurations and Wind Direction Characteristics at SMO

Date	PM Sampling Configuration				Wind Direction Frequency and Classification					
	NE	SW	N	W	Calm	NW	NE	SE	SW	Winds
07/03/2013	F	F			0	0	0	2	**98**	SW
07/04/2013	F	F	F		0	0	0	4	**96**	SW
07/05/2013	F	F	F		4	0	6	10	**79**	SW
07/06/2013	F	F	F		0	2	0	4	**94**	SW
07/07/2013	F,T	F,T			0	0	0	0	**100**	SW
07/08/2013	F,T	F,T			0	0	0	0	**100**	SW
07/09/2013	F,T	F,T			0	0	0	2	**98**	SW
07/10/2013	F,T	F,T			0	6	0	4	**90**	SW
07/11/2013	F,T	F,T			2	0	0	21	**77**	SW
07/12/2013	F	F	F	F	*0*	0	0	19	**81**	SW
07/13/2013	[F]	[F]	F	F	0	2	0	2	**96**	SW
07/14/2013	F	F	F	F	2	0	0	6	**92**	SW
07/15/2013	F	F	F	F	0	0	0	0	**100**	SW
07/16/2013	F	F	F	F	*58% of records missing*					
07/17/2013	F	F	F	[F]	0	0	0	0	**100**	SW
07/18/2013	F,T	F,T			0	0	0	10	**90**	SW
07/19/2013	F,T	F,T			0	0	0	0	**100**	SW
07/20/2013	F,T	F,T			0	0	0	17	**83**	SW
07/21/2013	F,T	F,T			0	2	0	10	**88**	SW
07/22/2013	F,F	F,F			0	0	0	0	**100**	SW
07/23/2013	F,F	F,F			0	0	0	0	**100**	SW
07/24/2013	F,F	F,F			0	0	0	2	**98**	SW
07/25/2013	F,F	F,F			0	0	0	0	**100**	SW
07/26/2013	F,F	F,F			0	0	0	6	**94**	SW
07/27/2013	F,F	F,F			0	0	0	0	**100**	SW
07/28/2013	T,T	T,T			0	0	0	0	**100**	SW
07/29/2013	T,T	T,T			0	0	0	0	**100**	SW
07/30/2013	T,T	T,T			0	6	0	0	**94**	SW

Notes: The row following each interior horizontal line is a Monday. PM Sampling: F = $PM_{2.5}$, T = TSP, [ ] = invalid sample, and empty cells = no sample collection. Wind Direction: percentage frequency of 15-minute average ASOS 10m wind direction; and wind direction classification for events with at least two-thirds of the 15-minute winds from a given quadrant.

Figure 24
Daytime (0800-1959 PDT) 15-minute Average 10m ASOS Winds at SMO, July 3 – 30, 2013

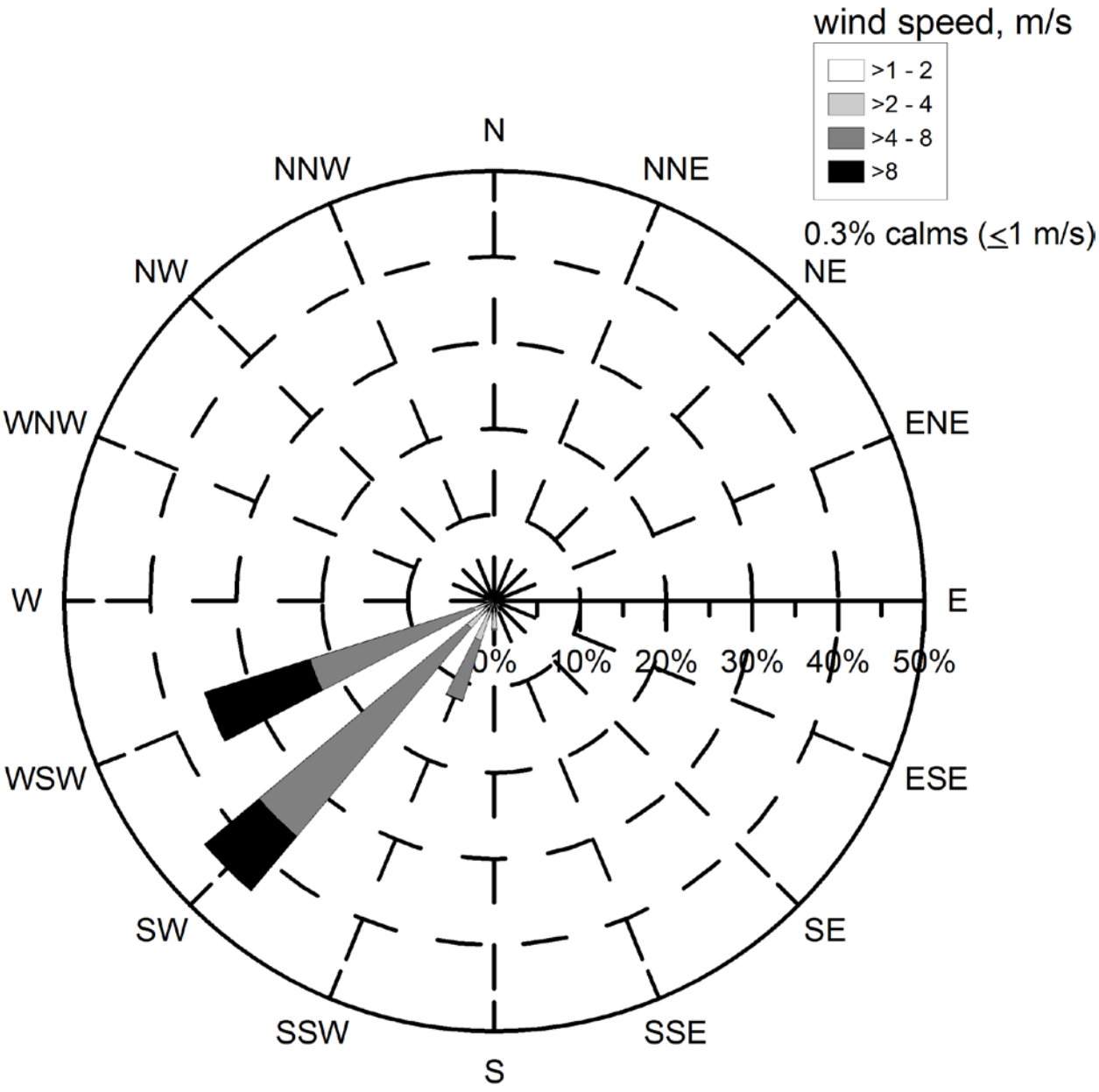

Wind direction persistence was examined by assigning each 15-minute average wind direction to a quadrant centered on the wind directions midway between the cardinal directions. A wind direction was assigned to a sampling event if at least two-thirds of the 15-minute average winds were from a given quadrant; otherwise, the winds were deemed to be variable. Table 42 above summarizes the daily wind direction patterns. Excluding the day with mostly missing wind data, all sampling events were classified as southwesterly winds. Winds were much more consistent at SMO than they were at either APA or RVS. While the criterion of winds being from a given quadrant for two-thirds of the time might seem relatively lax, for 22 of the 27 events with available ASOS wind direction the winds were from the southwest for at least 90% of the sampling period.

A laboratory contamination issue was discovered that affected samples from July 3 through July 21, with the exception of those samples sent for XRF analysis. The source of this contamination was determined to be the acid bath for cleaning the glassware used in sample preparation. To quantify the contamination, "glassware blanks" were collected prior to and following replacement of the acid bath and these samples were analyzed using ICP-MS. The median contamination level corresponded to 2.8 ng/m^3, and this value was subtracted from all samples digested in the contaminated batches. The overall impact of the contamination is quite modest for samples collected at the Northeast (downwind primary) site, with 21 of the 23 samples having a corrected concentration more than five times the correction value and 50% of the Northeast samples having corrected concentrations more than ten times the correction value. Corrected field blank concentrations ranged from -2 to +2 ng/m^3; for the Northeast site, six of the seven TSP-Pb values were greater than the corresponding $PM_{2.5}$-Pb values, with the one exception having a difference within the measurement error. The contamination had a greater impact on data collected at the remaining sites (Southwest, North, and West) where the PM-Pb concentrations are much lower. Appendix B discusses the rationale for voiding the Northeast and Southwest samples on July13 and the West sample on July 17.

Table 43 shows the PM-Pb data for all PM samples as measured by ICP-MS and including the correction for contamination. Of the 57 analyzed $PM_{2.5}$ samples, 45 (79%) have a Pb concentration at least three times the $PM_{2.5}$ median field blank. Additionally, 29 (97%) of the 30 analyzed $PM_{2.5}$ samples collected at the North and Northeast sites have a Pb concentration at least three times the $PM_{2.5}$ median field blank. Of the 30 TSP samples, 26 (87%) have Pb concentrations at least three times higher than the median TSP field blank. These results demonstrate that acceptable detectability was achieved for the airborne Pb data.

Figure 25 compares $PM_{2.5}$-Pb at the Northeast and Southwest sites. Of the 30 data pairs, 29 (97%) have downwind to upwind ratios of greater than five, and 20 (67%) have a ratio of greater than 20. This pattern clearly indicates the downwind Northeast site is impacted by aircraft operations. $PM_{2.5}$-Pb levels at the Southwest site were below or within the measurement error, as defined by the collocated precision, of the $PM_{2.5}$-Pb at the North site and West site for days without contaminated samples. These patterns support the assignment of the Southwest site as a background site for the airport. For 6 of the 9 days with sampling at the North site, $PM_{2.5}$-Pb at that site was at least double the Southwest site. This shows that the North site is likely impacted from aircraft climb-out and possibly ground operations.

Table 43
Airborne Pb Concentrations Observed at SMO

	Pb Concentration, n/m^3					
	Northeast		Southwest			
Date	Primary	Collocate	Primary	Collocate	North	West
07/03/2013	29.0		1.7			
07/04/2013	16.9		< 0		3.3	
07/05/2013	< 0		3.3		6.8	
07/06/2013	36.8		3.7		8.6	
07/07/2013	27.5	[35.3]	0.3	[4.5]		
07/08/2013	20.5	[50.5]	1.0	[2.5]		
07/09/2013	25.5	[39.6]	0.4	[2.9]		
07/10/2013	37.7	[46.6]	3.2	[3.9]		
07/11/2013	27.9	[37.8]	4.7	[2.9]		
07/12/2013	30.7		1.6		7.3	0.0
07/13/2013	--		--		10.7	7.6
07/14/2013	71.8		1.0		5.4	1.7
07/15/2013	6.8		< 0		5.5	< 0
07/16/2013	29.9		1.0		5.6	1.7
07/17/2013	30.5		< 0		3.4	--
07/18/2013	32.4	[42.4]	2.0	[0.8]		
07/19/2013	44.9	[61.4]	4.2	[2.3]		
07/20/2013	27.6	[26.8]	< 0	[1.7]		
07/21/2013	34.2	[47.1]	0.1	[0.9]		
07/22/2013	20.6	21.6	0.9	0.6		
07/23/2013	19.9	20.8	0.2	0.3		
07/24/2013	18.9	25.4	0.2	1.3		
07/25/2013	15.0	17.1	0.0	0.9		
07/26/2013	36.1	31.9	1.4	1.2		
07/27/2013	67.1	32.1	0.4	0.5		
07/28/2013	[33.2]	[35.1]	[1.0]	[1.4]		
07/29/2013	[26.0]	[29.3]	[1.7]	[1.8]		
07/30/2013	[59.6]	[57.2]	[2.0]	[1.0]		

Notes: The row following each interior horizontal line is a Monday. Data are $PM_{2.5}$-Pb unless otherwise noted. [ ] = TSP; and empty cells indicate no sample collection. 2.8 ng/m^3 was subtracted from the underlined samples through to correct for laboratory contamination; negative concentration values after applying this correction are denoted by "< 0". Samples denoted with a dash (--) were invalidated because of contamination.

Figure 25
$PM_{2.5}$-Pb at the Northeast and Southeast Sites at SMO

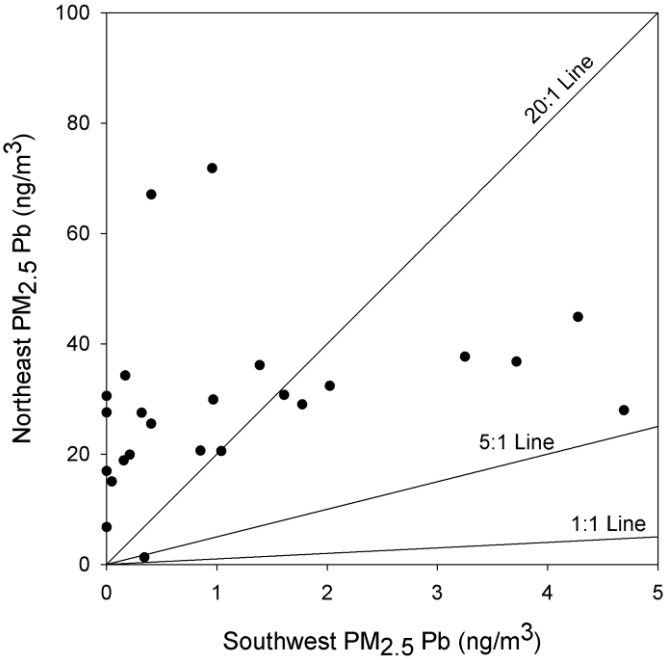

Note that the y-axis range is 20 times the x-axis range.

Figure 26 shows TSP-Pb versus $PM_{2.5}$-Pb for the Northeast and Southwest sites. One sample has a higher Pb concentration in $PM_{2.5}$ than in TSP, which is physically unrealistic; however, the difference is within the measurement error. The average $PM_{TSP-2.5}$ concentration at the Northeast site was 12 ng/m^3, which is 40% of the average $PM_{2.5}$-Pb for the same sample days. $PM_{2.5}$-Pb was 41-100% with only one sample pair below 64%. Thus, TSP-Pb at the Northeast site is dominated by $PM_{2.5}$-Pb, which supports the Pb at this site being predominantly from direct piston-engine aircraft exhaust, but with significant contributions from the tail of coarse mode PM-Pb extending below 2.5 µm.

Figure 26
TSP-Pb versus $PM_{2.5}$-Pb at the Northeast and Southwest Sites at SMO

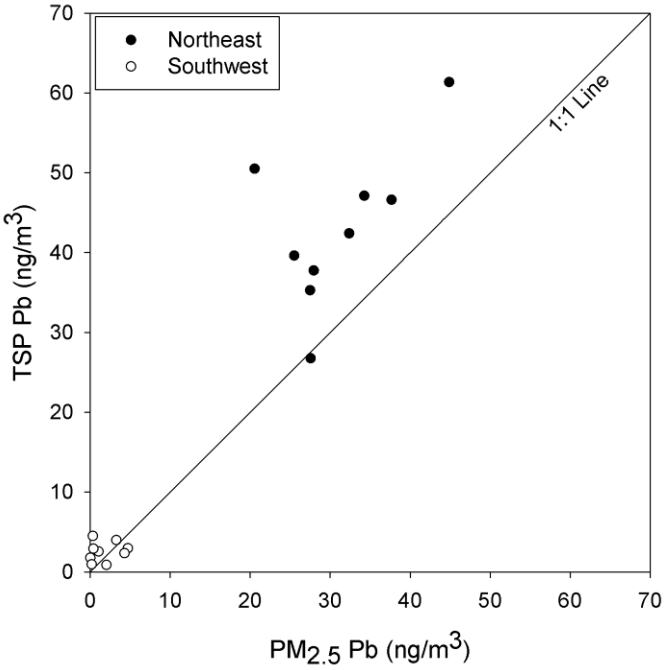

5.4.3 Avgas Data Collection

Because the SMO FBOs that sell avgas declined to provide gasoline samples, two avgas samples were collected from SMO-based planes. One sample was collected from an aircraft that had recently refueled at the American Flyers FBO and another sample was collected from an aircraft that was under maintenance (at Bill's Air Center). Avgas samples were analyzed by Intertek Caleb Brett for Pb content analysis using test method ASTM D5059. The lead content was 0.489 g/L (1.85 g/gal) from the plane fueling at American Flyers and 0.522 g/L (1.98 g/gal) from the plane under maintenance. The relative volumes of avgas in the aircraft tanks from fueling at SMO versus other airports are not known.

5.5 LTOs from On-Site Observations and ATADS

As described in Section 5.1, LTOs were captured using video cameras deployed during each 12-hour PM-Pb sampling period. ATADS data were obtained for each day of on-site data collection and are compared to the LTOs recorded by video camera. Figure 27 shows the distributions of the ratio of 12-hour (daytime) video recorded operations to corresponding daily ATADS-reported operations. For all three airports, LTOs from the video data are lower than ATADS data with mean ratios of ~60% at RVS and APA, and ~85% at SMO. Part of the video data deficit is from LTOs prior to or following the 12-hour video data collection period. However, at APA the FAA also provided hourly LTO counts used to generate the ATADS-reported data and only ~10% of all FAA counted

observations occurred outside the 12-hour video data collection period. For APA, this still leaves a difference of ~30% between the video data and ATADS data. The relatively better agreement at SMO might arise in part from the restrictions on nighttime activity, which reduce the LTOs outside the 12-hour daytime video data collection period. There are several factors that could contribute to the discrepancies, such as overflights that are counted by the FAA and requested operations that are cleared by the FAA but subsequently aborted. More work is needed to explain these differences, which do impact the emissions estimates.

Figure 27
Distributions of Daily Video-Recorded and ATADS-Reported LTOs

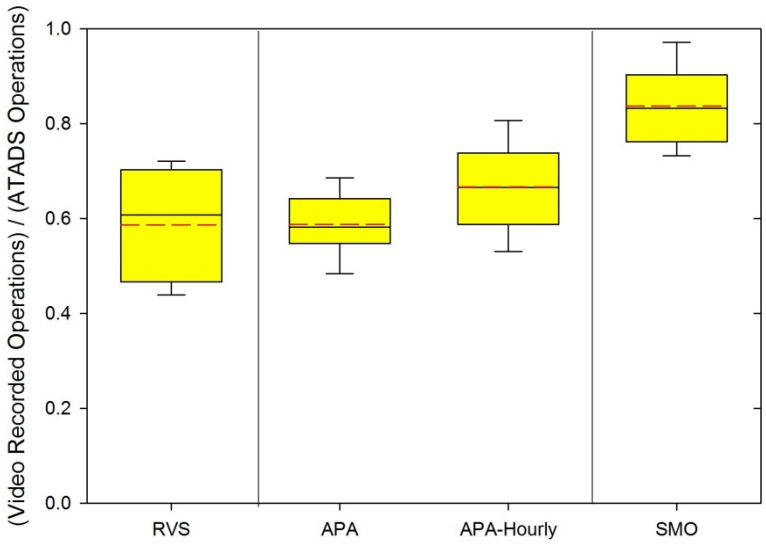

Notes: Interior solid lines are medians and interior dashed lines are arithmetic means, whiskers are 10^{th} and 90^{th} percentiles. RVS, APA, and SMO are 12-hour video data and daily ATADS data; APA-Hourly corresponds to 12-hour video data and FAA data, used to generate ATADS values, for the same 12-hour period as the video data.

5.6 Additional Lines of Evidence for the Origins of Airborne Pb

At each airport, the highest ambient PM-Pb concentrations were measured at the sites downwind of aircraft operations. $PM_{2.5}$-Pb at the aircraft-impacted sites accounted for most of the TSP-Pb, with ranges of 65-86% at RVS, 71-100% at APA, and 41-100% at SMO. The enrichment of Pb in the fine particulate matter size range is consistent with fresh exhaust emissions rather than exhaust emissions that previously deposited and are resuspended by wind or aircraft-induced turbulence during the sampling events. Additional lines of evidence for the contribution of aircraft exhaust—whether fresh or resuspended—are provided by Br/Pb ratios from XRF analysis and Pb isotope ratios from ICP-MS analysis.

5.6.1 $PM_{2.5}$ Br/Pb Ratios

Halide compounds such as ethylene dibromide and ethylene dichloride are part of the tetraethyl lead (TEL) additive blended into avgas. These compounds scavenge Pb in the engine and the resulting exhaust emissions are bromolead compounds such lead bromide ($PbBr_2$) and lead bromochloride (PbBrCl). There is only one supplier of the TEL additive (Innospec) and it supplies TEL-B, which contains only ethylene bromide (*http://www.innospecinc.com/market/octane-additives*). The Br/Pb ratio in ambient particulate matter has long been used as an indicator for combustion of leaded fuels and, in particular, motor gasoline (Harrison and Sturges 1998). A mixture of brominated and chlorinated additives was most commonly used in motor gasoline and the Br/Pb ratio of 0.386—which corresponds to the compound PbBrCl and is commonly termed the "ethyl ratio"—was used as a reference ratio. If brominated but not chlorinated additives are used, then a Br/Pb ratio of 0.772, corresponding to the compound $PbBr_2$, would be the reference. There are several caveats to use of the Br/Pb ratio as an indicator for combustion of leaded fuels. Most importantly, bromine is relatively volatile and volatility losses can lead to a decrease in the Br/Pb ratio. The loss can occur during transport in the atmosphere, during sample collection and storage, or during analysis using high energy beams such as XRF.

For this study, Br/Pb ratios were examined for evidence of Pb from piston-engine aircraft exhaust emissions. Br losses during atmospheric transport of fresh exhaust emissions are likely small because the time between emission and sample collection is on the order of seconds to minutes. Br losses from resuspended exhaust PM could have substantial losses. Precautions were taken to minimize losses after sample collection by transporting in coolers and storing in a freezer. A subset of the airborne $PM_{2.5}$ samples collected at each airport was sent to Cooper Environmental Services for elemental analysis by XRF. Details are provided in Appendix B, including a comparison of PM-Pb by XRF and ICP-MS.

Figure 28 shows the relationship between $PM_{2.5}$-Br and $PM_{2.5}$-Pb as measured by XRF. All but one sample are above a distinct edge with Br/Pb ~ 1/3. At low Pb concentrations, the samples can be enriched in Br.

Figure 29 shows the same data after classifying each sample as having expected high or low aircraft exhaust impacts. First, concentrations less than three times the XRF MDL values were screened out for this analysis. Next, expected high-impact samples were identified on an airport-by-airport basis. At RVS, expected high-impact samples were those collected at either the North or South sites, depending on the wind pattern. Samples from the East site or upwind of the airport based on the daily winds were categorized as low impact. Samples collected at RVS on days with variable winds are not included in Figure 29. At APA, all samples from the Central site were categorized as high impact while samples from the East site were considered low impact. At SMO, all samples from the Northeast site were categorized as high impact and the samples from the Southwest site were considered low impact. Br and Pb are highly correlated for the high-impact samples ($r = 0.92$). In contrast, Pb was weakly correlated with markers for resuspended soil, especially for the high-impact samples ($r = 0.00$ and 0.01 for Si-Pb and

Figure 28
$PM_{2.5}$ Br and Pb Measured by XRF and Stratified by Airport

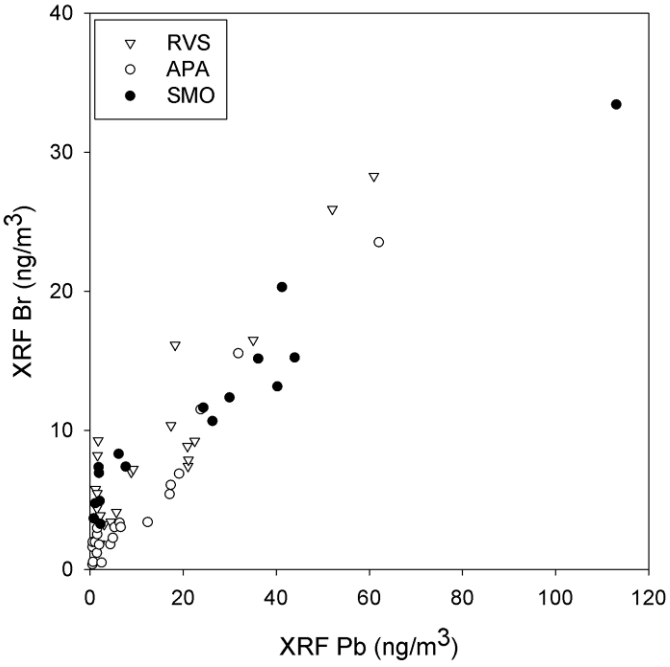

Figure 29
$PM_{2.5}$ Br and Pb Measured by XRF and Stratified as Samples with High or Low Expected Impacts from Aircraft Exhaust

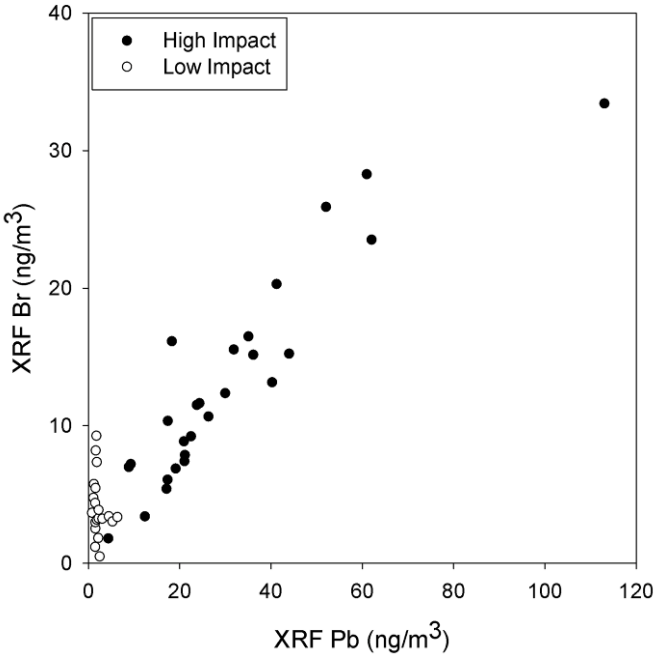

Ca-Pb, respectively). The strong correlation of Pb with Br and weak correlation of Pb with soil markers such as Ca and Si provide support that the $PM_{2.5}$-Pb originates from combustion of leaded fuel. The downwind Br/Pb ratio was then adjusted to correct for Br and Pb background contributions. The adjusted ratios were calculated as:

$$\frac{Br}{Pb} = \frac{Br_{downwind} - Br_{upwind}}{Pb_{downwind} - Pb_{upwind}}$$

The median adjusted downwind Br/Pb ratio is 0.30 with 25^{th} and 75^{th} percentile ratios of 0.24 and 0.39, respectively. These ratios are much smaller than the expected ratio of 0.772 if all the lead was present as $PbBr_2$. It is also less than the ethyl ratio. This discrepancy may be caused by volatilization of Br during the XRF process. Chlorine was also examined to determine if Pb was in the form of PbBrCl, and it was poorly correlated with Pb and Br; however, volatilization of Cl could also be an issue.

5.6.2 PM-Pb Isotopic Composition

Pb isotopes have long been used to identify sources of PM-Pb and in some cases to quantify the source contributions. Pb isotopes are stable, but fractionation that has occurred over geologic time leads to distinct isotopic signatures for Pb of different origins. In this study, if the Pb isotope ratios for both the native soil and other "background" Pb sources are different from the isotope ratios for Pb used in leaded fuels, these ratios can be used to evaluate the prevalence of PM-Pb from leaded fuel combustion. Given that lead was phased out of motor gasoline several decades ago, a leaded fuel signature at general aviation airports should be a good indicator for piston-engine exhaust emissions. While this approach cannot distinguish between direct exhaust emissions and exhaust emissions that have locally deposited and are subsequently resuspended, it may be able to discriminate Pb from avgas compared to other sources.

A common approach to examining Pb isotopes data is to make a scattergram of the $^{207}Pb/^{206}Pb$ versus $^{208}Pb/^{206}Pb$ ratios. The isotopic composition of airborne PM-Pb is a simple mixture of Pb from different geologic sources (whether native soil, or mined and refined such as the Pb in avgas). Emission source compositions are "end members" and the source contributions to Pb in airborne PM are estimated by the PM-Pb sample location along the mixing line between the end members. This construct is sound if there are only two end members, which is often the case, but becomes more complicated in the presence of three or more end members.

All PM-Pb samples were analyzed for Pb isotopes using the protocol described in Appendix B. While precise quantification of Pb isotopes is best performed using a high resolution ICP-MS, previous work conducted by the WUSTL team has determined that the ICP-MS available to this project was adequate for at least semi-quantitative analyses and the measurement precision has been quantified.

Figure 30 shows the $^{207}Pb/^{206}Pb$ versus $^{208}Pb/^{206}Pb$ ratios for all airborne PM samples collected in this study with the data stratified by airport. All of the samples lie along a line, albeit it with some scatter, which generally supports the notion of a two-source model for Pb. Four resuspended soil samples from each airport and 15 total avgas samples were also analyzed. Figure 30(b) shows the $^{207/206}Pb$ versus $^{208/206}Pb$ for all airborne PM samples and the soil and avgas samples collected for each airport. The avgas ratios are similar to measured ratios of lead mined in Australia, which is reported to be the source of the lead used in avgas (Townsend et al., 1998). Isotope ratios for resuspended soil are generally consistent with crustal material in the continental United States and are more similar to each other than to Australian lead. Therefore, samples with high Pb ratios likely contain more avgas contribution while samples with low ratios are likely indicative of background ambient Pb and in particular resuspended soil. It is not clear whether the soil samples include significant Pb originating from the use of avgas. However, isotopic compositions of soil samples collected at different locations within and between the three airports are indistinguishable. This suggests that avgas Pb does not dominate the Pb in these soils. A potential confounder to the soils analysis is that the airport topsoil samples can have dramatically different histories, and in some cases there was evidence of soil being moved. At high $^{208}Pb/^{206}Pb$ ratios, the APA data tend to fall below the mixing lines for the RVS and SMO data.

Figure 30
Pb Isotope Ratios for Airborne PM-Pb, Soil, and Avgas Samples Collected at the Three Airports

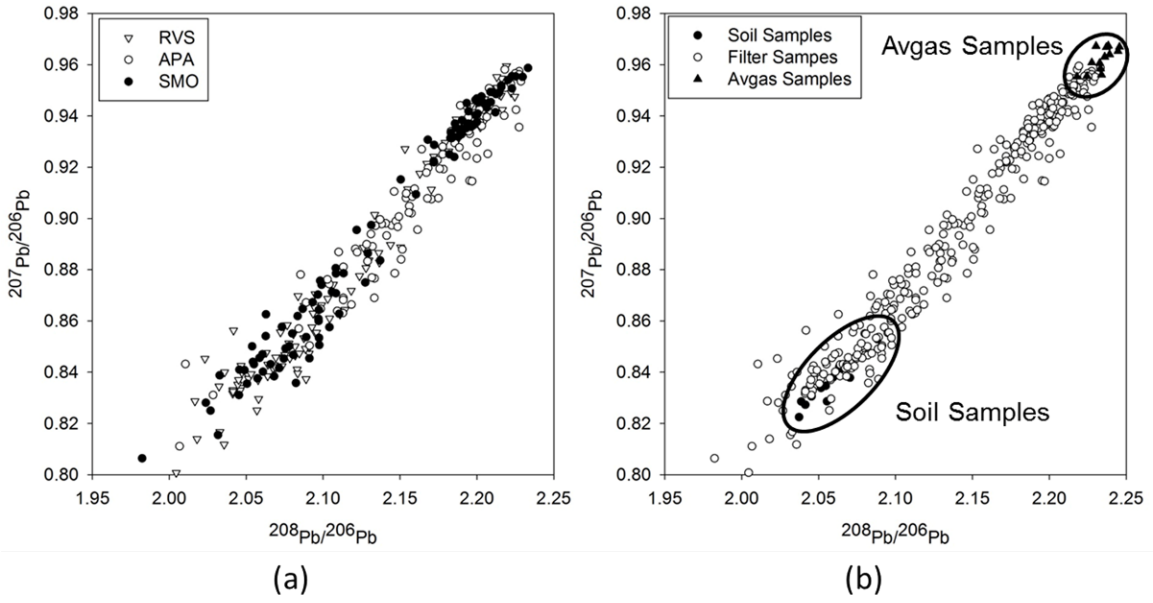

Figure 31 shows the same data but now stratified into samples expected to have low or high impacts from piston-engine aircraft emissions. Concentrations less than three times the ICP-MS MDL for Pb were screened out for this analysis, and the classification

scheme used for the Br/Pb ratios analysis was used for this analysis. Most of the high-impact samples are clustered towards the avgas end member, whereas most low-impact samples are at greater distances from the avgas end member. This pattern is consistent with Pb in high-impact samples being dominated by avgas combustion. The threshold composition between high- and low-impact samples is $^{208}Pb/^{206}Pb \sim 2.15$. All of the low-impact samples with $^{208}Pb/^{206}Pb$ above this threshold are from APA.

Figure 31
Pb Isotope Ratios for Airborne PM-Pb with Samples Stratified as High or Low Expected Impacts from Aircraft Exhaust

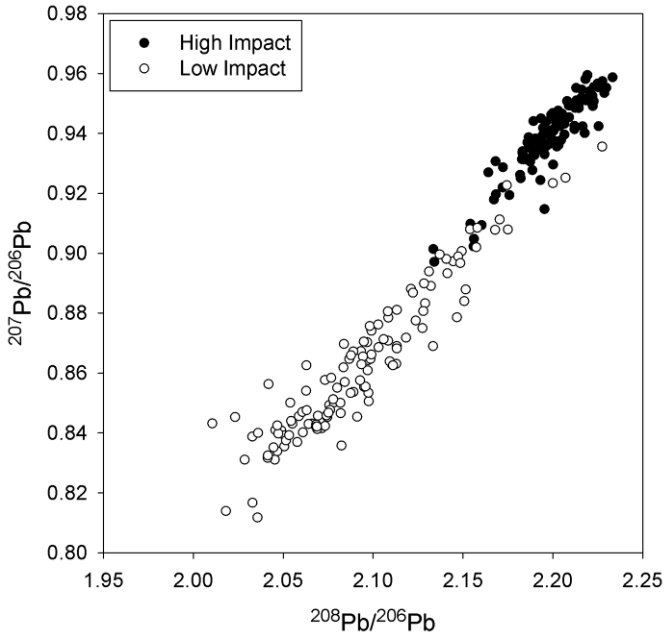

Data from collocated PM sampling can be used to gauge measurement precision. Shown in Figure 32 are the $^{208}Pb/^{206}Pb$ ratios and $^{207}Pb/^{206}Pb$ ratios for the collocated airborne PM samples collected at the three airports. Collocated sample isotope ratios are highly correlated, with $r^2 = 0.90$ for $^{208}Pb/^{206}Pb$ and $r^2 = 0.94$ for $^{207}Pb/^{206}Pb$. While the data are highly correlated, the high scatter suggests that even if the end member compositions are appropriately identified, caution should be used when quantitatively apportioning airborne PM-Pb to the end members. Again, this scatter is likely a limitation of not using a high resolution ICP-MS instrument.

Figure 32
Pb Isotope Ratios Collocated PM Samples Collected at the Three Airports

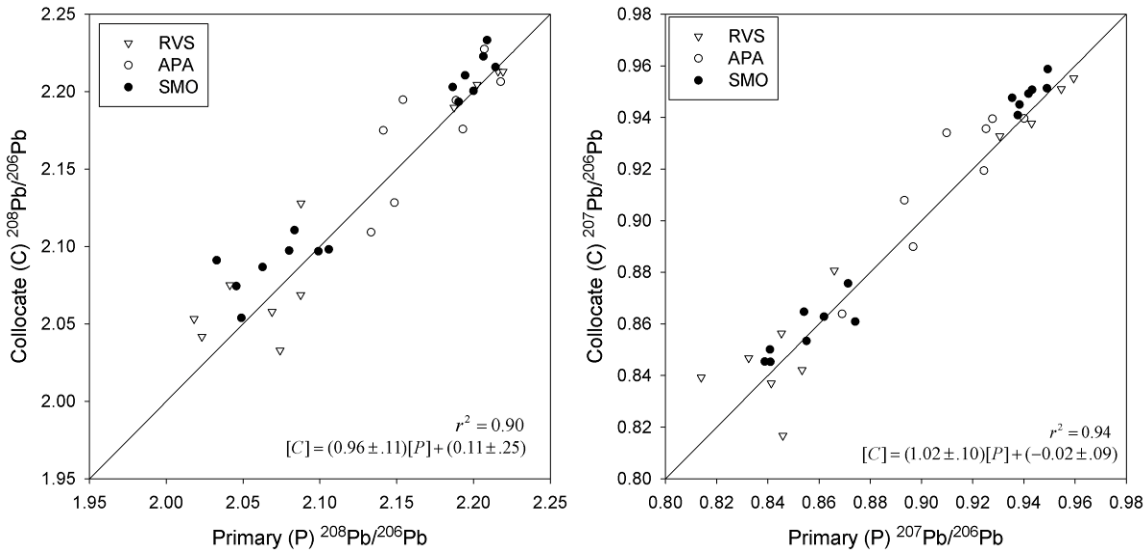

(a) (b)

Correlation was also observed between Pb isotope ratios and total lead concentration. Figure 33 shows total Pb concentration versus the $^{208}Pb/^{206}Pb$ ratio for airborne PM samples collected at the three airports. High Pb concentrations correspond to high $^{208}Pb/^{206}Pb$ ratios, suggesting that lead from avgas combustion is the primary driver of the high PM-Pb measured at each airport.

Some of these data represent paired $PM_{2.5}$ and TSP samples. For the high-impact data, there was no consistent trend in the directional difference of the $PM_{2.5}$-Pb and TSP-Pb isotope ratios and the differences were generally small. This pattern suggests that significant Pb in coarse particles at the high-impact sites originates from previously deposited TEL-Pb.

5.7 Comparison of SMO Data to Previous Studies

In addition to this ACRP study, there have been two other recent studies of PM-Pb at SMO. The South Coast Air Quality Management District (SCAQMD) conducted a study in 2006-2007 to assess the impact of airport operations for a suite of air pollutants, including PM-Pb (SCAQMD 2010). A 2009 study performed by ICF International for EPA (Carr et al. 2011) collected airborne PM-Pb samples towards evaluating an air quality modeling approach for local-scale impacts from general aviation activity. In this section, the results from the SCAQMD and ICF studies are compared to the results from this ACRP study.

Figure 33
Pb Total Concentration versus the $^{208}Pb/^{206}Pb$ Ratio for PM Samples Collected at the Three Airports

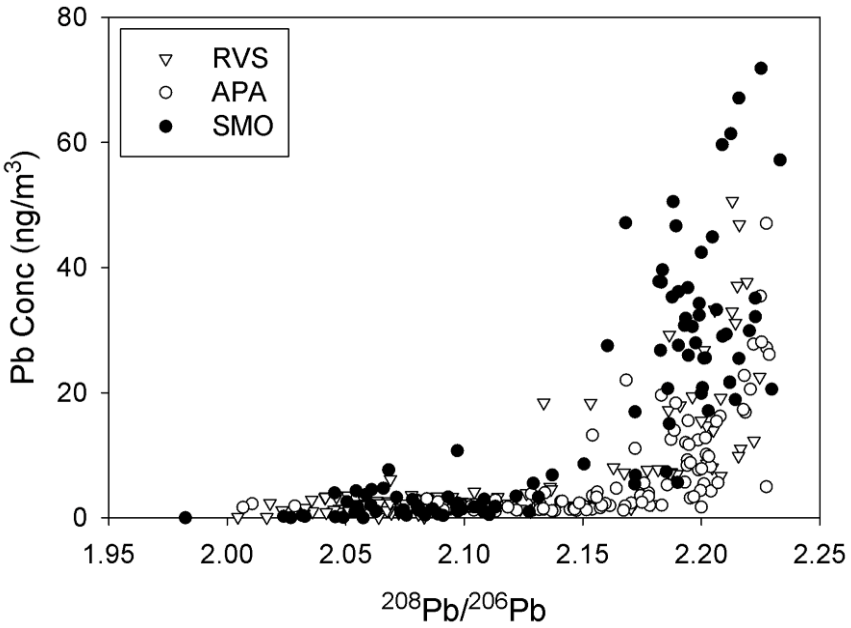

Table 44 summarizes the key attributes for each of the three SMO studies. Both the SCAQMD and ICF studies performed wintertime and summertime campaigns, and in both cases PM-Pb concentrations were higher in the winter than the summer. Comparisons to the ACRP study use only the summertime data because the ACRP study was conducted in July 2013.

Both the SCAQMD and ICF studies primarily focused on TSP-Pb sample collection using FRM High-Volume (Hi-Vol) samplers. This ACRP study focused primarily on $PM_{2.5}$-Pb measurements and secondarily on TSP-Pb measurements because the objective is to refine the inventory methodology for aircraft exhaust emissions, which are fine particles. BGI PQ100 samplers were used for both size ranges because they are portable and battery operated, which provided flexibility for siting and moving the samplers. ICF also used Mini-Vol samplers during the first, wintertime campaign. The Mini-Vol is attractive because it is a portable, battery-operated sampler. However, its performance for TSP-Pb measurements was deemed unacceptable and therefore only Hi-Vol samplers were used in the second, summertime campaign. During the SCAQMD summertime campaign, a BGI PQ100 sampler was used to collect TSP-Pb at a site near the runway to overcome the need for electrical service. MetOne SASS samplers were also deployed at multiple sampling locations to collect $PM_{2.5}$ samples.

Table 44
Measurement Attributes for the Three Airborne PM-Pb studies at SMO

Parameter	Study		
	SCAQMD[1]	EPA/ICF[2]	ACRP
Sampling Period	April-July 2006 (12 wks)	July 2009 (1 wk)	July 2013 (4 wks)
Sampling Frequency	1-in-3 day	Daily	Daily
Sampling Duration	24-hour	24- and 16-hour	12-hour
Sampling Locations	7	4	4
PM Size Sampled (Primary Size/Other Size)	TSP / $PM_{2.5}$	TSP / $PM_{2.5}$	$PM_{2.5}$ / TSP
Primary PM Samplers[3] Other PM Samplers	Hi-Vol FRM SASS, PQ100	Hi-Vol FRM	PQ100
Total Samples for Primary Size	191	28	77
Primary Size Samples Collected at Site Northeast of Runway 21[4]	12	7	27
Analytical Method (Primary Method /Other Method)	ICP-MS / XRF	XRF	ICP-MS / XRF
ATADS-reported daily mean aircraft activity LTOs)	385 (April-July 2006)	290 (July 25-31, 2009)	293 (July 3-31, 2013)

[1] Measurement attributes for the SCAQMD summertime campaign only.
[2] Measurements attributes for the ICF summertime campaign only.
[3] PM sampler manufacturers: Anderson Hi-Vol, MetOne SASS, BGI PQ100.
[4] Does not include collocated sampler data.

Finally, both the SCAQMD and ICF studies primarily collected 24-hour samples while this ACRP study collected 12-hour samples to focus on periods with highest aircraft activity. The SCAQMD and ICF studies included sampling locations outside the airport footprint while this ACRP study included locations only within the footprint.

Figure 34 shows the site locations at or immediately adjacent to the airport and including only the summer period sites from the ICF study. The SCAQMD and ICF studies had additional sampling locations in residential areas around the airport, some of which are not shown on the map. All three studies had sampling locations to the northeast of runway 21 (designated NE in ACRP, and East Tarmac in SCAQMD and ICF) as well as near the maintenance shed (designated West in ACRP). The ACRP and SCAQMD studies both had sampling locations west of runway 3 (designated SW in ACRP, West Tarmac in SCAQMD). For clarity, the remainder of this section uses only the ACRP site designations. The NE site zone is downwind of the activity on runway 21 for prevailing

Figure 34
Sampling Locations for the SCAQMD, ICF, and ACRP PM-Pb Studies

winds during the summertime. However, the precise locations are not identical across the three studies and this could lead to significant differences in measured concentrations because this is a zone of steep concentration gradients.

PM-Pb concentration data are summarized in Table 45. Since samples from the ACRP study were primarily $PM_{2.5}$, the measured $PM_{2.5}$-Pb concentration values were multiplied by a factor of 1.3, which was the mean ratio of TSP-Pb to $PM_{2.5}$-Pb for simultaneously collected TSP and $PM_{2.5}$ samples. For the SCAQMD study, the TSP-Pb to $PM_{2.5}$-Pb ratio ranged from 0.68 to 1.20; however, different sampler types, and possibly different analytical methods, were used for the TSP and $PM_{2.5}$ samples. For all three studies, PM-Pb concentrations measured on the airport footprint were highest at the Northeast site, with lower and similar concentrations at the West and Southwest sites. For the SCAQMD and ICF studies, PM-Pb concentrations at monitoring locations off the airport footprint were similar or less than the concentrations at the Northeast site.

Mean and Median TSP-Pb at the Northeast site were highest for the SCAQMD study, intermediate for the ICF study, and lowest for the ACRP study. Differences in aircraft activity may explain some of the differences. Overall airport activity as measured by ATADS was 11% higher for the SCAQMD study than the ICF and ACRP studies, which had similar levels of activity. As summarized below, there are several factors that potentially confound the comparison across studies.

Table 45
TSP-Pb (ng/m^3) Summary Statistics for the SCAQMD, ICF, and ACRP Summertime Studies

Site	Northeast			West			Southwest		
Study	SCAQMD[1]	ICF[2]	ACRP[3]	SCAQMD	ICF	ACRP	SCAQMD	ICF	ACRP
Number of Samples	12	7	27	32	7	5	31	-	28
Mean	**85**	**49**	**39**	**4**	**3**	**3**	**5**	**-**	**2**
Median	84	53	36	3	4	2	4	-	1
Maximum	135	62	93	14	6	10	18	-	6
Minimum	27	34	<MDL	0	<MDL	<MDL	0	-	<MDL

Note: ACRP TSP-Pb estimated as 1.3 times the measured $PM_{2.5}$-Pb; <MDL = concentration below the minimum detection limit.
[1] Source: South Coast Air Quality Management District 2010
[2] Source: Carr et al. 2011
[3] Current study

- First, ACRP sampling was conducted during the daytime 12 hours to collect PM only during periods with high aircraft activity. SCAQMD and ICF sampling durations were primarily 24 hours; the inclusion of nighttime hours would mix in periods with lower activity but perhaps also lower dispersion; therefore, the overall impact on the reported average concentrations is not clear.

- Second, based on the ICF and Sierra modeling, the sampling zone northeast of runway 21 is an area with steep PM-Pb concentration gradients. Thus, even modest differences in sampling location can have a large impact on observed PM-Pb levels. The ACRP northeast site was ~20 m north of the SCAQMD and ICF sites to be farther away from the blast wall.

- Third, there are likely differences in the actual TSP collection efficiencies between the different samplers. For example, the Hi-Vol TSP sampler has an inlet collection efficiency that depends on the sampler orientation with respect to the wind.

- Finally, there can be analytical biases. For example, the SCAQMD study included PM sample collection at the Northeast site using a BGI PQ100 with a TSP inlet and operated at 12 LPM. Pb as measured by both XRF and ICP-MS were highly correlated but with an absolute bias of ~25 ng/m^3 with XRF higher than ICP-MS. A similar comparison was made with 19 $PM_{2.5}$-Pb samples collected during the ACRP study. In this case, the data were highly correlated but with a relative bias of ~28% with the XRF higher than the ICP-MS.

Despite these potential confounders, the PM-Pb concentration data are generally consistent across the three studies. While the measurements are not directly comparable to the Pb NAAQS because of differences in data collection averaging times, it is noted that none of the summertime 12- or 24-hour samples had a TSP-Pb concentration above the three-month average NAAQS of 150 ng/m^3 and study mean concentrations were 25-57% of that value.

5.8 Key Observations

Field studies were conducted at three general aviation airports that each had distinguishing features in terms of airport layout and meteorology. Airborne PM-Pb samples were collected with high completeness, detectability, and precision.

Overall, aircraft activity patterns and PM-Pb patterns were similar across the three airports. The patterns outlined below were observed for all three airports.

- Aircraft LTOs measured by the video cameras were lower than the FAA ATADS counts. There may be several reasons for this discrepancy, including differences in counting methods and helicopter activity that is not necessarily well-captured by the video data.

- A small number of aircraft disproportionately contributed to total operations with 5% of the observed aircraft conducting one-third of the operations and 10-12% of the observed fleet conducting half of the operations.

- Run-up operation TIM was more variable than landing-and-takeoff TIM. PM-Pb hot spots tend to be downwind of run-up areas, so the run-up TIM variability will lead to variability in the hot spot intensity.

- PM-Pb concentrations were downwind of aircraft ground operations and especially downwind of run-up areas.

- Most of the PM-Pb at the high-impact sites is in the $PM_{2.5}$ size range, consistent with direct exhaust emissions from piston-engine aircraft, but there is considerable Pb in the $PM_{TSP-2.5}$ size range. The median TSP-Pb/$PM_{2.5}$-Pb ratio across all three airports was 1.3 with a narrow interquartile range of 1.2 and 1.4 for the 25^{th} and 75^{th} percentiles, respectively. While coarse mode particles are not the dominant contributor to PM-Pb, they cannot be neglected.

- PM-Br and PM-Pb are highly correlated at the high-impact sites, which is consistent with TEL-Pb origins. The Br/Pb ratio is much lower than predicted by the presumed form of $PbBr_2$. There are several possible reasons for the lower than expected ratio, which was also commonly observed in studies during the era of leaded automobile gasoline.

- The Pb isotopic compositions for PM samples collected at sites with expected high impact from TEL-Pb are distinct from those for samples collected at sites

with expected low impacts. Furthermore, PM-Pb isotopic compositions for the high-impact sites are consistent with avgas samples collected at the airports, while the isotopic compositions for the low-impact sites are generally consistent with resuspended soil samples collected at the airports.

- TSP-Pb at the high-impact sites does not systematically exhibit a shift in isotopic compositions towards background (e.g., resuspended soil) Pb compositions compared to the corresponding $PM_{2.5}$-Pb samples. This pattern suggests that the lead in the coarse particle size mode is strongly influenced by TEL-Pb.

PM data collection focused on size ranges and averaging times that do not support direct comparisons to the Pb NAAQS. Nonetheless, none of the individual 12-hour PM-Pb values exceeded the three-month average NAAQS of 150 ng/m^3, and the highest observed 12-hour concentration was a TSP-Pb value of 72 ng/m^3 at SMO. Study-average $PM_{2.5}$-Pb values at the highest concentration sites were 15 ng/m^3 at APA, 21 ng/m^3 at RVS, and 30 ng/m^3 at SMO.

###

6. APPLICATION OF THE REFINED METHODOLOGY USING SITE-SPECIFIC DATA

This chapter presents the application of the refined methodology using the site-specific aircraft activity data collected during the field studies. As described in Chapter 5, the three field studies assembled detailed aircraft activity data from the Richard Lloyd Jones Jr. Airport (RVS) in Tulsa, OK; Centennial Airport (APA) in Englewood, CO; and Santa Monica Municipal Airport (SMO) in Santa Monica, CA.

Temporally and spatially resolved daily emission inventories, covering the dates of the field study, were estimated for each airport. These inventories were used as inputs to the dispersion modeling presented in Chapter 7. These inventories were also used together with annual operations data from the FAA's ATADS to estimate annual lead emissions inventories for calendar year 2011 for purposes of comparison with the inventories presented in Chapter 4, which were based on publicly available data.

6.1 Site-Specific Inventory Method and Inputs

The refined methodology of Chapter 4 was modified to utilize the field study data. Figure 35 presents an overview of the inventory methodology applied using the site-specific data. As shown, the parallelograms illustrate the key data inputs, the rectangles illustrate the individual processing elements, and the rounded rectangles illustrate the inventory outputs. The inputs developed from the field study data, labeled in Figure 35, are summarized below.

- "Episodic operation counts" were the number of operations by hour by runway. Operation type distinctions included landings, takeoffs, and touch-and-go operations. Aircraft type distinctions included fixed-wing planes and rotorcraft (i.e., helicopters).

- "Survey of times and distances" was the collection of time-in-mode data for a representative sample of aircraft operations covering the complete set of movements of aircraft within the facility. Operating mode distinctions included taxiing, idling, magneto run-ups, other (i.e., maintenance) run-ups, takeoffs, and landings. The time data form the basis for the estimating the duration spent in each mode of operation. The distance data were the average wheels-up and wheels-down data to identify the spatial dimensions of landings, takeoffs, and touch-and-go operations; these dimensions are not needed for the emissions inventory but were needed for the air quality modeling discussed in Chapter 7.

Figure 35
Flow Chart of Airport Inventory Development Methods
Using Field Study Data Sources

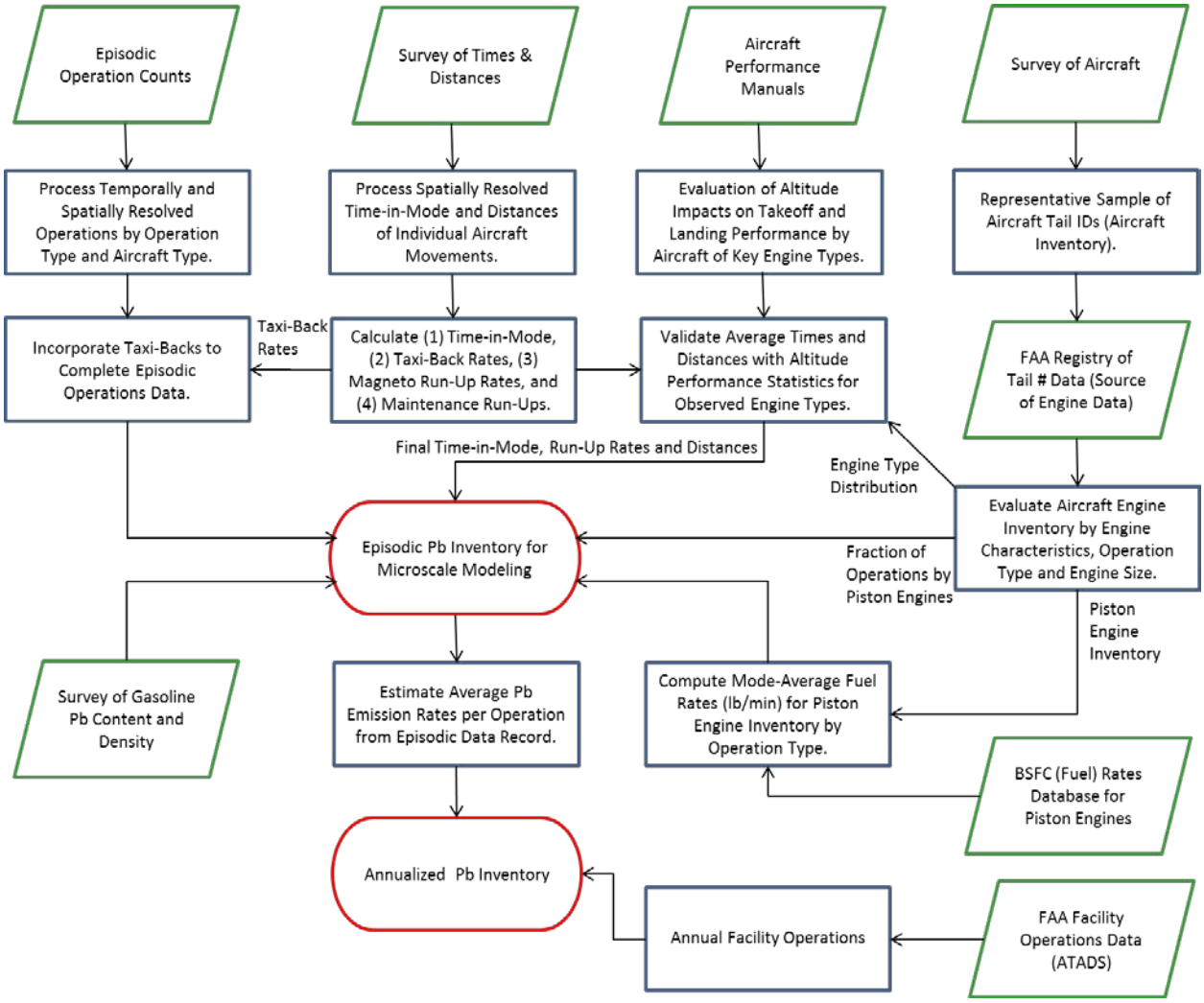

Note: Parallelograms illustrate the key data inputs, rectangles illustrate the individual processing elements, and rounded rectangles illustrate the inventory outputs.

- The "survey of aircraft" was still photography of tail numbers of a representative sample of aircraft. Aircraft-type distinctions included fixed-wing planes and rotorcraft. The tail number inventory was matched with registry data to obtain the aircraft and aircraft engine inventory. Data were also used to estimate the proportions of operation by piston-powered, turboprop, and jet engine types.

- The "survey of gasoline" data resulted in data regarding the lead content and density of aviation gasoline in use locally.

Figure 35 also shows additional inputs that were not collected as part of the field studies, as described below.

- "Aircraft performance manuals" from a range of piston engine technologies were used to evaluate the impacts of altitude on modeling parameters, including time-in-mode, takeoff and landing distances, and approach/climb-out angles. The impacts of altitude on modeling variables are significant particularly for Centennial Airport which is at 5,885 feet elevation.

- The "database of brake specific fuel consumption" (BSFC) for piston engines is the same database summarized and discussed in Chapter 4 of this report (see Table 10). BSFC—the mass of fuel consumed per unit work—is the preferred metric for extrapolating fuel consumption rates across engines.

- The FAA's registry of tail numbers provides the aircraft and aircraft engine information for each tail number.

- The FAA's ATADS provided the total annual operations for each facility. The ATADS data were not used for the episodic Pb inventory for microscale modeling (Chapter 7) because actual operations were counted during the field study. The ATADS data were used to generate the annualized Pb inventory, in this case for 2011.

These inputs were processed, as shown in Figure 35, to yield episodic (e.g., hourly) and annual lead inventories. Lead emissions were estimated from fuel consumption rates and modes of operation of the specific aircraft operating at each facility. The episodic inventories were also spatially resolved (by runway and taxiway) based on site-specific data for input into a dispersion model. The areas to which emissions were spatially distributed are shown for each airport in the figures presented in Appendix C.

The episodic lead inventories were converted to average lead emission rates (over the entire field study period) on a per-operation basis. Note this emission rate already accounts for the proportion of total operations that are conducted by piston engine aircraft and is expressed as the emission rate per aircraft operation—whether jet or piston engine. These average emission rates were converted into annual lead inventories using ATADS annual operations for each facility. The details of the inventory processing used using the locally collected data are described further below.

6.1.1 Operation and Mode Definitions

Under the standard FAA/EPA emission inventory procedures universally applied to evaluate general aviation airports in the U.S., every two operations consist of a landing and a takeoff, as summarized in Section 3.2 of this report. These two operations combined are termed a *landing-takeoff (LTO) cycle*, and agency inventory methods are based on a per-LTO basis with the underlying presumption that every two operations consist of a standalone takeoff and a standalone landing. "Standalone" in this context

signifies operation that either begins or ends with the engine off and the aircraft parked at the hanger/ramp location.

The standard LTO cycle approach was clearly inadequate for evaluating the site-specific activity data collected. A significant proportion of "continuous" operation—i.e., multiple operations executed in series such that the engine is not turned off—was observed. The refined methodology was expanded for the site-specific analysis to properly address continuous operation presumably present due to commercial flight school activity. One or more flights schools operated at each airport evaluated, and these schools are common at general aviation airports nationally, with FAA listing approximately 600 of these pilot schools. As explained below, two distinct types of continuous operation were explicitly evaluated, the "touch-and-go" and the "taxi-back."

- Touch-and-go operations for fixed-wing aircraft consist of an approach, brief ground roll (landing), an immediate takeoff, and a climb-out—all of which occur without exiting the runway. Specifically a touch-and-go operation counts as two operations in FAA procedures, because both a landing and a takeoff occur. Approach and climb-out modes for the touch-and-go were handled similarly as the procedure used for any standard landing and takeoff. However, the fuel rate for the ground-roll mode of the touch-and-go was handled distinctly as the average of the idling rate (typical for landing) and the takeoff rate.

- Taxi-back operations for fixed-wing aircraft consist of a standard approach, landing, and taxing off the runway, after which the aircraft taxis back to a runway and completes a takeoff and climb-out. The taxi/idle time on the ground is unique for this procedure (and accounted for separately in the methodology) and the run-up prior to takeoff may be omitted.

These two types of continuous operation represented a significant portion of the piston-powered aircraft activity observed at the three airports. Correctly addressing the continuous operation was key to the inventory development because the run-up procedures are generally omitted between successive takeoffs (if operation is continuous) and the time spent in each operation mode is otherwise distinct from a similar standalone operation.

Inventory modeling of standard aircraft activity is divided into four modes of engine operation: taxi/idle, takeoff, climb-out, and approach. Recently, a fifth mode was added specific to piston-powered aircraft engines to address the run-up procedure completed prior to takeoff (ICF International and T&B Systems 2010). These five modes of operation are retained in the refined methodology with some modifications. The distinct definitions related to the modes of operation used in the inventory development are provided below.

- The run-up mode encompasses the magneto test completed prior to takeoff, and the estimated fuel consumption rate for this mode is specific to the magneto test. The fuel consumption rate of the magneto test, as described in Chapter 4, is estimated at 52% of the maximum fuel consumption rate of the engine. Any

additional time the aircraft spends at a run-up location, in excess of the magneto test time, is counted as part of the total taxi/idle time on the ground. On average, it was observed that an aircraft spends about 5 minutes total at the run-up locations, of which about one minute is for completing the magneto test.

- The landing ground roll—the period from wheels down to turning off the runway—is included as part of the approach mode in the standard FAA/EPA modeling protocol for fixed-wing aircraft. We changed this assumption because the landing ground roll is completed at engine idle, whereas for the remainder of the approach mode the engine is assumed to be operating at 40% load. In this method, the period of the landing ground roll is explicitly counted as part of the on-the-ground idle/taxi time in order to apply the proper fuel flow rate to the landing roll operation.

- The touch-and-go ground roll is the brief period from wheels down to wheels up again. As noted above, the fuel rate for the ground-roll mode of the touch-and-go was handled distinctly as the average of the idling rate (typical for landing) and the takeoff rate. This ground roll operation is, in effect, a distinct mode.

- The maximum altitude included in the climb-out and approach modes is capped at the traffic pattern altitude (TPA) of each airport. The TPA, assigned by aircraft type, is typically between 500 and 1,500 feet above ground level (AGL). This is an improved assumption over the EPA default of 3,000 feet AGL, which is not typical for general aviation operation. The default time-in-mode for approach and climb-out modes for piston aircraft is defined by FAA/EPA based on flight to and from 3,000 feet AGL, the same altitude assumption the agency employs for commercial jet aircraft. This change in the maximum altitude assumption impacts the time-in-mode estimated for the climb-out and approach modes.

- "Maintenance run-ups" are separate run-up procedures that are not coupled with a takeoff event and are often completed in conjunction with engine maintenance for specific testing purposes. Airports have guidelines where maintenance run-ups are to occur. The field studies completed did not comprehensively evaluate the frequency/duration of maintenance run-ups, but maintenance run-ups were observed and factored into the inventory results when identified. Maintenance run-ups are accounted for separately from the magneto test run-ups (i.e., in effect this also represents a distinct mode) as the typical duration and fuel flow rates are distinct from the magneto test. Maintenance run-ups can be much greater in duration but have significantly lower fuel flow rates.

The assumed engine load for the four standard operating modes is shown in Table 46; load values are distinct for fixed-wing aircraft and rotorcraft. The fixed-wing engine load assumptions are those of the FAA/EPA. The rotorcraft engine load assumptions are those of the Swiss FOCA (Switzerland Federal Office of Civil Aviation 2009). Load, as defined in this method, represents the fraction of engine rated power applied at each mode. Load is combined with the engine power rating and is used to convert BSFC (lbs/hp-hr) to fuel consumption rates (lbs/hr), as was shown in Chapter 4.

Table 46
Piston Engine Load Points for Standard Operating Modes

Mode	Fixed-Wing Planes	Rotorcraft
Taxi/Idle	7%	20%
Takeoff	100%	N/A
Climb-Out	85%	95%
Approach	40%	60%

6.1.2 Time-In-Mode (TIM)

The sources of time-in-mode (TIM) data were as follows.

1. The site-specific TIM data were collected and used to define the amount of time for on-the-ground modes (i.e., taxi/idle, takeoff, run-up) for fixed-wing aircraft.

2. The TIM for the aloft modes (i.e., approach and climb-out) of fixed-wing aircraft was determined from the airport traffic pattern altitude (TPA) by scaling the EPA/FAA default TIM defined for 3,000 feet AGL. The TPA for fixed-wing aircraft at RVS and APA was 1,000 feet AGL; the TPA for single-engine and twin-engine fixed-wing aircraft at SMO was 1,200 and 1,700 feet AGL, respectively.

3. The TIM for rotorcraft was based on the Swiss FOCA estimates (Switzerland Federal Office of Civil Aviation 2009) except for the run-up mode, which was assumed to be equivalent to that measured for fixed-wing aircraft. The TPA for rotorcraft was 500 feet AGL. Note that rotorcraft operation was not recorded at APA (see Section 6.1.5 for further discussion of helicopter observations).

The site-specific TIM data went through a QA/QC process by tracking the individual planes over the entirety of their on-the-ground movements at each airport. The TIM data collection was complete for all operation on runways and taxiways. To account for the missing on-the-ground operation which occurred on ramps and in hanger areas, one minute of taxi/idle time was added to standalone landings and 2 minutes of taxi/idle time were added to standalone takeoffs.

The site-specific times for the run-up mode (i.e., the magneto test) were validated against information contained in Owner's Manuals. The TIM for the magneto test was log-normally distributed; three data points—in excess of 6 minutes duration and more than two geometric standard deviations from the mean (two at APA and one at RVS)—were

removed. The geometric mean of the remaining data was used to define the average magneto test time at each facility for the purposes of inventory development.

TIM data for piston-engine aircraft observed at each airport during the field studies are summarized in Tables 47–49. The tabulated data include the comparison of the Chapter 4 assumptions, generally employing FAA/EPA default values, with the site-specific results. Also shown in Table 49 for SMO are the TIM values from the ICF study at that airport. Overall, the site-specific TIM data show substantial differences compared to the FAA/EPA default and ICF study values.

Table 47
RVS Times In Mode (Minutes)

Aircraft	Engine Mode	Chapter 4 Analysis (FAA/EPA Default)	Site-Specific Data
Fixed-Wing Aircraft	Idle/Taxi (Takeoff)	12.00	9.24
	Run-Up	1.48[a]	0.92
	Takeoff	0.30	0.28
	Climb-Out	5.00	1.73
	Approach	6.00	2.15
	Idle/Taxi (Landing)	4.00	3.61
	Idle/Taxi (Taxi-Back)	n/a	3.63
	Ground Roll (Touch&Go)	n/a	0.28
Rotorcraft	Idle/Taxi (Departure)	n/a	4.00
	Run-Up	n/a	0.92
	Climb-Out	n/a	0.92
	Approach	n/a	0.67
	Idle/Taxi (Arrival)	n/a	4.00

n/a = not available

[a] The EPA/FAA default does not include the run-up mode; however, for this analysis the run-up mode was added for completeness as applied in Chapter 4 (see Table 13).

Table 48
APA Times In Mode (Minutes)

Aircraft	Engine Mode	Chapter 4 Analysis (FAA/EPA Default)	Site-Specific Data
Fixed-Wing Aircraft	Idle/Taxi (Takeoff)	12.00	10.16
	Run-Up	1.48 [a]	1.18
	Takeoff	0.30	0.42
	Climb-Out	5.00	1.73
	Approach	6.00	2.00
	Idle/Taxi (Landing)	4.00	4.33
	Idle/Taxi (Taxi-Back)	n/a	2.19
	Ground Roll (Touch&Go)	n/a	0.39

n/a = not available
[a] The EPA/FAA default does not include the run-up mode; however, for this analysis the run-up mode was added for completeness as applied in Chapter 4 (see Table 13).

Table 49
SMO Times In Mode (Minutes)

Aircraft	Engine Mode	Chapter 4 Analysis		Site-Specific Data
		ICF SMO	FAA/EPA Default	
Fixed-Wing Aircraft	Idle/Taxi (Takeoff)	5.07	12.00	10.28
	Run-Up	1.48	1.48 [a]	0.77
	Takeoff	0.27	0.30	0.28
	Climb-Out	1.30	5.00	1.81
	Approach	1.07	6.00	2.42
	Idle/Taxi (Landing)	2.53	4.00	4.29
	Idle/Taxi (Taxi-Back)	n/a	n/a	4.13
	Ground Roll (Touch&Go)	n/a	n/a	0.17
Rotorcraft	Idle/Taxi (Departure)	n/a	n/a	4.00
	Run-Up	n/a	n/a	0.77
	Climb-Out	n/a	n/a	0.92
	Approach	n/a	n/a	0.67
	Idle/Taxi (Arrival)	n/a	n/a	4.00

n/a = not available
[a] The EPA/FAA default does not include the run-up mode; however, for this analysis the run-up mode was added for completeness as applied in Chapter 4 (see Table 13).

It is important to note that the idle/taxi TIM data reported in Tables 47–49 are averages over the total observation period for the on-site data collection. Idle/taxi TIM values were calculated by individual runway and operation type. For example, the idle/taxi time observed in conjunction with a standalone takeoff at APA was calculated for each runway as shown below.

9.3 minutes (Runway 17R)
12.6 minutes (Runway 35L)
10.2 minutes (Runway 17L)
11.3 minutes (Runway 35R)
7.2 minutes (Runway 10)
9.9 minutes (Runway 28)

The operation data collected for the site-specific analysis were runway-specific. It was observed that runways were favored for operations depending on time of day, meteorology and congestion, and that specific runways were favored for continuous operations. Time of operation on the ground was clearly spatially distinct (as commercial hanger areas were the dominant origin and destination of activity) and runways were asymmetrically located relative to the busiest areas of each airport. Therefore, the methodology included total taxi/idle TIM mode estimates by operation type and by runway, which were then built up for the observations (by runway) over the duration of the on-site study period because activity was clearly asymmetrical.

It should be noted that the annual inventory estimates for each airport reported herein are based on average TIM for idle/taxi reported in Tables 47–49. The inherent assumption in the annual inventory is that the frequency distribution of runways used during the observation period is representative of the year as a whole.

6.1.3 Aircraft Fleet Composition and Fuel Consumption Rates

The site-specific data collection included the survey of aircraft from still photography of tail numbers of a representative sample of aircraft that was inherently activity or operation weighted. Aircraft-type distinctions included fixed-wing planes and rotorcraft. The tail number inventory was matched with FAA registry data to obtain the aircraft and aircraft engine inventory for piston-powered aircraft. These data were also used to estimate the proportions of operation by piston-powered, turboprop, and jet engine types.

The site-specific data were further processed to distinguish fixed-wing aircraft from rotorcraft and then to distinguish continuous operation from standalone operation for fixed-wing aircraft. Separately identifying the fleet of fixed-wing aircraft undergoing continuous operation was done because a few aircraft were disproportionately producing much of the activity. Continuous operations, presumably from commercial flight schools, were being completed from a distinct fleet—almost exclusively single-engine piston-powered aircraft. Aircraft involved in continuous operations were identified by the subset of aircraft appearing three or more times in a single hour's tail number recording. The maximum number of times a single aircraft was observed in one hour was 15.

The site-specific aircraft fleet data are summarized in Table 50, which also includes the results from Chapter 4 encompassing publicly available resources to determine aircraft fleet mix. Table 50 shows the site-specific data collection for the "raw data" encompassing all aircraft and operation types as observed. Overall, the Chapter 4 methods overstated the jet/turboprop proportions for two out of three airports and significantly understated the single-engine piston activity proportions for all three airports. In addition, the site-specific data analysis shows that continuous operations were completed by single-engine piston craft at a rate of greater than 90% for all three airports. An important observation in these results is that the Chapter 4 data sources (i.e., TFMSC and regional GAATA data) used to determine the proportion of aircraft by the engine types reported in Table 50 were not found to be accurate data sources for airport-specific activity. For this reason, it is concluded that these parameters are best determined locally.

Table 50
Proportion of Aircraft Activity by Engine Type

Airport	Engine Type	Chapter 4 Analysis (Fixed-Wing Only)	Site-Specific Data			
			Raw Observations (All Aircraft & Operation Types)	Fixed-Wing Aircraft, Standalone Operation	Fixed-Wing Aircraft, Continuous Operation	Rotorcraft
RVS	Jet & Turboprop	58%	10%	12%	1%	54%
	Single-Engine Piston	33%	79%	75%	92%	46%
	Multi-Engine Piston	9%	11%	13%	7%	0%
APA	Jet & Turboprop	29%	29%	36%	3%	n/a
	Single-Engine Piston	42%	64%	58%	92%	n/a
	Multi-Engine Piston	29%	7%	6%	5%	n/a
SMO	Jet & Turboprop	37%	20%	24%	0%	71%
	Single-Engine Piston	54%	78%	73%	100%	29%
	Multi-Engine Piston	9%	2%	2%	0%	0%

An important element for the Centennial Airport (APA) data collection and inventory evaluation was the presence of a B-17 aircraft at this airport during the field study. This aircraft—observed 11 times in the tail number recording—has four large, 1944-vintage, radially configured piston engines (1200 HP). The aircraft, known as the "flying fortress," has fuel consumption rates more than an order of magnitude higher than the typical piston-powered aircraft. For this reason, the B-17 was modeled separately (in terms of fuel flow rates and episodic activity levels) from the remaining aircraft at APA.

Using the site-specific aircraft fleet data and engine load assumption, the mean fuel consumption rates were calculated for the piston-engine aircraft operating at each airport while maintaining the distinction between continuous and standalone operation for fixed-wing aircraft. These results are shown are shown in Tables 51–53. As noted above, the B-17 aircraft in operation at APA (Table 52) is reported as a distinct aircraft/operation type as this aircraft was handled separately from the remaining aircraft. It should also be noted that a small number of Thielert piston engines were observed (at a frequency on the

Table 51
RVS Piston Aircraft Inventory, Mean Fuel Consumption Rates

Aircraft (Operation Type)	Gasoline Consumption by Activity Mode (lbs/hr)					
	Taxi/Idle	Takeoff	Climb-Out	Approach	Run-Up	Touch-and-Go Ground Roll
Fixed-Wing (Standalone)	17	125	98	54	55	N/A
Fixed-Wing (Continuous)	13	102	79	44	50	58
Rotorcraft	35	N/A	94	60	51	N/A

Table 52
APA Piston Aircraft Inventory, Mean Fuel Consumption Rates

Aircraft (Operation Type)	Gasoline Consumption by Activity Mode (lbs/hr)					
	Taxi/Idle	Takeoff	Climb-Out	Approach	Run-Up	Touch-and-Go Ground Roll
Fixed-Wing (Standalone)	17	131	103	58	62	N/A
Fixed-Wing (Continuous)	12	112	82	47	55	62
Boeing B-17	427	5,596	4,137	1,550	728	N/A

Table 53
SMO Piston Aircraft Inventory, Mean Fuel Consumption Rates

Aircraft (Operation Type)	Gasoline Consumption by Activity Mode (lbs/hr)					
	Taxi/Idle	Takeoff	Climb-Out	Approach	Run-Up	Touch-and-Go Ground Roll
Fixed-Wing (Standalone)	16	117	94	54	58	N/A
Fixed-Wing (Continuous)	12	86	69	42	45	49
Rotorcraft	46	N/A	136	85	74	N/A

order of a few tenths of a percent of total operations). These engines are unique in that these are based on a diesel automotive platform, and do not use aviation gasoline. The Thielert engines are retained in these site-specific results in the observed proportions by assigning a fuel consumption rate of zero, given that no aviation gasoline is consumed.

6.1.4 Altitude Impacts

One significant change made to the refined methodology subsequent to the original application to publicly available data described in Chapter 4 was the addition of the capability to account for the impact of airport altitude on emissions. Given that the altitudes of the study airports are 638 feet for RVS, 5,885 feet for APA, and 177 feet for SMO, this feature affected results for APA.

The altitude-specific modeling parameters were developed based on aircraft performance charts from a selection of piston-powered aircraft owner's manuals. Data for fuel, time, distance, and speed were pulled from climb, takeoff, and landing charts for the minimum increments of altitude reported—typically every 1,000 to 2,000 feet. Based on plots of the data and trend line, the initial examination showed that both the fuel consumed and times increased similarly with increasing altitude while fuel consumption rates remained relatively constant. Figure 36 illustrates this case using the climb data from the Lancair LC-40 Columbia owner's manual. "Time to climb" is the time needed to reach 50 feet above ground level. The 13 owner's manuals used to develop the adjustment are listed in Table 54.

Based on the number of engines and fuel metering type, the data from the 13 aircraft were assigned to the five groups listed below. Note that a turbocharged twin-engine aircraft manual was not found for evaluation in this effort.

- Single engine, fuel injected
- Single engine, turbocharged
- Twin engine, carbureted
- Single engine, carbureted
- Twin engine, fuel injected

Data for climb rates, time, distance, and speed were taken from takeoff and landing charts. Points were evaluated for multiple weights and wind directions and then averaged; a second-order polynomial was evaluated through the data of each aircraft such that any altitude could be evaluated. As an example, Figure 37 illustrates the takeoff-time data for the three single-engine carbureted aircraft.

Figure 36
Fuel and Time to Climb at Altitude, Lancair LC-40

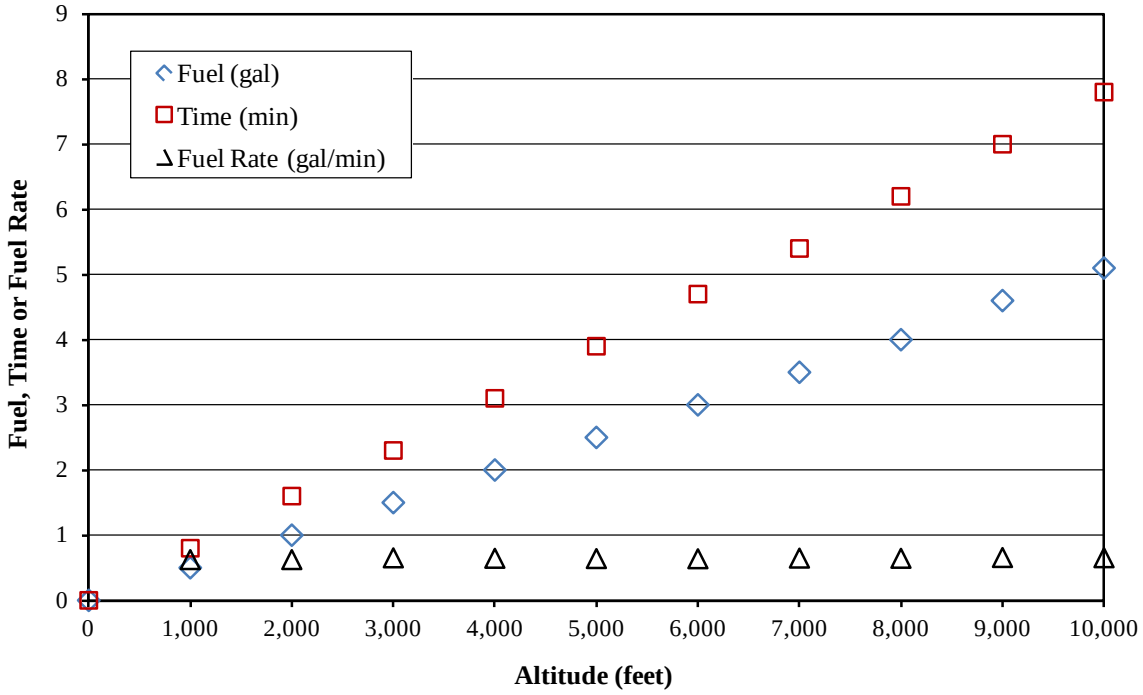

Table 54
Owner's Manuals Used for Developing Altitude Adjustments

Aircraft	Engines, Fuel Metering Technology
Cessna 150	Single Engine, Carbureted
Cessna 172M	Single Engine, Carbureted
Van's RV-12	Single Engine, Carbureted
Cessna 182T	Single Engine, Fuel Injection
Cessna 350 Corvalis	Single Engine, Fuel Injection
Rockwell Commander 112A	Single Engine, Fuel Injection
Mooney M20R	Single Engine, Fuel Injection
Cirrus SR22	Single Engine, Fuel Injection
Cessna 400	Single Engine, Turbo
Lancair LC-40 Columbia	Single Engine, Turbo
Piper PA-46	Single Engine, Turbo
Beechcraft Duchess	Twin Engine, Carbureted
Beechcraft Baron	Twin Engine, Fuel Injection

Figure 37
Altitude Impacts on Takeoff Time, Single-Engine Carbureted Aircraft

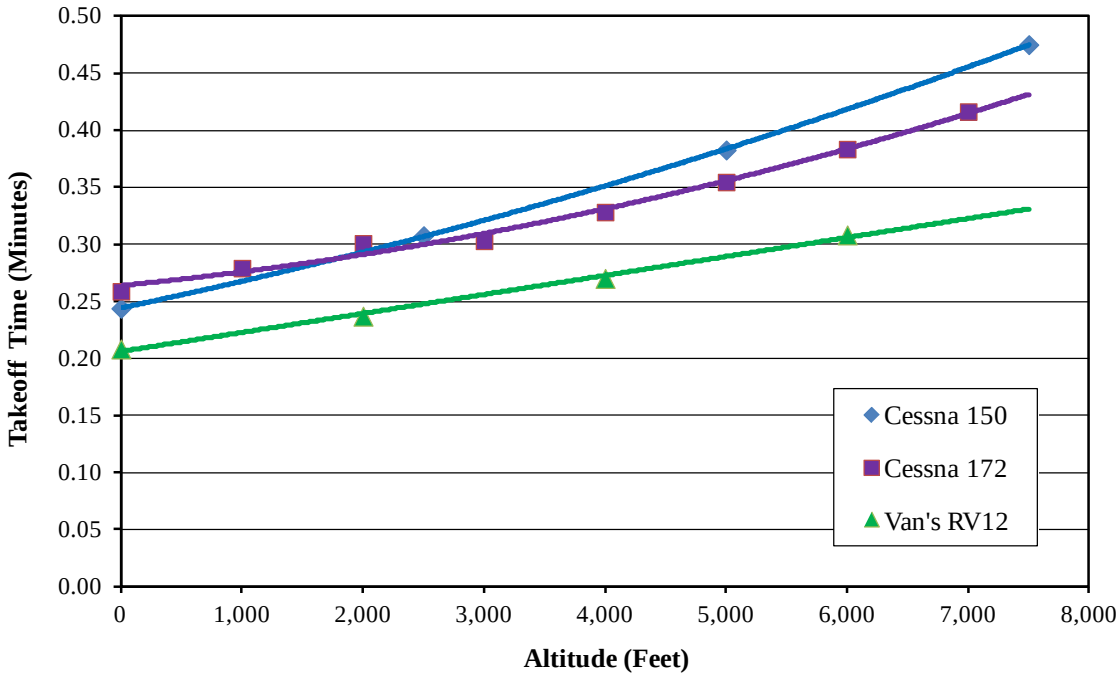

The data and regressions for each aircraft were used to evaluate key modeling parameters at the altitude of each airport. A simple mean of the aircraft results within each of the five technology groups was estimated. These results were combined in proportion to the technology group distribution observed in the aircraft inventory at each airport (for standard and continuous operating types distinctly). Table 55 summarizes the results for key modeling parameters. Overall, there is little difference observed between the RVS- and SMO-estimated parameters; however, the takeoff distances and times for APA are considerably larger, and landing angles are notably less. Note that the results reported in Table 55 are specific to the fleet of aircraft observed—hence, the reporting of separate results for standalone and continuous operation, as the aircraft fleets observed were different for the two types of operation.

Table 55
Selected Performance Results Evaluated at Altitude of Each Airport

Airport	Aircraft (Operation Type)	Takeoff Distance (Feet)	Takeoff Angle (Degrees)	Takeoff Time (Min)	Climb-Out Time to 50 Ft. AGL (Min)	Landing Angle (Degrees)
APA	Fixed-wing (Standalone)	1,285	3.4	0.42	0.15	3.2
	Fixed-wing (Continuous)	1,183	3.2	0.40	0.15	3.3
RVS	Fixed-wing (Standalone)	805	4.9	0.28	0.10	3.7
	Fixed-wing (Continuous)	752	4.9	0.27	0.11	3.7
SMO	Fixed-wing (Standalone)	837	5.0	0.28	0.10	3.7
	Fixed-wing (Continuous)	698	5.2	0.26	0.10	3.7

The altitude performance parameters were used for multiple purposes, including those described below.

- These data were used to validate and check the site-specific data collection for takeoff TIM and takeoff distances. It was generally observed that site-specific TIM estimates for takeoffs matched the performance parameters within a few seconds.

- These data were used to determine the range of takeoff and approach angles by aircraft type and from which the simple mean was determined (as reported in Table 55). This trajectory information was included in the episodic air quality modeling with AERMOD.

6.1.5 Other Airport-Specific Elements

There were several additional airport-specific elements and inventory methods applied. These are described as follows.

- Aviation Gasoline Pb Content – Pb content in gasoline was determined from local sample collections and varied between the three airports of study. The Pb content used in inventory development was 1.29, 1.60, and 1.91 g/gallon for RVS, APA, and SMO, respectively. Comparatively for the Chapter 4 analysis, the Pb content followed EPA procedures of modeling the Pb content at the maximum allowable of 2.12 g/gallon.

- Helicopter Operations – Helicopter operations were spatially and situationally distinct and accurately capturing the rotorcraft operations in the field studies was more uncertain. Helicopter operations were recorded at only two of the three airports (SMO and RVS); however, it should be noted that there are residence helicopters at APA based on the FAA Form 5010 filing. It is possible that helicopter operations were underrepresented in the field study data collection.

- Maintenance Run-Ups at RVS – Longer duration maintenance run-ups were assumed to be observed (audibly) at RVS which were not occurring at designated run-up locations on the taxiways. These loud engine noises were presumed to be due to maintenance operations occurring at FBOs. There were no similar observations at SMO or APA; however, a specific plan, such as surveying FBOs, was not completed at any of the airports. The inclusion of these maintenance run-ups as RVS was completed based on the proportion of time that they were observed (11 minutes out of each hour on average); and maintenance run-ups were assigned a fuel flow rate of 25% of the maximum based on a review of operations and repair manuals.

- Boeing B-17 Operation at APA – The Boeing B-17 "Flying Fortress" was present at APA for a specific event covering the period from June 3 to June 10, inclusive. The frequency, time of day, and location of B-17 activity was based on the narrative provided by the B-17 program manager. The B-17 aircraft was modeled distinctly from the remaining aircraft due to the order of magnitude higher gasoline consumption rates.

- Run-Up Procedures at APA – Common practice at general aviation airports is that fixed-wing aircraft run-up procedures occur at the run-up location proximate to the takeoff runway. APA had unique run-up procedures in that traffic control would, when conditions warranted, send aircraft to Taxiway C1 to perform run-ups prior to the takeoff runway being assigned. This additional variable procedure makes the spatial distribution of run-ups at APA more uncertain. The run-up location was modeled at APA as a frequency distribution from the on-the-ground observations (that was not temporally resolved).

- Variable Takeoff Points at APA – APA was the only airport where takeoffs would commence at multiple locations on the runway. All takeoffs at SMO and RVS (nearly all GA airports more generally) occur at the runway head only. However, at APA, planes were observed entering the runway (at various intersecting midpoints) and initiating takeoffs from that spot. Takeoffs at APA were treated by a distribution of start point based on on-the-ground observations. The primary runway at 10,000 feet in length is effectively twice as long as the longest runways at RVS or SMO.

- SMO Primary and Sensitivity Cases – There was an issue raised in the field study as to whether touch-and-go operations were underrepresented at SMO during the site data collection (where some touch-and-go operations were counted as landings). The SMO inventory analysis was completed by quantifying two bounding cases. The "primary case" retained the operations data as collected. The "sensitivity case" converted 20% of landings to touch-and-go operations, where 20% was determined by reducing the amount of landings such that total landings equaled total takeoffs over the field study period.

6.2 Results

This section compares the results from the application of the refined methodology with site-specific data for each airport to the results obtained for 2011 using the publicly available data as presented in Chapter 4. The site-specific data from the field studies makes notable improvements in local gasoline lead content, improves aircraft fleet characterization, and greatly improves characterization of the modes of operation.

The refined methodology common to the results of both Chapters 4 and 6 uses an expanded database of engine fuel consumption rates and uses engine efficiency (as measured by BSFC) to extrapolate fuel consumption rates to aircraft not covered by actual data. This method significantly improves the fuel consumption rate assignments to individual equipment.

6.2.1 RVS - Richard Lloyd Jones Jr.

Tables 56–58 compare the results obtained for RVS using site-specific data to those obtained using the publicly available resources of Chapter 4. Table 56 shows Pb emissions per piston-engine aircraft operation as a function of operating mode for fixed-wing aircraft and rotorcraft; these emissions are shown on a percentage basis in Table 57. As shown, Pb emissions per operation at RVS were considerably lower based on site-specific data. Another finding was that the inclusion of rotorcraft, data for which were not publicly available, had only a minor impact on per-operation Pb emissions.

Table 56
RVS Pb Emissions – Grams per Piston Operation

Aircraft	Engine Mode	Chapter 4 Analysis	Site-Specific Data
Fixed-Wing Aircraft	Idle/Taxi (Takeoff)	0.9726	0.1619
	Run-Up	0.3814	0.0526
	Takeoff	0.1483	0.0440
	Climb-Out	2.0565	0.2794
	Approach	1.4060	0.1880
	Idle/Taxi (Landing)	0.3242	0.0618
	Idle/Taxi (Taxi-Back)	n/a	0.0151
	Ground Roll (Touch&Go)	n/a	0.0060
Rotorcraft	Idle/Taxi (Departure)	n/a	0.0017
	Run-Up	n/a	0.0006
	Climb-Out	n/a	0.0008
	Approach	n/a	0.0007
	Idle/Taxi (Arrival)	n/a	0.0017
Total		5.29	0.81

Table 57
RVS Pb Emissions – Percent by Mode

	Engine Mode	Chapter 4 Analysis	Site-Specific Data
Fixed-Wing Aircraft	Idle/Taxi (Takeoff)	18.4%	19.9%
	Run-Up	7.2%	6.5%
	Takeoff	2.8%	5.4%
	Climb-Out	38.9%	34.3%
	Approach	26.6%	23.1%
	Idle/Taxi (Landing)	6.1%	7.6%
	Idle/Taxi (Taxi-Back)	n/a	1.8%
	Ground Roll (Touch&Go)	n/a	0.7%
Rotorcraft	Idle/Taxi (Departure)	n/a	0.2%
	Run-Up	n/a	0.1%
	Climb-Out	n/a	0.1%
	Approach	n/a	0.1%
	Idle/Taxi (Arrival)	n/a	0.2%
Total		100%	100%

Table 58
RVS Pb Emissions – CY2011 Operations (Tons)

	Engine Mode	Chapter 4 Analysis	Site-Specific Data
Fixed-Wing Aircraft	Idle/Taxi (Takeoff)	0.0886	0.0325
	Run-Up	0.0347	0.0238
	Takeoff	0.0135	0.0088
	Climb-Out	0.1873	0.0561
	Approach	0.1281	0.0378
	Idle/Taxi (Landing)	0.0295	0.0124
	Idle/Taxi (Taxi-Back)	n/a	0.0030
	Ground Roll (Touch&Go)	n/a	0.0012
Rotorcraft	Idle/Taxi (Departure)	n/a	0.0004
	Run-Up	n/a	0.0001
	Climb-Out	n/a	0.0002
	Approach	n/a	0.0001
	Idle/Taxi (Arrival)	n/a	0.0004
Total (all engine modes)		0.48	0.18
Total (ground modes only)		0.166	0.083

Table 58 presents the annual emission estimates for RVS during calendar year 2011 using the Chapter 4 analysis and the site-specific data. As shown, the site-specific annual Pb inventory at RVS was 63% and 50% less for all modes and for ground modes, respectively. The "ground modes only" excludes the aloft activity of climb-out and approach.

It is noteworthy to mention that RVS was the only facility that explicitly estimated emissions from the observed maintenance run-ups in the field study. The results presented in Tables 56 and 57 do not include the maintenance run-up emissions in the results reported as these tables are meant to convey emissions per unit of operation (and maintenance run-ups are independent of operation). However, the total inventory of Table 58 does include both magneto run-up and maintenance run-up. The maintenance run-up share is just over half (52%) of the total run-up emissions reported.

6.2.2 APA - Centennial

Tables 59–61 compare results obtained for APA using site-specific data relative to those estimated in Chapter 4. Table 59 shows Pb emissions per piston-engine aircraft operation as a function of operating mode for fixed-wing aircraft and rotorcraft; these emissions are shown on a percentage basis in Table 60. Again, as was the case at RVS, Pb emissions per operation at APA were considerably lower based on site-specific data.

Table 59
APA Pb Emissions – Grams per Piston Operation

Aircraft	Engine Mode	Chapter 4 Analysis	Site-Specific Data
Fixed-Wing Aircraft	Idle/Taxi (Takeoff)	1.4191	0.1740
	Run-Up	0.5588	0.0577
	Takeoff	0.2173	0.0681
	Climb-Out	2.9718	0.3785
	Approach	1.9987	0.2291
	Idle/Taxi (Landing)	0.4730	0.0761
	Idle/Taxi (Taxi-Back)	n/a	0.0006
	Ground Roll (Touch&Go)	n/a	0.0271
Total		7.64	1.01

Table 60
APA Pb Emissions – Percent by Mode

Aircraft	Engine Mode	Chapter 4 Analysis	Site-Specific Data
Fixed-Wing Aircraft	Idle/Taxi (Takeoff)	18.6%	17.2%
	Run-Up	7.3%	5.7%
	Takeoff	2.8%	6.7%
	Climb-Out	38.9%	37.4%
	Approach	26.2%	22.7%
	Idle/Taxi (Landing)	6.2%	7.5%
	Idle/Taxi (Taxi-Back)	n/a	0.1%
	Ground Roll (Touch&Go)	n/a	2.7%
Total		100%	100%

Table 61 presents annual emission estimates for APA during calendar year 2011 using the publicly available and site-specific data. As shown, the site-specific annual Pb inventory at APA was 63% and 50% less for all modes and for ground modes, respectively.

It is noteworthy to mention that the contribution of the Boeing B-17 to the APA site-specific inventory. The B-17 made up 0.2% of the operations and 9% of the Pb emissions. The annual inventory of Table 61 includes the B-17, presuming that its presence in the field study period is representative of the year as a whole.

Table 61
APA Pb Emissions – CY2011 Operations (Tons)

Aircraft	Engine Mode	Chapter 4 Analysis	Site-Specific Data
Fixed-Wing Aircraft	Idle/Taxi (Takeoff)	0.3274	0.0444
	Run-Up	0.1289	0.0157
	Takeoff	0.0501	0.0174
	Climb-Out	0.6856	0.0965
	Approach	0.4611	0.0584
	Idle/Taxi (Landing)	0.1091	0.0194
	Idle/Taxi (Taxi-Back)	n/a	0.0001
	Ground Roll (Touch&Go)	n/a	0.0069
Total (all engine modes)		1.76	0.26
Total (ground modes only)		0.616	0.104

6.2.3 SMO – Santa Monica

Tables 62–64 compare results obtained for SMO using site-specific data relative to those estimated in Chapter 4. Table 62 shows Pb emissions per piston-engine aircraft operation as a function of operating mode for fixed-wing aircraft and rotorcraft; these emissions are shown on a percentage basis in Table 63. The Chapter 4 results include two assumptions for TIM (FAA/EPA default and the ICF SMO study values). The site-specific results include both the primary and sensitivity cases (as described in Section 6.1.5). The sensitivity case includes an additional 20% of piston-powered aircraft operations assigned to touch and go, as it was believed that the touch-and-go operations were underrepresented in the data collection that makes up the primary case. Again, Pb emissions per operation at SMO are generally lower based on site-specific data, as was also the case at RVS and APA.

Table 64 presents annual emission estimates for SMO during calendar year 2011 using the publicly available and site-specific data. As shown (looking at the total ground mode results only), the site-specific annual Pb inventory at SMO was less than those estimated in Chapter 4 by a range of 29% to 65%, depending on which cases are compared.

It is noteworthy to comment on the ICF SMO study TIM data collection based on the comparable experience of TIM data collection for the three airports of this study. The ICF report (ICF International and T&B Systems 2010) did not detail how the times were recorded for the aloft engine modes (i.e., approach and climb-out) other than these were collected by "graduate students." For modeling purposes, the ICF report also states that the maximum altitude was 600 and 900 feet for fixed-wing and rotorcraft aloft modes, respectively, but this determination is not documented or justified. In contrast, the site-specific TIM data collection for this project found it impossible to accurately estimate time aloft for approach or climb-outs. We cannot qualify the accuracy of the TIM estimates for the aloft modes as reported by the ICF Study, but these were used here because the ICF SMO TIM data are part of the public domain of information for this airport.

Table 62
SMO Pb Emissions – Grams per Piston Operation

Aircraft	Engine Mode	Chapter 4 Analysis		Site-Specific Data	
		ICF SMO TIM	FAA/EPA Default TIM	Primary Case	Sensitivity Case
Fixed-Wing Aircraft	Idle/Taxi (Takeoff)	0.3757	0.8898	0.2421	0.2182
	Run-Up	0.3521	0.3521[a]	0.0638	0.0575
	Takeoff	0.1217	0.1369	0.0751	0.0677
	Climb-Out	0.4926	1.8945	0.3778	0.4248
	Approach	0.2301	1.2944	0.3636	0.3127
	Idle/Taxi (Landing)	0.1878	0.2966	0.1398	0.1005
	Idle/Taxi (Taxi-Back)	n/a	n/a	0.0317	0.0263
	Ground Roll (Touch&Go)	n/a	n/a	0.0005	0.0045
Rotorcraft	Idle/Taxi (Departure)	n/a	n/a	0.0027	0.0025
	Run-Up	n/a	n/a	0.0009	0.0008
	Climb-Out	n/a	n/a	0.0014	0.0012
	Approach	n/a	n/a	0.0012	0.0010
	Idle/Taxi (Arrival)	n/a	n/a	0.0027	0.0025
Total		1.76	4.86	1.30	1.22

n/a = not available
[a] The EPA/FAA default does not include the run-up mode; however, for this analysis the run-up mode was added for completeness as applied in Chapter 4 (see Table 13).

Table 63
SMO Pb Emissions – Percent by Mode

Aircraft	Engine Mode	Chapter 4 Analysis		Site-Specific Data	
		ICF SMO TIM	FAA/EPA Default TIM	Primary Case	Sensitivity Case
Fixed-Wing Aircraft	Idle/Taxi (Takeoff)	21.3%	18.3%	18.6%	17.9%
	Run-Up	20.0%	7.2%[a]	4.9%	4.7%
	Takeoff	6.9%	2.8%	5.8%	5.5%
	Climb-Out	28.0%	38.9%	29.0%	34.8%
	Approach	13.1%	26.6%	27.9%	25.6%
	Idle/Taxi (Landing)	10.7%	6.1%	10.7%	8.2%
	Idle/Taxi (Taxi-Back)	n/a	n/a	2.4%	2.2%
	Ground Roll (Touch&Go)	n/a	n/a	0.0%	0.4%
Rotorcraft	Idle/Taxi (Departure)	n/a	n/a	0.2%	0.2%
	Run-Up	n/a	n/a	0.0%	0.0%
	Climb-Out	n/a	n/a	0.1%	0.1%
	Approach	n/a	n/a	0.1%	0.1%
	Idle/Taxi (Arrival)	n/a	n/a	0.2%	0.2%
Total		100%	100%	100%	100%

n/a = not available

[a] The EPA/FAA default does not include the run-up mode; however, for this analysis the run-up mode was added for completeness as applied in Chapter 4 (see Table 13).

Table 64
SMO Pb Emissions – CY2011 Operations (Tons)

Aircraft	Engine Mode	Chapter 4 Analysis		Site Data Collection	
		ICF SMO TIM	FAA/EPA Default TIM	Primary Case	Sensitivity Case
Fixed-Wing Aircraft	Idle/Taxi (Takeoff)	0.0291	0.0689	0.0226	0.0209
	Run-Up	0.0272	0.0272[a]	0.0060	0.0055
	Takeoff	0.0094	0.0106	0.0070	0.0065
	Climb-Out	0.0381	0.1466	0.0353	0.0406
	Approach	0.0178	0.1002	0.0339	0.0299
	Idle/Taxi (Landing)	0.0145	0.0230	0.0030	0.0096
	Idle/Taxi (Taxi-Back)	n/a	n/a	0.0025	0.0025
	Ground Roll (Touch&Go)	n/a	n/a	0.0000	0.0004
Rotorcraft	Idle/Taxi (Departure)	n/a	n/a	0.0003	0.0002
	Run-Up	n/a	n/a	0.0001	0.0001
	Climb-Out	n/a	n/a	0.0001	0.0001
	Approach	n/a	n/a	0.0001	0.0001
	Idle/Taxi (Arrival)	n/a	n/a	0.0003	0.0002
Total (all engine modes)		0.136	0.376	0.122	0.117
Total (ground modes only)		0.080	0.130	0.052	0.046

n/a = not available
[a] The EPA/FAA default does not include the run-up mode; however, for this analysis the run-up mode was added for completeness as applied in Chapter 4 (see Table 13).

6.3 Conclusions

The primary conclusions from the site-specific inventory analysis are as follows.

1. Overall, the Pb emission inventory using site-specific data was significantly lower than inventories developed using public domain data as reported in Chapter 4.

2. Site-specific aviation gasoline samples collected showed a Pb content below the maximum allowed by 24% on average, with significant variation between the three airports. This contributed to the reduction in Pb emissions using site-specific data. The standard FAA/EPA emission inventory procedures that rely on the maximum Pb content allowed will be biased high based on these results.

3. Site-specific operations data show that “continuous” operations represent a significant portion (29 to 54%) of piston-powered activity at these three airports, which have one or more flight schools on site that is not taken into account by existing inventory methods. Accounting for continuous operations substantially reduced emission estimates for the ground operation modes.

4. The results for RVS indicate that maintenance run-ups may be a significant source of emissions. The evaluation of maintenance run-ups is not comprehensive, and warrants further study in future efforts.

5. The Traffic Pattern Altitudes (TPA) of each airport—which were used for determining the TIM for climb-out and approach—were substantially lower than the 3,000 foot default value used in the FAA/EPA methodology and more accurately represent airport operations.

6. The impacts of large, legacy aircraft such as the Boeing B-17 observed at APA can be significant and may require special inventory procedures given that this aircraft consumes fuel at a rate of 40 to 50 times that of the average piston aircraft. In the APA evaluation, the B-17 was treated as a separate aircraft type with aircraft-specific information collected to determine the exact dates and hours flown, trips per day completed, runway locations used, and run-up procedures. The inclusion of this B-17-specific activity data resulted in a 32% reduction in the estimated inventory for the APA facility, relative to a preliminary assessment that generically modeled the B-17 in the aircraft fleet in proportion to that observed in the raw video data. The special treatment of this aircraft was necessitated by its disproportionate impact on the inventory results and because its usage was not well represented by the fleet-average piston aircraft.

###

7. AIR QUALITY MODELING AND EMISSION INVENTORY EVALUATION

7.1 Air Quality Modeling

Using the spatially and temporally resolved Pb emissions estimates described in Chapter 6, an ambient air quality modeling assessment was performed for each study site to evaluate how well modeled and measured localized ground-level lead concentrations compare at the sampling locations for each of the three airports.

The modeling was performed using the American Meteorological Society/Environmental Protection Agency Regulatory Model Improvement Committee (AERMIC) modeling system, also known as AERMOD (version 13350). Because of the model's versatility, it is the most appropriate air quality modeling tool for assessing the Pb emission impacts from piston-engine aircraft. AERMOD has been used successfully by others in evaluating ambient impacts from aircraft operations, and was used to perform preliminary site modeling that determined the placement of the ambient monitors at the field study sites.

The AERMOD modeling system includes a steady-state, multiple-source, Gaussian dispersion model designed for use with discrete or more dispersed emissions sources (point, area, and volume sources). The model is capable of estimating concentrations for a wide range of averaging times (from one hour to one year, and multiple years). Both of these attributes—dispersed emission sources and a variety of averaging periods—were necessary for the modeling that was performed for this study.

The AERMOD modeling system includes two preprocessors in addition to the dispersion model itself: AERMET and AERMAP. AERMET is a meteorological preprocessor (which relies on two other preprocessors, AERSURFACE and AERMINUTE), while AERMAP is a terrain preprocessor that characterizes terrain for the generation of receptor grids. The AERMOD modeling system requires the following inputs:

- Model options;
- Meteorological data;
- Source characterization; and
- Receptor data.

The inputs used in each of these areas are discussed below.

7.1.1 Model Options

The model has a set of recommended default options for the user for some of these parameters. AERMOD was typically run using the following options:

- U.S. EPA regulatory default options;
- No treatment for building downwash effects; and
- Direction-specific, season-specific dispersion processing (based on land use designations from AERSURFACE).

AERMOD includes treatment for an urban boundary layer under stable conditions and a state-of the-science wet and dry deposition model. Only SMO is located within a large urban area (APA and RVS are located on the urban fringe). The URBANOPT option, with default urban surface roughness of one meter, is available in AERMOD for use when coupled with the URBANSRC keyword for developing an urban boundary layer under stable conditions. Nevertheless, the URBANOPT option was not used for any site, since aircraft activity and the modeling study concentrated on daytime, not nighttime, impacts.

7.1.2 Meteorological Data Selection

AERMOD uses hourly meteorological data to characterize plume dispersion. The representativeness of the data is dependent on the proximity of the meteorological monitoring site to the area under consideration, the complexity of the terrain, the exposure of the meteorological monitoring site, and the period of time during which the data are collected. Standard, hourly, extended National Weather Service Automated Surface Observing Stations (ASOS) date sets in TC-3505 ISHD format were used for all three sites, with low hourly wind speed data supplemented by one-minute ASOS data in TD-6405 format, per standard AERMINUTE methodology. The meteorological data sets used in these analyses combined surface meteorological data (e.g., wind speed and direction, temperature), surface data (cloud cover), and upper air data for the three selected study airports as summarized in Table 65.

Table 65
Sources for Meteorological Data

Airport/Surface Met Data/Cloud Cover	Upper Air Data
Centennial, CO (APA)	Denver, CO (Stapleton)
Tulsa, OK (RVS)	Norman, OK
Santa Monica, CA (SMO)	San Diego, CA (Miramar)[1]

1. Based on direction from the ACRP 02-34 Panel, data from Los Angeles International Airport (LAX) had been intended to be used rather than data from San Diego/Miramar; however, the radar wind profiler at LAX was inoperative during the July 2013 field study period at SMO. This precluded the use of upper air data from LAX.

The values for the surface characteristics of albedo, Bowen ratio, and surface roughness appropriate to the area around the surface meteorological monitoring stations were obtained from AERSURFACE. AERSURFACE is a surface-characteristic preprocessor that is part of the AERMOD modeling system. The preprocessor is designed to aid in obtaining realistic and reproducible surface characteristic values for AERMET, following EPA guidance. AERSURFACE uses as input the land cover data from the U.S. Geological Survey (USGS) National Land Cover Data 1992 archives (NLCD92). Land use in the areas surrounding the airport was surveyed using Google Earth images to confirm that no significant changes have taken place since the early 1990s that could be expected to affect dispersion characteristics. The specific sectors to be evaluated were determined by prevailing wind directions observed during the meteorological data collection period. Appropriate season-specific surface characteristics, corresponding to the periods during which observations were recorded at each airport, were used. Radii recommended by EPA modeling guidance were used to define the surface characteristics to be evaluated (one kilometer, centered on the meteorological tower, for surface roughness, and 10 kilometers for albedo and Bowen ratio).

7.1.3 Source Characterization: Runway Configuration and Aircraft Wake Turbulence

All Pb emission sources at each airports were characterized as line sources (represented as a string of volume sources) to represent the initial horizontal and vertical dispersion of the emissions depending upon the operating mode. Average wind speeds were calculated over the period during which airport activity data are collected to allow calculation of an initial vertical dispersion parameter for each airport, as described below.

Taxi/idle, takeoff, climb-out, and approach/landing traffic for each type of aircraft were allocated to specific airport locations according to operating mode observations made during the activity data collection phase of the project. Emissions during run-up activities were also allocated to airport areas based on observations. The activity locations for each airport are shown in Appendix C.

Common site-specific modeling parameters used for each airport are summarized in Table 66; site-specific parameters are summarized in Tables 67–69. All of these parameters are discussed in more detail below.

Table 66
Modeling Parameters Common to All Airports

Activity	Parameter	Value	Reference
Fixed-wing Aircraft			
Taxi	Source separation distance	18.29 meters	Based on CALINE assumptions
Takeoff	Source separation distance	50 meters	Based on ICF report
Climb-out_1	Initial portion of climb-out	50 feet	Based on performance statistics from aircraft owner's manuals[1]
Landing	Source separation distance	50 meters	Based on ICF report
Approach	Vertical extent of modeling domain	Traffic pattern altitude	Traffic pattern altitude – same as lead inventory
Run-up	Source separation distance	100 feet	Based on ICF report
	Width of volume source	100 feet	Assumed size of area in which run-up takes place
Touch and go	Source separation distance	50 meters	Based on ICF report
Helicopters			
Climb-out	Angle of climb	3.7 degrees	Variable – aircraft approach angle used
	Vertical extent of modeling domain	500 feet	Traffic pattern altitude – same as lead inventory
Approach	Vertical extent of modeling domain	500 feet	Traffic pattern altitude – same as lead inventory

[1] See Section 6.1.4 for a discussion of the development of these performance characteristics and modeling parameters.

Table 67
RVS Site-Specific Modeling Parameters

Activity	Parameter	Value	Reference
Fixed-wing Aircraft			
Taxi	Width of taxiway	40 feet	Taken from airport diagrams
Takeoff	Width of runway	50 or 100 feet	Taken from airport diagrams
	Location where aircraft leaves runway	1,145 feet from start of runway	Based on observations of aircraft activity
Climb-out_1	Angle of climb	4.9 degrees	Based on performance statistics from aircraft owner's manuals[1]
Climb-out_2	Angle of climb	4.9 degrees	Based on performance statistics from aircraft owner's manuals[1]
	Remainder of climb-out	50 feet to 1,075 feet	Traffic pattern altitude – same as lead inventory
Landing	Width of runway	50 or 100 feet	Taken from airport diagrams
	Location where aircraft touches down	890 feet from start of runway	Based on observations of aircraft activity
Approach	Glide slope angle	3.7 degrees	Based on performance statistics from aircraft owner's manuals[1]
	Vertical extent of modeling domain	1,075 feet	Traffic pattern altitude – same as lead inventory
Touch and go	Width of runway	100 feet	Take from airport diagrams
	Location where aircraft leaves runway	768 feet from start of runway	Based on observations of aircraft activity
	Location where aircraft touches down	2,161 feet from start of runway	Based on observations of aircraft activity
Helicopters			
Approach	Angle of descent	3.7 degrees	Variable – aircraft approach angle used

[1] See Section 6.1.4 for a discussion of the development of these performance characteristics and modeling parameters.

Table 68
APA Site-Specific Modeling Parameters

Activity	Parameter	Value	Reference
Fixed-wing Aircraft			
Taxi	Width of taxiway	40 feet for minor taxiways; 50 ft for major taxiways. For modeling, 40 feet use uniformly assumed	Taken from airport diagrams
Takeoff	Width of runway	75, 80 and 100 feet	Taken from airport diagrams
	Location where aircraft leaves runway	Distance from start of runway	Based on observations of aircraft activity
		2,785 ft	35L, 35R@A18, 17R, 10, 28@C5
		4,299 ft	35R @A16
		5,795 ft	35R @A14
		1,145 ft	17L
		4,173 ft	28@C4
Climb-out_1	Angle of climb	3.4 degrees	Based on performance statistics from aircraft owner's manuals[1]
Climb-out_2	Angle of climb	4.9 degrees	Based on performance statistics from aircraft owner's manuals[1]
	Remainder of climb-out	50 feet to 1,000 feet	Traffic pattern altitude – same as lead inventory.
Landing	Width of runway	75, 80 and 100 feet	Taken from airport diagrams
	Location where aircraft touches down	Distance from start of runway	Based on observations of aircraft activity
		1,503 ft	35L
		2,140 ft	35R
		1,638 ft	17L
		1,137 ft	17R
		723 ft	10
		614 ft	28
Approach	Glide slope angle	3.2 degrees	Based on performance statistics from aircraft owner's manuals[1]
	Vertical extent of modeling domain	1,000 feet	Traffic pattern altitude – same as lead inventory
Touch and go	Width of runway	100 feet	Taken from airport diagrams
	Location where aircraft leaves runway	1,226 feet from start of runway	Based on observations of aircraft activity
	Location where aircraft touches down	2,988 feet from start of runway	Based on observations of aircraft activity

[1] See Section 6.1.4 for a discussion of the development of these performance characteristics and modeling parameters.

Table 69
Site-Specific Modeling Parameters, SMO

Activity	Parameter	Value	Reference
Fixed-wing Aircraft			
Taxi	Width of taxiway	40 feet	Taken from airport diagrams
Takeoff	Width of runway	145 feet	Taken from airport diagrams
	Location where aircraft leaves runway	1,145 feet from start of runway	Based on observations of aircraft activity
Climb-out_1	Angle of climb	4.9 degrees	Based on performance statistics from aircraft owner's manuals[1]
Climb-out_2	Angle of climb	4.9 degrees	Based on performance statistics from aircraft owner's manuals[1]
	Remainder of climb-out	50 feet to 1,212 feet	Traffic pattern altitude – same as lead inventory
Landing	Width of runway	145 feet	Taken from airport diagrams
	Location where aircraft touches down	1,200 feet from start of runway	Based on observations of aircraft activity
Approach	Glide slope angle	3.7 degrees	Based on performance statistics from aircraft owner's manuals[1]
	Vertical extent of modeling domain	1,212 feet	Traffic pattern altitude – same as lead inventory
Touch and go	Width of runway	145 feet	Taken from airport diagrams
	Location where aircraft leaves runway	930 feet from start of runway	Based on observations of aircraft activity
	Location where aircraft touches down	1,600 feet from start of runway	Based on observations of aircraft activity
Helicopters			
Approach	Angle of descent	3.7 degrees	Variable – corkscrew approach used

[1] See Section 6.1.4 for a discussion of the development of these performance characteristics and modeling parameters.

Consistent with modeling performed previously at SMO, a source spacing of 50 meters was used for the runway. This distance balances the computational requirements with sufficient source density to preserve the horizontal geometry of the source configuration and accurately simulate the near-field concentration gradient. The approach used here is similar to the approach developed by Piazza (1999) but with some additional enhancements, particularly for the modeling of run-up.

For fixed-wing aircraft, initial horizontal dispersion (σ_y) was calculated as suggested in the AERMOD documentation (U.S. EPA 2004, Table 3-1) as the source separation distance divided by 2.15. Initial vertical dispersion (σ_z) was calculated using the mixing zone residence time as defined in CALINE3 model:

$$SZI = \left[(1.8 + 0.11) * \left(\frac{W2}{U}\right)\right] * \left(\frac{60}{30}\right)^{0.2}$$

where

SZI = initial vertical dispersion (m);

W2 = half-width of the runway or taxiway (m); and

U = average wind speed over the modeling period (m/s).

This equation accounts for the longer time an air parcel spends in the turbulent mixing zone and hence the greater initial vertical dispersion.

Dispersion Parameters: Taxiing – With the exception of touch-and-go operations, aircraft were assumed to be in taxi mode both prior to takeoff and following touchdown, and through landing roll and other post-landing movements, until parked. The rows of volume sources used to represent emissions during taxi operations were modeled as surface-based sources.

The source separation distance (the center-to-center distance of adjacent volume sources) was taken as 50 meters, following the ICF report (ICF International and T&B Systems 2010). The width of each taxiway was taken from airport diagrams presented previously and is shown in Tables 79–82. Initial sigma-z was calculated from the equation above using W2 = 24.4/2 = 12.2 meters. Initial sigma-y was calculated as the source separation distance divided by 2.15, or 23.3 meters.

Dispersion Parameters: Takeoff/Climb-out/Approach/Landing – These aircraft operation modes are defined below.

- *Takeoff* – The period during which the aircraft operates at full throttle, which lasts from the initial roll until wheels up.

- *Climb-out mode* – The end of takeoff until the aircraft reaches cruise altitude. For this modeling analysis, climb-out activity was modeled up to the traffic pattern altitude (TPA), consistent with the inventory calculations described in Section 6.1.4.

- *Approach/landing* – The period of operation between the time the aircraft elevation is below the traffic pattern altitude (as defined for climb-out) until the aircraft touches down on the runway.

- *Touch-and-go* – Approach/landing and takeoff/climb-out without intervening run-up or taxi activities.

The vertical extent used in the modeling analysis for each airport and aircraft type was the same as the dimension used in calculating lead emission inventories to ensure consistency between the inventories and modeling assumptions. Because of the lack of site-specific data, rotary-winged aircraft were assumed to use the same approach and climb-out flight trajectories as fixed-wing aircraft but with a lower TPA.

The value used for source separation was the same as those in the ICF report (50 meters).. Values used for the widths of runways were the physical widths, as shown in Appendix C. Calculated sigma-y and sigma-z for takeoff, climb-out, approach, and landing activities at each airport were the same as those used for taxiing activities. However, the rows of volume sources used to represent emissions during climb-out and approach operations were modeled as elevated sources.

An additional consideration was made to account for the wake turbulence created by the forces that lift the fixed-wing aircraft. High-pressure air from the lower surface of the wings flows around the wing tips to the lower-pressure region above the wings. A pair of counter-rotating vortices is shed from the wings where the right- and left-wing vortices rotate. It is within this region of rotating air behind the aircraft where wake turbulence occurs. To account for this effect, the effective emission height was adjusted for the angle of climb (takeoff) and glide slope angle for landing. This adjustment lowers the effective emission height to approximate the maximum downward extent of the aircraft's trailing wake. This resulted in an angle of climb-out for takeoff of approximately 4.9 degrees; for landing, this was 3.7 degrees. These angles were used for all airports because robust site-specific data could not be developed from the individual airport observations.

The locations at which takeoff and landing occur were determined based on observations of flight operations at each airport. Locations where the aircraft comes to a complete stop in approach mode were also defined for each airport, based on observation of flight operations. Specific locations are shown again in the airport diagrams.

As noted previously, SMO has a single runway, while RVS and APA have three runways each. Again, aircraft operations were allocated to runways based on observations of flight operations.

Dispersion Parameters: Run-up Sources – Source separation distance for the individual volume sources representing the run-up activities were taken from the ICF report as 100 feet. The width of each volume source was determined based on the size of the area at each airport where run-up activities were observed to take place. Initial sigma-y for these

sources representing fixed-wing aircraft was calculated as the sum of three components: wingspan wake, horizontal momentum, and propeller turbulence wake. The values for these components were taken from the ICF report. Wingspan wake was calculated as the source separation distance (30.48 m) divided by 2.15; the horizontal momentum (0.6 m) and prop turbulence wake (0.85 m) terms are constants.

Initial sigma-z also has three components: the elevation of the emissions release, exhaust buoyancy, and the effect of wind flow over the stationary aircraft. The height of the emissions release was assumed to be 1 meter and the exhaust buoyancy term was 0.65 meters (consistent with the values developed by ICF). This was done using the site-specific wind speed data collected at 10 meters, which the AERMET preprocessor automatically uses, along with the input roughness lengths, to calculate a log-wind profile down to ground level.

Dispersion Parameters: Helicopters – For helicopters, initial sigma-z during idle was based on a typical piston-engine helicopter height of approximately 4.0 meters divided by 2.15, or 1.86 meters. Initial sigma-y was based on a typical helicopter rotor width of 10 meters divided by 4.13, or 2.3 meters. The descent rate and angle of descent were assumed to be 3.7 degrees.

7.1.4 Receptor Grid Selection and Coverage

Receptor and source base elevations were determined from U.S. Geological Survey (USGS) National Elevation Dataset (NED) data in the GeoTIFF format at a horizontal resolution of 1 arc-second (approximately 30 meters). All coordinates were referenced to UTM North American Datum 1983 (NAD83). The AERMOD receptor elevations were interpolated among the data nodes according to standard AERMAP procedures. Cartesian coordinate receptor grids were used to provide adequate spatial coverage within and around the project area for assessing ground-level pollution concentrations, to identify the extent of significant impacts, and to identify maximum impact locations. Discrete receptors were also placed at the locations of the airborne PM sampling locations and in a 30-by-30 meter grid surrounding each sampling location (spaced at 10 meters within each grid) for use in comparing measured and modeled concentrations. The receptor grid layouts for each airport are illustrated in Figures 38–40.

The AERMOD model was used to generate one-hour average modeled ambient lead concentrations, which were converted into 12-hour average concentrations for purposes of comparison to the ambient monitoring results.

Figure 38
RVS Receptor Grid

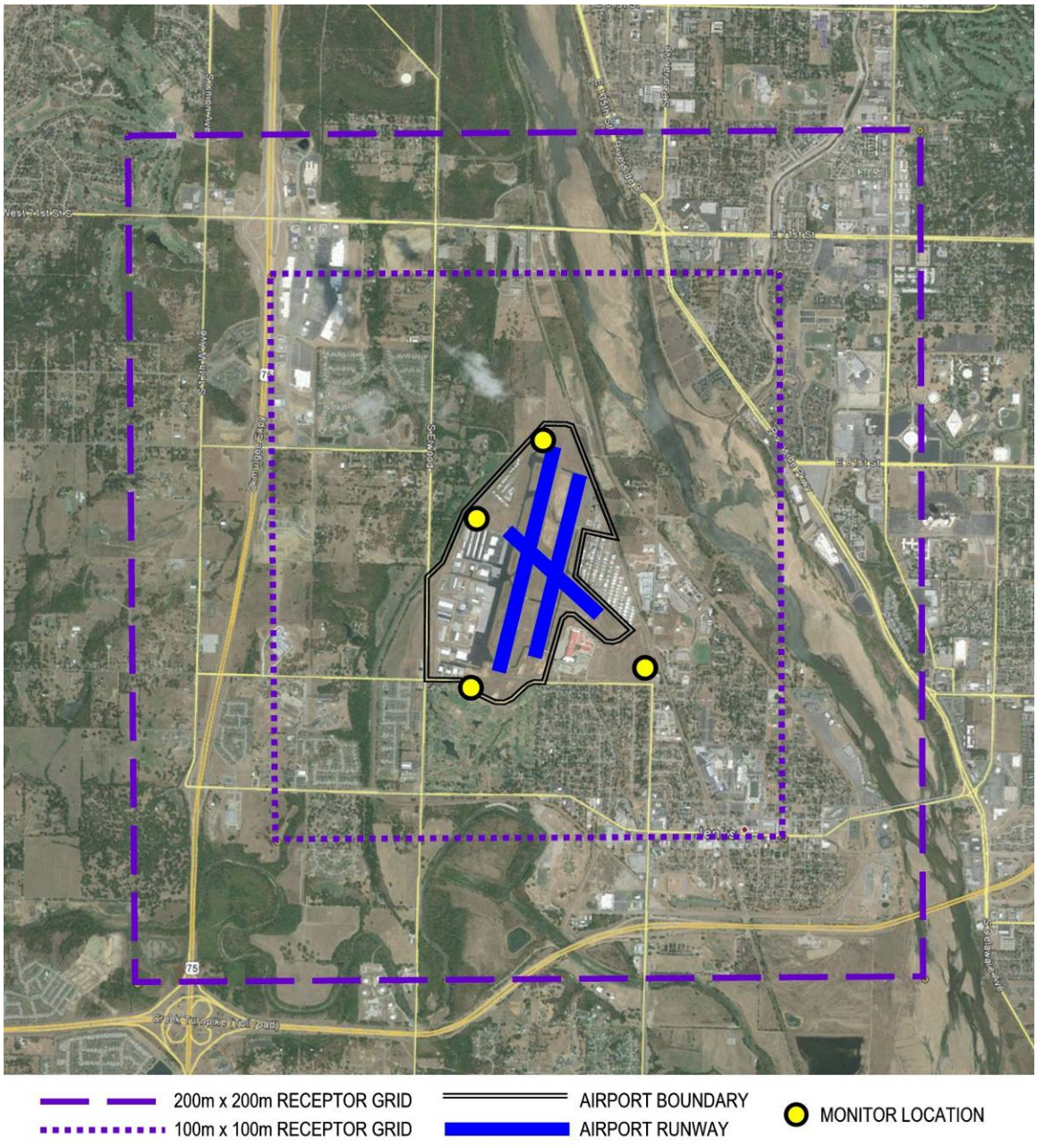

Figure 39
APA Receptor Grid

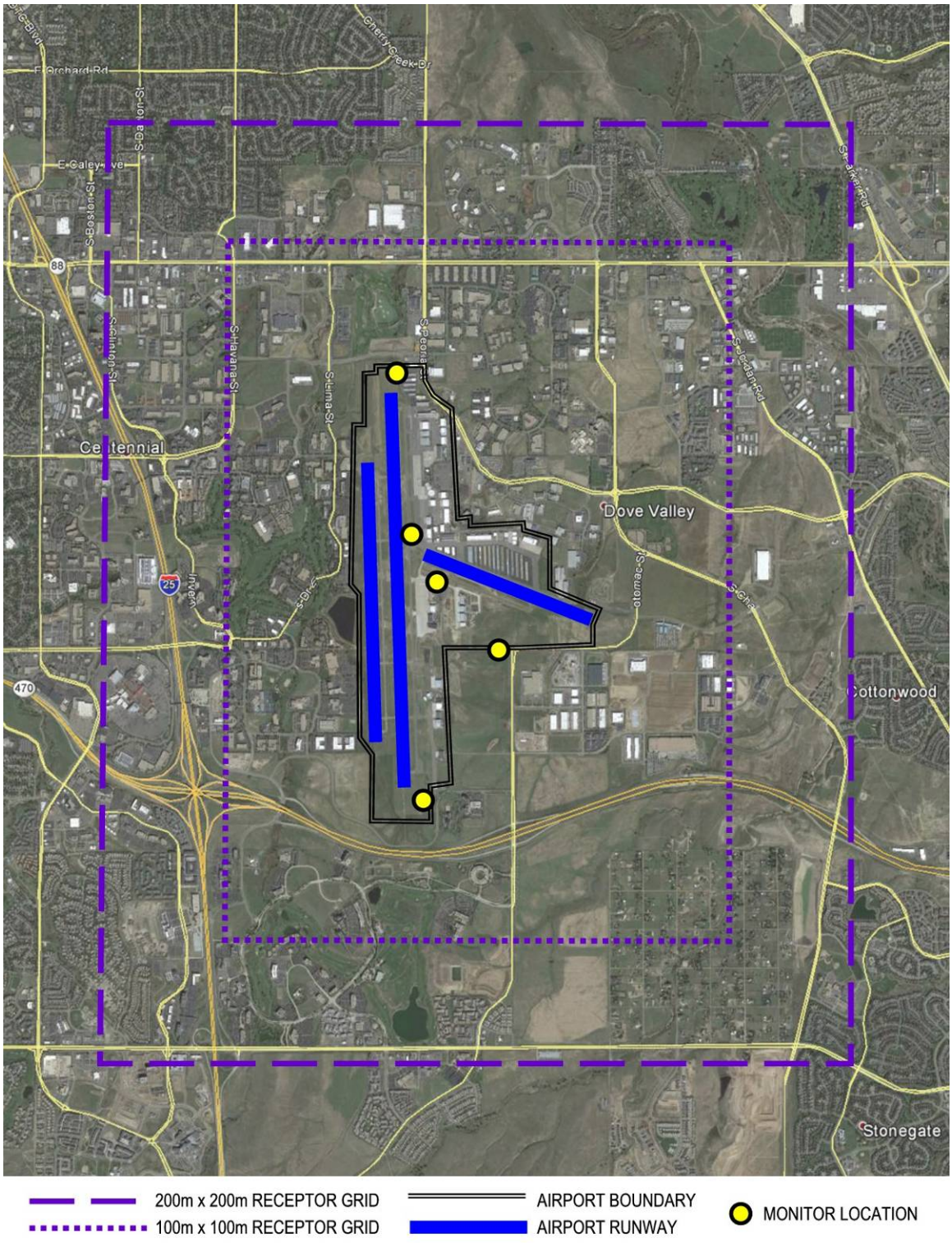

Figure 40
SMO Receptor Grid

7.1.5 Spatial Extent of Modeled PM-Pb Impacts

Hourly airborne PM-Pb concentration fields for each of the three airports were modeled using site-specific aircraft activity data. The modeled hourly concentrations were used to generate average impacts for the PM sampling field studies. These period-average concentrations include only those hours with PM sampling and valid aircraft LTOs data (collected from the video cameras); they do not include nighttime hours and days missing the hourly LTOs activity data. Figures 41–43 show the modeled period-average PM-Pb concentration fields for RVS, APA, and SMO, respectively. Consistent length scales are used to convey differences in the airport footprint sizes. Airport property boundaries are designated by a thick black line and the interior black lines are the runways. Sampling sites are denoted by the abbreviations used in Chapter 5.

Figure 41 shows the modeled period-average PM-Pb concentration fields at RVS. Modeled concentrations are highest near the runup areas and runway ends. The zone of Pb impacts, operationally defined as concentrations exceeding the 75th percentile measured $PM_{2.5}$-Pb background concentration of 3 ng/m^3, were generally confined to within the airport footprint with the exception of the northwest boundary. The North sampling site (primary downwind site for prevailing southerly winds) was near the area of highest modeled concentrations at the airport. Modeling predicts very low impacts at the East sampling site, consistent with the selection of this location as the primary upwind site for prevailing southerly winds.

Figure 41
Modeled Period-Average PM-Pb Concentrations at RVS

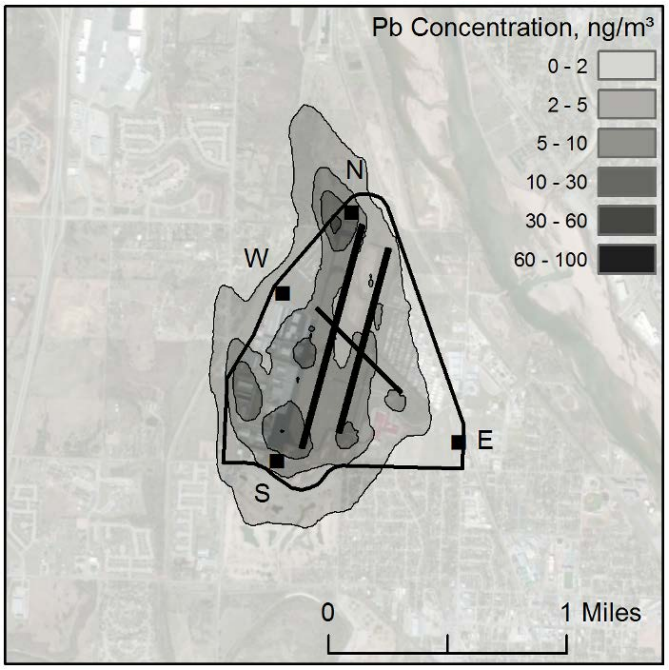

Note: Airport property boundaries are designated by a thick black line; dark interior lines indicate runways.

Figure 42 shows the modeled period-average PM-Pb concentrations at APA. The zone of Pb impacts—operationally defined as concentrations exceeding the 75th percentile measured $PM_{2.5}$-Pb background concentration of 2 ng/m^3—is again generally confined to within the airport footprint. Highest modeled period-average concentrations are at the center of the airport nearby multiple taxiways, a runup area, and the start of Runway 10. The Central sampling location is on the northern edge of the highest modeled concentrations. The East monitor was sited to capture background conditions and the modeling confirmed very low period-average impacts from aircraft activities.

Figure 43 shows the modeled period-average Pb impacts at SMO. Due to its small spatial extent and activities near the airport fence line, Pb impacts greater than the background—operationally defined as the 75th percentile measured $PM_{2.5}$-Pb background concentration of 2 ng/m^3—extend beyond the airport footprint. The highest period-average concentrations are near the start of Runway 21 and the northeast runup area. The Northeast sampling location is located on the northern edge of the modeled Pb hotspot. The Southwest monitor was sited to capture background conditions, and the modeling suggests there might be modest aircraft activity contributions to the PM-Pb measured at this location.

Figure 42
Modeled Period-Average PM-Pb Concentrations at APA

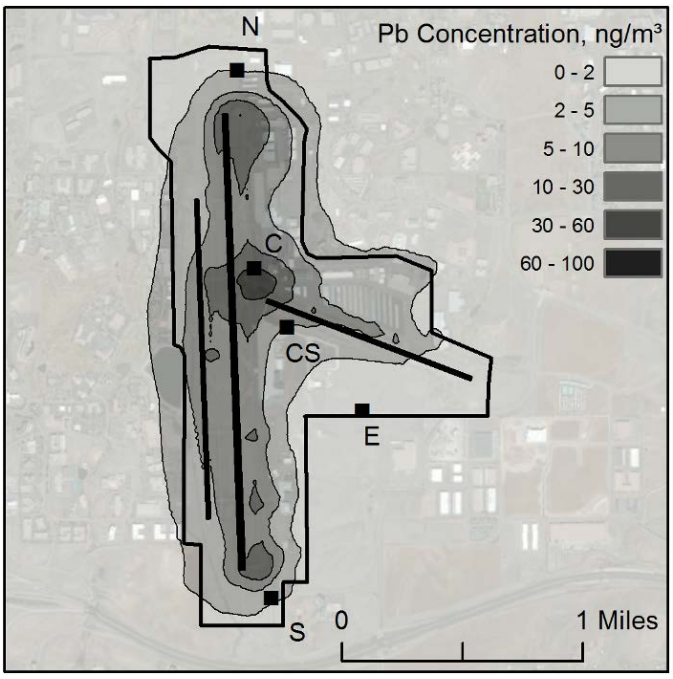

Note: Airport property boundaries are designated by a thick black line; dark interior lines indicate runways.

Figure 43
Modeled Period-Average PM-Pb Concentrations at SMO

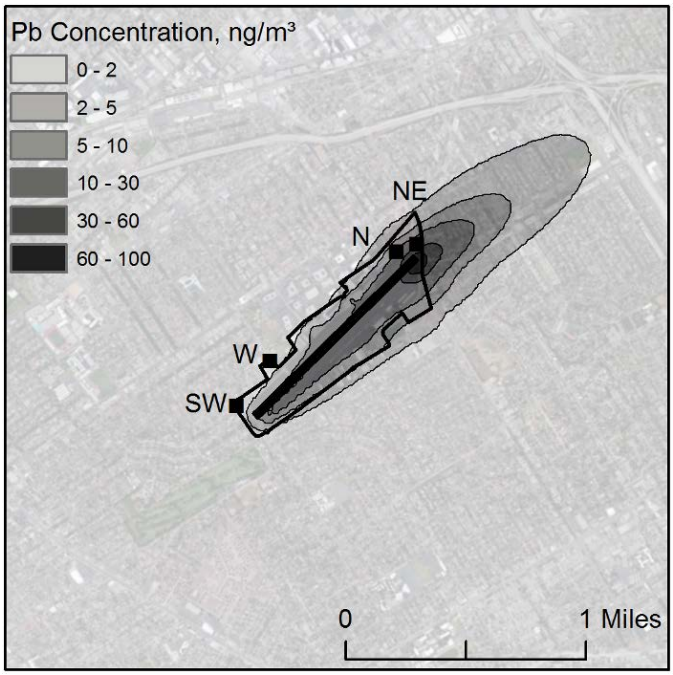

Note: Airport property boundaries are designated by a thick black line; dark interior lines indicate runways.

7.2 Comparison of Modeled and Monitored PM-Pb Concentrations

This section compares the results of the air quality modeling using PM-Pb emission estimates based on site-specific data to the results of the on-site ambient monitoring to evaluate the performance of the refined aircraft operations PM-Pb emissions estimation methodology.

Comparisons with modeled results based on site-specific data and monitored data were made based on $PM_{2.5}$ samples at the primary downwind site for each airport corrected for background using data from the primary upwind site. Days with wind patterns causing the primary upwind site to be impacted by aircraft activities, e.g., westerly winds at RVS, were excluded from the comparisons. Results for the primary downwind site are presented graphically while results for the other sites are briefly summarized with details presented in Appendix D.

Additionally, the modeled impacts from discrete airport activities and locations were grouped into the following nine source groups to determine their relative contributions across the airport in general and at the monitoring locations in particular:

- Runup,
- Taxiways,

- Takeoff,
- Climb-Out,
- Approach,
- Landing,
- Touch and Go,
- Hangars, and
- Helicopters.

The source groups were similar to those defined in the emission inventory (Chapter 6), with a few key differences:

- Runup includes both magneto test and idling emissions in the runup areas;
- Taxiways includes emissions from both taxiing and idling;
- Touch and Go includes emissions from all phases of a touch and go (Approach, Ground Roll, and Climb-out);
- Hangars includes all emission activities within a hangar area such as taxiing and idling; and
- Helicopters includes all phases of helicopter operation.

These relative contributions were determined on both a day-to-day and period-average basis.

7.2.1 RVS – Richard Lloyd Jones Jr.

Figure 44 compares the modeled results from RVS based on site-specific data to background-corrected measured concentrations for the primary downwind monitor. The first eight days of PM-Pb sampling were not modeled because of insufficient video camera data to capture airport operations. Additionally, two other days were not modeled because of malfunctioning video equipment. As shown, there was very good agreement between modeled and monitored PM-Pb concentrations, with the modeled results being distributed about the 1:1 line.

Modeled and measured concentrations were typically low at the other three sites. Six of the nine samples with excess PM-Pb concentrations (defined as a background-corrected concentration greater than two times the propagated measurement precision) had modeled concentrations within a factor of two of the measured values. The model both overestimated and underestimated PM-Pb concentrations across these six days.

Figure 44
Modeled versus Measured $PM_{2.5}$-Pb at the RVS North Site

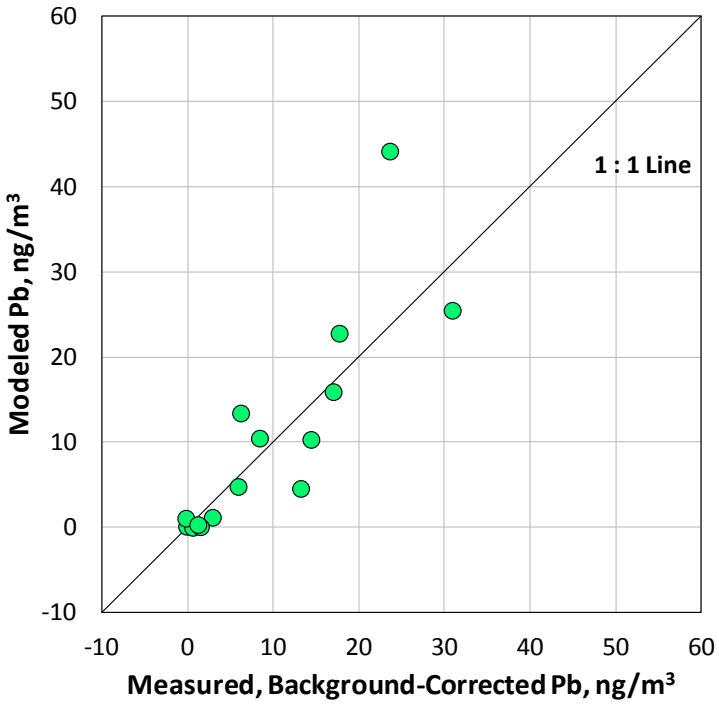

Table 70 shows the source group contributions to airport-wide PM-Pb emissions and to modeled concentrations at the North monitor. Taxiways, takeoffs, and runup activities were the largest contributors to the modeled period-average PM-Pb concentration at the North sampling location. The taxiway contribution was higher than anticipated; however the small taxiway that connects the ends of Taxiway A and Runway 19R is much closer than the northwest runup area to the North monitor. Forty percent of the estimated emissions from this taxiway were from idling while waiting for takeoff clearance. Taxiways and takeoffs exhibited a wide range of contributions to absolute concentrations at the North monitor. This variability, combined with the good agreement shown in Figure 44, suggests that the emission inventory and air quality modeling accurately represent these source groups at RVS. In contrast, the absolute contributions from runup activities are generally low and with modest sample-to-sample variability. Thus, the RVS study alone does not robustly evaluate the runup portion of the emission inventory. In addition to the North site data, there was one day at the South site during northerly winds with modeled runup contributions greater than 2 ng/m^3. For this day, the modeled and measured PM-Pb concentrations agreed very well.

Table 70
Airport-wide PM-Pb Emissions and Modeled Contributions at the North Monitor, RVS

Source Group	Percentage of Total Emissions (%)	Period-Average Contribution at North Monitor (%)	Range of Contributions at North Monitor[1] (%)	Range of Contributions at North Monitor[1] (ng/m^3)
Runup	22%	12%	2% - 15%	0.1 – 3.9
Taxiways	12%	52%	50% - 57%	2.3 – 22.2
Takeoff	5%	25%	18% - 36%	1.6 – 13.3
Climb-out	26%	3%	0% - 5%	0.0 – 0.9
Approach	17%	4%	2% - 7%	0.2 – 2.6
Landing	1%	1%	0% - 2%	0.0 – 0.2
Touch and Go	11%	2%	0% - 8%	0.0 – 0.8
Hangars	6%	1%	0% - 1%	0.0 – 0.3
Helicopters	1%	0%	0% - 0%	0.0 – 0.0

[1]Contributions for southerly winds only

Taxiways, runup areas, and takeoffs generally had the largest modeled contributions to ground level PM-Pb concentrations on the airport footprint, especially in areas with higher concentrations. Figure 45 shows the total modeled PM-Pb concentration (panel a, same as Figure 41) and the individual PM-Pb contributions from taxiways, runup areas, and takeoffs. Taxiways (panel b) had moderate Pb impacts over large portions of the airfield, with highest impacts near the ends of runways and at highly trafficked intersections. Runup areas (panel c) have the highest contributions to the hotspots shown in panel (a); however, concentration gradients were steep and the runup area impacts have relatively small spatial extent. Contributions from takeoffs (panel d) were constrained to the runway ends.

Figure 45
Modeled Total and Source-Group-Specific PM-Pb Concentrations at RVS

Note: Airport property boundaries are designated by a thick black line; dark interior lines indicate runways.

7.2.2 APA – Centennial

Figure 46 compares the modeled results from APA based on site-specific data to background-corrected measured concentrations for the primary downwind monitor. Two days were not modeled because of video camera malfunction; two additional measurement days are not shown because they were collocated TSP sampling days. In

Figure 46
Modeled versus Measured $PM_{2.5}$-Pb at the APA Central Site

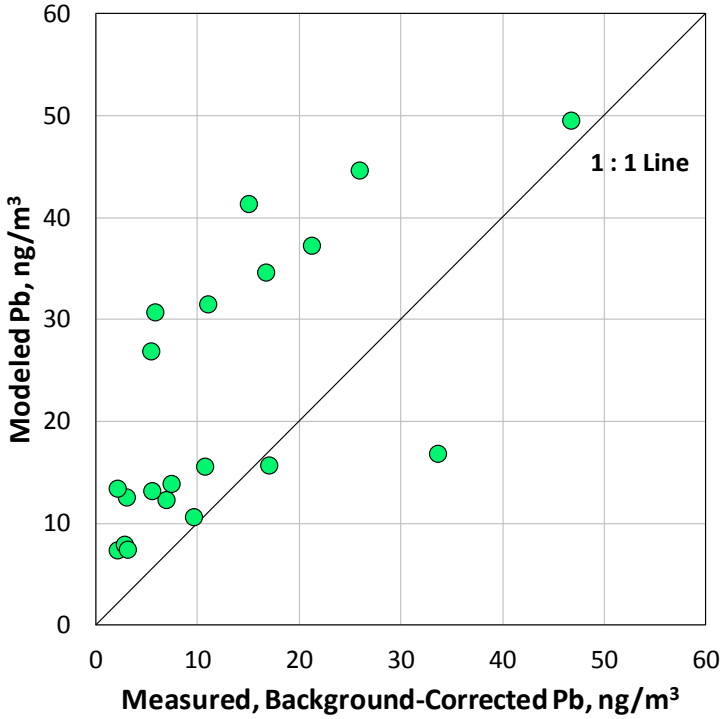

contrast to RVS, there is a bias at APA with the modeled concentrations persistently higher than the measured concentrations. For modeled concentrations above 20 ng/m^3, the modeled and measured values are well correlated.

The primary downwind sites at RVS and SMO were impacted by aircraft activities only for the prevailing wind direction; for other wind directions, the measured concentrations at the primary downwind sites approached background conditions. In contrast, the primary downwind site at APA was impacted by aircraft activities for a wide range of wind directions—this may be the reason for the poorer agreement between the modeled and measured concentrations. At APA, the primary downwind site was located north of the runway 10 run-up and takeoff area, with the expectation that most piston-engine aircraft operations were on runway 10 with virtually no piston-engine activity on runway 17L/35R immediately to the west. However, piston-engine activity was more evenly distributed across all three runways than expected and the site was therefore impacted by winds originating from the southeast clockwise through the northwest. As a result, the modeling for APA was very sensitive to the spatial and temporal allocation of activity because winds tended to shift during the sampling period, and thus the hour-by-hour characteristics at the Central site could vary dramatically. Furthermore, the site was very close to the eastern edge of Taxiway A and modeling of emissions from aircraft operating on this taxiway may have been affected by the short source-to-receptor distances.

Measured and modeled concentrations were typically low at the remaining three sampling locations. Two out of the six samples with excess PM-Pb had measured values within a factor of two of the modeled values. For the remaining four cases, two modeled South-site concentrations were two to four times the measured values, while two North-site measured concentrations were three to ten times the modeled values, although the worst case had both measured and modeled concentrations less than 5 ng/m^3.

Table 71 shows the source group contributions to airport-wide total PM-Pb emissions and to modeled concentrations at the Central monitor. Helicopters were not modeled at APA because of very low activity and lack of spatial activity information. Runup and taxiways were the highest modeled contributors to PM-Pb at the Central monitor, even though they were each only 12% of the total estimated emissions. In contrast to RVS, takeoffs from the nearby runways were not significant contributors to the period-average concentration at the primary downwind monitor. There was large day-to-day variation in the source group contributions to modeled concentrations at the Central monitor. For example, runup contributions ranged from 15% to 96% of total modeled impacts at the monitor. The large range of relative source contributions results from the day-to-day variations in meteorology.

Table 71
Airport-wide PM-Pb Emissions and Modeled Contributions at the Central Monitor, APA

Source Group	Percentage of Total Emissions	Period-Average Contribution at Central Monitor (%)	Range of Contributions at Central Monitor (%)	Range of Contributions at Central Monitor (ng/m^3)
Runup	12%	56%	15% - 96%	1.1 – 57.9
Taxiways	12%	33%	4% - 75%	1.8 – 23.7
Takeoff	7%	1%	0% - 4%	0.0 – 0.5
Climb-out	21%	2%	0% - 8%	0.0 – 1.6
Approach	12%	1%	0% - 2%	0.0 – 0.3
Landing	1%	1%	0% - 3%	0.0 – 0.8
Touch and Go	29%	3%	0% - 12%	0.0 – 1.9
Hangars	6%	4%	0% - 23%	0.0 – 2.6

Days with the largest differences between modeled and measured concentrations generally corresponded to above-average modeled contributions from runup sources. This suggests runup contributions may be overestimated at the Central monitor. The overestimation could result from multiple factors, including the runup emission inventory or the spatiotemporal allocation of these emissions in the modeling.

Similar to RVS, runup areas and taxiways generally had the largest modeled contributions to ground-level concentrations on the airport footprint, especially in areas with higher concentrations. Figure 47 shows the modeled total lead concentration (panel a, same as Figure 42) and the individual Pb contributions from taxiways, runup areas, and takeoffs. Taxiways (panel b) had moderate PM-Pb impacts over large portions of the airfield with highest impacts near the ends of runways and at highly trafficked intersections. Runup areas (panel c) have a more limited spatial extent of impacts above measured background PM-Pb concentrations on the airport footprint, but have the highest maximum impacts of all the source groups. Both taxiways and runup have high impacts near the intersection of Taxiways A and C, resulting in the modeled hotspot at the center of the airport footprint. Contributions from takeoffs (panel d) were constrained to the runway ends.

7.2.3 SMO – Santa Monica

Figure 48 compares the modeled results for SMO based on site-specific data to background-corrected measured concentrations for the primary downwind monitor. One day is not shown because of ICP-MS measurement contamination. There was good agreement between modeled and monitored lead concentrations. Data are distributed about the 1:1 line but, overall, the model tended to underestimate PM-Pb impacts at the Northeast site. There were, however, 2 days (shown with triangles, both occurring on weekends) where the monitored concentrations were much greater than the modeled values, and these differences cannot be explained.

Measured and modeled concentrations were typically low at the Southwest and West sampling locations, with no samples from these sites having excess PM-Pb (defined as a background-corrected concentration greater than two times the propagated measurement precision). All samples collected at the North site showed excess Pb, with modeled concentrations typically two to three times greater than the measured values.

Figure 47
Modeled Total and Source-Group-Specific PM-Pb Concentrations at APA

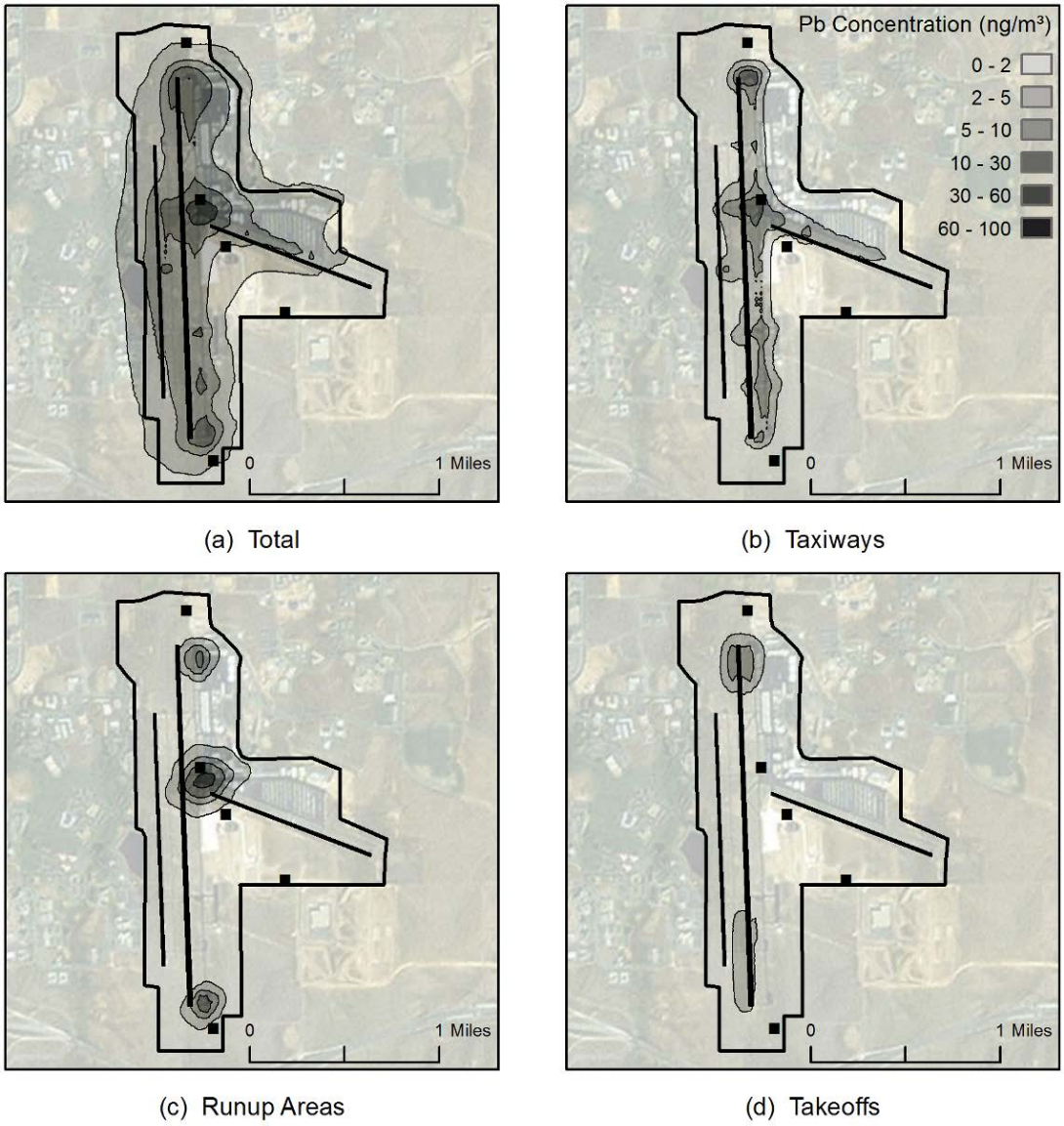

Note: Airport property boundaries are designated by a thick black line; dark interior lines indicate runways.

Figure 48
Modeled versus Measured $PM_{2.5}$-Pb Concentrations at the SMO Northeast Site

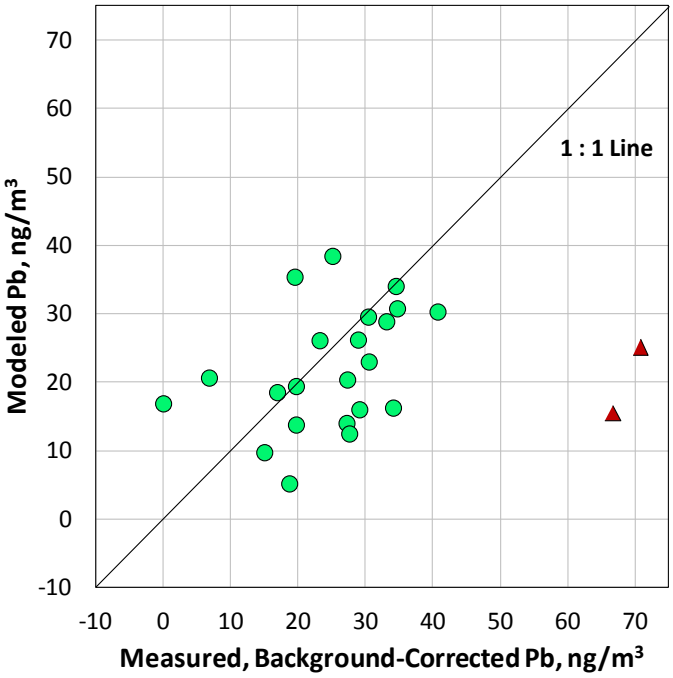

Modeled airport-wide total emissions contributions of the different source groups to modeled concentrations at the Northeast site are shown in Table 72. Runup, taxiways, and takeoffs collectively contributed about 90% of the modeled impacts at the Northeast monitor while accounting for only about 35% of the total emissions. Due to the compact size of the airport, approach and climb-out emissions had a larger impact at the Northeast monitor than at the downwind sites at RVS and APA. Relative source contributions at the Northeast sampling locations were much more consistent at SMO than at RVS and APA because of the wind consistency at SMO. There was wide variation in the absolute contributions from run-ups, takeoffs, and taxiways, implying that the SMO field study is appropriate for evaluating the emission inventory. However, the consistent relative contributions make it difficult to distinguish any particular source group as the source of model underestimation. Modeled source group contributions and measured airport operations data did not provide additional insights into the 2 days with poor model-to-monitor comparisons.

Again, runup, taxiways, and takeoffs had the largest relative contributions to high modeled PM-Pb areas. Figure 49 shows the modeled period-average PM-Pb concentration (panel a, same as Figure 43) and impacts of the taxiways, runup areas, and takeoffs. Similar to the total modeled PM-Pb impacts, the relative contributions of the taxiways and runup areas extend northeast of the airport footprint. Runup contributions were highest near the modeled hotspot shown in Figure 45, while taxiways had high relative contributions throughout the airport footprint. Takeoffs had a higher relative contribution to the modeled hotspot at SMO than at RVS or APA because of the compact nature of the SMO airport layout. However, takeoff impacts were still generally constrained to areas around the runway ends.

Table 72
Airport-wide PM-Pb Emissions and Modeled Contributions at the Northeast Monitor, SMO

Source Group	Percentage of Total Emissions	Period-Average Contribution at Northeast Monitor (%)	Range of Contributions at Northeast Monitor (%)	Range of Contributions at Northeast Monitor (ng/m^3)
Runup	13%	47%	37% - 52%	1.8 – 17.5
Taxiways	15%	23%	21% - 27%	1.1 – 9.0
Takeoff	6%	18%	15% - 21%	0.8 – 7.1
Climb-out	29%	4%	3% - 7%	0.3 – 1.3
Approach	27%	5%	3% - 9%	0.4 – 2.3
Landing	2%	1%	0% - 3%	0.0 – 0.7
Touch and Go	1%	0%	0% - 1%	0.0 – 0.3
Hangars	6%	2%	1% - 3%	0.2 – 0.8
Helicopters	1%	0%	0% - 4%	0.0 – 0.5

Figure 49
Modeled Total and Source-Group-Specific PM-Pb Concentrations at SMO

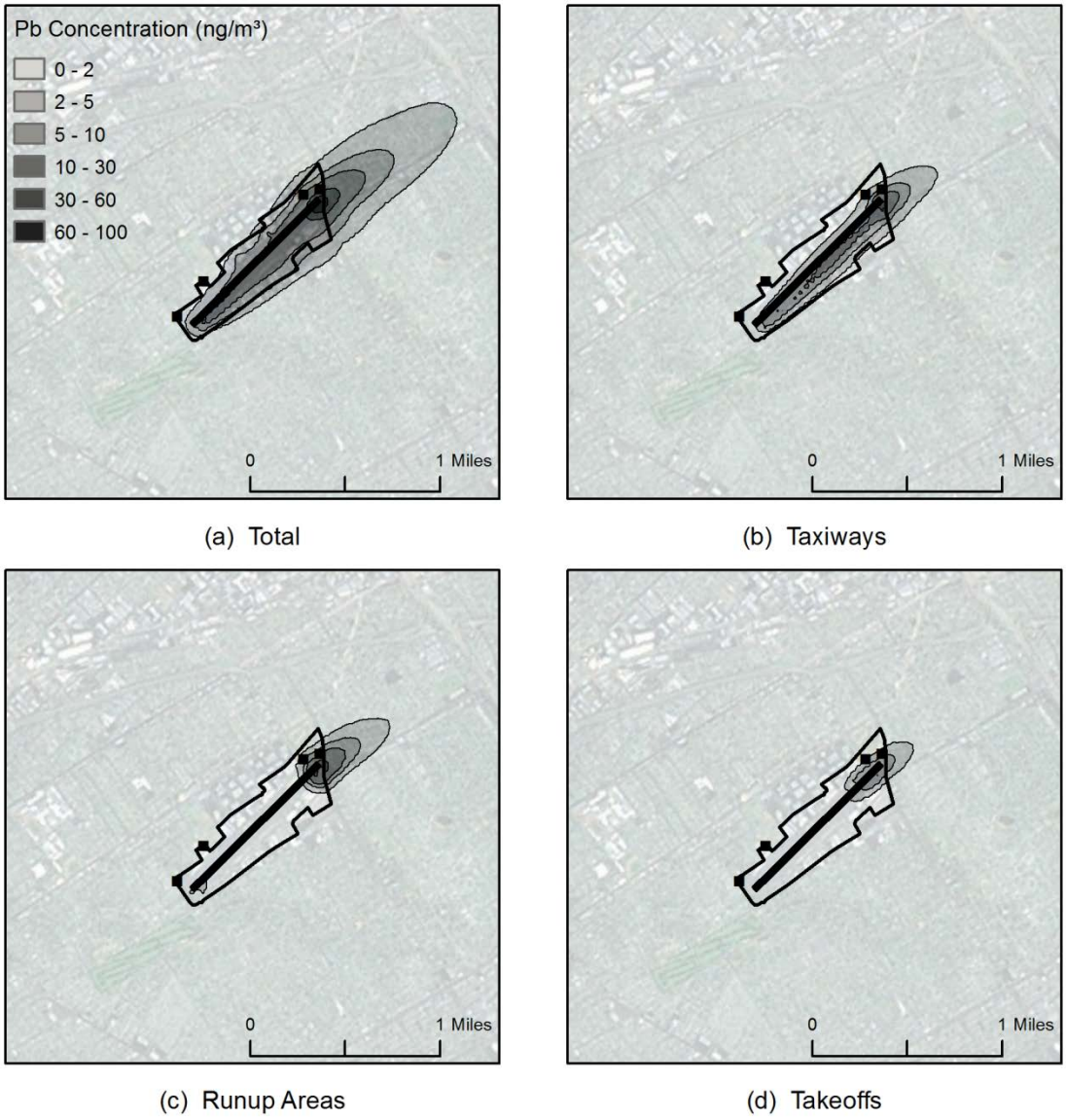

Note: Airport property boundaries are designated by a thick black line; dark interior lines indicate runways.

7.2.4 PM2.5-Pb Model Prediction to Measurement Summary

Modeled and measured 12-hour average $PM_{2.5}$-Pb concentrations for the downwind primary sites at each airport were presented as scattergrams in the previous section. Quantitative comparison metrics were also calculated using all data in Figures 44, 46, and 48 with the following exceptions. First, RVS samples with measured and modeled concentrations both less than 3 ng/m^3 were excluded. These samples correspond to days with northerly winds, and for these conditions the site is not impacted by aircraft

emissions. Second, the two SMO samples with measured values far exceeding the modeled values (triangles in Figure 48) were excluded.

Methods for comparing air quality models to measurements have been reviewed by Chang and Hanna (2004). Several common performance measures are presented in Table 73. FAC2 is the fraction of model-predicted concentration values (C_P) within a factor of two of the measured (observed) concentration values (C_O)—i.e., the fraction of data with $0.5 \le C_P/C_O \le 2$. FAC2 was ~75% at RVS and SMO and 45% at APA. Fractional bias (FB) is defined as follows:

$$FB = \frac{\overline{C_O} - \overline{C_P}}{0.5\left(\overline{C_O} + \overline{C_P}\right)}$$

The model overpredicts the measurements for negative FB and the model underpredicts the measurements for positive FB. As shown below, FB is related to the ratio of the arithmetic means, which is easier to understand.

$$\frac{\overline{C_P}}{\overline{C_O}} = \frac{1 - FB/2}{1 + FB/2}$$

Table 73
Performance Measures for Comparing PM-Pb Model Predictions to Measurements

Performance Measure	RVS	APA	SMO
Number of Samples	9[a]	20	22[b]
Mean $PM_{2.5}$-Pb, ng/m^3			
– Measured	15.3	12.2	24.7
– Model Predicted	16.9	22.2	22.1
FAC2[1]	0.78	0.45	0.77
Fractional Bias, FB	-0.11	-0.55	+0.11
Ratio of Arithmetic Means	1.11	1.76	0.89
Normalized Mean Square Error, NMSE	0.27	0.69	0.19
– NSME systematic error contribution	0.01	0.33	0.01
– NSME random error contribution	0.26	0.36	0.18

[a] Excludes seven samples with both measured and modeled $PM_{2.5}$-Pb less than 3 ng/m^3.
[b] Excludes two samples with measured $PM_{2.5}$-Pb much greater than modeled concentrations (triangles in Figure 48).
[1] The fraction of model-predicted concentration values within a factor of two of the measured (observed) concentration values.

Based on the ratio of means, the model is 11% high at RVS and 11% low at SMO, while the model is 76% high at APA. The normalized mean square error (NMSE) is defined as follows:

$$NMSE = \frac{\overline{(C_O - C_P)^2}}{\overline{C_O}\ \overline{C_P}}$$

A NMSE of 0.5 corresponds to a mean bias of a factor of two. NMSE is higher at RVS (0.27) than at SMO (0.19) in large part because the concentration values are lower at RVS. NMSE accounts for both systematic errors (bias) and random errors; the contributions of these error components are calculated as shown below.

$$\text{Systematic error component} = NMSE_S = \frac{4FB^2}{4 - FB^2}$$

$$\text{Random error component} = NMSE_R = NMSE - NMSE_S$$

NMSEs at RVS and SMO are dominated by the random error component while at APA there are nearly equal contributions from the systematic and random error components.

The quantitative performance measures collectively demonstrate good agreement between model predictions and measurements at RVS and SMO, but the model is biased high at APA. At RVS, the primary downwind site was largely impacted by taxiing and takeoffs; at SMO, it was largely impacted by taxiing and runup. Thus, across these two studies, the three major ground-based activities that contribute to emissions and to PM-Pb hot spots were evaluated and suggest the inventory methodology is sound. While model predictions and measurements were poorer at APA, if the error is ascribed to the emissions inventory then the methodology is conservatively high, which is preferred over being low. Approach and climb-out are also large contributors to the airport PM-Pb emission inventory, but the field studies were not designed to evaluate the methodology for these activities.

Modeling was also conducted using the refined methodology with publicly available data and the approach and results are summarized in Appendix D. For all three airports, the model performance was inferior to using site-specific data with significant underprediction at all three airports. Given that emissions per piston operation are much lower when using site-specific data compared to publicly available data (Section 6.2) for all three airports, the discrepancies must arise from differences in the number of piston operations or the spatiotemporal allocation of the emissions. While total observed operations were less than operations reported in ATADS, the observed fraction of total operations performed by piston engine aircraft was higher than predicted using publicly available data and this could be one reason for the model underpredicting the measured concentrations. Given the numerous potentially confounding factors, a detailed analysis was not conducted to identify the drivers for the relatively poor model performance when using publicly available data.

In summary, the refined emission inventory methodology with site-specific data consistently outperformed the refined emission inventory methodology with publicly available data when using dispersion modeling to compare to measured PM-Pb concentrations. Aircraft operations occur over large footprints and thus it is necessary to accurately specify the timing and especially the location of emissions to accurately predict airborne PM-Pb concentrations. While this was important for the model-to-monitor evaluation of the emission inventory, which was the focus of this project, it is also important for the prediction of PM-Pb hot spots. The emission inventory is not the only predictor—and perhaps not even the main predictor—of the potential for PM-Pb hot spot concentrations to approach or exceed the NAAQS. Air quality dispersion modeling presented in this chapter demonstrates that localized run-ups, takeoffs, and also taxiing in the runup/takeoff areas—potentially acting in isolation but more commonly in combination—result in the highest concentration zones. It is the localization and magnitude of these activities that, perhaps more so than the overall inventory, is a better predictor of hot spot concentrations.

###

8. REFERENCES

Atwood, D. 2007. *High-Octane and Mid-Octane Detonation Performance of Leaded and Unleaded Fuels in Naturally Aspirated, Piston, Spark Ignition Aircraft Engines*. Federal Aviation Administration Technical Report No. DOT/FAA/AR-TN07/5.

Atwood, D. 2009. *Full-Scale Engine Detonation and Power Performance Evaluation of Swift Enterprises 702 Fuel*. Federal Aviation Administration Technical Report No. DOT/FAA/AR-08/53.

Atwood, D. and J. Camirales. 2004. *Full-Scale Engine Knock Tests of 30 Unleaded, High-Octane Blends*. Federal Aviation Administration Technical Report No. DOT/FAA/AR-04/25.

Atwood, D. and K. Knopp. 1999. *Evaluation of Reciprocating Aircraft Engines with Unleaded Fuels*. Federal Aviation Administration Technical Report No. DOT/FAA/AR-99/70.

British Petroleum. 2011. Material Safety Data Sheet No. SAV2103 for 100LL Aviation Gasoline (low benzene) Produced by Air BP Fuels.

Carr, E., M. Lee, K. Marin, C. Holder, M. Hoyer, M. Pedde, R. Cook, and J. Touma. 2011. "Development and Evaluation of an Air Quality Modeling Approach to Assess Near-field Impacts of Lead Emissions from Piston-engine Aircraft Operating on Leaded Aviation Gasoline." *Atmospheric Environment* 45: 5795–5804.

Chevron Global Aviation. 2003. Material Safety Data Sheet No. 2647 for 100LL Avgas Produced by Chevron Aviation.

Conor Pacific Environmental Technologies, Inc. 2000. *Airborne Particulate Matter, Lead and Manganese at Buttonville Airport*. Prepared for Environment Canada under CPE Project 041-6710. Final Report.

ConocoPhillips. 2010. Material Safety Data Sheet No. 001769 for 100LL Aviation Gasoline Produced by ConocoPhillips.

Continental Motors, Inc. August 2011. *Continental Aircraft Engine Operator's Manual*. TSIO-360 Series of Engines, Publication X30583.

Coordinating Research Council, Inc. 2010. *Research Results: Unleaded High Octane Aviation Gasoline*. CRC Report No AV-7-07. CRC Project No. AV-7-07.

Coordinating Research Council, Inc. 2011. *Investigation of Reduced TEL Content in Commercial 100LL Avgas*. CRC Report No. 657, CRC Project No. CA-67-2010, Rev. A.

Eastern Research Group (ERG). 2011. *Documentation for Aircraft Component of the National Emissions Inventory Methodology*. ERG No.:0245.03.402.011.

Harris, A. and C. Davidson. 2005. "The Role of Resuspended Soil in Lead flows in the California South Coast Air Basin." *Environmental Science and Technology* 39: 7410–7415.

Harrison, R.M. and W.T. Sturges. 1998. "The measurement and interpretation of Br/Pb ratios in airborne particles." *Atmospheric Environment* 17: 311–328, 1998.

ICF International and T&B Systems. 2010. *Development and Evaluation of an Air Quality Modeling Approach for Lead Emissions from Piston-Engine Aircraft Operating on Leaded Aviation Gasoline*. U.S. Environmental Protection Agency. EPA-420-R-10-007.

Kenny, L., G. Beaumont, A. Gudmundsson, A. Thorpe, and W. Koch. 2005. "Aspiration and sampling efficiencies of the TSP and louvered particulate matter inlets." *Journal of Environmental Monitoring* 7: 1–7.

Lejano, R. and J. Ericson. 2005. "Tragedy of the Temporal Commons: Soil-Bound Lead and the Anachronicity of Risk." *Journal of Environmental Planning and Management* 48:2, 301–320.

Lycoming Engines. January 1977. "*Operator's Manual, Avco Lycoming O-320 and IO-320 Series Engines (Revised*).

Lycoming Engines. Undated. "*Lycoming Operator's Manual, O-540 and IO-540 Series Engines*.

Lycoming Engines. July 2008. *(L)IO-360-M1A Operation and Installation Manual*," Lycoming.

Petersen, T. 2008. *Aviation Oil Lead Content Analysis*. Report # EPA 1-2008. Available at *http://www.tc.faa.gov/its/worldpac/techrpt/avgaslead.pdf*

Petro-Canada. 2009. Material Safety Data Sheet for Aviation Gasoline 100LL Produced by Petro-Canada. 12/29/2009

Phillips Petroleum. 1996. Material Safety Data Sheet for 100LL Avgas Produced by Phillips 66 Petroleum.

Piazza, B. 1999. *Santa Monica Municipal Airport: A Report on the Generation and Downwind Extent of Emissions Generated from Aircraft and Ground Support Operations.* Prepared for the Santa Monica Airport Working Group.

Shell Energy North America. 2003. Material Safety Data Sheet No. 402095M-0 for 100LL Avgas Produced by Motiva Enterprises LLC.

South Coast Air Quality Management District. 2010. *General Aviation Airport Monitoring Study. Final Report*, prepared for the U.S. Environmental Protection Agency.

Switzerland Federal Office of Civil Aviation. 2007. *Aircraft Piston Engine Emissions*. Supporting Data.

Switzerland Federal Office of Civil Aviation. 2009. *Guidance on the Determination of Helicopter Emissions*. First Edition 0/3/33/33-05-20.

Townsend, A.T., Z. Yu, P. McGoldrick, and J.A. Hutton. 1998. "Precise lead isotope ratios in Australian Galena samples by high resolution inductively coupled plasma mass spectrometry." *Journal of Analytical Atomic Spectrometry* 13: 809–813.

U.S EPA. 1977. *Compilation of Air Pollutant Emissions Factors (AP-42).* Third Edition.

U.S. EPA. 1992. *Procedures for Emission Inventory Preparation Volume IV: Mobile Sources*. EPA420-R-92-009.

U.S. EPA. 1998. *Locating and Estimating Air Emissions from Sources of Lead and Lead Compounds*. EPA-454/R-98-006.

U.S. EPA. June 10, 2002. 40 CFR Part 51 – Consolidated Emissions Reporting: Final Rule. Published at 67 FR 39602.

U.S. EPA. 2004. *User's Guide for the AMS/EPA Regulatory Model – AERMOD.* EPA-454/B-03-001.

U.S. EPA. 2008. *Lead Emissions from the Use of Leaded Aviation Gasoline in the United States. Technical Support Document.* EPA420-R-08-020.

U.S. EPA. June 2012. *2008 National Emissions Inventory, Version 2: Technical Support Document (DRAFT).*

U.S. EPA. June 2013. *Program Update on Airport Lead Monitoring*. EPA-420-F-13-032, 4pp. http://www.epa.gov/otaq/regs/nonroad/aviation/420f13032.pdf

Young, T., D. Heraman, G. Sirin, and L. Ashbaugh. 2002. "Resuspension of Soil as a Source of Airborne Lead near Industrial Facilities and Highways." *Environmental Science and Technology* 36: 2484–2490.

9. ABBREVIATIONS AND ACRONYMS

ACRP	Airport Cooperative Research Program
AERMIC	American Meteorological Society/Environmental Protection Agency Regulatory Model Improvement Committee
AIP	Airport Improvement Program
APA	Centennial Airport in Denver, Colorado
ASOS	Automated Surface Observing System
ASTM	American Standards Testing Materials
ATADS	Air Traffic and Activity Data System
Br	Bromine
BSFC	brake specific fuel consumption
BTS	U.S. Bureau of Transportation Statistics
CDT	Central Daylight Time
CERR	Consolidated Emissions Reporting Rule
CI	Compression ignition
CRC	Coordinating Research Council
EDMS	Emissions and Dispersion Modeling System
EIIP	Emissions Inventory Improvement Program
EPA	U.S. Environmental Protection Agency
ETMSC	Enhanced Traffic Management System Counts (replaced by TFMSC)
FAA	Federal Aviation Administration
FAAED	FAA (Federal Aviation Administration) Aircraft Engine Emissions Database
FB	Fractional bias
FBO	Fixed Base Operator
FOCA	Federal Office of Civil Aviation (Switzerland)
FRM	Federal Reference Method
g/l	Grams per liter
GA	General aviation
GAATA	General Aviation and Air Taxi Activity
H_2	Hydrogen
ICAO	International Civil Aviation Organization
ICP-MS	Inductively Coupled Plasma – Mass Spectrometry
IFR	Instrument Flight Rules
ISH	Integrated Surface Hourly
LPM	Liters per minute
LTO	Landing and takeoff
m/s	Meters per second
MDT	Mountain Daylight Time

MSDS	Material Safety Data Sheet
ng/m^3	nanogram per cubic meter
NAAQS	National Ambient Air Quality Standard
NAS	National Academy of Sciences
NED	National Elevation Dataset
NEI	National Emissions Inventory
NLCD	National Land Cover Data
NMSE	Normalized mean square error
NPIAS	National Plan for Integrated Airport Systems
OPSNET	Operations Network
RVS	Richard Lloyd Jones Jr. Airport in Tulsa, Oklahoma
PM	Particulate matter
PM2.5	Particulate matter <2.5 microns in diameter
PM10	Particulate matter <10 microns in diameter
Pb	Lead
SCAB	South Coast Air Basin
SCAG	Southern California Association of Governments
SCAQMD	South Coast Air Quality Management District
SI	Spark ignition
SMO	Santa Monica Municipal Airport in Santa Monica, California
SO_2	Sulfur dioxide
SHP	Shaft horsepower
TAF	Terminal Area Forecast
TCDS	Type Certificate Data Sheets
TEL	TetraEthyl Lead
TFMSC	Traffic Flow Management System Counts (previously ETMSC)
TIM	Time in mode
TPA	Traffic Pattern Altitude
TSP	Total Suspended Particulate
USGS	U.S. Geological Survey
UTM	Universal Transverse Mercator
VFR	Visual flight rules
WUSTL	Washington University in St. Louis
XRF	X-Ray Fluorescence

Appendix A

Annotated Bibliography

Annotated Bibliography

Atwood, D. Full-Scale Engine Detonation and Power Performance Evaluation of Swift Enterprises 702 Fuel. Federal Aviation Administration Technical Report No. DOT/FAA/AR-08/53, 2009

- Comparative tests on Swift 702 fuel performance compared to 100LL in a TIO-540-J2BD and IO-540-K engine, in terms of peak power, energy content, fuel consumption, combustion temperatures, and detonation testing. Identifies TEL content and other physical properties of 100LL used in experiment, two blends which were purchased from a local FBO. The Swift 702 fuel had slightly lower energy content (in terms of mass), lower power, lower fuel consumption and higher combustion temperatures compared to 100LL.

Atwood, D. High-Octane and Mid-Octane Detonation Performance of Leaded and Unleaded Fuels in Naturally Aspirated, Piston, Spark Ignition Aircraft Engines. Federal Aviation Administration Technical Report No. DOT/FAA/AR-TN07/5, 2007

- Fuels of varying motor octane numbers and lead concentrations were tested in the IO-540-K and IO-320-B engines to determine and quantify the effects these parameters have on full-scale engine detonation performance. The main body of the document contains scatter plots of fuel flow rates as a function of brake horsepower. Appendix A contains load-point specific engine parameters, including mass fuel flow and brake specific fuel consumption, for all engines and fuels tested.

Atwood, D. and J. Camirales. Full-Scale Engine Knock Tests of 30 Unleaded, High-Octane Blends. Federal Aviation Administration Technical Report No. DOT/FAA/AR-04/25, 2004

- Thirty unleaded aviation fuels were tested at 100%, 85%, 75% and 65% engine power settings in a Lycoming IO-540-K engine, to determine their performance relative to leaded fuel. Ten leaded reference fuels of varying motor octane numbers were also created and tested by adding a specified amount of TEL to the fuel. Appendix A contains the detailed test data, including fuel flow, brake specific fuel consumption and power settings for all fuels tested. Appendix E contains information on the amount of TEL added per gallon to each reference fuel used in the study (0.076 to 1.285 mL TEL per gallon fuel).

Atwood, D. and K. Knopp. Evaluation of Reciprocating Aircraft Engines with Unleaded Fuels. Federal Aviation Administration Technical Report No. DOT/FAA/AR-99/70, 1999

- Study performed ground-based performance testing of the following engines powered with a variety of aviation fuels at a variety of load points: IO-550-D, IO-320-B, IO-540-K, TIO-540-J and TSIO-550-E. Flight testing also simulated using test cell on Lycoming GSO-480-B1A6 engine. Appendix A contains brake specific fuel consumption and mass fuel flow rates for the engines utilized in the ground-based testing for the following load points: 100%, 80%, and 70%. Select engines in this series were evaluated at multiple brake horsepower settings, enabling a comparison of how fuel flow varies with horsepower setting.

Blau, P. Compositions, Functions and Testing of Friction Brake Materials and Their Additives. Prepared for the U.S. Department of Energy by the Oak Ridge National Laboratory under Contract No. DE-AC05-00OR22725, 2001

- Describes typical aircraft brake formulations for a variety of aircraft. Identifies lead oxides as a potential additive as friction modifier in aircraft brake formulation, and those additives can comprise up to 2 percent by volume brake material.

Bocchinfuso, G.. L. Aiello, V. Ferone, A. Cinotti, and M. Bernabei. Toxicological Evaluation of Gasolines by GC-MS Analysis. Chromatographia 53,Suppl, S345−S349, 2001

- Provides tetraethyl lead (TEL) concentrations obtained using gas chromatography (GC) and mass spectroscopy (MS) for avgas and mogas samples. TEL concentrations were 490.5 and 530.4 µg/ml for the two avgas samples, respectively.

British Petroleum. Material Safety Data Sheet No. SAV2103 for 100LL Aviation Gasoline (low benzene) Produced by British Petroleum, 2011

- Contains between 0.05 and 0.1% alkyl lead compounds. Does not specify if percentages are by weight or by volume.

Camalier, L. and J. Rice. Memorandum from Louise Camalier and Joann Rice of the US EPA Office of Air Quality Planning and Standards on the Estimates of Precision and Bias for Lead in Total Suspended Particulate (TSP). U.S. Environmental Protection Agency Lead NAAQS Review Docket OAR-2006-0735, 2007

- Evaluates precision and bias of existing FRMs/FEMs for the measurement of lead as TSP using high-volume samplers. Precision data was evaluated from 32 high-volume collocated samplers located across the country; 21% of the data was excluded on the basis of being below detection limits leaving an sample size of n=2108 pairs. An average precision value of 11.7% ± 18.6% was obtained from the data, comparable both between and within methods, and consistent across the range of monitored TSP lead concentrations. Sampling and analytical bias was derived from National Performance Audit Program (NPAP) records for 1998 through 2005. The average sampling bias was -0.7% ± 4.2%; overall analytical bias was -1.1% ± 5.5%, making the total bias -1.7% ± 3.4%

Carr, E., M. Lee, K. Marin, C. Holder, M. Hoyer, M. Pedde, R. Cook, and J. Touma. Development and Evaluation of an Air Quality Modeling Approach for Lead Emissions from Piston-Engine Aircraft Operating on Leaded Aviation Gasoline. Atmospheric Environment 45: 5795−5804, 2011

- Applied ICF emissions inventory methodology as described in EPA-420-R-10-007. Activity data was provided by SMO personnel and via on-site surveys, fuel consumption rates were derived from EDMS for single-engine and twin-engine aircraft. Fuel consumption for the run-up mode of operation was derived based on data obtained from engine manuals for single-engine, fixed-wing aircraft. Times in mode utilized in the analysis were 304 seconds for taxi-out, 89 seconds for run-up, 16 seconds for takeoff, 78 seconds for climb-out, 79 seconds for approach and landing, and 137 seconds for taxi-in.

- AERMOD was used to model calculated aircraft emissions at 50 meter grid spacing. Model specifications accounted for wake turbulence, exhaust plume rise, and vertical allocation of climb-out and approach emissions at 50 meter elevation increments. Run-up emissions were determined to be the largest contributor the maximum modeled concentrations via sensitivity analysis, followed by the assumed content of lead in avgas and the share of twin-engine aircraft in the emissions inventory. Maximum model bias when validated with ambient monitoring was 19 nanograms

per cubic meter of air. Better validation was obtained during the summer modeling campaign.

- The winter monitoring campaign associated with this study was conducted over 8 days in March and comprised 43 miniVol TSP samples taken at the East Tarmac, West Tarmac and Clarkson sites. 24-hour average values ranged from 39.3 to 70.6 nanograms per cubic meter of air using x-ray fluorescence. Summer monitoring was conducted for one week in late July 2009 at two residences northeast of the airport and at the airport maintenance shed located near the airport blast fence, using high-volume samplers and XRF. Measured values were highest at the maintenance shed and lowest at the residences, and ranged from 17.0 to 62.2 nanograms lead per cubic meter of air.

Cassella, R., D. Brum, C. Lima, and T.C.O. Fonseca. Stabilization of Aviation Gasoline as Detergent Emulsion for Lead Determination by Electrothermal Atomic Absorption Spectrometry. Fuel Processing Technology 92: 933–938, 2011

- Refinement of analytical methods used to determining lead in aviation gasoline samples using electrothermal atomic absorption spectrometry (ETAAS). Six samples analyzed by this method yielded lead concentrations between 11.6 ± 0.6 and 64.2 ± 1.2 µg/L of fuel. Avgas samples were supplied by PETROBRAS.

Cavender, K. and S.M. Schmidt. Memorandum from Kevin Cavender and S. Mark Schmidt of the US EPA Office of Air Quality Planning and Standards on the Review of Collocated Lead in Total Suspended Particulate and Lead in Particulate Matter Less than Ten Micrometers. U.S. Environmental Protection Agency Lead NAAQS Review Docket (OAR-2006-0735), 2007

- Collected collocated Pb-TSP and Pb-PM_{10} data from AQS monitors at 22 sites, spanning years 1996-2006. Computing a simple ratio between the two measurements showed that there was considerable variation both within and between AQS sites, implying that relating TSP to PM_{10} based on a simple ratio is not reliable. Performing linear regression with TSP as the dependent variable and PM_{10} as the independent variable showed strong correlation ($r2>0.9$) at some locations but weak correlation ($r2<0.5$) at others, implying that a relationship based on linear regression could help relate the two variables on a site-by-site basis, given that the level of error in the method was accounted in the comparison.

Chevron Global Aviation. Aviation Fuels Technical Review (FTR-3), 2006

- Describes physical and chemical properties of various avgas blends as they relate to operational performance and safety. Outlines avgas specifications and test methods, as well as the chemical composition and processes by which the fuel is refined during manufacture. Describes properties of piston engines including combustion cycling, air intake and carburation, fuel injection and engine configurations.

Chevron Global Aviation. Material Safety Data Sheet No. 2647 for 100LL Avgas Produced by Chevron Global Aviation, 2003

- Contains less than 4 ml/gal TEL. Applicable to product numbers CPS200205, CPS200239, CPS200285 and CPS200456

Cho, S., J. Richmond-Bryant, J. Thomburg, K. Portzer, R. Vanderpool, K. Cavender, and J. Rice. A Literature Review of Concentrations and Size Distributions of Ambient Airborne Pb-Containing

Particulate Matter. Atmospheric Environment, In Press. Accepted Manuscript, DOI 10.1016/j.atmosenv.2011.05.009, 2011

- Anthologizes recent and available literature on PM_{10} FRM and TSP monitoring studies. Identifies lack of substantiated literature with sufficient detail on concentrations, location, techniques and full suite of particle size fractions. Overall the literature suggests that mode of size distributions of particle-bound Pb has increased due to phase-out of leaded mogas, leaving industrial and fugitive sources with larger particle sizes to dominate. Presents emissions data for piston aircraft from previous literature.

ConocoPhillips. Material Safety Data Sheet No. 001769 for 100LL Aviation Gasoline Produced by ConocoPhillips, 2010

- Contains 0.13% by weight TEL. Manufacturer is based in Houston, TX.

Conor Pacific Environmental Technologies, Inc. Airborne Particulate Matter, Lead and Manganese at Buttonville Airport. Prepared for Environment Canada under CPE Project 041-6710. Final Report, 2000

- Collocated high-volume sampling of PM_{10} and $PM_{2.5}$ was conducted at four sites adjacent to the airport runway ends and at an upwind site ~10 km WSW. Relative to PM_{10}, lead concentrations measured during the campaign averaged 0.030 $\mu g/m^3$ with a maximum of 0.302 $\mu g/m^3$, compared to background values of 0.007 and 0.012 $\mu g/m^3$, respectively. Monitored lead concentrations in the $PM_{2.5}$ size fraction were 0.028 $\mu g/m^3$ average and 0.308 $\mu g/m^3$ maximum, compared to background levels of 0.007 and 0.018 $\mu g/m^3$ respectively. Despite the elevated concentrations over background values, the greatest lead concentrations were observed at the end of the least frequently used runway, and the lowest concentration was measured at the runway of most frequent use.

- Triplicate soil samples were taken from ten locations around the runway complex up to a 5 cm sampling depth. No discernable pattern was observed between soil lead levels and airport proximity/operations. Soil lead values ranged from 21.7 to 60.9 µg/g of soil (with the highest sample located at one of the background locations.

Coordinating Research Council, Inc. Investigation of Reduced TEL Content in Commercial 100LL Avgas. CRC Report No. 657, CRC Project No. CA-67-2010, Rev. A, 2011

- A survey of 89 avgas samples from FAA FBOs (representing nine refineries) indicated a range of motor octane numbers between 101.6 and 108, and TEL concentrations ranging between 0.34 and 0.56 g/L. Additionally, 23 avgas samples obtained from engine manufacturers for use in certification testing exhibited a motor octane number range of 101.1 to 107.6 and TEL concentrations ranging between 0.08 and 0.6 g/L. Further, 39% of the FBO samples could meet a 20% reduction in TEL proposed in general aviation stakeholder meetings, 51% could meet a 15% reduction in TEL and 64% could meet a 10% reduction in TEL. 44% of the certification fuel samples could meet the 20% reduction and 67% could meet the 15% reduction in TEL. It is noted that an IO-540-K engine can experience a 4.9% impact in knock-limited fuel flow by a 20% reduction in TEL content.

Coordinating Research Council, Inc. Research Results: Unleaded High Octane Aviation Gasoline. CRC Report No AV-7-07. CRC Project No. AV-7-07, 2010

- Engine test data investigating unleaded avgas alternatives compared to a 100LL baseline. Alternatives represent a variety of alkylate, toluene, ETBE, ethanol and other additive blends with unleaded avgas and mogas. Knock test results provide plots of brake-specific horsepower vs. fuel flow at engine power settings >65% for all fuels tested, including the baseline 100LL fuel.

Czarnigowski, J., P. Jalkinski, and M. Wendeker. Fuelling of an Aircraft Radial Piston Engine by ES95 and 100LL Gasoline. Fuel 89: 3568−3578, 2010

- Testing on radial piston engine Asz-621R performed using 100LL and ES95 automotive gasoline, observing effects on power, fuel consumption, cylinder head temperature, mean pressure, peak pressure and crank angle. Physiochemical properties of both fuels are reported. Using ES95 caused negligible change in engine power, 6% increase in fuel consumption, negligible change in engine performance (including knock), temperature and pressure. Cycle-to-cycle variation increased by about 8% using ES95.

ENVIRON International Corporation. Teterboro Airport Detailed Air Quality Evaluation. Prepared for the New Jersey Department of Environmental Protection. Project No. 08-14189A, Final Report, 2008

- Details monitoring methods and locations, laboratory analysis methods, and results for $PM_{2.5}$, black carbon and VOC measurements taken in the areas surrounding TEB. Lead is not segregated from PM measurements.

Fang, G., Y. Wu, W. Lee, T. Chou, and I. Lin. Ambient Air Particulates, Metallic Elements, Dry Deposition and Concentrations at Taichung Airport, Taiwan. Atmospheric Research 84: 280−289, 2007

- CY 2004 air monitoring campaign measuring TSP, dry deposition flux, PM_{10} and $PM_{2.5}$ at Taichung Airport. Metallics within PM_{10} and $PM_{2.5}$ were also measured. Average Pb as $PM_{2.5}$ was 28.04 ± 6.57 ng/m^3. Average Pb as PM_{10} was 16.15 ± 2.88 ng/m^3. Average Pb as TSP was 40.18 ± 9.58 ng/m^3. Dry downward deposition flux for Pb was measured at 50.16 ± 25.87 µg/m^2/day, at a velocity of 1.21 ± 0.42 cm/s.

Ferrara, A. Avgas/Autogas Comparison: Winter Grade Fuels. Federal Aviation Administration Technical Report No. DOT/FAA/CT-86/21, 1986

- Dynamometer testing was conducted on general aviation aircraft engines fueled with avgas and automotive gasoline to ascertain the effects of fuel properties on engine performance parameters such as vapor lock. For this study, a Cessna 172 fuel system was used equipped with a test engine the authors claim to operate similarly to a Lycoming O-320 engine. Fuel consumption curves as a function of engine power (in rpm) are presented for all fuels evaluated in the study.

General Aviation Manufacturers Association. 2010 General Aviation Statistical Databook and Industry Outlook, 2010

- Contains detailed statistics on general aviation sector, including shipments and billings, fleet and flight activity, fuel consumption, pilots, forecasts, safety data and international figures. May contain usable information for allocating fleet and operations at a national and/or state level with respect to piston aircraft emissions inventories.

Harris, A. and C. Davidson. The Role of Resuspended Soil in Lead flows in the California South Coast Air Basin. Environmental Science and Technology 39: 74107415, 2005

- Emissions from piston aircraft operating in the South Coast Air Basin are quantified using EDMS and CY 2001 LTO data from FAA for 28 airports. EDMS aircraft used in the analysis were the Cessna 172, Piper PA28 and Cessna 150. It was assumed that of an average 64.9 minute LTO cycle, 42.1% occurs below the local mixing height. The study calculates lead emissions by converting SO_2 emissions from EDMS to lead using a factor of 0.739 and an uncertainty estimate of 17.5%. The resulting emissions load is 267 kg Pb/year.

- A crustal rock background of 12.5 ppm of Pb was assumed in the analysis. Lead outflows from the air basin were estimated as a function of the temporally averaged ratio of Pb to CO. Lead deposition was estimated using a dry deposition velocity of 0.0026 ± 0.0013 m/s and an average airborne lead concentration of 0.0310 µg/m^3, resulting in a downward flux of 11,300 ± 5,630 kg/year. This information was applied to a mass balance model using a range of resuspension rates. Model results using resuspension rates of 1^{e-10} µg/s and 1^{e-11} µg/s best matched measured airborne concentrations.

Ho, T., F. Kennedy, and M. Peterson. Evaluation of Materials and Design Modifications for Aircraft Brakes. Prepared for the National Aeronautics and Space Administration under Grant NGR 33-018-1552. NASA CR 134896, 1975

- Identifies lead tungstate (PbWO4) as a friction modifier in nickel-based aircraft brake strators tested in this study, present at 5 percent by composition. Stator wear rates for nickel-based brakes ranged between 0.001 and 0.008 grams per second of braking.

Hoyer, M. and M. Pedde. Memorandum from Marion Hoyer and Meredith Pedde of the U.S. Environmental Protection Agency Office of Air and Radiation on the Selection of Airports for the Airport Monitoring Study. U.S. Environmental Protection Agency Lead NAAQS Review Docket EPA-HQ-OAR-2006-0735, 2010

- Outlines the criteria used to determine the 15 airports selected for additional monitoring as promulgated at 75 FR 81126. The main criteria used to select the airports were 1) emissions of 0.5 tpy of lead or more, 2) runway configurations and meteorological data indicating a greater frequency of operations from one or two runways, and 3) public access within 150 meters of the location(s) of maximum emissions.

Hsu, Y. and F. Divita, Jr. SPECIATE4.2 Speciation Database Development Documentation. EPA/600-R-09/038, prepared by E.H. Pechan & Associates, Inc., 2009

- Describes data sources, quality ratings, compositing methodology, limitations and other considerations used to develop both gas and particle phase speciation profiles in the SPECIATE version 4.2 database.

Hu, S., S. Fruin, K. Kozawa, S. Mara, A. Winer, and S. Paulson. Aircraft Emission Impacts in a Neighborhood Adjacent to a General Aviation Airport in Southern California. Environmental Science and Technology 43: 8039−8045, 2009

- Ultrafine particulates, particle bound polynuclear aromatic hydrocarbons and black carbon were monitored in the vicinity of SMO in the summer of 2008. When compared to background, peak levels of UFP, PB-PAH and BC measured during the study were elevated by factors of 440, 90 and 100, respectively, in areas of jet departures. Lead emissions are not segregated from the particulate measurements. Concentrations remained elevated for extended periods of time when there was a lot of sustained jet activity.

Illinois Environmental Protection Agency. Chicago O'Hare Airport Air Toxic Monitoring Program: June−December 2000. Final Report, 2002

- Lead levels downwind of the airport were 87.5% higher than concentrations measured upwind. Lead concentrations measured at IEPA air toxics monitoring sites both upwind and downwind of the airport over the same study timeframe ranged from 12.0 to 31.5 ng/m^3, with the highest levels measured ~23 miles southeast of the airport at the Chicago-Washington high school station, which neighbors industrial areas.

Lejano, R. and J. Ericson. Tragedy of the Temporal Commons: Soil-Bound Lead and the Anachronicity of Risk. Journal of Environmental Planning and Management 48:2, 301320, 2005

- Mean concentrations of lead in mg/kg of soil taken from Whiteman Airport were 232.5 when considering an outlier value, and 111.6 without the outlier value. Even without the outlier in the data set, Whiteman Airport soil levels were highest second only to samples collected along San Fernando Road, which runs adjacent to the airport property. Mean concentrations of bioavailable lead in the same airport soils were approximately 72.5 mg/kg of soil regardless of whether the outlier was included. Cluster analysis of all soil samples collected during the campaign suggests that the airport contributed to elevated soil concentrations along San Fernando Road, and that historical vehicular contributions to soil lead levels are significant in airborne exposure levels.

Lovestead, T. and T. Bruno. Application of the Advanced Distillation Curve Method to the Aviation Fuel Avgas 100LL. Energy and Fuels 23: 2176−2183, 2009

- Researchers test a refinement of distillation methods used in ASTM D-86 and D-2887 to characterize enthalpy of combustion and the molar percentage of TEL throughout distillation, measured by gas chromatograph mass spectrometry (GC-MS). Neat avgas prior to distillation possessed a TEL molar % of 0.038, corresponding to 6.43 mL of TEL per liter of avgas at a density of 0.7 g/mL. TEL molar % increases were observed as distillate volume fraction increased, with most of the increase occurring at higher temperatures (i.e., higher % distillate).

Michigan Department of Environmental Quality - Air Quality Division. Michigan's 2012 Ambient Air Monitoring Network Review, 2011

- Indicates monitoring network design, parameters and justification for Oakland County International (PTK) ambient lead monitoring. The airport emits 0.76 tpy of lead according to the 2008 NEI. Using the number of based aircraft the airport emits 0.53 tpy of lead. Site selection was centered on the 27R end of 9L/27R because airport officials indicate the majority of piston aircraft activity occurs there.

Morin, B. TF Green Airport Air Monitoring Study. Presentation delivered by Barbara Morin of the Rhode Island Department of Environmental Protection at the EPA Air Toxics Data Analysis Workshop, 2007

- Presents monitoring methodology and results for $PM_{2.5}$, black carbon, and organic air toxic species in the areas surrounding PVD. Lead is not segregated from PM measurements.

Morris, K. Emissions from Aircraft Airframe Sources: Tyre and Brake Wear. Presentation delivered by Kevin M Morris, Manager of Environmental Affairs at British Airways on April 12, 2007

- Presents tire rubber loss data as a function of maximum landing weight, maximum takeoff weight and aircraft classification number (ACN). The range of rubber loss is <0.1 to <0.9 g/landing. Brake material loss reported as a function of maximum takeoff weight. Note, few data points for aircraft weighing less than 50,000 kg. The range of brake loss is between 0.012 and 0.014 g/landing.

Petersen, T. Aviation Oil Lead Content Analysis. Report No. EPA 1-2008, 2008

- Basis of quantifying lead retention in piston engine oil for 2008 NEI calculations. Samples of 100W in IO-360, O-300, O-320, C85, O-235 L2C, IO-550 and new oil (n=11) operated between 0 and 100 hours. Lead ppm in oil samples ranged between 226 for new oil and 10,286 ppm for Sample J (O-320 D2J). The samples with the two highest values were flight school airplane engines, and the author notes that this may have impacted the concentrations due to improper fuel leaning procedures. EPA's retention value may correspond to the ratio of new oil ppm to the average of all other samples, resulting in ~5%.

Petro-Canada. Material Safety Data Sheet for 100LL Avgas Produced by Petro-Canada, 2009

- Contains between 0 and 0.56 g/L of TEL

Phillips Petroleum. Material Safety Data Sheet for 100LL Avgas Produced by Phillips 66 Petroleum, 1998

- Contains less than 2.1 g/gal of TEL. Product No. 1014050 (21223)

Piazza, B. Santa Monica Municipal Airport: A Report on the Generation and Downwind Extent of Emissions Generated from Aircraft and Ground Support Operations. Prepared for the Santa Monica Airport Working Group, 1999

- Aircraft emissions were calculated using input from the Santa Monica Airport Working Group for fleet mix, emissions indices from AP-42 and FAEED, using calculation methodology according to EPA's Procedures for Emissions Inventory Preparation Volume 4: Mobile Sources. Time in mode was not considered. Rather hourly operational profiles, aircraft speed and route lengths were used to develop a uniform line source emissions load according to the EPA PAL2 dispersion model. Airport traffic and stationary source emissions contributions were also considered.

- Emissions source strengths were input to the ISCST3 dispersion model as volume sources for all mobile and fixed-based sources considered in the emissions inventory using a 50m grid resolution. DEM data was obtained from USGS and hourly surface weather data was obtained from SCAQMD's West Los Angeles Monitoring station.

Monitored quarterly Pb concentrations for 1995-1997 ranged between 0.03 and 0.05 $\mu g/m^3$, compared to modeled Pb concentrations from piston operations totaling 0.057 $\mu g/m^3$.

Platt, M. and E. Bastress. The Impact of Aircraft Emissions Upon Air Quality. Society of Automotive Engineers Paper No. 720610, DOI 10.4271/720610, 1972

- Dated paper presenting emissions inventory data for LAX, DCA, JFK, ORD, VNY and Tamiami airports. The source of Pb emissions factors and computation methodology are not disclosed. According to this study VNY emitted 0.003, 0.005 and 0.0069 kg of lead in 1970, 1975 and 1980 respectively, most of which purportedly came from aircraft.

RTI International. Scaling Factor: PM10 versus TSP. Final Report, 2008

- Assesses the feasibility of developing a scaling factor to relate Pb-PM_{10} to PB-TSP to support EPA's proposal to allow Pb-PM_{10} sampling. Outlines the criteria for developing scaled Pb-PM_{10} data as reported at 73 FR 29285 and proposes alternative methods. These methods were applied to collocated data from 21 locations that met sampling suitability criteria. Of these 21 locations, only four were suitable for development of a scaling factor based on quarterly statistical criteria ($r^2 = 0.60$), and only one was suitable based on monthly criteria. A method for statistically censoring the data to reconcile this deficiency is proposed in Appendix A.

Sheets, R., J. Kyger, R. Biagioni, S. Probst, R. Boyer, and K. Barke. Relationship Between Soil Lead and Airborne Lead Concentrations at Springfield, Missouri, USA. Science of the Total Environment 271: 79−85, 2001

- TSP monitoring data for 1975-1981 shows a strong correlation ($r^2 = 0.91$, $P < 0.005$) with current soil lead samples, irrespective of proximity to high-traffic sites. Soil concentrations are attributed to historical vehicular emissions.

Shell Energy North America. Material Safety Data Sheet No. 402059M-0 for 100LL Avgas Produced by Motiva Enterprises LLC, 2003

- Contains 0.53 ml TEL/L of fuel. Manufacturer is Motiva Enterprises, LLC, based in Houston, TX

Sierra Research. Alaska Aviation Emission Inventory. Report No. SR2005-06-02. Prepared for the Western Regional Air Partnership, 2005

- Detailed report outlining methodology and results for emissions inventories conducted for all Alaskan public use airports. Appendices contain detailed LTO data for each airport facility derived from the National Flight Data Center, Alaska DOT, FAA's Terminal Area Forecast, and airport surveys. Lead emissions were not quantified in this effort.

South Coast Air Quality Management District. General Aviation Airport Monitoring Study: Follow-up Monitoring Campaign at the Santa Monica Airport. Final Report, 2011

- A follow-up study was conducted at SMO while the airport was closed for a six-day period in 2010 for pavement renovations, to gauge how measured concentrations

change in the vicinity when the airport is not operational. Lead was not monitored during this campaign.

South Coast Air Quality Management District. General Aviation Airport Monitoring Study. Final Report, 2010

- At VNY, monitored TSP lead concentrations decreased with increasing distance from the runway area and ranged between 26.1 and 8.45 ng/m^3 during Phase I of sampling, and between 3.88 and 7.11 during Phase II. The basin average during these two phases were 12.3 and 5.92. For SMO, lead levels during phase I ranged between 3.30 ng/m^3 up to 85.2 ng/m^3 at the east tarmac measurement site. During Phase II, levels ranged between 5.5 and 77.0. The basin averages during these two phases were 9.47 and 13.1.

South Coast Air Quality Management District. Multiple Air Toxics Exposure Study in the South Coast Air Basin (MATES-III). Draft Report, 2008

- Average TSP Lead concentrations measured at ten monitoring locations throughout the South Coast Air Basin ranged between 6.9 ng/m^3 and 22.7 ng/m^3 during year 1 at the study, and between 6.2 and 14.6 ng/m^3 during year 2, with individual measurements ranging from 3.0 to 156.0 ng/m^3 across both years. 1,2-dibromoethane was also measured but was below the detection limits of the instrumentation at all sites for all samples.

- A simulated annual average concentration of both TSP and $PM_{2.5}$ lead was modeled using CAMx/RTRAC with MM5, using a 2002 emissions inventory projected to 2005 from the 2007 Air Quality Management Plan for the district. Simulated annual averages underestimated concentrations for Pb as $PM_{2.5}$ by 2.94 ng/m^3 and as TSP by 2.28 ng/m^3.

Switzerland Federal Office of Civil Aviation. Guidance on the Determination of Helicopter Emissions. First Edition 0/3/33/33-05-20, 2009

- Describes typical times in mode derived from in-flight testing for both single- and twin-engine turboshaft helicopters, as well as piston engine helicopters. Provides fuel flow and emissions index calculation methodology for these engine categories, accounting for variations in shaft horsepower.

Switzerland Federal Office of Civil Aviation. Guidance on the Determination of Helicopter Emissions. Supporting Data, 2009

- Spreadsheet containing detailed data on 86 helicopter engines, including shaft horsepower, modal fuel flow, and modal emissions indices. Information developed using methodology reported in FOCA publication 0/3/33/33-05-20 (Guidance on the Determination of Helicopter Emissions, 1st ed.).

Switzerland Federal Office of Civil Aviation. Aircraft Piston Engine Emissions - Summary Report. 0/3/33/33-05-003 ECERT, 2007

- Provides performance and emissions data for a range of piston aircraft engines. Outlines a preferred methodology for calculating emissions, including modal power settings and operating times within the LTO cycle. Also provides cruise emissions calculation methodology. Specifies avgas can contain up to 0.8 g of TEL per kg of

fuel. Pb emissions per LTO presented in the document range from 1.45 to 17.2 g. Lead emissions during cruise range between 16.6 and 84.2 grams, assuming a 1-hour cruise duration.

Switzerland Federal Office of Civil Aviation. Aircraft Piston Engine Emissions. Supporting Data, 2007

- Spreadsheet containing detailed data on 20 piston engines, including specific horsepower, modal fuel flow and modal emissions indices (criteria pollutants). Information developed using methodology and test results reported in FOCA publication 0/3/33/33-05-003 (Aircraft Piston Engine Emissions Summary Report).

Switzerland Federal Office of Civil Aviation. Aircraft Piston Engine Emissions Appendix 1: Measurement System. 0/3/33/33-05-003 ECERT, 2007

- Describes technology and methods used to obtain exhaust gas concentrations of criteria pollutants from piston engines included in the study. Lead emissions were not directly measured during this campaign.

Switzerland Federal Office of Civil Aviation. Aircraft Piston Engine Emissions Appendix 2: In-flight Measurements. 0/3/33/33-05-003 ECERT, 2007

- Describes methodology and approach for taking in-flight emissions, fuel flow and other performance measurements from piston engines included in the study, comprising O-360, IO-360, IO-550, O-320 engines. Lead emissions are not addressed in this document.

Switzerland Federal Office of Civil Aviation. Aircraft Piston Engine Emissions Appendix 3: Power Settings and Procedures for Static Ground Measurements. 0/3/33/33-05-003 ECERT, 2007

- Presents methodology and data used to measure fuel flow and correlate to engine power setting for piston aircraft engines included in the study. Discussion is relative to development of criteria pollutant emissions factors based measured concentrations, accounting for engine power and fuel flow. Documentation does not address lead as a pollutant.

Switzerland Federal Office of Civil Aviation. Aircraft Piston Engine Emissions Appendix 4: Nanoparticle Measurements and Research for Cleaner Avgas. 0/3/33/33-05-003 ECERT, 2007

- Provides SMPS particle size and mass distributions from exhaust emitted from two Lycoming O-320 series engines fueled with 100LL and 91/96 UL, fitted to two different airframes. Provides spectroscopic data for 100LL derived using EDX.

Switzerland Federal Office of Civil Aviation. Aircraft Piston Engine Emissions Appendix 5: Calculation of Emissions Factors. 0/3/33/33-05-003 ECERT, 2007

- Outlines process by which emissions exhaust testing results were translated into criteria pollutant emissions factors for engines included in the study. Used a molar mass balance approach. Lead emissions are not addressed in this methodology.

Tetra Tech, Inc. Destin Airport Air Sampling Project Executive Summary. Prepared for the City of Destin, Florida, 2007

- TSP lead measurements were collected around Destin Airport at background sites and at sites impacted by the airport (i.e., surrounding airport runways). TEL and ethylene dibromide were also measured. Background TSP concentrations were considered to be 30.6 mg/m^3. Two sites designated as impacted by the airport were above the background level, by nearly twice as much at one of the sites. TSP-lead background concentrations were measured at 2.5 ng/m^3, with all three impacted sites exceeding this concentration (although one non-impacted site did as well). The study implicates fireworks activity as a cause for anomalously high concentrations on the fourth of July. No measurements exceeded the current NAAQS during the study timeframe.

Turner, J. Missouri/Illinois Perspective on Pb Isotopic Abundance in Soils and Sediments. Presentation delivered via personal communication with Sierra Research, 2011

- Compares $^{208}Pb/^{206}Pb$ isotopic ratios to $^{207}Pb/^{206}Pb$ ratios for sediments both sampled directly and summarized from literature. Isotope measurements from smelters and refineries, as well as ambient PM_{10} and $PM_{2.5}$ measurements, are compared. Smelter data plots close to sediment values for Viburnum Ore, and Lamotte Sandstone samples. Ambient samples cannot be site-segregated, and lower bound of measurements may be artifact of detector saturation of ^{208}Pb. Isotope abundance ratios are consistent with mixing of known Pb sources, and samples isotopically closest to viburnum ore sediments were taken on highest Pb concentration days.

U.S. Environmental Protection Agency. 2008 Lead Emissions by Airport (3/9/2011), 2011

- Spreadsheet summarizing LTO data and other pertinent information, by facility, used to calculate lead emissions for the 2008 NEI both within the LTO cycle and in flight.

U.S. Environmental Protection Agency. Documentation for Aircraft Component of the National Emissions Inventory Methodology. Prepared by Eastern Research Group under Contract No. EP-D-07-097 (January 2011 Revision), 2011

- Outlines calculation methodology for criteria pollutant emissions from aircraft for inclusion in the 2008 NEI. Appendix B is a reproduction of EPA-420-B-10-044, which outlines methodology used by EPA to calculate lead emissions from piston aircraft fueled with 100LL both within the LTO cycle and above the mixing height for inclusion in the 2008 NEI. Uses emissions factor of 2.12 g Pb/gallon of avgas, representing the ASTM maximum allowable lead concentration. Also assumes 5% of lead from avgas is retained in the engine and engine oils. Describes data sources consulted to develop inventory input data for aircraft fleet and operational levels.

U.S. Environmental Protection Agency. Integrated Review Plan for the National Ambient Air Quality Standards for Lead. External Review Draft. EPA-452/D-11-01, 2011

- Summarizes key policy-relevant issues, science assessments, risk and exposure assessments, ambient air monitoring network considerations and requirements, and policy/rulemaking assessments associated with the most recent Pb NAAQS review. Includes discussion of the requirements for airport-oriented lead monitoring and proposes associated sampling and analysis methods.

U.S. Environmental Protection Agency. Integrated Science Assessment for Lead. EPA/600/R-10/075A, 2011

- Chapter 3 contains detailed information on ambient lead measurement, including: sources of atmospheric lead, a summary of the inputs and results of the 2008 NEI, source apportionment, fate and transport into various environmental media, monitoring methodology and network design, and concentration data up to CY 2009.

U.S. Environmental Protection Agency. Calculating Piston-Engine Aircraft Airport Inventories of Lead for the 2008 National Emissions Inventory. EPA-420-B-10-044, 2010

- Outlines methodology used by EPA to calculate lead emissions from piston aircraft fueled with 100LL both within the LTO cycle and above the mixing height for inclusion in the 2008 NEI. Uses emissions factor of 2.12 g Pb/gallon of avgas, representing the ASTM maximum allowable lead concentration. Also assumes 5% of lead from avgas is retained in the engine and engine oils. Describes data sources consulted to develop inventory input data for aircraft fleet and operational levels

U.S. Environmental Protection Agency. Development and Evaluation of an Air Quality Modeling Approach for Lead Emissions from Piston-Engine Aircraft Operating on Leaded Aviation Gasoline. Prepared by ICF International and T&B Systems. EPA-420-R-10-007, 2010

- Describes methodologies for calculating lead emissions from piston aircraft, conducting and reconciling air monitoring and dispersion modeling of lead concentrations, and sampling soil and dust from areas on and around SMO. Activity data was obtained from airport personnel. An emission factor of 2.12 g/gallon of avgas was used, assuming 5% retention of lead in the engine and lubrication oil. 25% of the helicopter activity was assumed to be performed by piston-powered helicopters. Fuel consumption rates for IO360, IO320, GSO480, IO550, TIO-540-J2B2 and TSIO550 were obtained from engine operating manuals.

- Modeling indicates that elevated concentrations of lead can be observed at receptors ranging between 500 and 900 meters downwind of the airport, with potential modeled concentrations as high as 150 ng/m^3. Model was most sensitive to changes in engine run-up time, Pb concentration in the fuel, and the fraction of multi-engine aircraft in operation.

- Winter monitoring program concentrations using HiVol and MiniVol samplers ranged below detection limits all the way up to 99 ng/m^3 at the East Tarmac. During the summer, HiVol samplers monitored concentrations ranging below detection limits to 79 ng/m^3. Soil lead measurements ranged between 9 and 150 mg/kg and were well below applicable EPA standards. Only three of the 18 dust samples collected were above detection limits, and measured as high as 684 $\mu g/ft^2$ at one residence, exceeding applicable EPA standards.

U.S. Environmental Protection Agency. Documentation for Aircraft Component of the National Emissions Inventory Methodology. Prepared by Eastern Research Group under Contract No. EP-D-07-097 (April 2010 Version), 2010

- Outlines calculation methodology for criteria pollutant emissions from aircraft for inclusion in the 2008 NEI.

- Appendix B is a reproduction of EPA-420-B-10-044, which outlines methodology used by EPA to calculate lead emissions from piston aircraft fueled with 100LL both within the LTO cycle and above the mixing height for inclusion in the 2008 NEI. Uses emissions factor of 2.12 g Pb/gallon of avgas, representing the ASTM

maximum allowable lead concentration. Also assumes 5% of lead from avgas is retained in the engine and engine oils. Describes data sources consulted to develop inventory input data for aircraft fleet and operational levels.

- Appendix C is a reproduction of EPA420-R-08-020, which outlines methodology used by EPA to calculate lead emissions from piston aircraft fueled with 100LL within the LTO cycle based on that employed for the 2002 NEI. Uses emissions factor of 2.12 g Pb/gallon of avgas, representing the ASTM maximum allowable lead concentration. Recommends refinements to methodology for future inventories including accounting for lead retention in the aircraft engine and lubrication oil, assessing lead emissions outside of the LTO cycle, and accounting for facilities for which data was unavailable in the 2002/2005 NEI. Summarizes 2002 emissions by facility for 3,414 airports.

U.S. Environmental Protection Agency. 40 CFR Part 58 - Revisions to Lead Ambient Air Monitoring Requirements, Final Rule. Published at 75 FR 81126. December 27, 2010

- Describes source-oriented lead air monitoring network requirements promulgated as a results of the 2008 Lead NAAQS revision. Airports designated for monitoring are those exceeding a 1 tpy emissions threshold. Additionally, 15 airports whose emissions are between 0.5 and 1.0 tpy have been identified for monitoring due to individual characteristics that could lead to infractions of the NAAQS. These airports are summarized on Table 5 of the document (p. 81131).

U.S. Environmental Protection Agency, Lead Emissions from the Use of Leaded Aviation Gasoline in the United States. Technical Support Document. EPA420-R-08-020, 2008

- Outlines methodology used by EPA to calculate lead emissions from piston aircraft fueled with 100LL within the LTO cycle based on that employed for the 2002 NEI. Uses emissions factor of 2.12 g Pb/gallon of avgas, representing the ASTM maximum allowable lead concentration. Recommends refinements to methodology for future inventories including accounting for lead retention in the aircraft engine and lubrication oil, assessing lead emissions outside of the LTO cycle, and accounting for facilities for which data was unavailable in the 2002/2005 NEI. Summarizes 2002 emissions by facility for 3,414 airports.

U.S. Environmental Protection Agency. National Ambient Air Quality Standards for Lead, Final Rule. Published at 73 FR 66964 on November 12, 2008

- EPA outlines supporting evidence and justification to revise the NAAQS to 0.15 $\mu g/m^3$ over a rolling three-month average. Provides updates to the language at 40 CFR Parts 50,51,53 and 58 on reference conditions, treatment of data during exceptional events, reference methods for TSP, PM10, test procedure methods, monitoring network requirements, assessments, and design criteria.

U.S. Environmental Protection Agency. SPECIATE v.4.2. Developed by E.H. Pechan and Associates, 2008

- Contains gaseous and particulate speciation profiles for numerous natural and anthropogenic emissions sources, including particle speciation profiles for piston aircraft, crustal sources, soil and road dust. Could be a useful data source in determining lead species in particulate emissions inventories.

U.S. Environmental Protection Agency. Lead Human Exposure and Health Risk Assessments for Selected Case Studies Volume II: Appendices. Draft Report EPA-452/D-07-001b, 2007

- Summarizes inputs and outcomes of the 2002 NEI as it pertains to piston aircraft emissions. Also summarizes Pb-TSP, Pb-PM_{10} and Pb-$PM_{2.5}$ monitoring network, methods and data for the period spanning 2003-2005

U.S. Environmental Protection Agency. Air Quality Criteria for Lead: Volume I or II. EPA/600/R-5/144aF, 2006

- Describes chemistry, sources and transport of lead, and summarizes toxicological, epidemiological and environmental studies used in establishing NAAQS for lead, including a synopsis of lead emissions from piston aircraft and related sources.

U.S. Environmental Protection Agency. Air Quality Criteria for Lead: Volume II of II. EPA/600/R-5/144bF, 2006

- Volume II of the criteria document is a series of annexes addressing literature and data sources consulted with respect to the following categories: human toxicology, animal toxicology, epidemiological studies of exposure, and environmental effects.

U.S. Environmental Protection Agency - Persistent, Bioaccumulative and Toxic Pollutants (PBT) Program. PBT National Action Plan for Alkyl Lead, 2002

- Gives synopsis of different types of avgas available (as of 2002), their use relative to market share, and TEL content. States that aviation was the largest contributor to evaporative emissions of lead from all sources considered in an inventory prepared by EPA in 1998. Identifies additives to avgas that have additional toxic effects.

U.S. Environmental Protection Agency. Procedures for Emission Inventory Preparation Volume IV: Mobile Sources. EPA420-R-92-009, 1992

- Aircraft emissions inventory methodology for general aviation aircraft involve either 1) factoring time in mode versus fuel flow rates to derive aircraft fuel consumption, and applying the fuel consumption estimate to specific engine emissions indices; or 2) applying fleet average emissions factors, in tons per LTO, to the LTO data derived from FAA's Air Traffic Activity. Fleet average emissions factors are only provided for HC, CO, NO_x, and SO_2. No guidance is provided for estimating Pb emissions from the use of avgas.

U.S. Environmental Protection Agency. Compilation of Air Pollutant Emissions Factors (AP-42). Third Edition, 1977

- The third edition of this compendium is not the latest, but contains a chapter on internal combustion sources (chapter 3), within which an aircraft emissions inventory methodology and supporting data (i.e., emissions rates, times in mode) are presented. No methodology on quantifying emissions of lead from airport sources is described.

URS Corporation. Select Resource Materials and Annotated Bibliography on the Topic of Hazardous Air Pollutants (HAPs) Associated with Aircraft, Airports and Aviation. Prepared in support of CSSI Contract: DTFA 01-99-Y-01002 under Technical Directive Memorandum D01-010, 2003

- Useful annotated bibliography describing sources of literature and data pertinent to aircraft HAPs and other air toxics, including lead.

Vanderpool, R., S. Kaushik, and M. Houyoux. Laboratory Determination of Particle Deposition Uniformity on Filters Collected Using Federal Reference Method Samplers, 2008

- Previous studies have indicated that particle deposition on FRM filters favors the outer border (5% of the total filter area), implying that uncertainty in filter sampling can be introduced due to the spatial non-uniformity of the particle distribution on the filter surface. Because EPA has allowed use of EDXRF filters in PM10 FRM samplers, this study seeks to assess the level of uncertainty caused by sampling the filter in differing areas of the filter surface. The study reveals that a 10 mm punch sample yields an accuracy ratio of 0.981, 0.994 and 0.982 for PM2.5, PM10 and TSP filters, respectively. Punch diameters of 20 mm yielded accuracy measurements of 0.972, 0.993 and 0.985 for the three size fractions, respectively. (Note, an accuracy ratio is a measure of particle deposition uniformity, with 1.0 being completely uniform. In addition, no difference in deposition uniformity was observed in particles ranging from 0.035 to 12.5 micrometers in diameter.

Webb, S., P. Whitefield, R. Miake-Lye, M.T. Timko, and T. Thrasher. *ACRP Report 6: Research Needs Associated with Particulate Emissions at Airports*. Transportation Research Board of the National Academies, 2008

- Identifies gaps in methodology and data pertinent to estimating particulate matter emissions from airport sources, including general aviation aircraft. Limitations identified in the report include a lack of engine emissions data for PM, lack of data regarding volatile PM sourced from engine oil, and lack of adequate modeling/knowledge of volatile PM evolution in aircraft exhaust plumes. Contains a reasonably comprehensive annotated bibliography of literature and research on these topics.

Young, T., D. Heraman, G. Sirin, and L. Ashbaugh. Resuspension of Soil as a Source of Airborne Lead near Industrial Facilities and Highways. Environmental Science and Technology 36: 2484–2490, 2002

Bulk samples were analyzed using XRF Spectroscopy to determine lead levels in soils surrounding industrial facilities and a roadway. Measurement of PM_{10} formation via resuspension was also tested using these bulk samples in a resuspension chamber, sampled on 25 mm Teflon filters. Pb concentrations exceeded the benchmark average for California soils (23.9 mg/kg), and a downwind effect on concentrations was observed for two of the sample sites, implying that these two sites influence soil lead levels to a greater degree. PM_{10} formation via resuspension ranged from 0.169 mg PM_{10}/g of soil for roadside samples to 0.869 for a sandblasting facility. Enrichment factors of between 5.36 and 88.7 were computed for Pb as PM10 from the samples analyzed.

Appendix B

Additional Field Study Information

Additional Field Study Information

PM Sample Collection Protocols

Airborne PM samples were collected using Model PQ100 portable samplers (BGI, Waltham, MA). The PQ100 is a U.S. EPA Federal Reference Method (FRM) for PM_{10} sampling and for this study was used with BGI Very Sharp Cut Cyclones (VSCC) to achieve $PM_{2.5}$ cutpoints. A louvered inlet with PM_{10} impactor—the standard configuration for ambient PM_{10} sampling—was used upstream of the $PM_{2.5}$ cyclone. Total Suspended Particulate (TSP) samples were collected using PQ100 samplers with BGI TSP inlets.

Samples were collected onto 47mm, 2.0 µm pore size Teflon® filters (PT47, MTL Corp., Minneapolis, MN). Prior to use, all filters were visually inspected for puncture holes or other impurities. Filter holders and screens were cleaned daily with de-ionized water. After sampling, the filters were again visually inspected for puncture holes and other irregularities and were then placed in a freezer for storage. All filters were transported using ice packs and insulated shipping containers.

The BGI samplers were operated at an actual flow rate of 16.7 LPM, which is the design flow rate for the aforementioned inlets. Flow rates were calibrated using a NIST-traceable flow meter (deltaCal, BGI, Waltham, MA). Flow rates were checked nominally every 3 days and with recalibration performed if the deviation from setpoint exceeded 5%. In such cases, the flow rate was rechecked after the end of the sampling event.

ICP-MS Analysis for Total PM-Pb and Pb Isotopes

Exposed filters were digested and analyzed for Pb by ICP-MS. Filters were first cut from their support rings and placed into polypropylene vials. Particulate matter on the filters was extracted using a two-stage digestion process. In the first stage, nitric and hydrofluoric acid were added to the sample vials and the samples were digested for 2 hours using a hot-block (ModBlock, CPI International, Santa Rosa, CA) at 90°C. After the first stage, samples were allowed to cool and then boric acid was added to enhance recovery and complex the excess hydrofluoric acid. The second-stage digestion was then performed, again with the hot-block at 90°C for 2 hours.

QA/QC measures for each set of digestions included (1) a reagent blank, prepared using the same amount of acid that was added to a vial which was subjected to the digestion process; (2) a spiked reagent blank, prepared identically to the reagent blank and spiked with a known amount of the multi-element standard before the first hot-block digestion stage; (3) a filter blank that used an unexposed filter that was subjected to the same digestion method as the exposed filter samples; and (4) a digested acid matrix matched blank (DAMMB), prepared identically to the reagent blank but in greater volume and using different glassware for the purpose of making ICP-MS calibration and concentration verification standards. Digested samples and QA/QC blanks were filtered using 0.45 µm pore size Acrodisc filters (Pall Corp., Port Washington, NY) and then

diluted to a final volume of 15 ml with de-ionized water to have a nitric acid content of 5% (v/v).

Samples were analyzed using an ELAN DRC II Inductively Coupled Plasma Mass Spectrometer (PerkinElmer, Waltham, MA). The ICP-MS nebulizer flow rate and lens voltage was optimized prior to each analysis batch. The instrument was calibrated using a number of DAMMB samples with known amounts of Pb. Calibration concentrations ranged from 0.001 to 50 ppb. For each analysis batch, the performance of the ICP-MS was re-evaluated after every 10 samples using blank DAMMB solution and a concentration verification solution made from DAMMB and 1ppb Pb. Total Pb (and select other elements) signal intensities were corrected using rhodium and rhenium internal standards, with rhodium used to correct the Pb intensities. Calibration curves were used to determine Pb concentration in solution, and the ambient air volume sampled was used to calculate ambient PM-Pb mass concentrations.

NIST Standard Reference Material (SRM) were digested and analyzed for PM-Pb content. Recoveries were 100±1 % (N=3) for SRM 1648a (urban particulate matter) and 102% (N=1) for SRM 2783 (urban $PM_{2.5}$ collected on polycarbonate filter media).

Lead isotope ratios were analyzed using a second ICP-MS analysis with a thallium internal standard. Thallium isotope ratios were first calibrated using a NIST Pb standard solution with quantified isotopic composition. The thallium ratios were then used as internal standards to correct Pb isotope ratios for the digested filter samples. The consistency of thallium internal standard isotopic ratios during ICP-MS analysis was evaluated by running a verification solution made from the NIST Pb isotopic standard after every 10 digested filter samples.

Soil and Avgas Analysis Protocols

Four soil samples were collected at each airport, one from each of the four sampling locations. Topsoil was collected into glass jars, transported from the field sites to the laboratory using ice packs and insulated shipping containers, and stored in a freezer. A portion of each sample has been analyzed total Pb and Pb isotopes. Soil samples were first sieved to remove small rocks and then ground into a coarse powder. The powdered soil was resuspended using a custom-made resuspension chamber generally based on the designs of Dobrzhinsky et al. (2012) and Martuzevicius et al. (2011). Resuspended soil was sampled onto Teflon filters using a MetOne SASS filter canister and $PM_{2.5}$ cyclone. Deposited samples were analyzed for total Pb and Pb isotopes using the same methods as the ambient PM filter samples.

A total of 15 avgas samples were collected from the three airports. Samples were collected in tin-plated steel cans, with caps sealed with Teflon tape to prevent volatile losses. A small portion of each sample was withdrawn and sent to Intertek Caleb Brett for total Pb analysis. Additional samples were sent to Washington University for Pb isotopes analysis using ICP-MS. The gasoline samples cannot be directed injected into the ICP-MS and thus Pb was extracted using the methodology presented by Lord (1994). A 3% m/v iodine in toluene solution was added to 1 mL of avgas. The lead was allowed

to react with the iodine and then an ICP-MS standard bismuth solution was added as an internal standard. A 10% nitric acid solution was then added and thoroughly mixed. The solution was allowed to separate with the reacted Pb, partitioning from the organic phase to the aqueous phase. The aqueous phase was diluted to form a 5% nitric acid solution with expected Pb concentrations within the calibrated range of the ICP-MS. The diluted extracts were then analyzed by ICP-MS using rhodium as an internal standard to quantify total lead and thallium as an internal standard to quantify Pb isotope ratios. Thallium isotope ratios were first calibrated using a NIST Pb standard solution with quantified isotopic composition. The consistency of thallium internal standard isotopic ratios during ICP-MS analysis was evaluated by running a verification solution made from the NIST Pb isotopic standard after every 10 extracted avgas samples.

PM-Pb Data Validation

Field operator and laboratory analyst comments were entered into a database that tracks each sample. This information was used to flag or invalidate samples for reasons such as specks observed on the filter after sampling, sampler flow rate or duration out of range, or laboratory contamination. Table B-1 summarizes the samples that were invalidated.

Table B-1
PM-Pb Samples That Were Invalidated

Airport	Date	Site	Sample Type	Reason
RVS	03/30/13	East	$PM_{2.5}$ collocate	Sample duration < 9 hours (75%)
RVS	04/06/13	North	$PM_{2.5}$ collocate	Low Pb isotope ratios, poor agreement with collocated sample, large bias compared to XRF Pb
RVS	04/08/13	South	$PM_{2.5}$	Filter fell in dirt during retrieval
RVS	04/13/13	West	$PM_{2.5}$	Sample duration < 9 hours (75%)
APA	05/15/13	Central Sec.	$PM_{2.5}$	Sample duration < 9 hours (75%)
APA	06/07/13	Central	$PM_{2.5}$ collocate	Sample duration 10 hours with poor collocated precision
APA	06/07/13	East	$PM_{2.5}$ collocate	Sample duration < 9 hours (75%)
SMO	07/13/13	Central	$PM_{2.5}$	Contamination identified by Pb isotopes analysis (**Figure B-1**)
SMO	07/13/13	East	$PM_{2.5}$	Contamination identified by Pb isotopes analysis (**Figure B-1**)
SMO	07/17/13	South	$PM_{2.5}$	Contamination identified by Pb isotopes analysis (**Figure B-1**)

Analysis of reagent, filter, and spiked blanks identified contamination in two batches of ICP-MS sample runs accounting for 55% of the SMO samples. Blank concentrations were high as 5 ng/m^3 (reported as effective ambient Pb concentrations). The source of contamination was traced to the acid bath used to clean the glassware for sample digestion and extraction. Ten new blank samples were made by processing DAMMB through the glassware used for normal samples. The acid bath container was then cleaned and a new acid bath was made. All the glassware was cleaned with the new acid bath and three additional blank samples were prepared. The 13 blanks were then analyzed using ICP-MS. The median effective Pb concentrations before and after cleaning the acid bath were 2.8 ng/m^3 and 0.2 ng/m^3, respectively. Pb levels after cleaning the bath were equal to the MDL. Based on this analysis, 2.8 ng/m^3 was subtracted from all Pb sample concentrations measured in these two SMO sample batches.

Lead isotope ratios were then examined to determine if there were any samples with extreme levels of contamination. Figure B-1 shows the ^{208}Pb/^{206}Pb isotope ratio versus measured Pb concentration for the samples in the two contaminated SMO batches. Three samples, denoted by the solid black circles, were determined to have extreme levels of contamination as evidenced by the combination of high concentrations and low ^{208}Pb/^{206}Pb ratios. Even if these samples were not contaminated by the sample digestion process, they indicate high levels of Pb with isotopic composition that does not correspond to TEL-Pb.

Figure B-1
^{208}Pb/^{206}Pb Ratio versus PM-Pb Concentration
for Contaminated SMO Digestion Batches

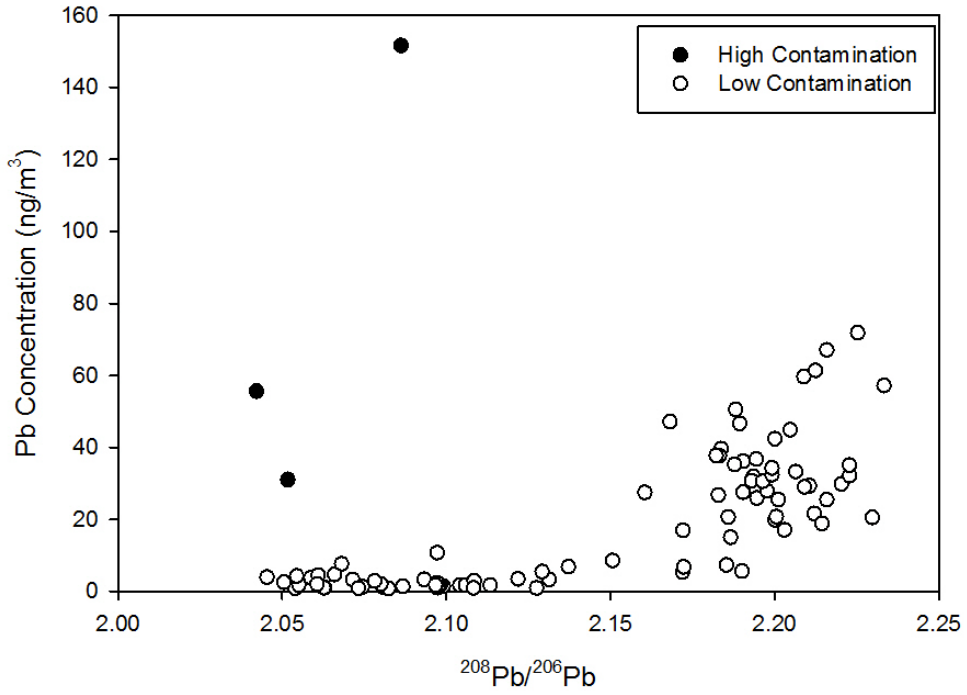

PM-Pb Field Blanks

Eight $PM_{2.5}$ and four TSP field blanks were collected at each airport (three field blanks per sampler per airport). Table B-2 presents the effective ambient field blank concentrations. One extreme value was observed (38 ng/m^3) and cannot be explained. Summary statistics are presented in the main body of the report.

Table B-2
Effective Ambient Pb Concentrations for the Field Blanks

Collection Date	Airport	Inlet	PM-Pb (ng/m^3)
04/11/2013	RVS	2.5	0.21
04/11/2013	RVS	2.5	0.25
04/11/2013	RVS	2.5	38.66
04/11/2013	RVS	2.5	0.13
04/18/2013	RVS	2.5	0.09
04/18/2013	RVS	TSP	0.42
04/18/2013	RVS	2.5	0.08
04/18/2013	RVS	TSP	1.78
04/27/2013	RVS	2.5	0.13
04/27/2013	RVS	TSP	0.17
04/27/2013	RVS	2.5	0.16
04/27/2013	RVS	TSP	0.42
05/27/2013	APA	2.5	0.5
05/27/2013	APA	TSP	0.3
05/27/2013	APA	2.5	-0.1
05/27/2013	APA	TSP	0.3
05/29/2013	APA	2.5	-0.2
05/29/2013	APA	2.5	0.0
05/29/2013	APA	2.5	-0.1
05/29/2013	APA	2.5	0.4
06/05/2013	APA	2.5	0.3
06/05/2013	APA	TSP	-0.2
06/05/2013	APA	2.5	-0.2
06/05/2013	APA	TSP	0.3
07/10/2013	SMO	2.5	0.2
07/10/2013	SMO	TSP	0.9
07/10/2013	SMO	2.5	0.0
07/10/2013	SMO	TSP	1.6
07/16/2013	SMO	2.5	-1.1
07/16/2013	SMO	2.5	0.0
07/16/2013	SMO	2.5	-0.8
07/16/2013	SMO	2.5	-0.3
07/19/2013	SMO	2.5	1.3
07/19/2013	SMO	TSP	-2.0
07/19/2013	SMO	2.5	0.3
07/19/2013	SMO	TSP	2.0

Collocated Precision

Given the importance of characterizing data quality at high PM-Pb concentrations, $PM_{2.5}$-Pb precision was further examined. Collocated sample pairs were ranked by the mean concentration for each pair and the precision was repeatedly calculated adding one pair at a time, starting with the highest concentration and adding sample pairs with decreasing concentration. Figure B-2 shows the evolution of relative precision using this approach. Relative precisions when including only a few sample pairs can be noisy and the values for $N \leq 3$ pairs are excluded from the figure. With increasing sample pairs (i.e., moving from right to left on the plot), including a large concentration gap between 8 and 16 ng/m^3, the relative precision is relatively constant. This asymptotic behavior is consistent with the relative precision being a constant value at high concentrations. Further increasing the number of sample pairs to include lower concentrations yielded a monotonic degradation in relative precision with a maximum value of 17% when including all data. In this region of lower concentrations, the additive contribution to precision is also important.

The upper tertile mean concentration value is 16.1 ng/m^3 and the maximum mean concentration value is 48.8 ng/m^3. Precision was calculated 25 times by re-sampling with replication the ten sample pairs in this concentration range. The mean relative precision was 12% with 1σ standard deviation of 3%. This result demonstrates that 12% is a stable estimate of the relative precision at high concentrations.

Figure B-2
Ripening of the $PM_{2.5}$-Pb Collocated Precision

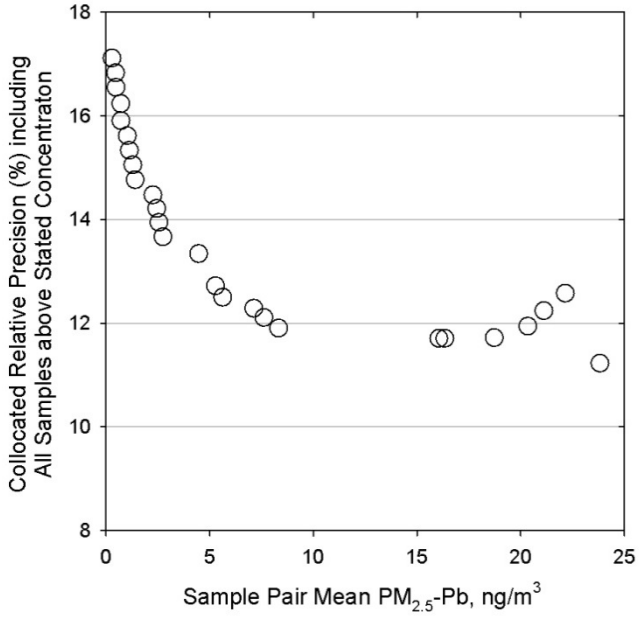

PM-Pb Analysis by XRF with Comparison to ICP-MS

Twenty-two airborne $PM_{2.5}$ samples from each airport were sent to Cooper Environmental Services (CES) for elemental analysis by XRF. Fourteen field blanks, including at least four from each airport, and six laboratory blanks were also analyzed, with the latter used to develop the spectral blank correction for the specific make and model of filters used in this study. Samples were analyzed by CES Protocol C, which is the most sensitive of the three routine protocols offered with a Pb MDL of 0.24 ng/m^3 effective ambient concentration. Pb effective ambient concentrations for each of the 14 field blanks were less than 0.5 ng/m^3.

Figure B-3 compares ambient $PM_{2.5}$-Pb measured by XRF and ICP-MS. Samples with ICP-MS $PM_{2.5}$-Pb less than three times the ICP-MS MDL of 0.2 ng/m^3 were excluded. The data are highly correlated, with $r^2 = 0.99$ (N = 57). The regression intercept is statistically indistinguishable from zero, but from the regression slope the XRF data are biased 20% high compared to the ICP-MS data. The quantitative SRM recoveries provide compelling evidence for the accuracy of the ICP-MS data.

Measurement differences in Pb are not unusual. For example, in the South Coast Air Quality Management District airport study (SCAQMD 2010), XRF and ICP-MS data were highly correlated ($r^2 = 0.97$) with regression slope of 1.06 and intercept of 25.6 ng/m^3. Compared to this study, the SCAQMD-reported slope is closer to unity, but the intercept is much larger.

Figure B-3
$PM_{2.5}$-Pb measured by XRF and ICP-MS

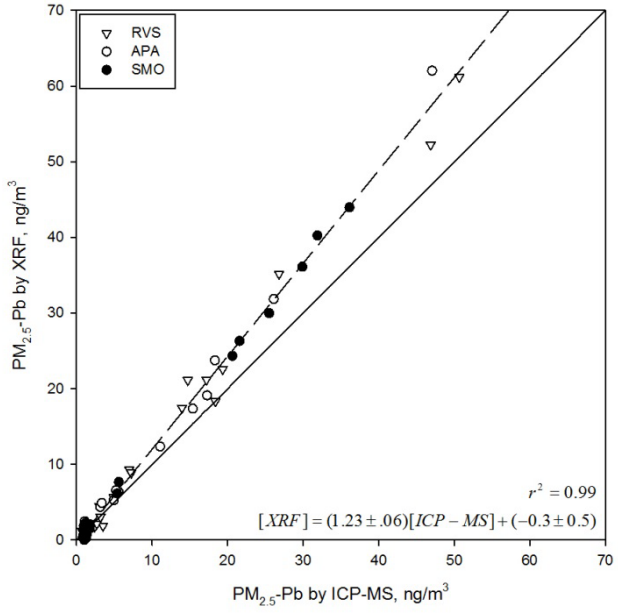

Note: Regression coefficients including 95% confidence intervals are from a constant variance Deming regression. The solid line is the 1:1 line and the dashed line is the regression line.

References

Dobrzhinsky, N., E. Krugly, L. Kliucininkas, T. Prasauskas, M. Kireitseu, A. Zerrath, and D. Martuzevicius. 2012. "Characterization of desert road dust aerosol from provinces of Afghanistan and Iraq." *Aerosol and Air Quality Research* 12: 1209–1216.

Lord, C.J. 1994. "Determination of lead and lead isotope ratios in gasoline by inductively coupled plasma mass spectrometry." *Journal of Analytical Atomic Spectrometry* 9: 599–603.

Martuzevicius, D., L. Kliucininkas, T. Prasauskas, E. Krugly, V. Kauneliene, and B. Strandberg. 2011. "Resuspension of particulate matter and PAHs from street dust." *Atmospheric Environment* 45: 310–31.

South Coast Air Quality Management District (SCAQMD). 2010. *General Aviation Airport Monitoring Study, Final Report*. Prepared for the U.S. Environmental Protection Agency.

Appendix C

Location of Airport Emissions Areas

Figure C-1
RVS Hangar Activity Locations

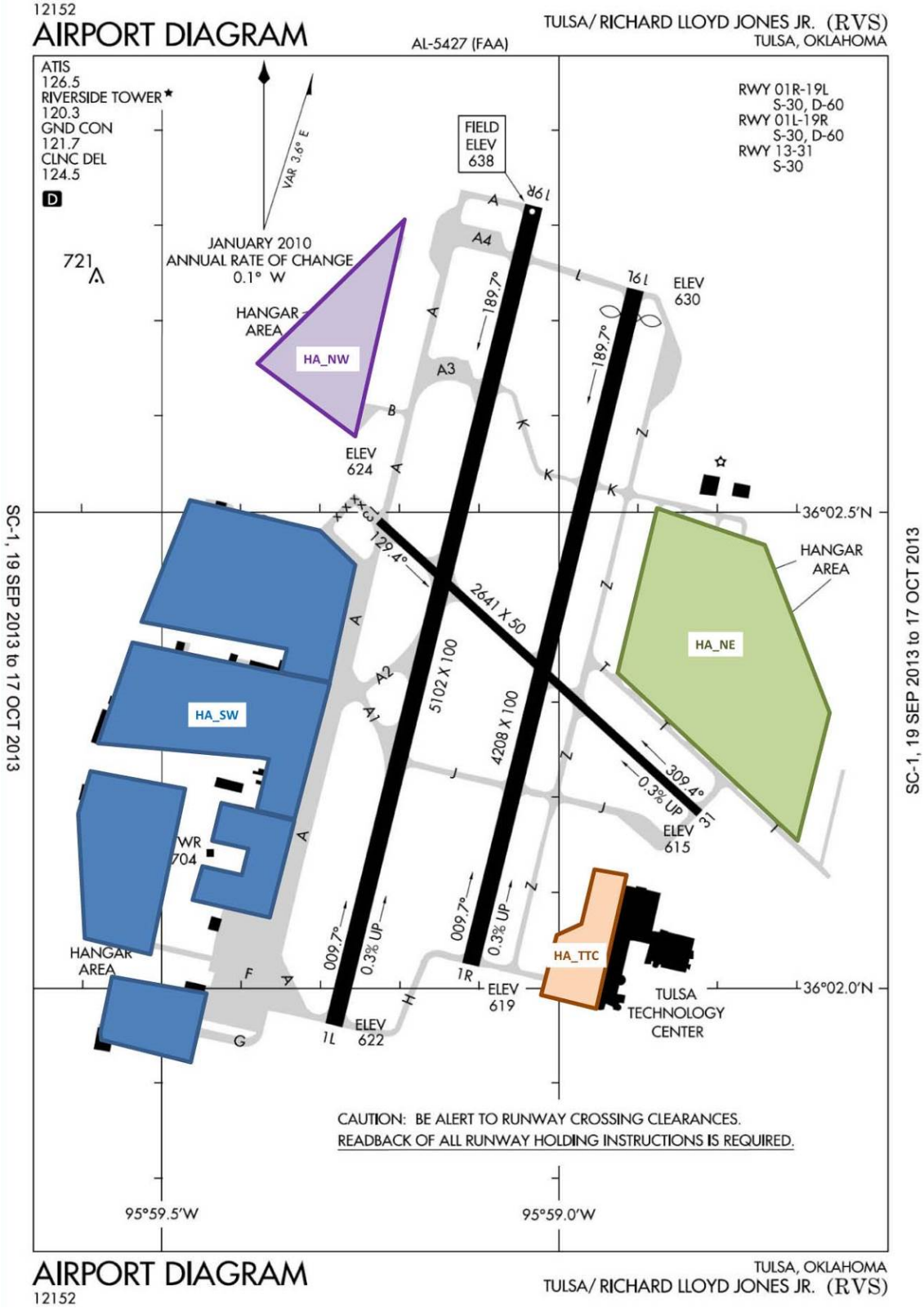

Figure C-2
RVS Runup Activity Locations

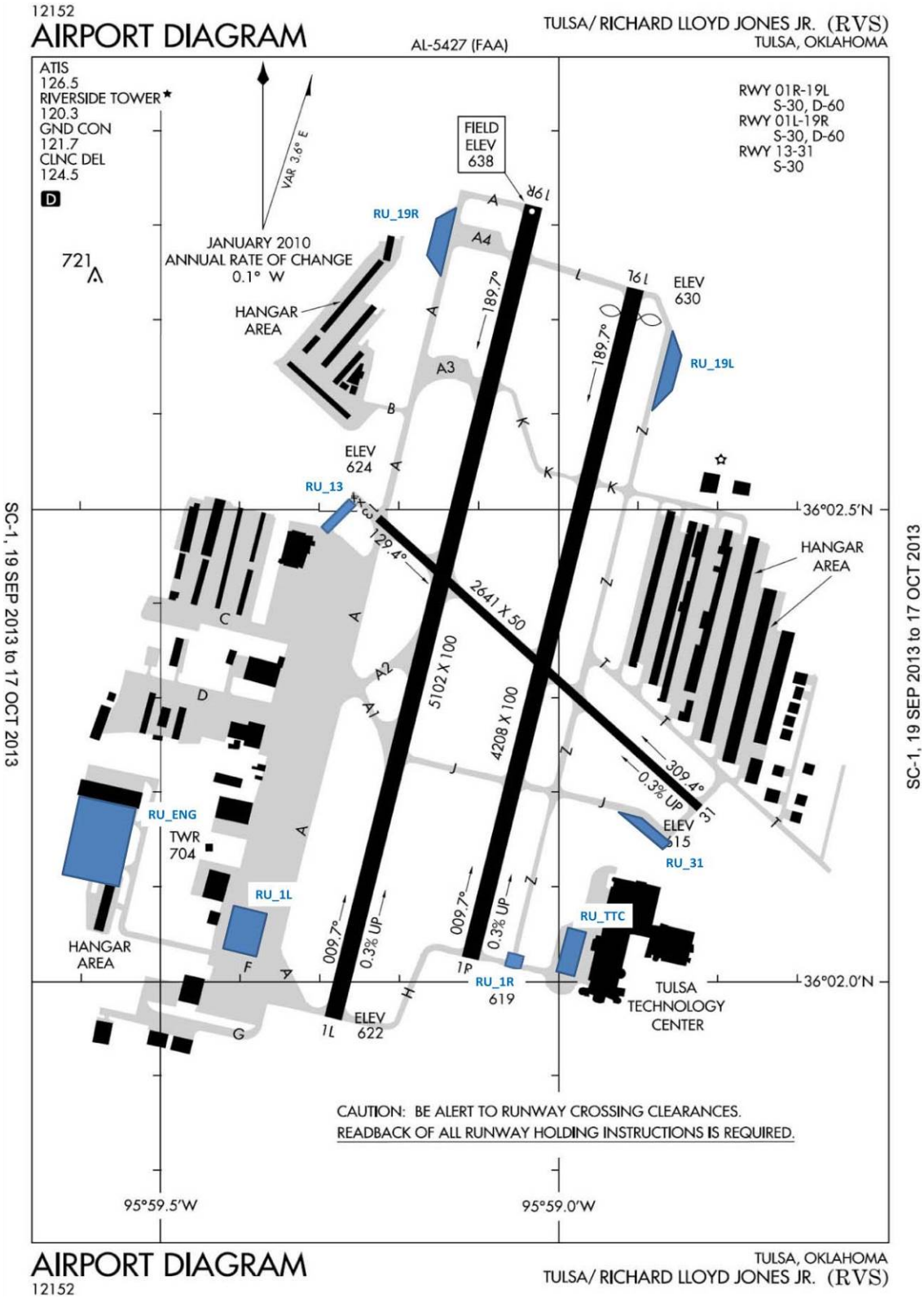

Figure C-3
RVS Taxiway Locations

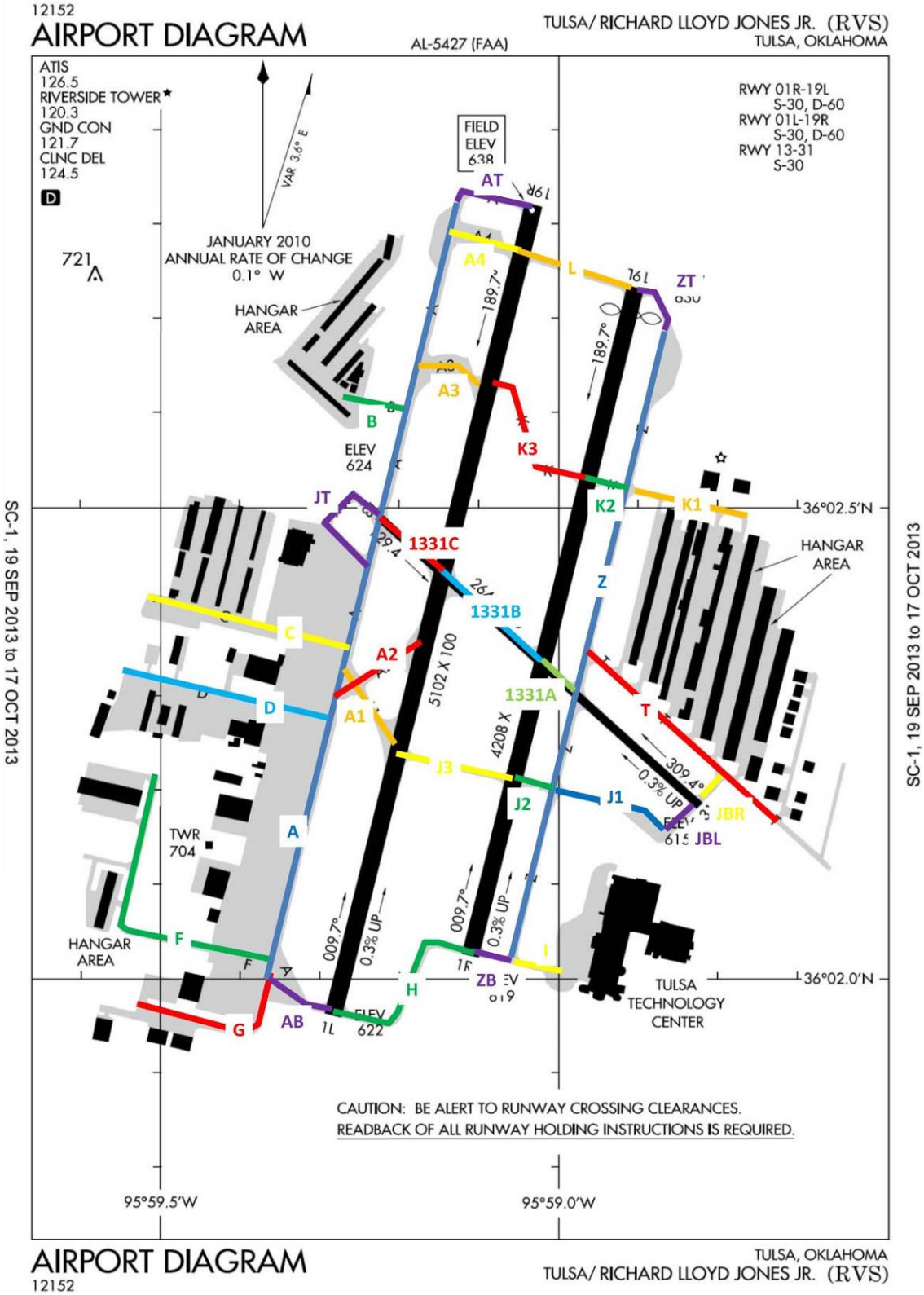

Figure C-4
RVS Helicopter Activity Locations

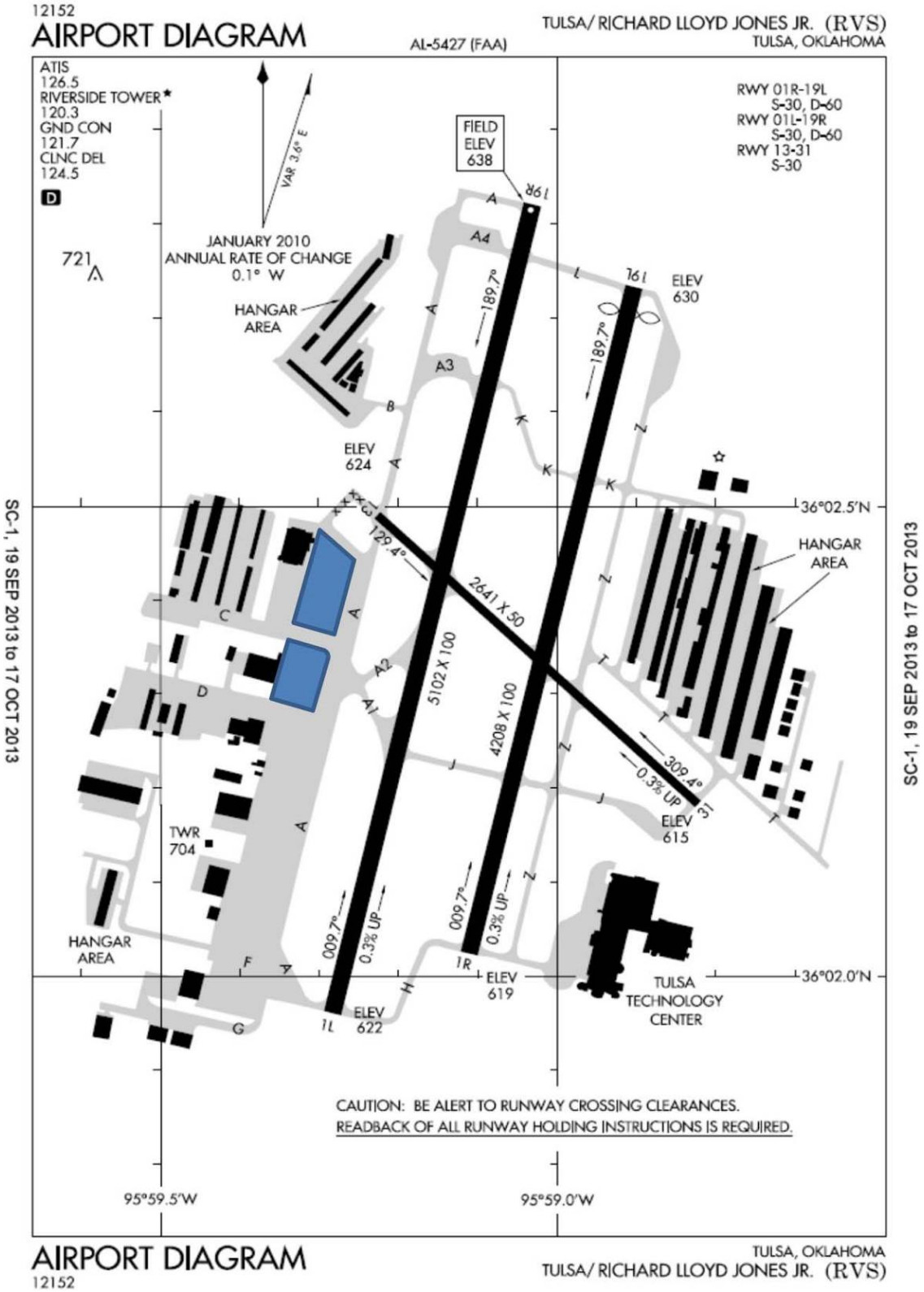

Figure C-5
APA Hangar Activity Locations

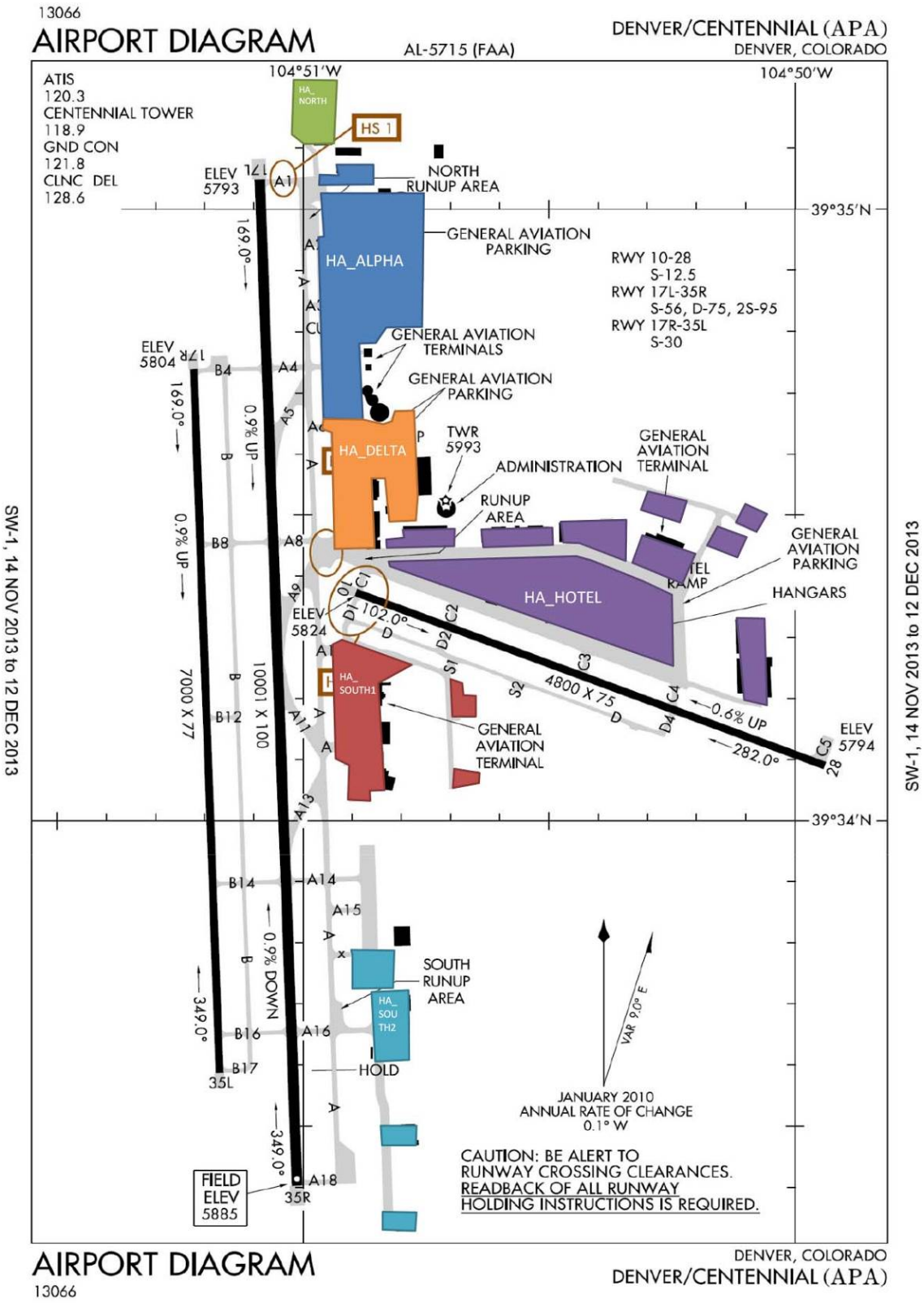

Figure C-6
APA Runup Activity Locations

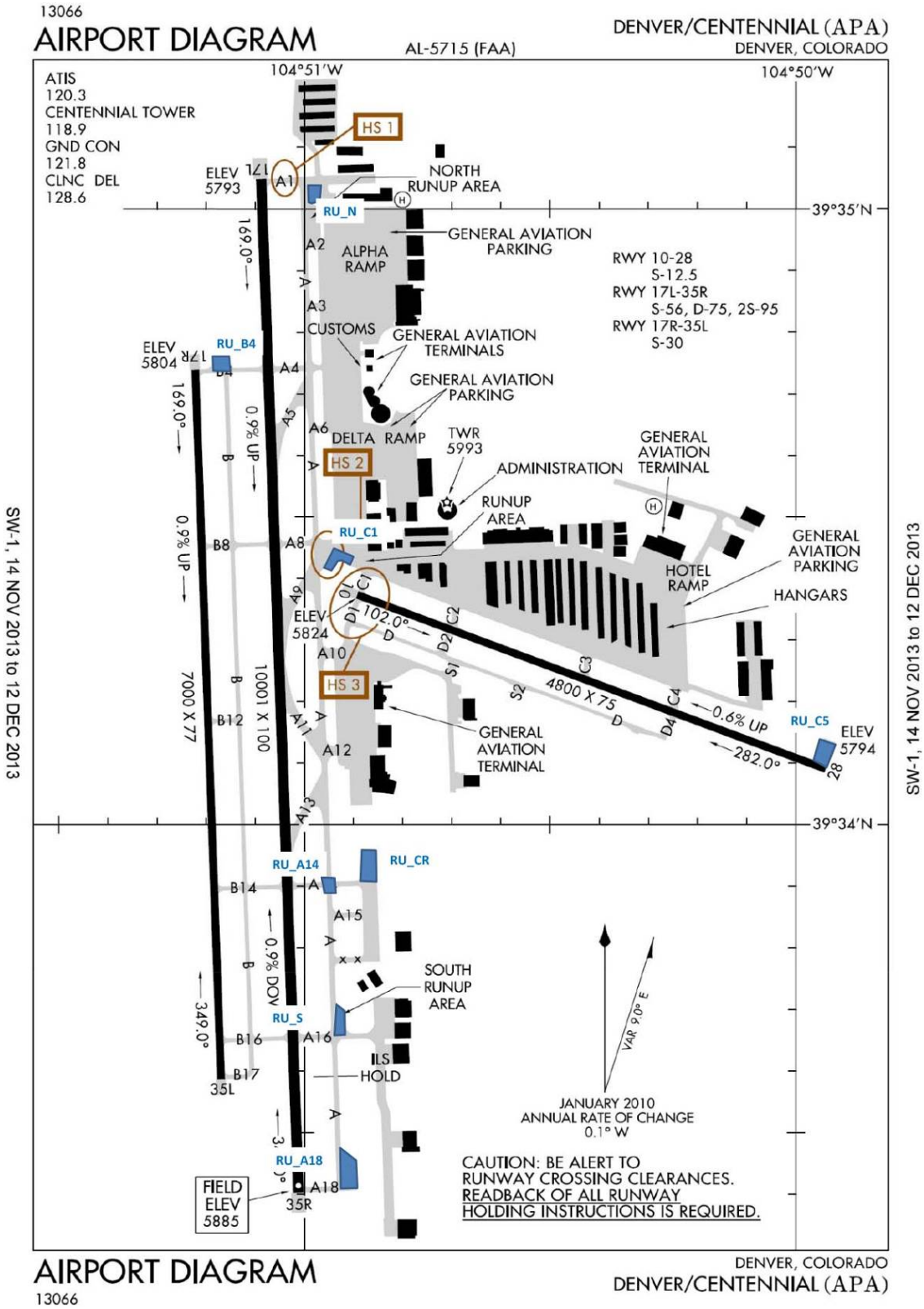

Figure C-7
APA Taxiway Locations

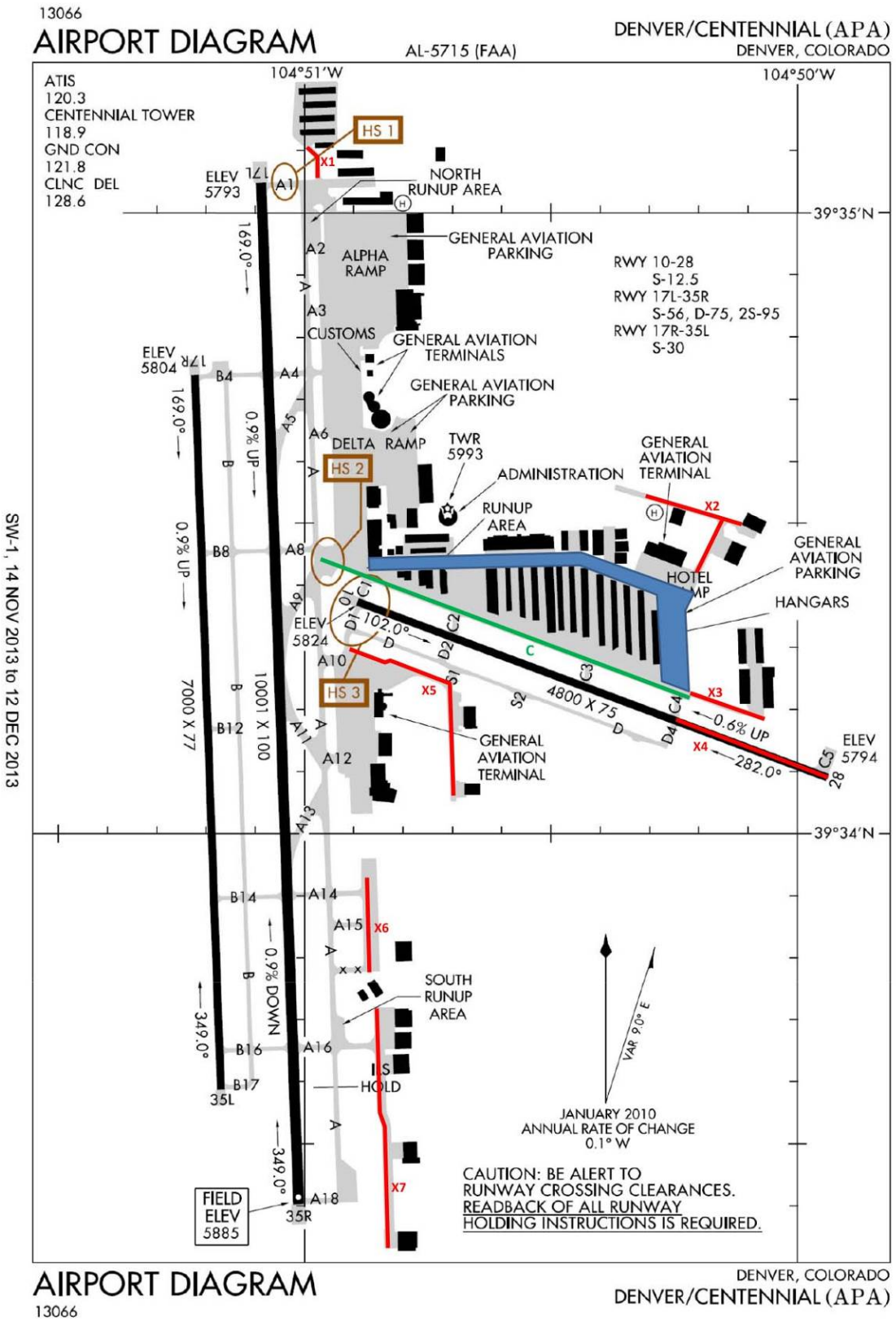

Figure C-8
SMO Hangar Activity Locations

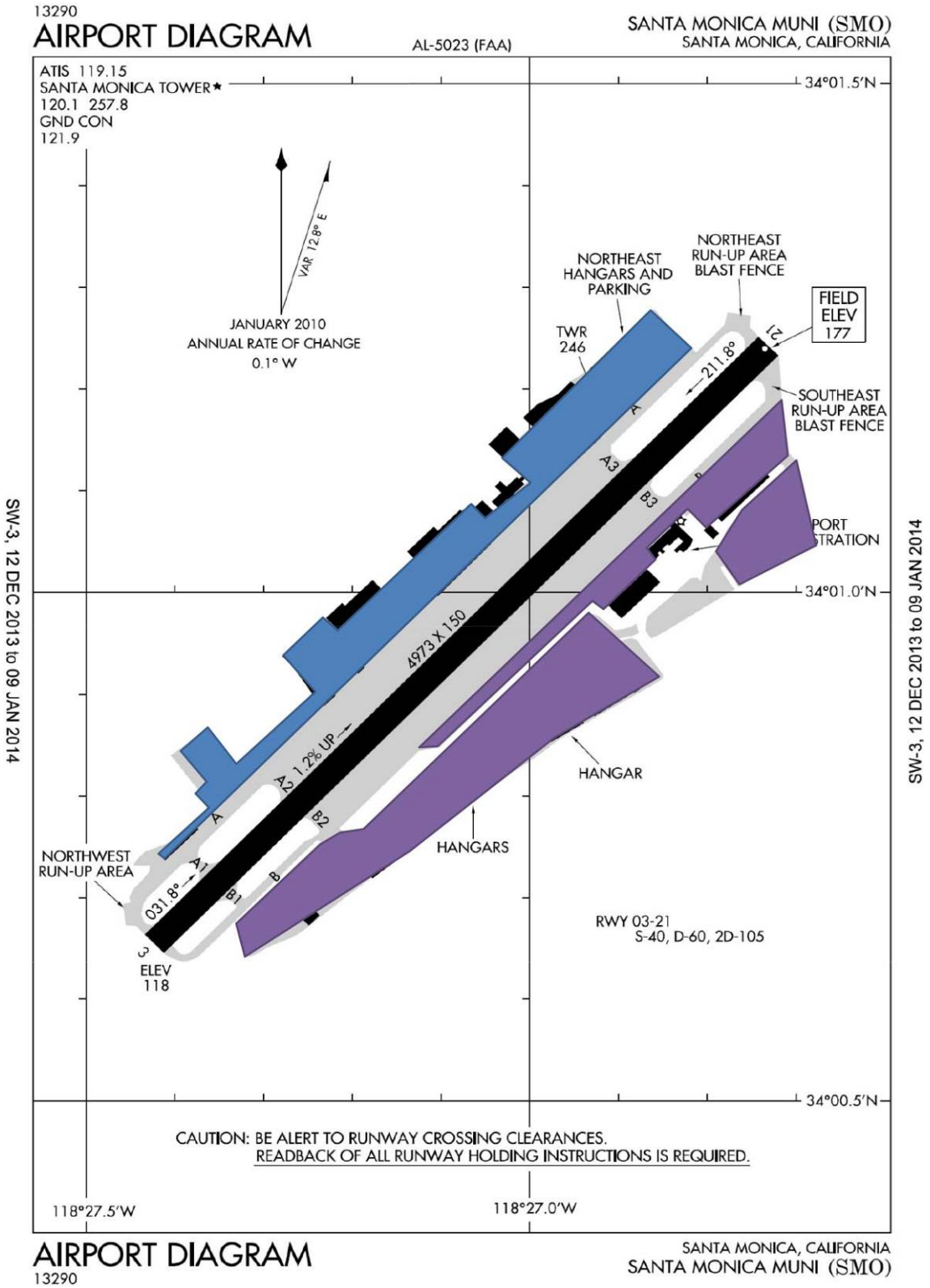

Figure C-9
SMO Runup Activity Locations

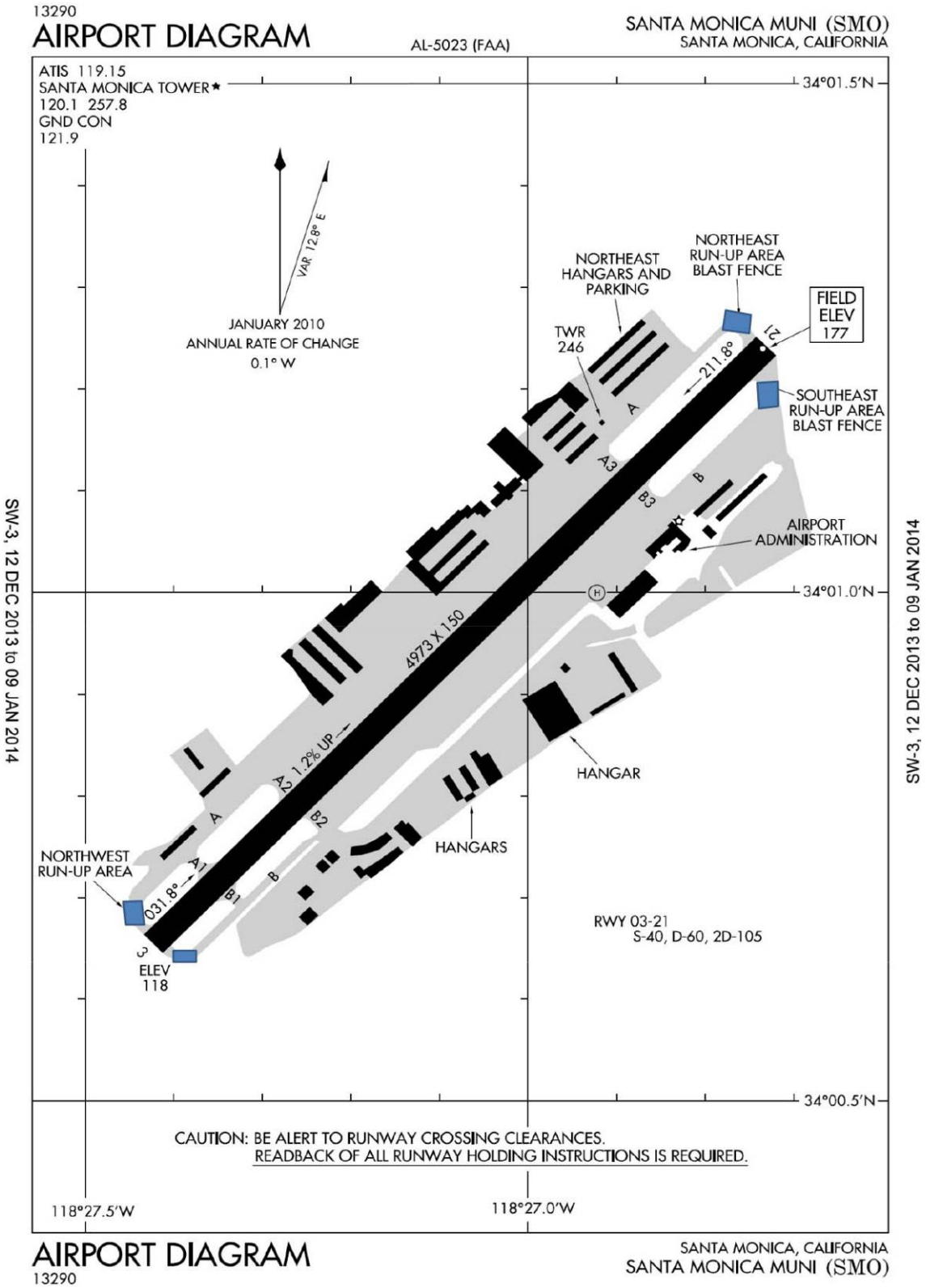

Figure C-10
SMO Taxiway Locations

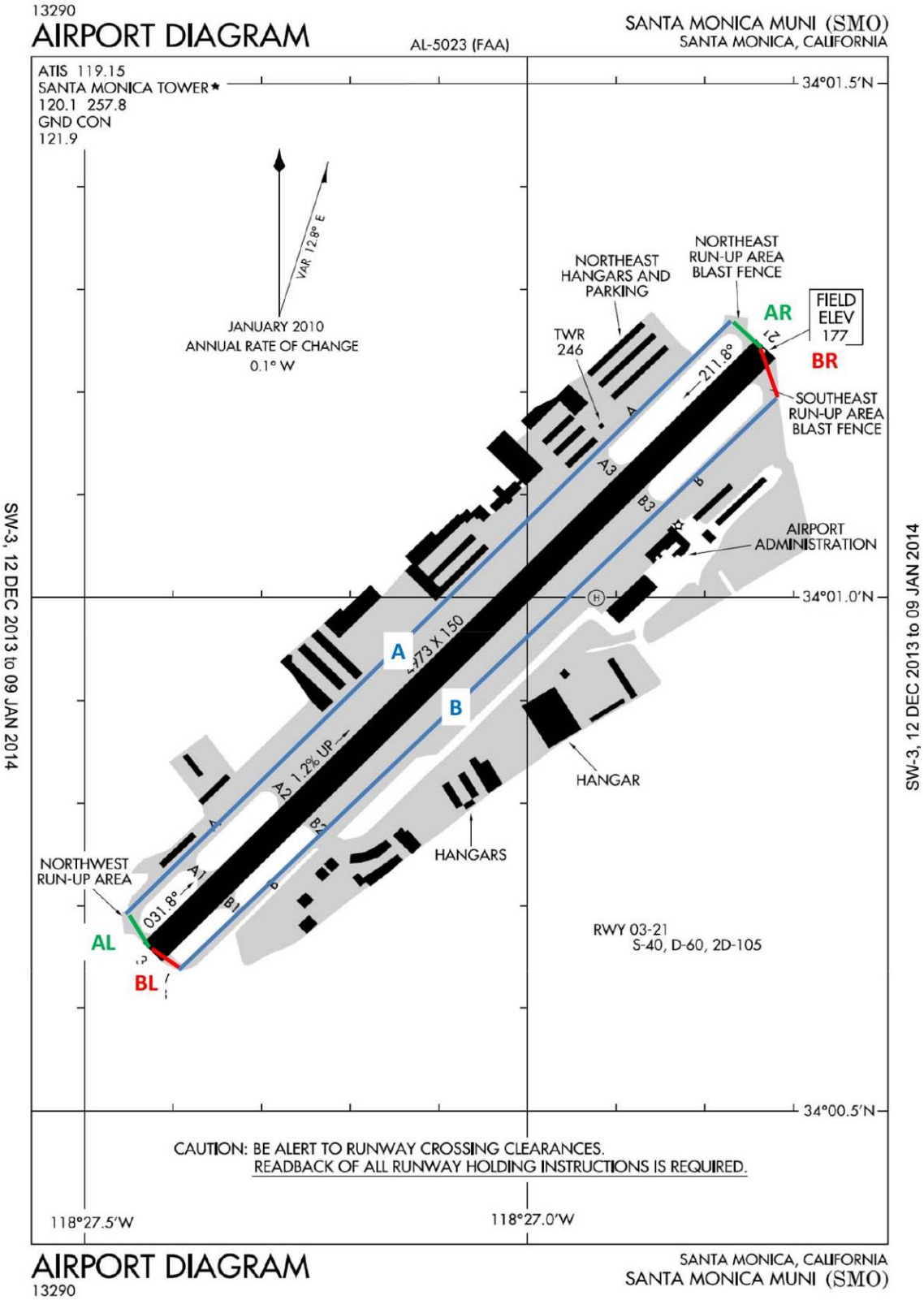

Figure C-11
SMO Helicopter Activity Locations

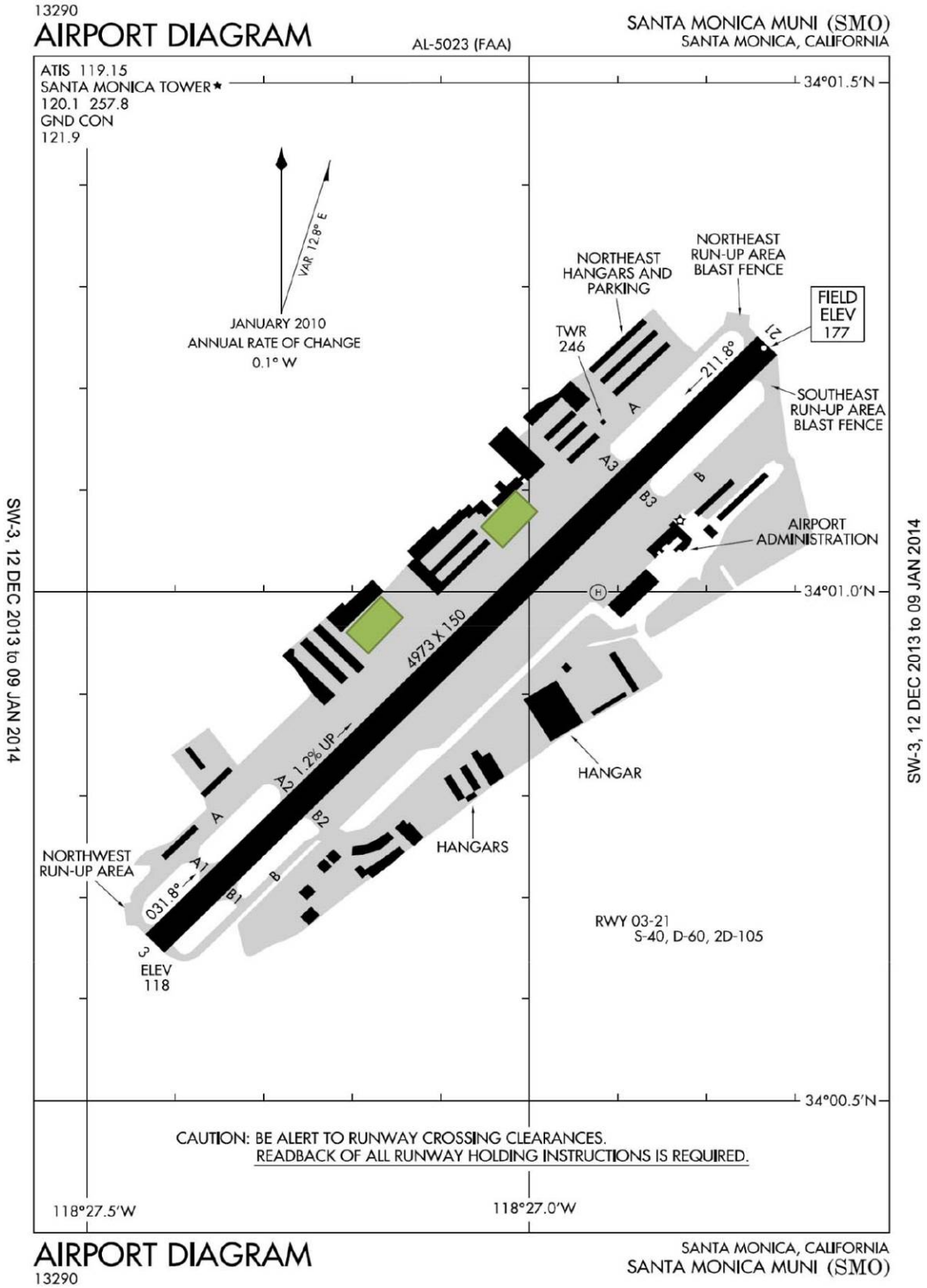

Figure C-12
SMO Additional Aircraft Idling Activity Locations

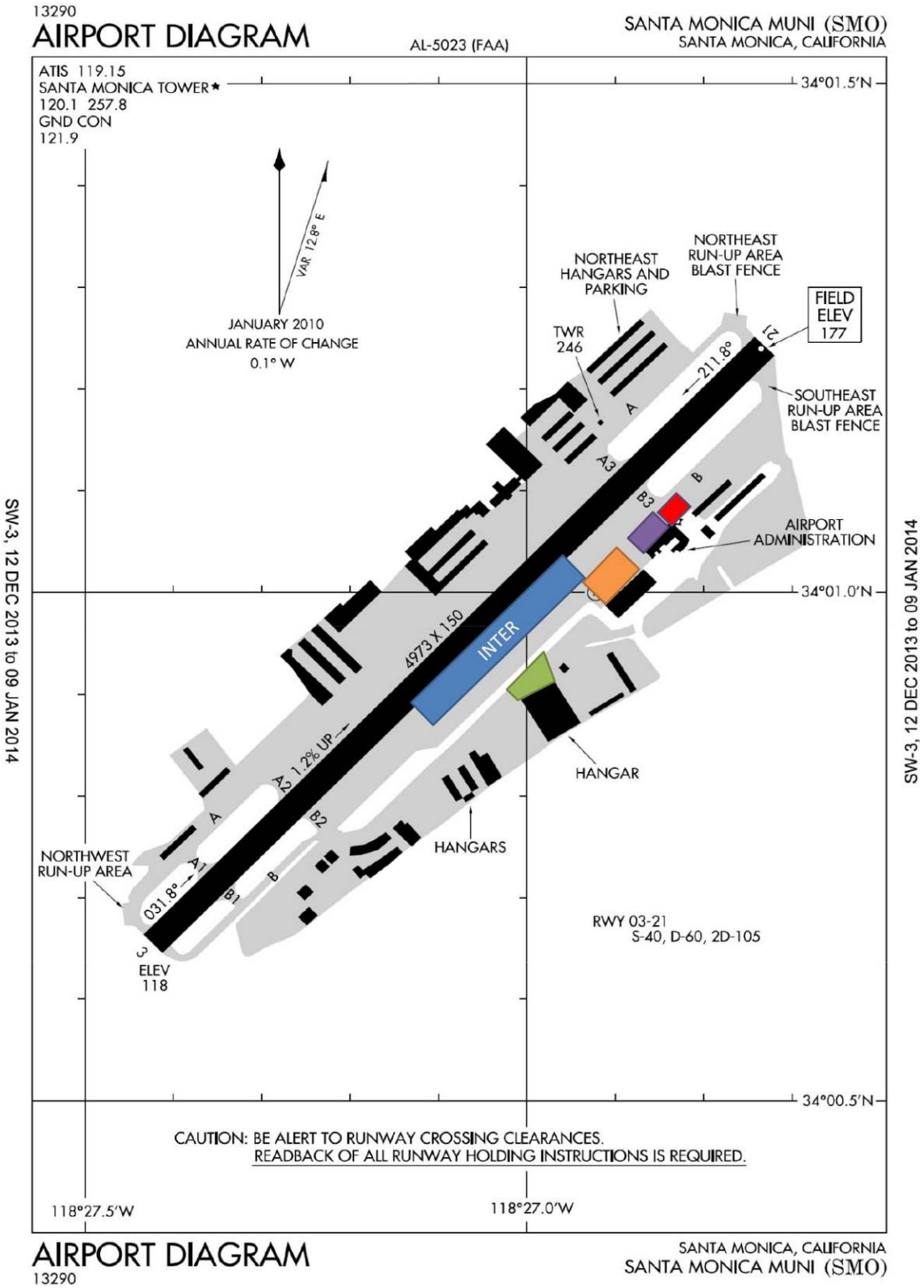

Appendix D

Model-to-Monitor Comparisons Using Publicly Available Data

Model-to-Monitor Comparisons Using Publicly Available Data

Model-to-monitor comparisons using the refined emission inventory with site-specific data were presented in Section 7.2. This appendix summarizes the comparisons using the refined inventory with publicly available data. In this case, the 2011 emission inventories presented in Chapter 4 were scaled using ATADS data for the sampling days during the 2013 field studies. Emissions were spatially and temporally allocated based on conversations with the airport operators and engineering judgment, consistent with the information that would be available in the absence of on-site data collection. Daily emissions were uniformly distributed across the 12 daytime hours with PM sampling. At RVS, two-thirds of the LTOs were assigned to runway 19R/1L and one-third to runway 19L/1R. At APA, all LTOs were assigned to runway 10/28, since little piston engine traffic was anticipated on runway 17R/35L. The runway activity splits were used to allocate run-up emissions to the run-up areas corresponding to each runway. SMO has only one runway. Taxi/idle activities are distributed over the second half of the runway(s) to account for aircraft roll on the runway after landing, and also movement on the taxiways. At RVS, the emissions were equally distributed between aircraft roll after landing and movement on taxiways. At APA and SMO, one-third of the taxi/idle emissions were assigned to aircraft roll after landing and two-thirds were assigned to movement on taxiways. Air quality dispersion modeling was conducted as described in Chapter 7 and with the same meteorological data that were used for the comparisons presented in that chapter. Exceptions are the data elements in Table 7-1 to 7-4 that were based on the on-site data collection (e.g., runway locations where aircraft touch down); in such cases, engineering judgment without prior knowledge of true airport activity was used.

Figures D-1 to D-3 show the model-to-monitor comparisons for RVS, APA, and SMO, respectively. For each airport the model typically underpredicts the measured concentrations except near the origin, which corresponds to sampling days with winds such that the monitor was upwind of the airport activities. PM-Pb emission inventories presented in Chapter 6 show the refined inventory with publicly available data was higher than the inventory with site-specific data. Furthermore, ATADS daily operations were higher than the 12-hour daytime on-site observations, and in the case of APA it was demonstrated that operations outside of the on-site data collection period could not explain the differences. Thus, the direction of bias in the modeling results with publicly available data cannot be explained by differences in the overall emission inventory. It is likely that errors in the spatial allocation of emissions significantly contribute to the bias, with additional contributions from errors in the TIM estimates. These results reinforce the importance of on-site data collection to accurately model PM-Pb concentrations.

Figure D-1
RVS North Site
Measured vs. Modeled Pb in PM2.5 Using Publicly Available Data

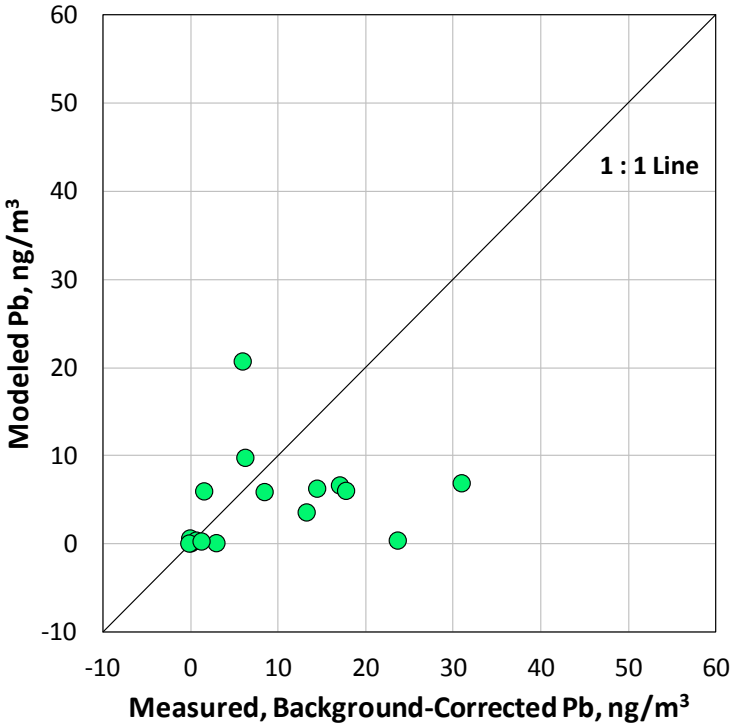

Figure D-2
APA Central Site
Measured vs. Modeled Pb in PM2.5 Using Publicly Available Data

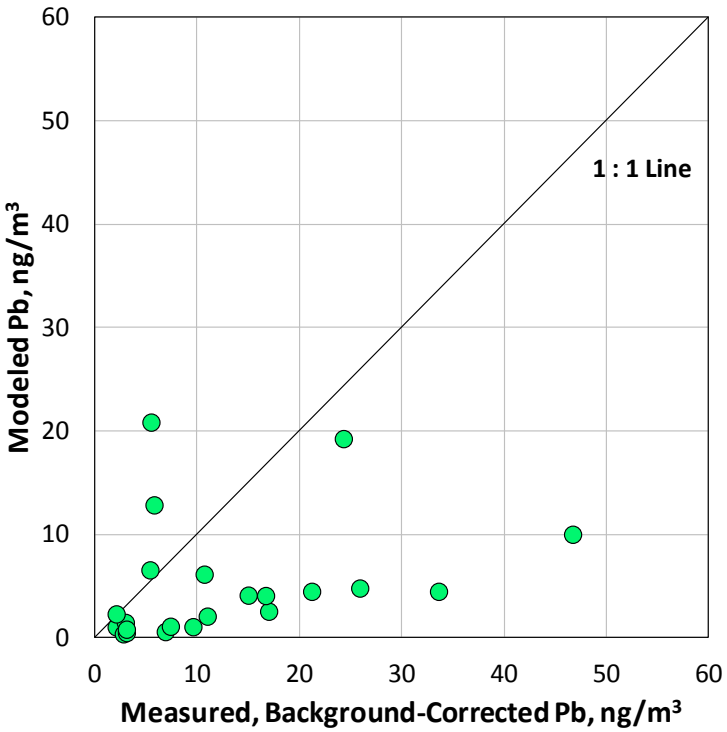

Figure D-3
SMO Northeast Site
Measured vs. Modeled Pb in PM2.5 Using Publicly Available Data